Plasticisers in Historic Plastics: Spectroscopic and Chromatographic Approaches for Cellulose Acetate and Polyvinyl Chloride

Rose King

A thesis presented for the degree of

Doctor of Philosophy

Institute of Sustainable Heritage

University College London

July 2023

Supervisors

Dr. Katherine Curran, Dr. Josep Grau-Bové

Abstract

The presence of plastic objects in museum collections reflects their use as a material for artistic expression, and their widespread use in our everyday lives. Their conservation is tailored to the plastic type or polymer, but the role of additives within a plastic formulation can be overlooked. Plasticiser additives are used to manufacture CA and PVC and are designed to remain within the plastic to impart flexibility. Instead, they can migrate out of the plastic due to the surrounding environment or the plasticiser's chemical characteristics. As such the additive can influence the migration rate and consequently aging behaviour of a plasticised object, but few studies have linked an objects degradation behaviour with the additives present.

Non-destructive methods were developed for PVC identification using new ATR libraries and ER-FTIR spectroscopy. ER-FTIR spectra were also used to identify aromatic plasticisers without requiring destructive GC-MS or NMR methods. Additionally, a minimally invasive sampling method using surface swabs were shown to allow sampling of degradation products, before a simple, cost-effective thin layer chromatography method can be used to widen the range of observable analytes versus the ER-FTIR spectroscopy method.

For CA, a preliminary attempt at magnetic resonance imaging suggested water and plasticiser content could be studied across three-dimensional CA samples. Additionally, a new data processing method for ^{1}H NMR data allows for the measurement of additive and acetic acid concentrations, as well as the degree of substitution within a single sample. It is hoped the method can be developed further

and used to identify links between chemical composition and degradation behaviour for objects.

Overall, the proposed techniques aim to enable conservation practitioners to assess the condition and composition of plastic objects in museum collections. By employing these methods, conservators can gain insights into the effect of a plastic object’s additive formulation on its aging behaviour.

Declaration

“I, Rose King confirm that the work presented in my thesis is my own. Where information has been derived from other sources, I confirm that this has been indicated in the thesis.”

Impact Statement

This thesis aims to contribute towards the heritage sector's efforts to preserve plastic objects; by advancing our understanding of their composition with respect to plasticiser additives. Within the heritage sector, practitioners including heritage scientists and conservators, were the target audience for much of the work presented here.

For conservators, the literature review in Chapter 1 can be used to expand domain knowledge as it incorporates findings from adjacent research sectors such as material emissions studies and details the current state of the sector. For scientists, Chapter 3 illustrates opportunities for polymer and plasticiser analysis from existing spectroscopic data, and Chapter 4 offers a simple method of plasticiser analysis which can be performed with minimal resources and without destructive sampling. Chapter 3 also expands the methods available for the analysis of cellulose acetate.

Beyond the heritage sector, the statistical analysis in section 4.3.9 may be more broadly applicable to monitoring plastic formulations over time, and section 3.3.11 offers a novel application of magnetic resonance imaging for plastics analysis. The data analysis method used in section 3.3.10 also seems promising for natural polymer analysis.

In terms of disseminating outputs, the literature review in Chapter 1 was adapted for publication in the *Heritage Science* journal and is the first heritage-specific publication seeking to summarise the issue of plasticiser migration from culturally valuable items. The Practitioner Survey in Chapter 2 is intended for publication in an open-source conservation journal. A summary of the proposed additive analysis methods was shared at the *Festival of Plastics* for conservation professionals.

Finally, on the back of knowledge gained during this work the author supported and contributed to projects at the *Museum of London* and *Tate,* the later resulting in a publication in the *Polymers* journal [1].

UCL Research Paper Declaration Form
referencing the doctoral candidate's own published work(s)

Please use this form to declare if parts of your thesis are already available in another format, e.g. if data, text, or figures:

- *have been uploaded to a preprint server*
- *are in submission to a peer-reviewed publication*
- *have been published in a peer-reviewed publication, e.g. journal, textbook.*

This form should be completed as many times as necessary. For instance, if you have seven thesis chapters, two of which containing material that has already been published, you would complete this form twice.

1. For a research manuscript that has already been published (if not yet published, please skip to section 2)

a) **What is the title of the manuscript?**
Plasticiser loss in heritage collections: its prevalence, cause, effect, and methods for analysis

b) **Please include a link to or doi for the work**
https://doi.org/10.1186/s40494-020-00466-0

c) **Where was the work published?**

Heritage Science

d) **Who published the work?** (e.g. OUP)

Springer

e) **When was the work published?**

2020

f) **List the manuscript's authors in the order they appear on the publication**

Rose King, Josep Grau – Bove, Katherine Curran

g) **Was the work peer reviewed?**

Yes

h) **Have you retained the copyright?**

Yes

i) **Was an earlier form of the manuscript uploaded to a preprint server?** (e.g. medRxiv). If 'Yes', please give a link or doi)

No

If ‘No’, please seek permission from the relevant publisher and check the box next to the below statement:

☐

*I acknowledge permission of the publisher named under **1d** to include in this thesis portions of the publication named as included in **1c**.*

2. **For a research manuscript prepared for publication but that has not yet been published** (if already published, please skip to section 3)

   a) **What is the current title of the manuscript?**

   Click or tap here to enter text.

   b) **Has the manuscript been uploaded to a preprint server?** (e.g. medRxiv; if ‘Yes’, please give a link or doi)

   Click or tap here to enter text.

   c) **Where is the work intended to be published?** (e.g. journal names)

   Click or tap here to enter text.

   d) **List the manuscript’s authors in the intended authorship order**

   Click or tap here to enter text.

   e) **Stage of publication** (e.g. in submission)

   Click or tap here to enter text.

3. **For multi-authored work, please give a statement of contribution covering all authors** (if single-author, please skip to section 4)

4. RK critically analysed the literature and drafted the manuscript, KC and JGB helped to review and edit the manuscript. All authors read and approved the final manuscript.

5. **In which chapter(s) of your thesis can this material be found?**

   Edited in chapter 1

6. **e-Signatures confirming that the information above is accurate** (this form should be co-signed by the supervisor/ senior author unless this is not appropriate, e.g. if the paper was a single-author work)

   Candidate

   Rose King

   Date:

   8/7/23

   Supervisor/ Senior Author (where appropriate)

   Date

Acknowledgements

An immense thank you to my supervisors Josep and Katherine for your guidance through the years, and to Simoni and Miriam for your help in the lab. To Isa, Morena, and Rosie you made my time at UCL even more enjoyable, and laughter filled. Thanks also to the ESPRC, Smithsonian MCI, and Getty Conservation Institute for their financial support.

To my friends, Beth, Chelsea, Danielle, Erin, Laura, Lauren, and Josie, I am writing this just shy of 20 years since meeting you all, so thank you for letting me witter on, offering wise council, and being the most wonderful friends!

To my wonderful family, Mum, Alice, Steven, and Noah, you are the most loving and encouraging family, thank you for your endless patience and support. It's done! I would like to dedicate this thesis to my Dad and my grandparents who saw me start this journey but are sadly not here to celebrate the end. Thank you for sharing your love, thirst for knowledge, and encouraging me to make the most of any opportunity that arose. My Dad's favourite refrain was to try and 'have fun' with whatever I am doing, and I can honestly say that I did

Table of Contents

List of abbreviations

ATR: Attenuated total reflectance

AER: Air Exchange Rate

AFM: Atomic Force Microscopy

ATBC: acetyl tributyl citrate

ATD: Attenuated Thermal Desorption

BBzP: benzyl butyl phthalate

CA: Cellulose Acetate

CN: Cellulose Nitrate

DBP: dibutyl phthalate

DBS: dibutyl sebacate

DEP: diethyl phthalate

DEHA: diethylhexyl adipate

DEHP: bis(2-ethylhexyl) phthalate

DOTP: diethylhexyl terephthalate (also known as DEHT)

DIDP: diisodecyl phthalate

DINCH: 1,2-Cyclohexane dicarboxylic acid diisononyl ester

DINP: diisononyl phthalate

DiHpP: diisoheptyl phthalate

DIUP: diisoundecyl phthalate

DHEH: 1,2-cyclohexane dicarboxylic acid, diethylhexyl ester

DMP: dimethyl phthalate

DOA: dioctyl adipate

DOP: dioctyl phthalate

DOTP: dioctyl terephthalate

ER: External reflectance

ESBO: epoxidized soybean oil

FTIR: Infrared Spectroscopy

GC-MS: Gas Chromatography – Mass Spectrometry

KKT: Kraemer Kroning Transformation

KM: Kubelka-Munk

LDA: Linear discriminant analysis

LDPE: Low-Density Polyethylene

MRI: Magnetic Resonance Imaging

NIR: Near-Infrared Spectroscopy

NMR: Nuclear Magnetic Resonance

PCA: Principal Component Analysis

PEV: pentaerythritol valerate

PMMA: Poly(methylmethacrylate)

PU: Polyurethane

PVC: Poly(vinyl chloride)

Py-GC-MS: Pyrolysis Gas Chromatography – Mass Spectrometry

SEM-EDX: Scanning Electron Microscopy - Energy-dispersive X-ray spectroscopy

SPME: Solid Phase Microextraction

SVOC: Semi-volatile organic compound

TGA: Thermogravimetric Analysis

THz: Terahertz Spectroscopy

THz-TDS: Terahertz – Time-Domain Spectroscopy

TLC: Thin Layer Chromatography

TOTM: trioctyl trimellitate

TPP: triphenyl phosphate

VOC: Volatile organic compound

Introduction

The presence of plastic objects in museum collections reflects their ubiquity in society. Plastics are pervasive in society due to their versatility in manufacturing, cost, and arguably unrivalled variety of applications. While polymerisation reactions were first reported in the 19th century, the development of commercial plastic production is most associated with the 20th century. They have been acquired into heritage collections as a record of everyday modern life, to represent technological and medical advancements, and as a medium of artistic expression. As with other heritage objects, conservation priorities may be driven by a balance of historical, aesthetic, scientific and social values and influenced by an object's provenance, the magnitude of the plastics collection, the available budget, and the interests of stakeholders. However, plastics present a particular challenge for conservators and scientists seeking to maintain collections due to the variety of formulations used.

Plastics comprise one or more polymers, alongside a variety of additives such as colourants, inorganic fillers, flame retardants, heat stabilisers, and plasticisers [2,3]. The history of additives is therefore as long the history of plastics. Cellulose Nitrate (CN) was the first commercialised plastic, its production in the 1870s was enabled by the discovery of camphor's plasticising ability for CN. However, applications of CN were limited due to its flammability and inability to be moulded. Instead, non-plasticised plastics such as 'Bakelite'; a dark-coloured mouldable synthetic plastic, and casein formaldehyde (CF), 'Galalith' or 'Erinoid;' a light-tinted cast semi-synthetic plastic, were developed at the turn of the century and proved the varied markets for plastics; from electrical devices to imitation gemstones. Later, the development of phthalate plasticisers enabled the commercial production of flexible poly (vinyl chloride) (PVC) by the Goodrich Co. in 1933, and cellulose acetate (CA) which was

patented in 1932 [4,5]. CA's transparent appearance and suitability for injection moulding meant it was an alternative for CN film and CF consumer goods, whereas plasticised PVC (pPVC) offered an alternative to rubber.

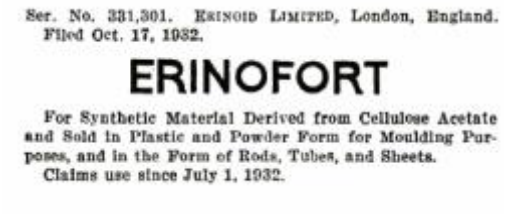

Ser. No. 331,301. ERINOID LIMITED, London, England.
Filed Oct. 17, 1932.

ERINOFORT

For Synthetic Material Derived from Cellulose Acetate and Sold in Plastic and Powder Form for Moulding Purposes, and in the Form of Rods, Tubes, and Sheets.
Claims use since July 1, 1932.

Figure 1: US patent announcement for cellulose acetate in 1932

While nature has evolved to produce polymers of high thermal and kinetic stability, e.g. cellulose and DNA, the synthetic plastics discussed above have proven less robust. Some synthetic polymers require heat stabilisers, antioxidants, and plasticisers to achieve stability and longevity of the resultant plastic. Together the additive formulation can modulate the desirable chemical and physical properties of the polymer and final plastic, such as the glass transitition temperature and elastic modulus. Consequently, alongside chemical reactions that alter the polymer (e.g. oxidation, hydrolysis, photolysis), additive (typically plasticiser, and stabiliser) migration is a degradation pathway which can result in visible changes and physical instability of an object [6]

Plasticiser migration has been observed in three 'malignant plastics' frequently found in collections; CN, CA, and PVC. Preventive environmental guidelines to slow polymer degradation rates and additive migration rates were introduced following key research contributions from multiple authors for CN and CA, and Yvonne Shashoua's studies of PVC [7,8] . As such, conservation case studies typically describe a preventive response to observable damage or active degradation, such as low temperature

storage, adsorbent used when a vinegar smell indicates deacetylation of cellulose acetate, or isolation when visible surface accretions and stickiness from plasticiser migration are evident for PVC.

Figure 2: Marketing of cellulose acetate for consumer goods and industrial components by Erinoid Ltd c. 1940s-50s. Images courtesy of 'Museum in the Park', Stroud, Gloucestershire, England.

In 2014, after recounting the previous three decades' developments, Learner et al. summarised the field of plastics conservation as follows [9];

> *… our understanding of plastics' stability remains rudimentary. We have a menu of mechanisms that potentially explain degradation, but there is a tendency to default to them and recite them, rather than investigate sceptically what is actually going on …*

Progress has been made in the intervening eight years; polymer identification using non-destructive reflectance spectroscopy, volatiles analysis, and conservation cleaning methods have been recurring and fruitful topics of study, alongside expanding environmental research to include the light sensitivity of plastics [10–12]. However, for many plastics, there remains a gap between achieving polymer identification and understanding how and on what time scale an object will degrade. As additives contribute significantly to the final chemical and physical properties of a plastic object, a deeper understanding of additive behaviour and its influence on aging may help to close the gap.

Structure in brief

The literature review (*Chapter 1*) collates previous observations of additive-influenced aging behaviour, and key indoor air/material emissions studies from other research sectors which describe the influence of environmental and intrinsic factors on additive loss. Examples focus on how differences in aging behaviour can be observed with different plasticisers. *Chapter 1* also collates analytical methods used for plastics analysis and includes the background of the analytical techniques used in later chapters.

The literature review also attempted to understand conservation strategies used to date, but examples were limited. Therefore, *Chapter 2* includes a professional survey which sought to understand how plastic objects are acquired and conserved in collections. The results show that in-depth scientific analysis of plastic objects is infrequent and uncommon, due to limited resources. However, non-analytical tools, and less commonly non-destructive analytical methods such as FTIR spectroscopy are used for polymer identification. No attempts which include additive analysis were documented.

Therefore, *Chapter 3* evaluates how PVC may be identified and how additives in PVC may be analysed by external reflectance and attenuated total reflectance FTIR spectroscopy, with comparison to destructive gas chromatography and NMR spectroscopy methods more commonly used in material and food science studies. The samples studied represent a variety of manufacture dates from the 1960s to present day.

Chapter 4 considers the limited resources available for plastic analysis during conservation work identified in *Chapter 2*, by developing a thin layer chromatography

method for PVC additive analysis. The accuracy of the method is evaluated with the characterised samples from *Chapter 3*. *Chapter 4* also considers how the TLC method can be used in practice by minimising invasive sampling and illustrates the minimum equipment required. Inspired by conservation cleaning and conditions surveys, *Chapter 4* details how swab sampling can be used for non-destructive sample collection. The method can be performed in a high-throughput manner, for example, during collection surveying. A statistical analysis of additive combinations found in literature data was also used to assess the limitations of the method.

Finally, *Chapter 3 also* considers the analysis of cellulose acetate. A novel data processing method used in metabolomics has been adapted for the analysis of the degree of substitution and plasticiser content of CA, and builds upon published work to maximise the information obtainable from ^{1}H NMR spectroscopy. Finally, the first exploratory attempt at non-destructive analysis of plasticised CA by Magnetic Resonance Imaging is described.

1. Literature Review

Plasticisers are small molecules used in plastic formulations to ease the processing of synthetic and semi-synthetic polymers and impart flexibility to plastics such as PVC and cellulosic esters [13,14]. From the 1930s onwards, patent literature records the evaluation of various plasticisers' compatibility with cellulosic and vinyl polymers [15]. Cellulose acetate (CA) formulations included dimethyl phthalate, diethyl phthalate (DEP), triphenyl phosphate (TPP), toluene sulphonamide, *N*-ethyl toluene sulphonamide, or mixtures of the same [16]. Phthalates (the esterification product of phthalic acid and alcohol) account for the majority of the plasticiser market today. PVC is predominately plasticised with long chain (C_{4+}) and branched ortho-phthalates (e.g. DINP) [17], but a variety of other plasticisers including terephthalates, sebacates, adipates, and trimellitates are also effective and increasingly used [14]. Some examples are shown in Figure 3.

Unlike some additives, such as lubricants which only aid the manufacturing process, plasticisers are designed to remain in the plastic matrix and contribute to the plastic article's final properties. However, plasticiser migration is well documented in medical literature, ecological pollution, food packaging studies, and studies of consumer products such as furniture, flooring, and toys [18,19]. Research into the effect of some ortho-phthalate plasticisers on human and animal health means their use is now regulated, and the use of non- phthalate and bio-based plasticisers (e.g. DINCH and ATBC) is increasing [20–22]. Plasticisers may be selected for specific applications such as food packaging (e.g. citrates), or their low migration in high-temperature (e.g. trimellitates) or low-temperature applications (e.g. adipates). Some polymeric plasticisers such as polyadipates are also marketed for applications requiring low migration rates.

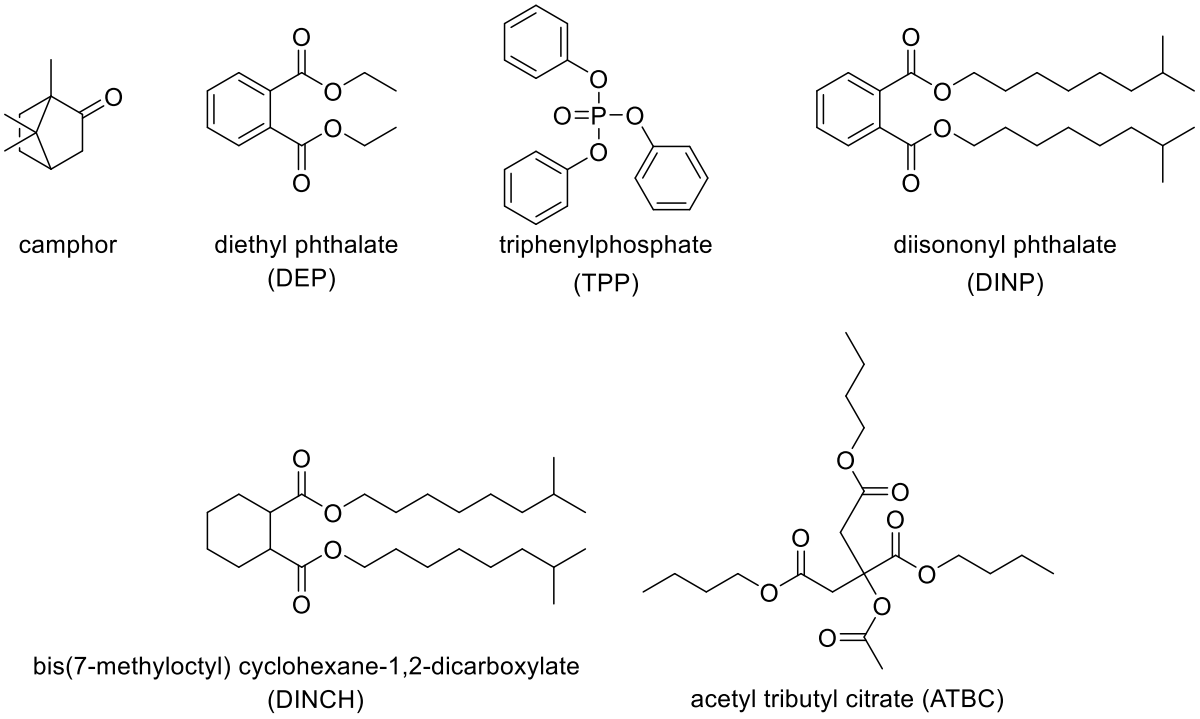

Figure 3: Examples of plasticisers used with cellulose nitrate (camphor), cellulose acetate (DEP, TPP) and polyvinyl chloride (DINP, DINCH, ATBC).

Plasticiser migration occurs when interactions between polymer chains and weakly bound additives are overcome, for example, on contact with a solvent, with the application of heat, or due to changes to the molecular structure of the polymer or additive, which modifies the strength of interaction at ambient temperature. The loss of additives, which are typically volatile or semi-volatile organic compounds (VOC/SVOCs) and are present in high concentrations (up to 50%), can cause visible and physical changes to objects, including a loss of mass, distortion, and embrittlement. Such changes can make an object more fragile and vulnerable to damage from handling, exhibition, or when supporting its own weight [23,24].

The appearance of surface deposits can also result from additive migration, examples are shown in Figure 4. In traditional polymer science, the terms ‘bloom’ and ‘bleeding’ describe the appearance of additives such as stabilisers, lubricants, or plasticisers on

a plastic surface. IUPAC defines bloom as “the process in which one component of a polymer mixture…undergoes phase separation and migration to the external surface” [25]. In conservation literature, observational terms such as “[crystalline] deposits” or “tacky surface” are used to describe visible evidence of additive migration. References to sticky/tacky deposits, ‘weeping’ or ‘sweating’ are equivalent to ‘bleeding’ whereby liquid plasticiser is observed exuding onto the surface. Krieg et al. have made efforts to standardise terminology with a comprehensive damage catalogue to aid the interpretation of damage phenomena on historic plastics [26]. Furthermore, residues can trap dust, adhere storage materials to the object, and transfer to adjacent materials. As Shashoua notes, this can “reduce [an objects] value both commercially and culturally” [27].

Figure 4: (Left) Bloom of triphenyl phosphate plasticiser and (right) phthalate plasticiser exudation from dolls made of cellulose acetate. Images are reproduced with the permission of Tate, London. Both dolls form a part of ‘Mouth Open, Teeth Showing (I)’, 2000, Zoe Leonard, Tate X717743 L04293.

1.1 Conservation strategies to date

Surveys have frequently found plasticised objects to be some of the most vulnerable in collections. Keneghan's survey of 7900 plastic objects within the Victoria and Albert Museum's collection showed evidence of chemical damage (classified as bloom, brittleness, discolouration, or sweating) in ~10% of surveyed objects [28]. A more detailed output arose from the use of a condition form including terms specific to additive migration in the pan-European 'POPART' survey [29]. Evidence of additive migration was classified by plastic type; bloom, bleeding, and 'solid exudates' were each observed in 30% of the CA and CN objects surveyed, and "sweating" or a "sticky surface" was observed in 23% of PVC objects.

Strategies proposed for the conservation of vulnerable plastics are primarily rooted in environmental control, including cold storage to reduce degradation rates following the assumption that the kinetic parameters follow an Arrhenius relationship. However, the storage space required along with refrigeration infrastructure costs is typically prohibitive for a whole collection. Refrigeration also impedes access to the object and typically is not used during exhibition. Therefore, non-refrigerated storage with macro environment climate control is theoretically more achievable.

For cellulose acetate (CA), early research found that cold storage reduces the auto-catalytic reaction rate of polymer hydrolysis or 'vinegar syndrome' [30,31]. Others recommend ventilated storage or scavengers to minimise a build-up of acidic species arising from hydrolysis of CA and CN [32,33]. However, a recent study suggests replication as the only viable long-term preservation method for triacetate film [34]. Plasticiser migration occurs alongside the deacetylation of CA, although its relative rate, importance, and impact are understudied.

For PVC, evidence of both dehydrochlorination and plasticiser migration has been observed in collections. Thermal and/or photo-oxidative degradation mechanisms have been extensively studied [35–37]. A comprehensive review by Wypch highlights varied ageing behaviour between formulations, that plasticiser loss generally occurs before dehydrochlorination during thermal ageing experiments, but also that plasticiser evaporation, plasticiser hydrolysis, and polymer degradation can be interlinked [38]. Yellowing provides visible evidence of dehydrochlorination, and the appearance of surface exudates and hardening generally result from additive migration.

Thermal ageing experiments have shown that enclosure reduces the migration rate of plasticisers from PVC samples relative to non-enclosed samples [39,40]. Royaux et al. have used similar experiments to investigate the effect of wrapping materials for new and historic PVC samples. Colour changes were particularly evident for samples wrapped in LDPE and PET during thermal ageing, and phthalate hydrolysis was also induced on contact with PET. Conversely, rates of yellowing and phthalate migration did not increase for samples wrapped in silk paper versus non-wrapped. However, migration of an oil-based co-plasticiser and proteinaceous component were slowed, which led the author to suggest that wrapping in suitable materials could be used to slow dirtying and protect the visible appearance of the surface [41,42].

1.2 Plasticiser loss mechanism and rate

Briefly, the migration process is governed by two mass transfer steps illustrated in Figure 5;

- Internal diffusion of additive molecules through the material bulk to the surface

- External mass transfer of additive molecules from the surface to the surroundings (sometimes generalised as evaporation)

The slowest step or ‘rate-limiting step’ controls the overall loss rate from the object. Therefore, the loss may be either “diffusion-controlled” or “evaporation-controlled”. In some cases, a change in the dominant transport step can occur during the ageing period.

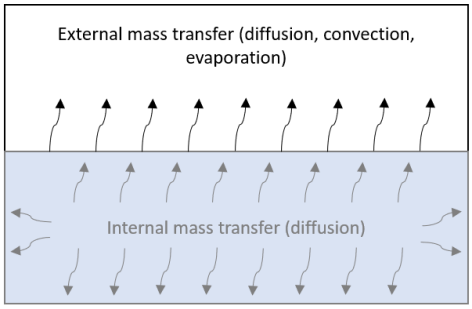

Figure 5 Simplified schematic showing the two mass transfer steps of plasticiser migration and loss.

The term ‘evaporation-control’ describes the case where the convective mass transfer of molecules between the material surface and adjacent air controls the loss rate. When this process is slower than the internal diffusion rate, thin films of additives can build up on surfaces, as seen in conservation studies of PVC [23].

Diffusion-controlled loss occurs when the rate of plasticiser emission from the surface is faster than the rate at which additive molecules are replenished by diffusion from the bulk. Without surface accumulation, no direct observation of the process occurs, but a concentration gradient along a cross-section may be measured [43].

Inhomogeneous concentrations may be hypothesised to result in internal stresses or risk of moisture gradients developing, for example, if plasticisers lend hydrophobic properties to the plastic.

The shapes of concentration distance profiles for both diffusion and evaporation-controlled loss are shown in Figure 6. Evaporation-controlled systems show a relatively flat concentration profile throughout the sample thickness, while a clear gradient develops under diffusion-controlled conditions. Due to the low volatility of some additives at room temperature, thermal ageing may be used to accelerate the loss rate and ensure measurable changes in additive concentration over shorter experimental times.

Aside from concentration-distance profiles, the change in additive concentration as a function of time or the square root of time can be plotted by analysis of the sample or environment. For example, evaporation-controlled loss results in a sigmoidal-shaped profile of mass loss as a function of the square root of time [44]. While beyond the scope of this review, the concentration-time profile shapes derive from ratios between key evaporation and diffusion parameters [45–47].

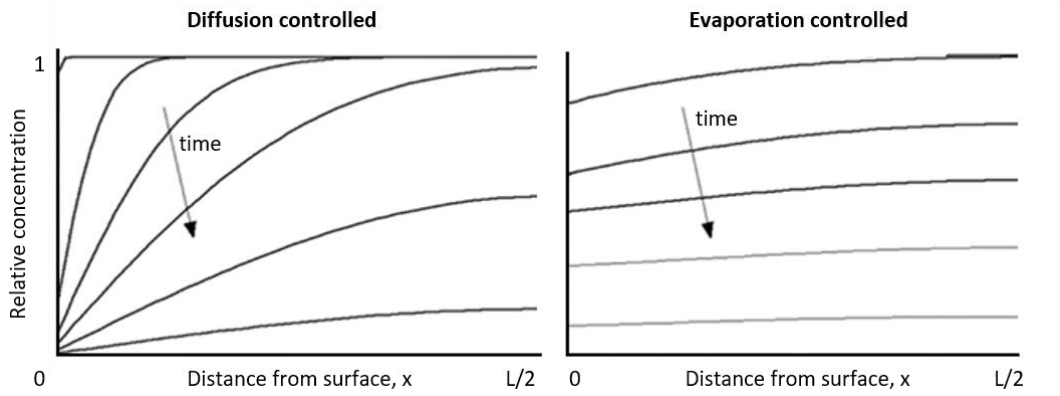

Figure 6: Concentration-distance profiles for evaporation and diffusion-controlled migration. Image adapted from [45]*, licensed under CC BY 4.0.*

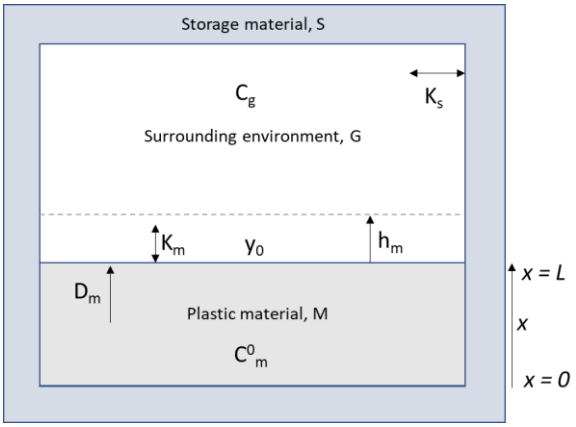

Figure 7: Schematic showing key mass transport parameters used to describe the emission of additives into the surrounding environment. The dashed line illustrates the conceptual air-boundary layer used in many emissions models. Parameters used in emissions models include the diffusion coefficient through the material, Dm, the material/air partition coefficient Km, the convective mass transfer coefficient, hm, and the concentration in the air boundary layer at the surface, y0.

The key parameters shown in Figure 7 are used to model either VOC or SVOC emission rates from solid materials. The World Health Organisation classifies VOCs as having a boiling point range between 50/100 °C and 240/260 °C and SVOCs between 240/260 °C and 380/400 °C; others classify SVOCs by vapour pressures of 10^{-9} to 10 Pa at room temperature [48].

VOC emission is typically diffusion-controlled and can be modelled if specific parameters are known:

- the material phase diffusion coefficient of the additive, D_m
- a material/air partition coefficient to describe the equilibrium between material surface and adjacent air, K_m

- the additive's initial material phase concentration, C^0_m (generally assumed constant within the material) [47,49].

Later VOC models have incorporated the external mass transfer parameter (h_m) to describe the initial loss from the surface into adjacent air, which occurs early in the emission period, and others have sought to incorporate sink effects.

Conversely, for SVOCs, evaporation-controlled emission modelling requires knowledge of:

- the gas-phase concentration of the SVOC in equilibrium with the material phase, y_0
- the convective mass transfer coefficient from the material surface to air, h_m [50].

In non-ideal environments (e.g. indoors), the partitioning of SVOCs from the gas-phase to surfaces, particles and settled dust is significant; therefore, models also require:

- the concentration of dust and particles
- the mass transfer coefficient from air to the surrounding surfaces, h_s
- Partition coefficients that describe transfer to condensed phases, such as airborne particles (K_p) and settled dust (K_d) or onto indoor surfaces (K_s) [49].

These parameters are challenging to measure, and research is ongoing to improve the accuracy of the measurement methodology [51–53]. System parameters including the emitting surface area, room volume, ventilation rate, and room surface area are also required.

It should be noted that the validity of ignoring the diffusion process for other SVOCs has been evaluated with limited formulations. To date, the evaporation-controlled SVOC emission models best describe low-volatility phthalates (e.g. DEHP, DINP, BBzP) in solid materials with a high initial concentration. Furthermore, diffusion and partitioning coefficients may become influential as additive concentration decreases over time.

Other examples highlight the variation in behaviour which may be observed in plastic collections where many additive/polymer combinations will be present. Benzenesulfonamide plasticisers have been found in plastics dating from the 1950s and are classified as VOCs with a boiling point at the higher end of the range [23]. A recent study reported the diffusion-controlled migration of n-butyl benzenesulfonamide from a polyamide pipe [44]. Organophosphate flame retardants were also found to migrate under diffusion-controlled rates from rigid foam materials, despite their classification as SVOCs [46].

1.3 Factors affecting the migration behaviour of plasticisers from plastics

Table 1 shows the range of environmental and intrinsic factors have been extensively researched and reviewed for indoor air quality audiences [54,55]. The relevance of their findings to conservation research is outlined below.

The cornerstones of environmental control in preventive conservation; temperature, relative humidity, light, and ventilation or enclosure, provide accessible means for conservators to exert influence on the rate of degradation. There is also evidence that storage type and material can influence the emission rate. Intrinsic factors of the

plastic formulation also play a significant role, including the concentration, chemical, and physical properties of the plasticiser. For example, short-chain phthalates (e.g. dimethyl phthalate and diethyl phthalate) have vapour pressures four orders of magnitude greater than longer chain analogues such as di(2-ethylhexyl) phthalate (DEHP) [48].

Table 1 Factors affecting migration rate

Extrinsic factors (environmental)	***Intrinsic factors (material dependent)***
• Temperature • Relative humidity • Volume of surrounding air and airflow rate • Light exposure • Storage material and air quality	• Plasticiser concentration • Plasticiser properties (e.g. volatility) • Sample thickness and surface area

Temperature

Evaporation-controlled rates and gas-phase concentrations increase with temperature, a trend observed in multiple studies of phthalate emissions [56–59]. Increasing the temperature also leads to a larger solid diffusion coefficient and thus a faster diffusion rate, as described by an exponential Arrhenius type relationship; $D = D_0 \exp\left(-\frac{E_a}{\mathrm{RT}}\right)$. Deng has proposed a modified equation to account for the temperature dependence of the diffusion coefficient for VOCs in porous materials; $D = B_1 \exp\left(\frac{B_2}{\mathrm{T}}\right)$. Where B1 and B2 are constants for a specific VOC/material pair [60].

Storage at a low temperature is regarded as a constructive action for plastics conservation, as it reduces the rate of both mass transfer processes. However, lowering the temperature has induced additive bloom in at least one conservation treatment; lubricant bloom appeared on PVC dolls stored at a yearly average temperature of 11–12°C over ten years [61]. Phthalate and citrate plasticisers were identified in a cohort of the dolls by ATR-FTIR spectroscopy, although GC-MS analysis of the bloom showed stearyl alcohol as the dominant component. Bloom reappeared within six months of cleaning and a return to the same cool conditions. Despite the reappearance, objects were returned to cool storage to retain high plasticiser levels, as plasticiser loss was judged more likely to cause long-term stability issues compared to the migration of the lower concentration moulding lubricant.

Relevance for ageing studies

The Arrhenius relationship relating temperature and the diffusion rate constant is the basis of accelerated ageing studies. Thermal ageing accelerates the rate of the degradation processes which occur at lower use temperatures (e.g. room/storage temperature in heritage contexts) to ensure the chemical and physical changes are measurable over a shorter period than the years/decades-long natural ageing process. Accelerated ageing is used in the conservation community to understand long-term ageing behaviour under controlled environmental conditions (typically temperature and relative humidity) [62–64]. However, some caveats apply; the polymer, degradation mechanism and rate-limiting step should remain unchanged at both temperatures; a change in the slope of an Arrhenius plot (log(measured variable) vs 1/T) occurs when the rate-limiting step changes [44,65,66]. If so, diffusion-controlled migration behaviour initiated by a high ageing temperature will not be representative of an evaporation-controlled system at room temperature. Wei et al. collated examples

of plasticiser loss studied by thermal ageing and found that most evaporation-controlled regimes generally become diffusion-controlled around 100 °C [45].

While Wei's critical temperature range is useful to consider when conducting ageing experiments on specific formulations, it cannot be considered alone. The importance of other environmental parameters is demonstrated by Shashoua's accelerated ageing of 30-year-old DEHP-plasticised PVC at 70°C [67]. Ageing in a sealed container led to evaporation-controlled migration, but the removal of the enclosure enhanced the evaporation rate so that diffusion became rate-limiting. Indeed, ageing environments are not always able to replicate natural conditions; therefore, the potential for influence by other environmental factors is discussed below.

Relative Humidity

The effect of humidity is highly dependent on the formulation. For evaporation-controlled regimes, two studies of 20 wt.% DEHP/PVC samples at 100 °C have suggested that the emission rate was not affected by humidity changes [12,13]. An accelerated ageing study for CA thin films also suggested that plasticiser loss is independent of relative humidity between 30-70% [68]. However, the opposite was recently reported for thicker phthalate plasticised CA samples by Kemper et al. [69].

To date, no study has conclusively reported if relative humidity, deacetylation, and plasticiser migration are related in CA degradation. Hydrolysis of phthalate esters is also known in humid conditions on surfaces and, under non-neutral pHs, has been postulated to cause the formation of phthalic acid crystals. However, no case studies are available [70,71]. The water contents within the object and the air may also have different effects, which makes a full assessment challenging; for example, surface

sorption of SVOCs is known to be affected by relative humidity changes in some cases [54].

Ventilation

In chamber studies approximating a sealed enclosure, SVOC emission from the material phase reaches a steady-state equilibrium over time. In chamber studies more closely representing indoor environments, the impact of the air exchange rate (AER) or ventilation rate is more challenging to study. As noted by Rackes et al., 'mass transfer from a material surface-air interface to the bulk room air depends on the air concentration, which in turn depends on the AER' [72].

For evaporation-controlled systems, the emission rate from a material is governed by the mass transfer coefficient, surface area, and the difference in concentration between the surrounding air (C_g) and the air adjacent to the material's surface (y_0) or $ER = h_m A(y_0 - C_g)$. Theoretically, increasing the air flow rate will reduce the gas-phase concentration (C_g) by dilution. Little et al. noted that AER has only a small impact on the air speed over a surface, suggesting y_0 is not significantly affected by ventilation rate [73]. This combination creates a greater concentration gradient between the source and surrounding air which increases the driving force for emission as ventilation and the air exchange rate increases. Additionally, Liang et al. suggested the convective mass transfer coefficient, h_m, was increased by a higher air velocity above an emission source [74]. These findings support the experimental work of Shashoua and others, where a greater loss was measured over the same period when ventilation was enhanced [40,67,75]. Ekelund et al. also observed that the loss rate of DEHP increases linearly with gas flow rate before reaching a limiting flow rate (75 ml min^{-1}), beyond which no effect was observed [76].

In non-steady state environments (e.g. real environments such as open shelf storage), the precise effects of ventilation are challenging to quantify. However, higher emission rates would be expected versus stagnant environments. For CA, the relative rates of polymer deacetylation and plasticiser loss are unknown and no method which enables simultaneous measurement has been published; therefore, the effectiveness of ventilated containers has been questioned [34].

As enclosure is not theorised to have any adverse effect on polymer degradation for PVC, Royaux has proposed wrapping PVC objects [41]. Furthermore, an enclosure can minimise the amount of airborne particles and dust in contact with an object and protect other objects in its proximity [77]. Some gas-phase SVOCs can sorb to (and desorb from) airborne particulate matter and settled dust present in the surrounding environment, a process called 'dynamic partitioning' [78–80]. A study of DEHP emission from vinyl flooring found that the emission rate was enhanced when airborne particles were introduced [81]. One hypothesis is that the emission rate is driven by a more significant concentration difference (y_0-C_g), owing to a reduced gas-phase SVOC concentration when partitioning occurs.

Light

The effect of light exposure on plastics is well studied; UV exposure is commonly linked to photo-oxidative discolouration of plastics, for example, causing the yellowing commonly observed with PVC and attributed to a radical dehydrochlorination process. A few studies have considered the effect of different plasticisers on samples exposed to UV wavelengths, including those found in sunlight.

Lee et al. compared DOP, DOA and TOTM plasticisers in TiO_2-PVC samples aged under UV-A light (340 nm, 0.76 W m^{-2}) for four weeks. The DOA plasticised sample

lost 4% by weight versus <1% for TOTM and DOP. Whereas a surface colour change (dE) was barely measured with DOA, DOP and TOTM samples visibly yellowed, and TOTM was exuded at the surface [82]. It is reasonable to attribute greater weight loss and lack of visible accumulation for DOA to it's volatility.

However, the difference in yellowing behaviour suggests a dependence on plasticiser type versus migration tendency. Biggin et al. similarly observed different extents of dehydrochlorination when DOP and TOTM plasticised samples were exposed to a variety of wavelengths, including solar irradiation outdoors for 1 year. Biggin proposed that PVC dehydrochlorination was enhanced when peroxide radicals of TOTM and DOP formed and transferred to the PVC chain under solar irradiation. The greater dehydrochlorination observed with the TOTM sample was attributed to it's broader adsorption range versus DOP [83]. Hollande et al. also proposed that the discolouration of DOP itself under irradiation contributed to the overall yellowing process [84].

Conversely, but over a much shorter exposure time of 5 hours, Hankett et al. demonstrated that whereas molecular changes to DEHP occur with short-wave UV (254 nm), no molecular changes were observed at the longer-wavelength UV (365 nm) more representative of daylight [85]. Under shortwave irradiation, cleavage of the ester group was evident from production of the mono-ester (MEHP) and phthalic acid.

The experimental variations between these studies including exposure time, power, and sample formulation make comparison challenging, but evidently the nature of the plasticiser is known to affect the dehydrochlorination process in PVC.

Storage material

Both VOCs and SVOCs will also rapidly partition from the gas phase onto surfaces at room temperature in indoor environments [86]. Indoor surfaces such as glass, painted surfaces, plaster, wood, and plastics can host reservoirs of SVOCs; by adsorption onto the surface or absorption into the material [58,74,87]. A study by Wu et al. measured similar phthalate partition coefficients across non-absorbing materials (glass, stainless steel, and acrylic), which suggests partitioning can also occur into thin films of organic grime on a surface independent of the surface's chemical or physical properties [88]. Once again, partitioning to adjacent surfaces can enhance emission rates from the source.

In the context of heritage conservation, potential sink materials include adsorbents, packing materials, and even different materials found in composite objects. Sink behaviour explains Shashoua's observation of a greater DEHP migration rate from PVC during aging experiments where silica, Ageless© oxygen absorber, and activated charcoal absorbents were included in the aging chamber. The same trend was observed for samples aged in an LDPE bag versus the sealed glass container [67].

For mixed material objects, partitioning to adjacent components could occur, including other plastics. Curran et al. have begun this work by demonstrating the effect of VOCs emitted from plastics on paper [89]. Other examples highlight the potential for cross migration between different plastics; DEHP migrated from a PVC object and plasticised the LDPE tray it was stored in, causing irreversible damage [70]. Royaux et al. recently observed phthalate and azelate plasticiser migration from a PVC object through an LDPE wrap during artificial ageing in a closed container but found no significant difference in migration rate versus the unwrapped reference material. Ageing in contact with a PET product (Melinex®) appeared to induce the hydrolysis of

dioctyl phthalate to phthalic acid. However, it is unknown if similar behaviour would be replicated under less extreme museum standard 70 F & 50% RH environmental conditions [42].

Examples of plasticiser migration into other plastics provides evidence that some plasticised PVCs should not be stored with rigid PVC, polystyrene, ABS, and polycarbonate plastics. Damage observed included solvation, and induced environmental stress cracking (ESC) [90–93]. Lactus et al. suggested 'microvoids' and surface defects on glassy thermoplastics' surfaces can lead to microscopic crazing and cracks on contact with small penetrant molecules [94]. Comparison between plasticisers suggests there is a difference in behaviour, most notably between polymeric and monomeric plasticisers where there was no evidence of polymeric plasticisers causing ESC. ESBO also performed well in tests on mechanically strained plastics, and TOTM is considered a good choice for ESC resistance, before DOTP, with aliphatic alternative plasticisers causing ESC the quickest [95–98].

Material surface area & thickness

Material thickness and surface area are import parameters for SVOC emission models. For surface area, the larger the exposed area of an object, the greater the emission rate [50]. As the diffusion rate is dependent on diffusion distance, the material thickness will have a significant role in the loss rate in diffusion-controlled emissions. It follows that loss from thin samples is more likely to be evaporation controlled. Uniformity cannot be assumed in a plastic object as thickness variations are possible from manufacture; for example, variable shrinkage is common in amorphous and semi-crystalline polymers used in injection moulding. The longer-term creep behaviour of plastics under load can also cause significant non-uniform deformation [99].

Plasticiser characteristics

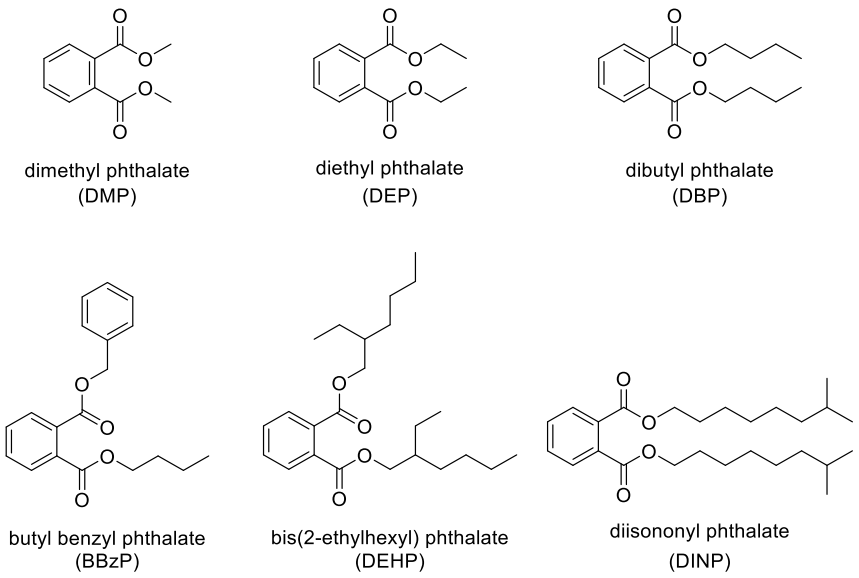

Figure 8: Examples of phthalate esters used as plasticisers. DINP is represented here as a singular species, however, it is formed from an isomeric C9 alcohol mixture.

No covalent bond exists between polymers and external plasticisers. Their retention within the matrix relies on intermolecular interactions [100] between the plasticiser and polymer to disrupt the network of polymer chains, increases polymer chain mobility, and decreases the polymer's glass transition temperature.

The presence of plasticisers such as dimethyl, diethyl and dibutyl phthalate plasticisers can be a sign of early plastics, as they were key to the development of CA and PVC in the 1920s and 1930s [55,93]. A variety of other dicarboxylic acid scaffolds were trialled and continue to be explored, but short chain phthalates dominated the plasticiser market, before higher molecular weight phthalates derived from C_{4+} alcohols were introduced for PVC by the 1950s [94–96]. Figure 9 shows some 'alternative' non-phthalate plasticisers. Many have been in production since at least

the 1970s, but the market share for non-phthalate plasticisers has grown following regulatory controls on the use of phthalates in 2006 [101,102]. Other classes include polymeric plasticisers (typically polyesters) which give lower migration rates and volatility at the expense of higher glass transition temperatures, hydrolytic stability, and a material which is more challenging to process [98,99].

Some plasticisers have additional roles when included in a plastic formulation. For example, ESBO is often used as a 'secondary plasticiser' in combination with a phthalate or alternative plasticiser. It is a composite epoxide-containing oil which also serves as a stabiliser due to its sequestration of evolved hydrochloric acid [103]. Similarly, phosphate esters can also act as flame retardants in PVC, PU, and historically, CA.

Phosphates offer the clearest example of a specific plasticiser influencing degradation behaviour as the presence of triphenyl phosphate (TPP) appears to induce significant degradation and damage in some CA objects [17]. Two studies have proposed that recrystallisation of TPP occurs within historic CA objects. TPP was historically used as a phthalate co-plasticiser and was solubilised by DEP. Therefore, McGath et al. suggested that the crystallisation of TPP occurs as phthalate plasticisers migrate away over time [100]. It is unclear if migration occurs for TPP, but mapping of phosphorous signals suggested aggregation of phosphorus-rich species. More recently, a study of 20th century Chinese CA microfilm linked deacetylation of the film substrate to the migration of TPP and the formation of 'microbubbles'. The study also found increased hydrophilicity in areas of the film affected by microbubble formation [101]. In other studies, TPP's hydrolysis products of phenol and diphenyl phosphate have been detected, suggesting plasticiser and migration of by-products can also occur [5,102].

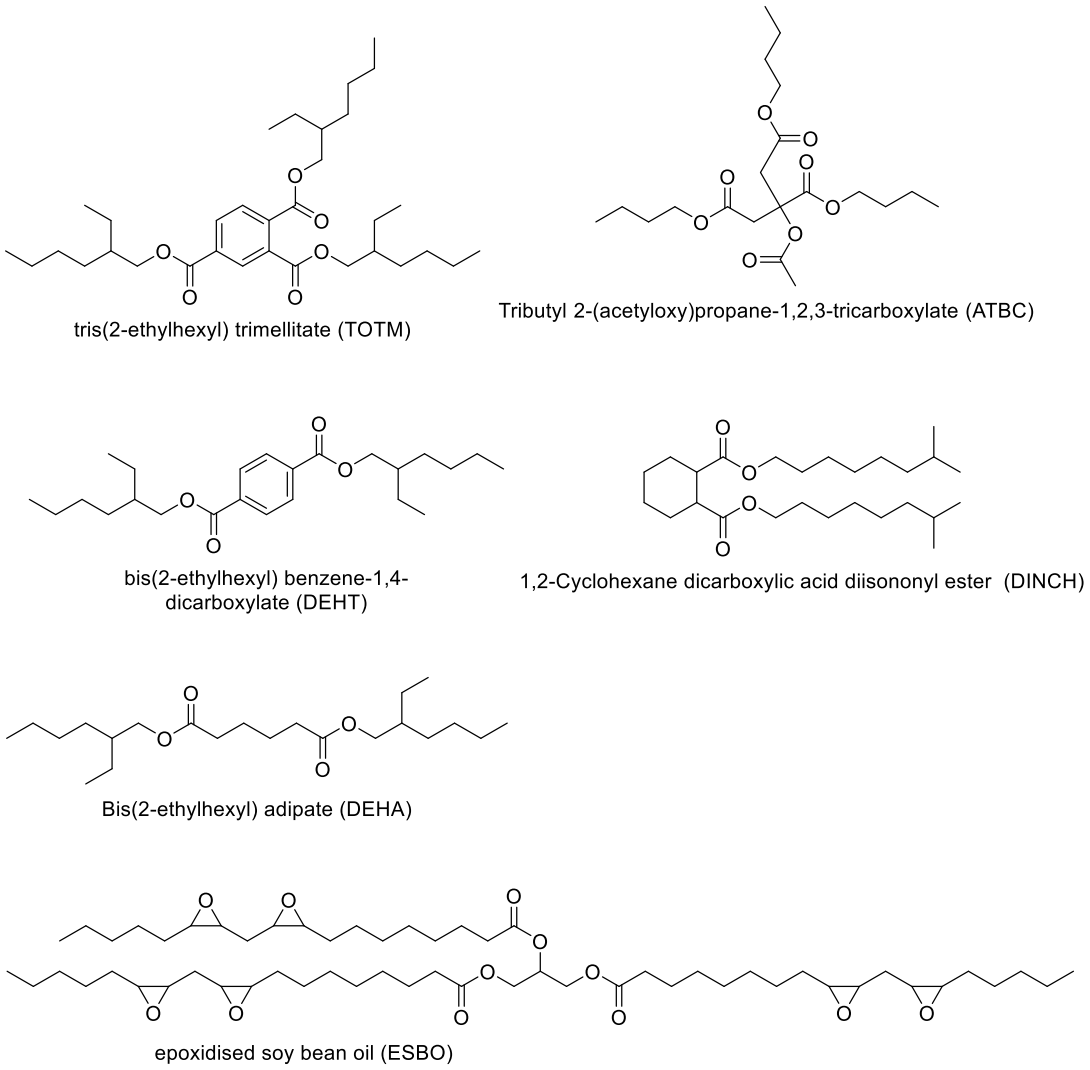

Figure 9: Examples of alternative 'non-phthalate' plasticisers (TOTM, ATBC, DOTP, DINCH, DEHA, and ESBO).

Under the same environmental conditions, plasticisers can differ by chemical reactivity (hydrolytic, photolytic) but their physical properties also influence migration. However, as recently summarised by Li et al., comparing the migration tendencies of different plasticisers is complicated by the variety of experimental methods used across multiple literature studies, including the extraction medium (air, solid, solvents) and temperature used [104].

Therefore, Li et al. used molecular modelling of PVC with multiple plasticisers, to examine the effect of plasticiser properties such as alkyl chain length, and chain branching on the heat of mixing (as a measure of thermodynamic compatibility), mean square displacement distance (for molecular mobility) and Youngs Modulus (to quantify 'the [efficiency] improvement brought by a given plasticiser dosage.') The overall conclusion is that molecular mobility and therefore diffusivity is dominated by kinetic factors including the complex relaxation dynamics of plasticiser molecules. In general, Li et al.'s results are supported by experimental studies. However, to translate mobility to a diffusion rate, modelling over much longer timescales would be needed, and the authors caution that 'although it seems plausible to expect the [displacement distance] at those scales to correlate with the ultimate diffusion rate, the possibility of a later crossover cannot be ruled out'.

In terms of mobility of the plasticiser molecule, Li et al.'s model suggested increased branching reduces diffusivity (e.g. DEHP vs DIOP), para-substituted DOTP shows reduced diffusivity vs ortho-substituted DEHP, and 'adding a third leg substantially improves migration resistance' in the case of TOTM. Among the non-aromatic plasticiser, citrates were found to have a thermodynamic disadvantage as the quaternary carbon 'severely restricts the molecule's configurational freedom'. Li et al. argue this reduces the citrate's ability to interact strongly with the PVC and similarly means slow molecular mobility despite faster rotation of leg groups. Aliphatic esters such as adipates and sebacates are considered more highly mobile due to confirmational flexibility compared to the aromatic 'torso' of DEHP.

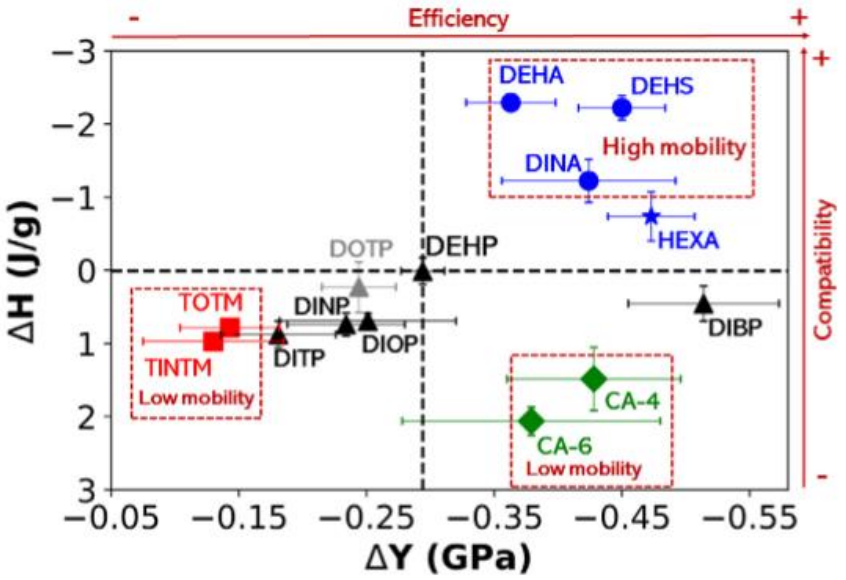

Fig. 6. Scatter plots of plasticizer performance in the ΔH–ΔY space. Error bars in ΔY show the uncertainty in the Young's modulus (i.e., the same as the smaller error bars in Fig. 4). Text annotations "high mobility" and "low mobility" are in reference to comparison with DEHP.

Figure 10: Clustering of plasticisers by modelled values for heat of mixing, and young modulus. From Li et al.[104].

An object's plasticiser concentration will also influence the rate of loss; the diffusion rate is more correctly described by a concentration-dependent diffusion coefficient and is explained more thoroughly elsewhere [105–107].

Finally, it has been claimed that the incorporation of inorganic additives including nanoparticles of SiO2 and to a lesser extent $CaCO_3$ may reduce the migration rate of plasticisers; a finding which is attributed to the large surface area of the nanoparticles and their ability to interact with the plasticiser [108].

1.4 Conservation cleaning methods

Plasticiser migration can result in visible deposits or accretions on an object's surface. However, multiple studies have produced evidence of scratch formation and residue

contamination due to the action of cleaning, which conflicts with the need to preserve the aesthetic value of an object [109,110]. The balance between conservation and inducing further damage was comprehensively studied during the POPART study; five types of plastic were assessed for changes in their appearance, including after dry and wet cleaning with a range of aqueous solutions and organic solvents [11]. The study confirmed that wet cleaning products lubricate surface deposits and reduce scratching visible compared to dry cleaning, but damage to surfaces can occur with both organic and aqueous solutions. Microfiber cloths were also shown to minimise scratching compared to cotton cloths. Further studies have reinforced the benefit of using microfiber cloth over cotton due to its ability to ‘lift’ dirt versus redeposit it [111].

However, Fricker's study of rigid polystyrene (PS) using SEM & AFM found scratches 'were present on all substrates, regardless of the cleaning agent under investigation'. The POPART study concluded that scratching became noticeable only when 3-10% of the surface was scratched.

POPART flow charts were produced to direct conservators to appropriate cleaning solutions and carrier material for each plastic type (Table 2). For all plastics, a proprietary alcohol alkoxylate surfactant 'Dehypon 54' was recommended to remove oily deposits. The efficacy of a cleaning solution is also judged by the residue left on the cleaned surface; Fricker also noted that 'a monolayer of surfactant is still present on the surface after multiple rinses' for the anionic and non-ionic aqueous surfactant solutions trialed with PS [110,112].

Table 2: Recommended cleaning solutions for removing oily and waxy deposits from various plastics [11].

Plastic-type	**Recommended cleaning solutions**		**Recommended cleaning material**	**Ref.**
	Aqueous	Solvent		
CA	1 w/w% Dehypon LS 45	Ethanol, IPA	Cotton, microfibre	[11]
HDPE	1 w/w% Dehypon LS 45	Ethanol, IPA	Cotton, microfibre	
HIPS	1 w/w% Dehypon LS 45	Ethanol, IPA	Cotton, microfibre	
PMMA	1 w/w% Dehypon LS 45	Ethanol, Xylene	Cotton, microfibre	
Plasticised PVC	1 w/w% Dehypon LS 45	Ethanol, IPA	Cotton, microfibre	
Plasticised PVC	0.5% Orvus Paste (aq)	-	Hydrogel (Nanorestore Peggy)	[113]
Plasticised PVC	Microemulsion solution - effective at removing assumed plasticiser residue and adhered dirt.	Non-ionic surfactant, a non-polar silicone solvent, and deionized water.	Cotton swab	[114]

Alcoholic solvents were recommended for the removal of waxy substances but using organic solvents on plastics risks solvating colourants leading to discolouration and softening. Environmental stress cracking can also be induced by localised fluid absorption [115].

Polymeric gels loaded with aqueous solutions (hydrogel) or organic solvents (‘organogels’) have been used to 'control solvent diffusion', 'permit solvent penetration into the surface, while minimising the risk of material dissolution', and reduce 'mechanical damage during treatment' in two studies of PMMA cleaning [111,116]. Gels were found to offer advantages versus traditional swabbing, including ease of application and removal, localised application, and minimal abrasion of the surface, but others such as Angelova et al. have noted the challenges in applying and removing spreadable gels, where mechanical clearance could induce surface damage [111].

In a later study of additional gels, the authors reinforced that whilst there was evidence that gelation of solvents moderated their activity, applying organic solvent-loaded gels can also "increase solvent diffusion [into the surface] and contact time, aggravating the condition of the sample" [117]. Additionally, when applied with a swab, evaporation of the solvent from the surface can compete with diffusion through the surface, whereas in the gelled form, the evaporative loss is minimised, and greater action on the plastic surface may result.

1.4.1 Surface cleaning of plasticised PVC objects

Cleaning swabs and hydrogels loaded with aqueous solutions, organic solvents, and microemulsion surfactant solutions have been trialled for their ability to remove artificial carbonaceous and sebum-based soils [11,109,118–120].

Shaushoa observed scratches across 5-10% of the surface area from cotton or microfibre cloths at 5x optical magnification, whereas Munoz Morales et al. found a marginal benefit using a polyester/polyamide blend cloth versus cotton [113,119]. Munoz Morales et al. also measured a 7% increase in plasticiser surface concentration after dry cleaning, but given the heterogeneity of plasticiser distribution and therefore

the ability to measure loss by infrared spectroscopy, the significance of the result is unknown.

Table 3: Cleaning solutions recommended for plasticized PVC

Study & findings	Recommended Cleaning Solution	Carrier	Reference
PoPART	Isopropanol	Cotton swab	[11]
Hydrogel cleaning - effective at removing carbonaceous soil, plasticiser assumed unchanged	0.5% Orvus Paste	Hydrogel (Nanorestore Peggy)	[113]
Microemulsion solution - effective at removing assumed plasticiser residue and adhered dirt.	Non-ionic surfactant, a non-polar silicone solvent, and deionized water.	Cotton swab	[114]

1.5 Qualitative and quantitative methods for the analysis of plasticised objects

Analytical techniques suitable for use in heritage applications are typically assessed in terms of their destructive and invasive sampling requirements. However, the analysis of additives is often simplified by their removal from the host polymer matrix to avoid interference from the polymer. Therefore, to date, methods have generally involved destructive sampling and matrix separation by solvent extraction before spectroscopy, chromatography, or spectrometry. Increasingly non-destructive surface analysis and minimally invasive passive sampling methods have been employed.

Bernard et al. reviewed analysis techniques for PVC additives in 2014 [121], and sample preparation methods, including solvent extraction were evaluated for CA [122],

and in multiple studies for PVC [123–127]. Therefore, the publications highlighted here are either published after 2014, have relevance to heritage studies where sampling ethics are considered, or are of relevance to the work in this thesis.

Table 4 shows the typical amounts of samples required for common techniques. Table 5 gives examples of additive analyses undertaken on historic plastics.

Table 4: Analytical techniques used for plasticiser analysis.

Method	**Mass of sample required**
GC-MS	Dependent on sampling procedure: 1 ug (pyrolysis), ug - mg scale for liquid injection.
TLC	1 ug
NMR Spectroscopy	1-5 mg
Benchtop NMR Spectroscopy	>100 mg
Infrared Spectroscopy	1 mg

.

Table 5: Plasticiser identification methods used in conservation literature

Reference	Method	Amount	Notes	Quantitative /Qualitative	Polymer	Plasticisers identified
[128]	Direct inlet Py-GC/M.S.	Estimated at a 'few ug'	Specialist thermal separation probe required to pyrolyze sample	Qualitative	CA	Triacetin Dimethyl phthalate 2,2,4-trimethyl-1,3-pentanediol diisobutyrate Diethyl phthalate N-ethyl toluene sulphonamide N,N-diethyl toluene sulphonamide N-ethyl toluene sulphonamide N,N -diethyl toluene sulphonamide Dibutyl phthalate Dimethoxyethyl phthalate Triphenyl phosphate Diisooctyl phthalate Tricresyl phosphate
[129]	NMR	1 cm^2 area	Methanol was applied to the surface, and 'leachate' was collected. Shown to find more additives vs GC-MS and u-FTIR. Referred to as 'non-invasive'.	Qualitative	CA, CN	N-ethyl-o-toluene-sulfonamide N-ethyl-p-toluene-sulfonamide Triphenyl phosphate Dimethyl phthalate Camphor Trace phthalates Phthalates o-toluenesulfonamide p-toluenesulfonamide Diethyl phthalate

[130]	FT-Raman	Direct analysis of surface or deposits	TPP in a sample was associated with surface deposits	Qualitative	CA	Triphenyl phosphate Diethyl phthalate
[131]	FTIR, GC-MS	Surface was scraped to remove deposits	Bloom is characterized as a fatty alcohol, phthalate and citrate plasticiser suspected by FTIR. GC-MS was required to confirm stearyl alcohol, stearic acid, DINP, and ATBC.	Qualitative	PVC	Diisononyl phthalate Acetyl tributyl citrate Stearyl alcohol Stearic acid
[132]	FTIR	Liquid and crystals removed	Deposits or liquid exudates sampled from space suit tubing. DEHP stated, but spectra are known to be similar to other phthalates by visual inspection only.	Qualitative	PVC	Di(2-ethylhexyl) phthalate
[133]	GC-MS and Py-GC-MS	Py-GC-MS - unknown size. GC-MS liquid exudate (1-2 ul)	All analytes were identified using both py-GC-MS and GC-MS; phthalates are typically minor components by intensity.	Qualitative	PVC	Poly(1,3-butylene adipate) Poly(1,2-propylene adipate) Di(2-ethylhexyl) phthalate Dibutyl phthalate Diethyl phthalate

1.5.1 Environment sampling (non-invasive)

Environmental sampling can be advantageous when no visible signs of additive migration are present, including under diffusion-controlled loss regimes. Due to the volatile nature of some species emitted from degrading plastics, passive sampling of the environment has previously been used to monitor historic plastics by SPME-GC-MS[134], and thermal desorption (TD-GC-MS) [135]. At its most simple, passive colormetric detection strips are used to monitor acetic acid evolution from CA [136].

Kearney et al. showed the utility of SPME fibres for the sorption of phthalates emitted from a visibly degraded CA object where it was not possible to sample via contact [137]. Qualitative analysis by GC-MS was possible, but the variability of measurements in non-controlled museum environments discounts their use in quantitative studies [138].

GC-MS analysis of analytes captured in passive samplers (sorbent tubes, activated charcoal disks, SPME fibres) from sealed chamber emission studies have also been used for measurement of key parameters (y_0 and K_m) to model semi-volatile phthalate migration from vinyl flooring at 25 °C [139]. The models focus on emissions from flat materials rather than the complex geometries found in heritage objects. However, a similar approach could be used to research emissions rates for samples of relevance to conservation. For example, active sampling in a stainless-steel chamber using pumped air and TENAX sorbent tubes followed by TD-GC-MS has been successfully used to detect and measure the concentration of volatile naphthalene pesticide residues from intact collection objects [140].

1.5.2 Surface sampling (non/minimally-invasive)

Deposits formed under evaporation-controlled conditions are ideal candidates for collection with a scalpel or swab because there can be enough of the deposit to observe [141]. Depending on the amount of sample that can be collected from a surface, $^{1}H/^{13}C/^{31}P$ NMR, Infrared, and Raman spectroscopy have been used in heritage settings [23,142–145].

Non-visible samples can also be collected by swab sampling, a common method used in forensic and environmental analysis [146–150]. Trace amounts of phthalate and alternative plasticisers were sampled from PVC surfaces in two studies before solvent extracts from the swabs were analysed by GC-MS [151,152]. As summarized in Table 6, there were significant differences in swab size, method, and solvent loading, and the samples were also different in their composition.

Table 6: Experimental details and results from Xie and Clausen's plasticiser sampling studies.

	Clausen et al. [152]	**Xie et al.** [151]
Experiment features		
Swab properties	Dry and solvent wetted Effective surface area = 4.9 cm^2 (single side of cotton cloth)	Dry and solvent wetted Effective surface area = 116 cm^2 (double sided cloth)
Solvent loading	Methanol (0.15 mL)	Isopropanol (3 mL)
Sampled surface area	66 cm^2	Variable; 155-428 cm^2
Extraction method	Accelerated solvent extraction into methanol	Soxhlet extraction into dichloromethane
Sample features		
Sample description	Four flooring samples	Seven 3D toys and six thin PVC backpack fabrics

PVC sample concentration	DIBP (6 wt.%), DnBP (15 wt.%), DEHP (10-24 wt.%), DINCH (31 wt.%)	DOTP (8 – 21 wt.%), DINCH (23 wt.%), ATBC (0.2 -1.7%) with trace DIBP, DnBP, DEHP, DEHA (<0.1 wt.%)
Equivalent surface concentrations measured*		
Dry sampling (ng/cm^2)	240-670	33-304
Wet sampling (ng/cm^2)	610-1520	656-20397

**Assumed complete extraction from swab into the solvent*

Assuming complete extraction into solvent, microgram amounts per squared centimeter were transferred to alcohol-wetted swabs in both studies, whereas the amount transferred to dry swabs was variable. Xie et al. found dry transferred masses were an order of magnitude lower and showed a high relative standard deviation (RSD) across repeats, which were not improved by the efforts of Clausen et al. to control pressure or contact time with a sampling apparatus.

Xie et al. found a positive correlation between mass transfer to wet wipes and mass content of DOTP in samples, but there was limited data for other plasticisers to conclude. Conversely, Clausen et al. found that surface concentration was not correlated to the bulk sample concentration. Table 7 shows the extract concentrations which can be achieved. The method developed by Xie et al. produced the highest concentration extracts which would be suitable for the analysis techniques shown in Table 4.

Table 7: Extract concentrations calculated from supplementary information provided by Clausen et. al.

Study	Sample	Mass extracted from the solvent-wetted cloth per unit area sampled (ug/cm^2)	Absolute mass transferred to sample cloth (ug)	Extract concentrations* (ug/ul)
Clausen et al.	DEHP - Blue PVC	1.52	100.32	0.02
	DEHP - Red PVC	1.64	108.24	0.02
	DiBP - Red PVC	0.61	40.26	0.01
	DnBP - Red PVC	1.03	67.98	0.01
	DINCH - White PVC	8.16	538.56	0.10
Xie et al.	DINCH - WA-t1	26.9 ± 10.5	4283.3	4.3
	DOTP-WA-t2	1.1 ± 0.3	148.2	0.2
	DOTP-TA-t1	1.5 ± 0.6	150.7	0.2
	DOTP-DO-t1	3.8 ± 1.0	600.4	0.6
	DOTP-DO-t2	1.7 ± 0.7	430.4	0.4
	DOTP-BK-t	1.1 ± 0.3	484.9	0.5

*Calculation assumed complete extraction into solvent. Methanol volume = 5.15 mL (Clausen et al). DCM volume assumed 1 mL (quoted range 0.5 - 1 mL, Xie et al.).

1.5.3 Extractive sampling (destructive)

Extensive literature has investigated the optimal extraction method for PVC additives from a variety of matrices [127]. Dissolution of the polymer followed by antisolvent precipitation is frequently used for PVC, requiring dissolution in THF and precipitation by methanol, hexane, or acetonitrile, although co-precipitation of additives, including polyadipate plasticisers, is known [153]. Alternatively, extraction of phthalates without polymer dissolution can be achieved by immersion at room temperature, Soxhlet, ultrasonic or microwave-assisted extraction with chloroform, hexane, ethyl acetate, acetone, methanol, or their mixtures [142,154–156].

Table 8 summarises a study of plasticiser extraction from PVC tubing. Room temperature extraction with hexane, ethyl acetate, or chloroform gave the highest yields versus polymer dissolution or Soxhlet extraction for all plasticisers [123]. Chloroform was the most efficient extraction solvent at room temperature with yields of >80% within 15 mins and a 500-fold excess (mL/g) of solvent to PVC.

Due to the limited solubility of CA, the triacetate form of cellulose is only soluble in dimethyl sulfoxide, and no antisolvent precipitation method has been established. Instead, polymer dissolution with dimethyl sulfoxide or additive extraction into ethanol or methanol is favoured [157]. To avoid volatilisation of small molecule additives if the solution is heated, slow extractions at room temperature are favoured [158].

Table 8: Extraction yield from PVC medical tubing, reproduced from [123]*.*

Extraction yield (% ± SD)							
		Soxhlet (250 mL, 24 h)		**Polymer dissolution**	**Solvent extraction (50 mL, 24 h)**		
Sample ID	**Plasticiser**	**Diethyl ether**	**Ethyl acetate**	**Tetrahydrofuran**	**Ethyl acetate**	**Hexane**	**Chloroform**
R4	DEHP	75.2 ± 3.2	96.2 ± 1.1	54.4 ± 3	99.4 ± 1.4	96.6 ± 1.7	98.5 ± 2.1
R3	DOTP	57.1 ± 4.2	80.0 ± 3.11.8	48.4 ± 2.8	94.6 ± 6.3	67.9 ± 2.8	95.5 ± 4.2
R1	TOTM	76.4 ± 3.5	87.6 ± 3.11.2	53.3 ± 3.1	85.3 ± 6.3	90	100.0 ± 3.3
R2	DINCH	78.8 ± 1.4	69.9 ± 2.2	36.6 ± 4.4	98.9 ± 1.9	76.7 ± 1.9	91.6 ± 2.3

1.5.4 Gas Chromatography and Mass Spectrometry

Multiple studies have optimised GC-MS methods for the analysis of additives. Aside from solvent extraction, thermal methods, such as pyrolysis or thermal gravimetry (e.g. EGA-MS, Py-GC-MS, TD-GC-MS) are also used to separate an additive from the sample matrix before GC-MS analysis [16,65,68,141,159]. Thermal protocols typically use much lower sample amounts (micrograms) versus the milligram amounts which can be required for solvent extraction methods.

The most comprehensive GC-MS method includes non-phthalate plasticisers but requires secondary derivatisation steps for the volatilisation and analysis of ESBO and polymeric plasticisers [160]. Figure 11 illustrates that chromatography cannot resolve the multiple low-intensity peaks of DINP, DIDP and DINCH, so identification relies on distinction by mass fragmentation. A continuous wavelength transformation post-processing method was also proposed as a method for DINP/DIDP peak resolution [161].

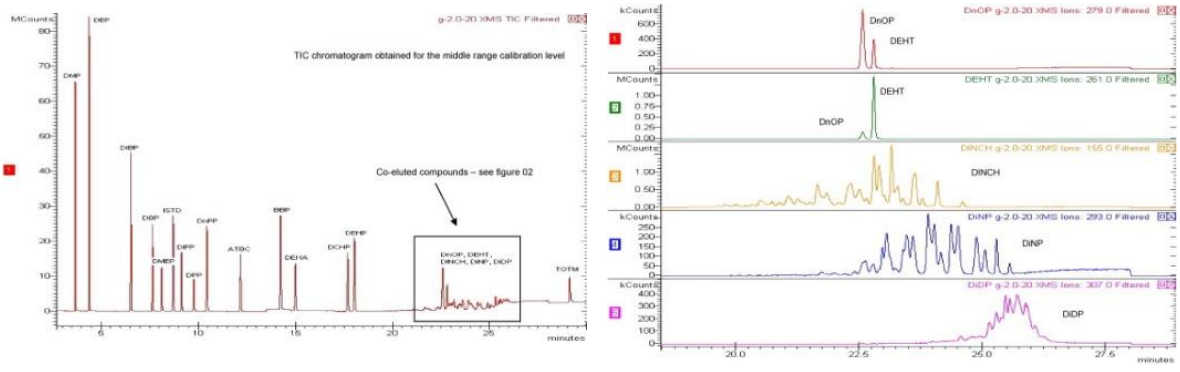

Figure 11: Coelution of higher molecular weight plasticisers, reproduced from Gimeno et. al.[162]

Ambient ionization techniques, such as DART-MS, can also be used for analysis by mass spectrometry without any prior sample preparation or chromatographic separation [163]. Sampling can be performed in a non-destructive, or minimally invasive manner as minute solid and/or liquid samples are placed at the ion source. Sampling can also be achieved through a localised solid-liquid extraction mechanism, such as DESI-MS, which allows charged solvent droplets to desorb and solvate analytes from a surface, including phthalates [164]. A similar approach has been demonstrated with a portable mass spectrometer and liquid micro-junction sampling pen, although the authors highlighted the risk of solvent-induced damage to the surface of valuable objects [165]. Identification relies on fragmentation patterns to distinguish the analyte, and it has been demonstrated to distinguish phthalate isomers although mixed analytes were more challenging to identify [166].

1.5.5 Thin Layer Chromatography

Thin layer chromatography (TLC) is commonly used in synthetic chemistry, but as more advanced chromatography instrumentation has developed and become cheaper, its use for qualitative analysis has declined. Sensitivity (limit of detection) to sample amount and type can also be limiting versus liquid or gas chromatography [167,168]. However, TLC offers a rapid, non-instrumental, and less costly method that works particularly well for routine analysis.

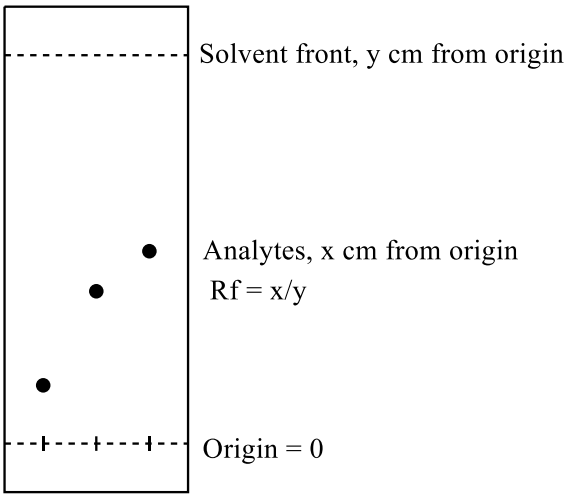

Figure 12: Exemplar TLC plate after elution

TLC is an ascending chromatography technique whereby a solid stationary phase and tailored mobile phase are used to separate the components of a mixture. Mobile phase selection can be guided by the eluotropic series, but there is no universal method to translate between different mobile or solid phases. The distance travelled (Rf) by an analyte relative to the solvent mobile phase is determined by polarity and can be considered characteristic for an analyte under the same conditions illustrated in Figure 12. However, many variables can influence the exact R_f value, including analyte loading, and the temperature and humidity of the environment. R_f ranges targeted between 0.2 – 0.8 can help to ensure baseline distinction and avoid analytes being lost in the solvent front. More nuanced experimental parameters such as spotting solvent can also influence the analytes spread and subsequent resolution.

Resolution by retention factors (R_f) of some homologous phthalates is also possible, and mixtures can be identified. TLC is, therefore, most effective when applied to a

sample with a limited set of expected or known analytes. However, known references should be run at the same time as unknown samples to improve the reliability of the interpretation.

Multiple studies from the 1950s to 1980s reported protocols to separate common plasticiser additives in PVC using paper [169], ion-exchange, and thin-layer chromatography with a range of stationary phases and elution solvents [170–176]. Table 9 illustrates solvent systems and visualization methods previously used for the analysis of additives on normal phase silica. The separation of homologues within adipate, sebacate, and phthalate classes is achievable with a non-polar hydrocarbon and polar ester or ketone solvent mix, although the isomeric and similar phthalates (e.g. DEHP, DINP, and DIDP) have not been resolved.

Table 9: Solvent systems previously used for plasticiser additive analysis on Silica G and quoted RFs

	Solvent system (v:v %)				
Analyte	**Dichloromethane (100)**	**Isooctane: Ethyl acetate (85:15)**	**Isooctane:Amyl acetate (85:15)**	**Hexane: Ethyl acetate (90:10)**	**Isooctane: Ethyl acetate (90:10)**
ATBC	-	-	-	-	0.53
DEHA	0.44,0.40	0.67,-	0.72	-	-
DBS	0.41,-	-	0.61	-	1
ESBO	-	-	-	-	0.09-0.92
DINCH	-	-	-	-	-
TOTM	-	-	-	-	-
DOTP	-	-	-	0.98	-
DEP	-,0.35	-,0.30	-	0.42	0.51
DBP	-,0.45	-,0.46	-	0.72	0.74
DEHP	-,0.65	-,0.66	-	-	1.14
DINP	-	-	-	0.93	1.01
DIDP	-,0.67	-,0.65	-	-	-
Visualisation	F254 plates, PMA. R_f are calculates relative to DBS.			UV light (254 nm)	0.005% Ultraphor in UV light (365 nm)
Citation	[173]			[175]	[172]

Visualisation of analytes

Table 10 shows common TLC visualization methods and reagents, known applications, hazards and references to other uses in the heritage sector. Plasticisers are hydrocarbon esters without additional functional groups, and there is no universal stain for the ester functional groups common to most additives. Instead, esters may be converted to another functional group for visualization, typically via an intermediate hydrolysis product [177,178].

PMA, resorcinol, vanillin, and Dragendorff reagents were previously used for phthalate visualization [171,173,174,179]. PMA, while simple, to prepare is relatively expensive and offers poor contrast for the visualization of spots. The Dragendorff stain is impractical and costly; it requires multiple reagents and steps to prepare. The resorcinol stain is also a three-step process, including a caustic hydroxide spray. Unlike the generality of the PMA and Dragendorff reagents, the condensation of resorcinol and the ester under acidic conditions was reported to distinguish (at >10 ug/spot) plasticiser class by colour; orange for phthalates, red for adipates, and yellow for sebacates [174]. Early qualitative colourimetric tests for diethyl phthalate in alcohol similarly relied on a reaction with resorcinol under acidic conditions to produce a fluorescein derivative [180]. A reaction with resorcinol is also understood to proceed under basic conditions but forms a non-fluorescent red product [181]. The reaction of resorcinol with various dicarboxylic acids has been similarly studied but has not been reported for esters aside from adipate and sebacate esters [182–184].

Two of the most simple TLC stains are vanillin and bromocresol green. Vanillin is prepared with a stoichiometric amount of sulfuric acid or hydrochloric acid, and produces a range of colours in response to various nucleophiles. Bromocresol green

(BCG) is a blue-yellow acid indicator dye, and is prepared with an excess of sodium hydroxide in ethanol.

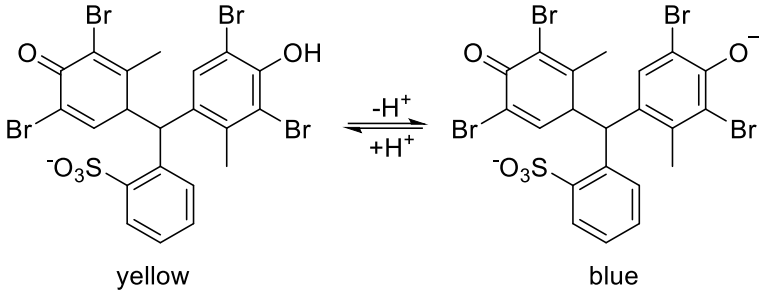

Figure 13: Bromocresol green, monoanionic yellow form under acidic conditions (left), dianionic blue form under basic conditions (right)

Figure 13 illustrates the generally accepted mechanism for BCG's yellow-blue transition where the di-anionic blue form is protonated on contact with acids with pKa <5 to form the mono-anionic yellow form of the dye. A BCG stain can be prepared from either the free acid with sodium hydroxide or the commercially available monosodium salt. The sodium salt form is used in 0.04% commercial blue indicator solution, prepared in industrial methylated spirits (5% methanol / 95% ethanol) without the need for additional sodium hydroxide [185].

BCG was previously used as a non-specific stain for short-chain phthalate esters (DMP, DEP, diallyl phthalate) separated by column chromatography in post-war explosives research when Ovenston described a green band evolving against a sky-blue background 10 minutes after staining, enhanced clarity was observed if the elution solvent was allowed to evaporate before the stain was applied [186].

Table 10: Common TLC visualization methods highlighting their preparation and ease of use.

Visualization method	**Preparation**	**Known applications** [187]	**Other**	**Hazards**	**Conservation sector use**
Short wave U.V. light	Illuminate with 254 nm UV lamp	Aromatics and conjugated systems act to quench the fluorescent indicator, showing dark spots on a fluorescent green background.	"F254" fluorescent indicator TLC plates required	Avoid eye and skin exposure to UVC light.	Used in spectroscopic imaging
Iodine stain	Expose to iodine crystals in a sealed container	Unsaturated functional groups including aromatics	Small amounts are required. Reversible by evaporation at room temperature.	Acute toxicity, irritant.	Recently proposed as a method to show organic

			Can stain background causing poor contrast.		soiling on PVC. [113]
Vanillin stain	Spray with 20 wt% vanillin in ethanol. Heat 80 °C – 10 mins. 2M sulfuric acid. Heat 110 °C – 30 mins.	Nucleophiles (alcohols, amines) and carboxyl (aldehyde, ketones) show various colours on a yellow background which progresses to purple over time (<1 hr)		Strong acid.	No uses known in the heritage sector
Bromocresol green (BCG)	Bromocresol green (sodium salt), ethanol solution *OR* Cholesterol derivatives	Carboxylic acids (pKa <5)	Commercially available.	Not a hazardous substance or mixture according to	Used in acetic acid detection strips [136]

	Bromocresol green (free acid), 0.1 M sodium hydroxide, ethanol.			Regulation (E.C.) No 1272/2008.	
Resorcinol	Spray with 20 wt% resorcinol in ethanol. Heat 150 °C. Spray with 2M sulfuric acid, heat 120 °C. Spray with 7M potassium hydroxide.	Plasticisers	Colours produced are variable if exact conditions are not met.	Strong acid and alkali. Highly caustic.	No uses known in the heritage sector

Phosphomolybdic acid (PMA)	PMA in water or ethanol.	General – green spots		Oxidizing agent.	No uses known in the heritage sector
Dragendorff	Multiple variations include a bismuth salt and Group 1 halide salt. E.g. acetic acid, ethyl acetate, sodium iodide, sodium tetraiodobismutate.	General – orange/yellow/red/brown spots	Commercially available, some require daily preparation.	Strong acid.	No uses known in the heritage sector

1.5.6 NMR spectroscopy

Given the interdisciplinary nature of this work, including chemistry, heritage science, and plastics conservation, NMR spectroscopy's fundamental theory is provided as background for all readers. Nuclear magnetic resonance (NMR) spectroscopy is a spectroscopic technique used to analyze molecules and macromolecules which possess nuclei with non-zero spins, i.e. they have an odd number of protons and/or neutrons. NMR spectroscopy measures the transition between quantized nuclear energy levels on excitation of the nucleus by a radio frequency pulse under an applied magnetic field. Nuclei with paired protons and neutrons will possess no magnetic moment and are therefore inactive to NMR spectroscopy. Both proton and carbon nuclei are accessible for organic molecules, and NMR spectroscopy is routinely used to elucidate structures (Table 11).

Table 11: Example nuclei with non-zero spins

Nuclei	**Number of protons**	**Number of neutrons**	**Spin state (I)**
^{1}H	1	0	½
^{13}C	6	7	½
^{14}N	7	6	1
^{31}P	15	16	½

Nuclei carry a positive charge and are considered for NMR spectroscopy to spin about their nuclear axis. This motion generates a small magnetic field, and the nucleus possesses a magnetic dipole moment proportional in strength to its spin (*I*). On

application of an external magnetic field, the nuclei precess at the Larmor frequency is defined by the applied magnetic field (B0) and the specific nuclei's gyromagnetic ratio (a constant).

If we consider a simplified quantized model of the energy levels in a molecule, the number of energy states of a nucleus is defined by $2I + 1$. In the absence of an external magnetic field, energy levels are degenerate. In a magnetic field, the energy (ΔE) difference between the two levels is described by Equation 1.

Equation 1: The energy difference between energy levels in a magnetic field depends on the gyromagnetic ratio of the nucleus; γ, the external magnetic field; B_0 and Planck's constant; h.

$$\Delta E = \frac{\gamma B_0 h}{2\pi}$$

Equation 2: Population difference between quantized energy levels

$$\frac{N_\alpha}{N_\beta} = e^{\frac{\Delta E}{k_b T}}$$

It then follows that we perturb the equilibrium (by applying a magnetic field and RF pulse) and measure the difference in energy levels. For example, a proton spectrum recorded at 400 MHz (B0 = 9.4T) will result in a population difference of 64 between

the two spin states (Equation 2). The consequence is that a recorded NMR signal is weak due to the low number of observable transitions.

Sensitivity

The nuclei will also determine how easy it is to observe. The cube of the gyromagnetic ratio governs the sensitivity or reciprocity of a nucleus; y^3. Some NMR active isotopes are also not very abundant, e.g. ^{13}C, which accounts for only ~1.1% of carbon atoms in a sample. Given that SNR ratios increase with magnetic field strength ($\propto B_0^{3/2}$), higher field instruments improve the signal intensity and signal/noise ratios.

Chemical shift

The chemical shift plotted in NMR spectra is the frequency at which a given nucleus resonates under a magnetic field (both local and externally applied). Chemical shifts are reported in ppm to allow values that may be quoted independent of spectrometer field; δ(ppm) = resonant frequency/spectrometer frequency.

Protons in similar nuclear environments will resonate at similar frequencies; therefore, assigning peaks in spectra can be aided by knowledge of characteristic chemical shift ranges, for example, aromatic ring protons usually correspond to peaks at 6.5-8 ppm.

The vector model

The physical basis of NMR can be described in a general sense by the vector model. When nuclei are placed in a magnetic field, bulk magnetization results from the alignment of spins with the applied field. Once the spins are aligned in the z-direction, a short 90° radiofrequency pulse is applied across the entire frequency range, causing the spins to align with the xy plane. With time the magnetization decays to zero, and the spins return to their alignment in the z-direction and return to thermal equilibrium. The magnetization is recorded by monitoring the interference of the nuclei with a coil.

The decay of the signal with time is recorded as the free induction decay (FID). The time-domain interferogram produced is converted to a frequency-domain spectrum using a Fourier Transform, whereby signal intensity is plotted against the resonance frequency of each spin system.

Relaxation

In the most basic pulse sequence, after the RF pulse has been applied, the process of the magnetization returning to equilibrium is termed ‘relaxation’. Along the z-axis, the magnetization returns to a steady-state thermal equilibrium with a rate ‘T1’ (longitudinal relaxation), while along the xy plane, the magnetization returns to zero at a rate ‘T2’ (transverse relaxation). Inhomogeneities in the magnetic field or sample itself (paramagnetic species) cause the transverse magnetization to decay more quickly; thus, the observed or measured value is denoted T2*. The decay of the transverse magnetization determines the broadness of the signals recorded.

Quantitative use (qNMR)

Besides qualitative use, NMR allows a quantitative assessment of a mixture’s purity or can be used to determine a compound’s absolute concentration. Optimization of instrument and sample parameters is required to achieve accurate and precise results. For example, to ensure complete relaxation of the nuclei of interest, a delay between pulses should be at least five times the largest T1 value. T1 is measured using an inversion recovery experiment and will vary with concentration and the solvent so that the delay time can influence the method's accuracy. The ideal 90° pulse maximizes the signal-to-noise ratio (SNR), but a 30° pulse quickens the analysis in practice. Accurate phasing, a flat baseline, line broadening, and zero-filling are critical for accuracy when processing the spectra[188].

The limit of detection (LOD) for a given analyte is “the minimum concentration or mass of analyte that can be detected at a known confidence level”. The limit of quantification (LOQ) is the “lowest amount of analyte (concentration) in a sample that can be determined with acceptable precision and accuracy under the stated experimental conditions”. Both are dependent on the SNR, which is influenced by experimental parameters such as the magnetic field strength and the analyte’s characteristics such as peak shape and splitting pattern [189].

LOD can be determined visibly. Alternatively, mathematical approaches can be adopted where the peak shows an SNR>3 or following ICH guidelines LOD= 3.3*σ/S, where σ is the standard deviation of the response a calibration curve and S is the slope. LOQs are determined mathematically; the most recent analysis suggests the uncertainty introduced by integration of a peak with SNR = 86 is 1% due to integration errors and that SNRs above this should be adopted as a rule of thumb [190].

Low-field NMR

Alongside the technological advancements which have led to high and ultra-high-field NMR instruments (>300 MHz) becoming available to academic and commercial laboratories, there has been a resurgence of interest in low-field instruments (<300 MHz). Low field instruments use permanent magnets to produce homogenous magnetic fields with much lower running costs, maintenance costs, and space requirements versus a high field instrument’s electromagnets and cryogenic cooling. These qualities have allowed 40-100 MHz ‘benchtop' spectrometers and relaxometry to be commercialized. Since 2010, the number of publications has increased considerably with various academic and commercial applications demonstrated in food science, healthcare, and forensics [191–198]

Challenges when using low field NMR versus high field NMR instruments can be discussed in terms of the sensitivity, resolution, and dispersion of resulting spectra [199]. Sensitivity is proportional to the field strength and concentration of the analyte. Therefore, samples analyzed using low field instruments benefit from high concentrations. Peak separation can be considered in terms of both dispersion and resolution. Resolution is the distinction of two peaks and depends on each resonance's chemical shift and line width. The line width is related to the analyte's T_2; therefore, faster-relaxing peaks can show broader peaks [200]. Dispersion refers to the spacing of chemical shifts across the available axis. For example, when recording a spectrum across a spectral width of 12 ppm on a 700 MHz spectrometer, peaks will be spaced over 8400 Hz, whereas the same spectrum recorded at 60 MHz spans 720 Hz. Consequently, there can be less separation, which may reduce resolution between adjacent peaks.

For low field spectra, these factors mean that splitting patterns may not be identifiable. Complex multiplet peaks such as those seen with substituted aromatic protons are generally not resolved, and fine details such as coupling constants are inaccessible. Furthermore, when visual inspection of a spectrum is not trivial due to these changes, peaks may be deemed 'second [or higher] order', and analysis using standard integration and multiplet identification methods are inappropriate. Second-order effects occur at high-field strengths; coupled peaks can cause 'roofing' with the consequence that integrals do not follow Pascal's triangle. In more severe cases of poor resolution, which is exacerbated at low-field strength, overlap can be significant enough to remove all identifiable features. Therefore, multivariate analysis is particularly useful for low-field NMR instruments, which can be hard to interpret versus traditional high-field spectra.

Quantification can be performed, either with an external reference, calibration of a known response, or internal standard, but it can be challenging to avoid overlapping resonances with internal standards [191,201]. More advanced sequences available with high-field systems are also being implemented; examples include solvent suppression [202], and DOSY NMR [203]

Applications of NMR spectroscopy in polymer science

Both solution and solid-state NMR spectroscopy are essential methods for analyzing macromolecules, including proteins and synthetic polymers. For example, NMR has been used to study polymer defects, end-groups, stereochemistry and tacitity [204–206].

To date, NMR has found limited use in the study of historical materials; the main limiting factor is cost and equipment availability, although cheaper, low-field 'benchtop' NMR systems are increasingly used in academic research [196–198,201,207,208]. Key findings and features from the NMR analysis of common historic plastics are discussed below.

Analysis of Cellulose Acetate (CA) with NMR spectroscopy

The physical properties of CA polymers depend on the proportion of acetyl substituents on the glycosidic rings ('degree of substitution' or DS). Deacetylation of the glycosidic rings is the primary mechanism of CA degradation; multiple case studies have found that deacetylation occurs over time, and lower DS values are associated with more visibly degraded CA objects. High-field NMR is one of the most sensitive ways to measure the degree of substitution and monitor deacetylation. NMR spectroscopy offers a direct DS measurement method, obviating any need for chemical transformation beyond dissolution, unlike titration methods [209].

DS was initially measured by analysis of ^{13}C NMR spectra before Kono et al. assigned the ^{1}H NMR spectra of unplasticized CA and enabled the DS to be calculated from the integral ratio of glycosidic ring protons and acetyl protons [210,211]. As cellulose acetate is typically formulated with small-molecule additives, its NMR spectrum contains broad complex polymer resonances which overlap sharper, well-resolved peaks associated with small molecules. The resulting convoluted spectra can hinder quantitative and qualitative analysis. In a previous study, we modified Kono's sample preparation method for historic samples plasticized with DEP [158]. Additionally, integrals from overlapping plasticisers and CA peaks were subtracted to allow the quantification of additives (DEP and DMP). To date, no single method can be used for simultaneous DS measurement and quantification of residual acetic acid, and additive quantification.

Compared to the study of small molecules that exhibit well-defined and resolved resonances, the assignment and analysis of some polymer peaks are not trivial. Line broadening results from slow relaxation of protons as a result of larger mass or viscous samples and can lead to coalescing peaks.

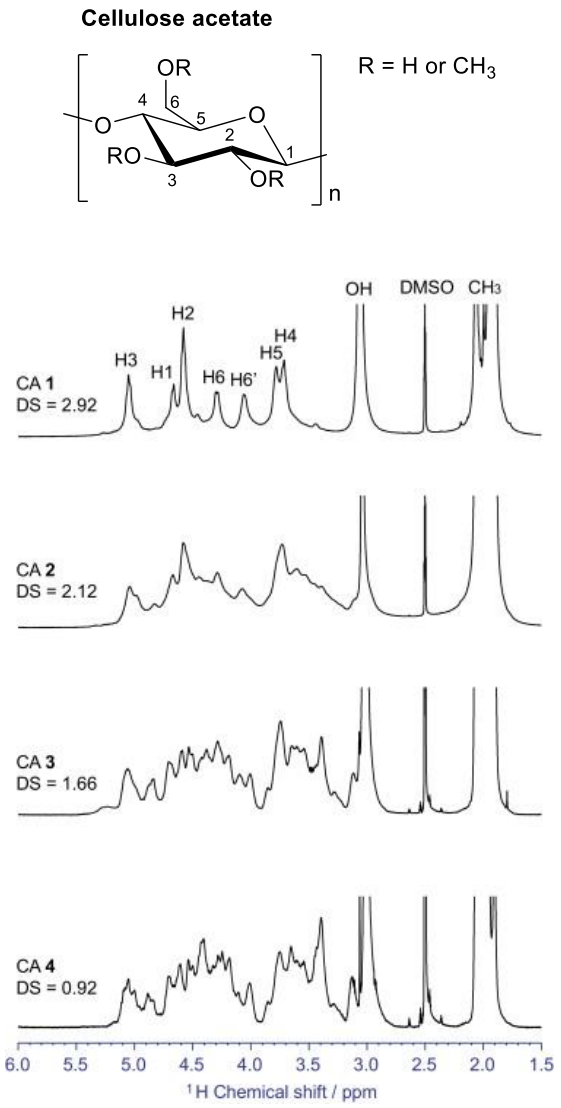

Figure 14: ^{1}H NMR spectra of cellulose acetate with varying degrees of substitution (DS). Image adapted from Kono et al. [5].

NMR methods for PVC analysis

Genay et al. developed a method for plasticiser quantification with high field NMR, including the distinction of isomeric phthalates by splitting patterns [212]. Adams et al. recently published a low-field NMR method able to distinguish between single additives (DEHP, DIBP, DINCH, DINP, TOTM) extracted from PVC in hexane and chloroform [213].

Mixed systems

The examples discussed above represent NMR methods which can be used to characterise either polymer or additives. The analysis of mixtures by NMR is most commonly performed for biological applications, either relying on bespoke NMR methods or advanced data processing techniques. Some relevant examples are discussed below. Mixtures can be harder to interpret without more advanced pulse sequences or processing methods [214–216], which have primarily been developed for the field of metabolomics.

Carr-Purcell-Meiboom-Gill (CPMG) pulse sequences filter by T_2 relaxation constants, which are generally shorter for macromolecular species than for small molecules [6]. By delaying the acquisition part of the pulse sequence, the fast-relaxing signals can decay without forming part of the recorded spectrum. A recent study by Aiello et al. investigated the suitability of a CPMG experiment to study additives in plastic samples; two model additives (a terephthalate and substituted benzene) were used as model additives in polyethene glycol (PEG) and polystyrene (PS) solutions [7].

The authors used Design of Experiments with factorial design to determine how sample preparation and experimental parameters could be used to attenuate polymeric signals. Increasing sample concentration and hence viscosity caused greater attenuation by decreasing the T_2 of polymer signals for PEG. However, it was not possible to attenuate PEG-derived signals by more than 45%. Statistical analysis using the analysis of variance (ANOVA) model showed that all factors (including polymer molecular weight (MW), solution concentration, and echo time) contributed to the filtering effect. Therefore, opportunities for further optimization were limited within the confines of the CPMG experiment.

Conversely, the relaxation filter was efficacious for PS, with polymer signal attenuation of up to 98%. Attenuation was independent of molecular weight, but the authors achieved an SNR>10 suitable for quantifying small molecules by considering the polymer's MW, echo time, and the number of cycles performed. For example, short echo times were most effective for high MW (>120 kDa) PS samples. In both experiments, aliphatic polymer proton signals were attenuated to a greater extent than aromatic protons.

The main disadvantage of the CPMG method is the need to optimize experimental parameters for specific samples and the potential for off-target suppression of non-macromolecular signals. Therefore, further experiments are required to determine the validity of quantification and fine-tune the pulse sequence parameters used. Similar approaches would be costly, impractical, and speculative for less standardized and unknown samples, which would be expected in heritage studies.

Spectra processing methods

The ability to tailor the acquisition method as required in the experiments above is unavailable to most routine users, yet complex and overlapped peaks are typical in spectroscopic analysis of mixtures. Instead data processing may be used to resolve minor and overlapped peaks from broader signals. Most NMR processing software includes deconvolution tools which use an iterative method to fit Lorentzian, Gaussian, or a weighted combination of line shapes to the observed peaks in solution state spectra.

Spectral differentiation is computationally less expensive and requires minimal user expertise or input. Most recently, the utility of spectral differentiation has been demonstrated in the field of metabolomics, where Takis et al. have used it to study small molecules (metabolites) and their concentrations in macromolecular matrices (e.g.

blood serum, plasma, and urine). The metabolomics field's workhorse is a standardized 1D-^{1}H-NOESY experiment used to suppress background water signals. However, broad macromolecular signals remain if the sample is not pre-treated by filtration or extraction, so multivariate statistical methods available through specialist software are required, or a CPMG experiment is used where interference from protein or lipid signals complicates data analysis.

SMolESY differentiation method

Takis et al. used derivative post-processing of ^{1}H-NOESY spectra as “an efficient and quantitative alternative to on-instrument macromolecular ^{1}H-NMR signal suppression” [8]. The ‘Small Molecule Enhanced Spectroscopy’ or ‘SMolESY’ process is simple and automated with a MATLAB package. Application to 3300 biological samples validated its resolution of overlapping small molecules from macromolecular signals. The SMolESY method’s novelty lies in using the imaginary spectrum's derivative for more robust quantitative analysis; it retains positive peak maxima and a larger SNR than the real component (see Table 12). Quantitative accuracy was greater versus the standard CPMG method used on the same samples. The processing method is newly published and was only applied to biological and food samples.

The peaks present in a Fourier transformed ^{1}H NMR spectrum can be described by a Lorentzian distribution, including peak intensity(I), chemical shift (x,δ) and peak width at half height ($\Delta\nu_{1/2}$) (Equation 3). The first derivative (Equation 4) shows how the derivative tends to zero as peak width at half height ($\Delta\nu_{1/2}$) increases.

Equation 3:

$$f(x) = \frac{I_\delta}{1 + \left(\frac{(x-\delta)}{\Delta v_{\frac{1}{2}}}\right)^2}$$

Equation 4:

$$f'(x) = \frac{-I_\delta(2x - 2\delta)}{\Delta v_{\frac{1}{2}}\left(\frac{(x-\delta)^2}{\Delta v_{\frac{1}{2}}} + 1\right)^2}$$

Therefore, broad signals give rise to low values, and their contribution to overlapped signals in spectra is minimized. Table 12 illustrates the transformation of peaks in a standard frequency domain spectrum to the derivative spectrum.

Table 12: Illustration of derivative spectra shape. Adapted from [217].

	Fourier transformed frequency domain spectra	First derivative spectra
The Lorentzian function used to describe line shapes	$f(x) = \frac{I_\delta}{1 + \left(\frac{(x-\delta)}{\Delta v_{\frac{1}{2}}}\right)^2}$	$f'(x) = \frac{-I_\delta(2x - 2\delta)}{\Delta v_{\frac{1}{2}}\left(\frac{(x-\delta)^2}{\Delta v_{\frac{1}{2}}} + 1\right)^2}$
Phased spectrum	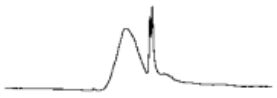	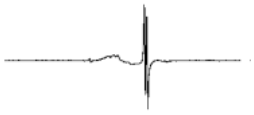
Real component of the spectrum	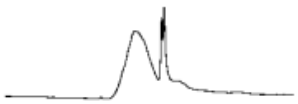	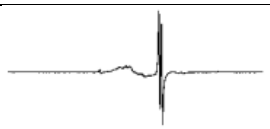
Imaginary component of the spectrum	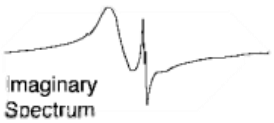	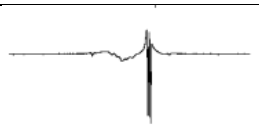

The finite difference method used to obtain the derivative is affected by noise; therefore, a low SNR in the original spectrum can lead to a poor-quality derivative spectrum. The method seems particularly promising for post-processing of samples containing small molecules and polymers where broad resonances impede simple analysis, such as cellulose acetate.

1.6 Methods for the identification of plastics

Literature examples of plastic identification primarily use FTIR spectroscopy, as a variety of sampling methods and optical setups exist to accommodate various sample characteristics, including transmission, attenuated total reflectance (ATR), diffuse reflectance (DRIFTS), and external reflectance (ER) FTIR spectroscopy. Increasingly, conservation scientists have used ER instruments to avoid destructive sampling or accommodate non-planar sample geometries which are unable to be analysed with ATR [218–221]. Bruker Alpha II instruments with interchangeable attenuated total reflectance (ATR) and external reflectance (ER) accessories are frequently used in heritage settings, including several plastics identification studies [219–223].

Interpretation of spectroscopic data is a key challenge for polymer and additive analysis. To date analysis of infrared spectra has largely relied on comparison to spectral libraries, where Pearson's correlation coefficient is a widely used method to rank similarity between a sample spectrum and all library spectra. For more complex samples such as those containing high additive concentrations or co-polymer blends, library matches to the base polymer may be penalised such that manual interpretation of characteristic bands remains crucial. Increasingly, infrared spectra are analysed using chemometric approaches including multivariate analysis and machine learning models.

Aside from scientific analysis, the diversity of material form and appearance can aid identification. The ResinKit and Samco kits are the first examples of known sample kits used in the heritage sector [224]. Most recently, the 'Plastics Identification Kit' (PIK) formalized an identification strategy using observations [225]. After an item is

categorised as a foam, film, elastomer or rigid, the user is asked optional and targeted questions covering age, smell, feel and form alongside microchemical test results. Answers are used to assign a probability score to the candidate plastics shown in Table 13. The PIK is the first resource for museum professionals which links form to material type. It is targeted to collections professionals without access to scientific equipment but could be used to provide additional context during polymer identification using spectroscopic data.

Table 13: Candidate plastics by category in the Plastic Identification Kit [225]

Category	**Candidate plastics**
Film	Cellulose Acetate (CA) Cellophane (CE), Cellulose nitrate (CN), Ethylene Vinyl Acetate (EVA), Polyamide (PA), Polybutyrate adipate terephthalate (PBAT), Polycarbonate (PC), Polyethylene (PE), Polyethylene terephthalate (PET), Polylactic Acid (PLA), Polypropylene (PP), Polystyrene (PS), Plasticized Polyvinyl chloride (PVC - P)
Elastomer	Natural rubber (NR), Flexible Polyurethane (PUR flexible),

	Plasticized Polyvinyl chloride (PVC - P), Silicone rubber (SI), Synthetic rubber (SR)
Foam	Ethylene Vinyl Acetate (EVA), Natural rubber (NR), cross-linked polyethylene (PE cross-link), non-cross-linked polyethylene (PE non cross-linked), Expanded Polyethylene (PE, EPE expanded), Phenol Formaldehyde (PF), Polypropylene (PP), Expanded Polystyrene (PS, EPS expanded), Extruded polystyrene (PS, XPS extruded), Soft Polyurethane ester (PUR ester soft), Soft polyurethane ether (PUR ether soft), Expanded Polyurethane (PUR expanded), Hard Polyurethane (PUR hard), Plasticized Polyvinyl chloride (PVC - P), Synthetic rubber (SR)
Rigid - sheet	Acrylonitrile butadiene styrene (ABS), Cellulose Acetate (CA), Cellulose nitrate (CN), Melamine formaldehyde (MF), Polyamide (PA), Polycarbonate (PC), Polyethylene (PE),

	Polyethylene terephthalate (PET), Phenol Formaldehyde (PF), Poly(methyl methacrylate) (PMMA), Polypropylene (PP), Polystyrene (PS), Non-plasticized Polyvinyl Chloride (PVC - U)
Rigid - industrial product	Acrylonitrile butadiene styrene (ABS), Cellulose Acetate (CA), Casein Formaldehyde (CF), Cellulose nitrate (CN), Epoxy (EP), Hard Vulcanized Rubber (HVR), Melamine formaldehyde (MF), Polyamide (PA), Polycarbonate (PC), Polyethylene (PE), Polyethylene terephthalate (PET), Phenol Formaldehyde (PF), Polylactic Acid (PLA), Poly(methyl methacrylate) (PMMA), Polypropylene (PP), Polystyrene (PS), Flexible Polyurethane (PUR flexible), Hard Polyurethane (PUR hard), Plasticized Polyvinyl chloride (PVC - P),

	Non-plasticized Polyvinyl Chloride (PVC - U), Styrene acrylonitrile (SAN), Urea Formaldehyde (UF), Unsaturated polyester (UP)

The following sections discuss examples where infrared spectroscopy was used for polymer and additive analysis and explores the advantages and limitations of ER and ATR-FTIR spectroscopy methods for those purposes.

1.6.1 Characterisation of historic plastics with ER and ATR-FTIR spectroscopy

Multiple authors have used NIR and mid-IR spectroscopy for polymer identification, including with ATR and ER instruments. Recording an ATR spectrum requires pressurized contact between the sample and the ATR crystal to maximise the quality of a spectrum, but this can be impossible with fragile or vulnerable heritage objects. Conversely, ER configurations may be used when destructive sampling or using pressurized contact is undesirable as the object only needs to cover the aperture. However, the optical setup of ER instruments differs from ATR instruments such that the quality and signal to noise ratio from ER spectra is generally lower than ATR. Corrections are typically applied for ER, although Rosi et al.'s recent methodology did not make use of any correction [226].

At least two studies have sought to compare spectra recorded using different configurations (transmission, ATR, and reflectance modes). Picollo et al. found that transmission, ATR, and 'total reflectance' (comparable to ER) spectra were all comparable for one PVC sample, and for a CA sample only the transmission spectra differed [227]. The samples were part of the 'ResinKit' sample set, which are flat

coupons ideally suited for close contact with the spectrometer. Bell et al.'s study examined and compared the use of ER and ATR sampling methods for 3D historical samples, and sought to consider how a samples physical properties such as colour and surface texture affected spectral quality. Key quotes are reproduced here;

- *ATR clamped sampling [of] transparent materials (PC, PMMA, PET, PVC) produced lower SNR than opaque (PE, PF, PA, PP, CSF, ABS, PS, CN, MF) or semi-opaque materials (CA, PUR) due to the normal dispersion of light.*

- *Close contact [for ER and ATR] is more easily maintained with softer materials (PVC, PUR).*

- *Whereas glossy, smooth surfaces (ABS, PS, PMMA, PF) produced higher SNR… their [ABS, PS] dark coloring… impact the spectra resulting in lower overall spectrum intensity with all sampling techniques.*

- *Upward baseline shift (more significant at low wavenumbers) in … CA and PVC sample absorbance spectra are attributable to the infrared radiation scattering from additives, such as fillers or colourants, including carbon black and titanium dioxide.*

These observations were used to produce a guide for practitioners with ER or ATR recommended after consideration of the object's form including shape and surface texture.

1.6.2 The effect of ATR vs ER sampling methods on observed spectral features

Sample properties can have a significant effect on the quality of the spectra recorded, to the extent that peaks present in ATR spectra may be obscured in ER spectra. Thus ER-FTIR spectra are generally more challenging to interpret than ATR-FTIR spectroscopy and transmission spectra, and this subject has recently been addressed in two studies [221,226].

In brief, 'external reflectance' strictly refers to infrared light reflected from a sample's surface (Rs) without penetration into the sample. However, if a material has any capacity to absorb infrared light, volume reflectance (Rv) of the infrared beam inside the sample can also contribute to the spectrum. ER bands deriving from surface reflectance (Rs) appear derivative-like, which may be corrected by a Kramers-Kroning Transformation (KKT) to produce a spectrum more similar in appearance to ATR-FTIR spectra. Meanwhile, volume reflectance describes light which 'propagates greater path lengths before it is scattered, transmitted, and reflected to the detector [resulting in the] enhancement of the low absorption bands' [228], and the resulting spectra is unsuitable for correction by KKT.

Additionally, the reflected light (Rs and Rv) contains both specular (reflected at the same angle of incidence) and diffuse (reflected at different angle to the angle of incidence) components. In general, diffuse reflectance dominates for samples with rough and matte textures, whereas specular reflectance dominates for smooth shiny surfaces. As such a material's surface properties can significantly affect the appearance of a collected external reflectance spectrum.

The chemical composition of the sample can also induce further distortions. Rosi et al. recently described how Restrahlen bands and Christiansen scattering may occur

in ER-FTIR spectra where inorganic additives are present [226]. Restrahlen bands are ‘inverted bands at wavelengths corresponding to high absorption’. One example showed how an ER-FTIR spectra of a PVC cable contained calcium carbonate filler but was a poor match to PVC reference spectra as the filler ‘strongly modifies both the morphological and optical properties of the surface generating a Reststrahlen peak‘ [226].

1.6.3 Additive identification by infrared spectroscopy

Table 14 shows some reported peaks for PVC, calcium carbonate and other inorganic additives used in addition. Metal stearates are used as heat stabilisers in PVC and may be identified in ATR-FTIR spectra although the infrared profile of mixed stearates was shown to vary with their preparation method [229]. It is unknown if they induce distortion in ER spectra.

Table 14: Characteristic peaks for PVC and inorganic additives used as fillers and heat stabilisers in PVC formulations in ATR-FTIR spectra.

Component	**Characteristic ATR-FTIR spectroscopy peaks (cm^{-1})**	**Notes and citations**
Calcium carbonate	1396-1413 1426	asymmetric carbonate stretch of pure $CaCO_3$. Vichi et al. 'applied different levels of pressure between the sample and the ATR crystal' and recorded a range which was attributed to an 'anomalous dispersion effect in ATR mode' [230] Broad peak, recorded in plasticised PVC samples [231]
Calcium stearate	1575	[232]
Zinc stearate	1535	[229]

Heat treated or mixed Ca/Zn stearates	1520-1600	Complex formation and polymorphism are known to affect IR profile [229]
PVC	2970 2912 1435 & 1427 1331 & 1255 1099 966 690 & 615 635	C—H stretch in CHCl C—H stretch in CH2 CH_2 deformation C—H deformation in CHCl C—C stretch CH_2 rocking atactic / non-crystalline crystalline / tactic C-Cl stretch [233–235]

Organic additives do not cause such extreme spectral distortion, but plasticiser-derived peaks have been observed to shift on incorporation within PVC samples along with changes to the C-Cl bands [235,236]. A recent study used deconvolution of the plasticiser-derived carbonyl peaks, to show that the deconvoluted peak maxima in 'plasticiser mixtures were shifted relative to the single plasticisers' in samples containing DOTP, DOP and ESBO plasticisers and mixtures of the same [237]. Therefore, known shifts for singular plasticisers are not reliable for identification as mixtures could be present. Peaks derived from the C-Cl bonds of the polymer have also been observed to shift. Both shifts can be explained by the interaction between the plasticiser C=O and polymer C-Cl groups and are considered a measure of compatibility between polymer and plasticiser [235,236].

Finding distinct peaks for all major plasticisers is not achievable due to the shared ester and aliphatic or aromatic hydrocarbon functional groups. However, distinction *between* aromatic plasticiser class (phthalate vs. trimellitate vs. terephthalates) is easily achieved with ATR-FTIR spectra. The different substitution patterns of the benzoate esters alter the vibrational characteristics of the sp^2 C-H bonds, giving the visibly distinct peaks between ~730-750 cm^{-1} detailed in Table 15.

.

Table 15: Organic plasticiser classes used in PVC formulations, and associated peaks in ATR-FTIR spectra.

Plasticiser class (R = hydrocarbon)	**ATR-FTIR spectroscopy peak wavenumbers (cm^{-1}), characteristic peaks are in bold**	**Citations**
Phthalate 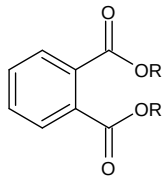	1580, 1600, 741	[229,235]
Trimellitate 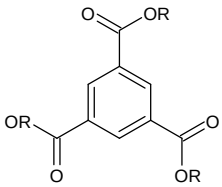	1575, 1610, 751	[229,238,239]
Terephthalate 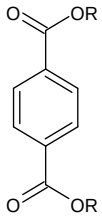	728	[229]

More advanced multivariate analysis and machine learning models are increasingly used where differences in spectra are subtle or imperceptible by visual inspection,

such that Pearsons's correlation coefficient are poor separators of library matches. They have also been used in studies seeking to use mid-infrared, near-infrared and Raman spectroscopy for plasticiser identification. During the preparation of this thesis, Rijavec et al. evaluated multiple machine learning models, from which a PCA-LDA model was able to classify ATR spectra between some long-chain phthalates (DEHP vs DINP vs DIDP vs mixed DINP & DIDP) with 99.8% accuracy against test data [240]. Initially PCA was used to reduce the raw spectral data to 12 principal components, which were sufficient to describe the variance across the sample set. The principal component scores were then used as the input to the LDA model and associated with the plasticiser type identified by GC-MS. The same approach with NIR spectra yielded a model with only 72% accuracy.

To date, *in situ* identification of additives within historic polymeric objects has been most successfully demonstrated with a portable dispersive Raman instrument (excitation at 785 nm) and laboratory-based FT-Raman instruments (excitation at 1064 nm) [241–243]. In general, fluorescent interference has been found to impede peak detection for some plastics, and skilled control over the incident laser energy is also required to avoid burning and minimise the invasiveness of Raman spectroscopy for collection objects.

Madden et al. identified camphor in CN, alongside dimethyl phthalate, diethyl phthalate and TPP in CA using a portable spectrometer to survey historic aviation glasses [244]. Similarly, Neves et al. used Raman microscopy to analyse CN film [245]. For PVC, destructive sampling and GC-MS analysis was needed to distinguish DMP, DBP, and DEHP in conserved PVC sculptures after analysis by a portable Raman instrument [246].

The inability to distinguish PVC plasticisers using visual inspection or traditional spectral matching methods is well established. Most PVC studies were designed for regulatory testing and therefore focus on distinguishing ‘phthalate’ vs non-phthalate class samples instead of aiming to characterise the specific plasticiser. As such Norbygardd et al. first reported that homologous alkyl phthalates showed a characteristic peak at 1040 cm^{-1} when analysed with a 1064 nm laser. Less common phthalates with R groups other than n-alkyl chains were distinguishable from the highly similar spectra of the homologous n-alkyl phthalates, but the finding is of limited practical use as they are not widely used in PVC formulations.

More recently, chemometric methods enabled differences between ‘ortho-phthalate’ and ‘non-phthalate’ plasticised PVC samples to be identified using PCA on a subset of the spectral region (1100-900 cm^{-1}), for 22 food-grade tubing samples analysed with a handheld Raman (785 nm) spectrometer. However, interference from other additives ($CaCO_3$ at 1084 cm^{-1}), and fluorescent interference were all observed to effect accurate classification. In testing, three citrate and an adipate plasticised sample were also misclassified as phthalate plasticised. Most importantly for the heritage sector three samples were observed to burn with a laser power of 250 mW. The lowest power achievable for the instrument was 75 mW, although the authors noted that this also caused rubber samples, which may be visibly confused for PVC, to burn.

In a follow-up publication, the same authors used a portable 1064 nm Raman system to identify individual plasticisers [247]. ATBC, DOTP, DEHP, DINP and ESBO were correctly identified in real samples by limiting the spectral matching region to 1810-974 cm^{-1}. DIDP samples match more closely to a longer chain phthalate (DTP) which

is rarely used, so further refinement of the library matching window to 1900-1210 cm^{-1} was required to correctly discriminate DIDP.

In summary, with ATR-FTIR spectroscopy limited plasticiser classes may be distinguished by peak picking (trimellitate, terephthalate, and phthalate), and individual phthalates and DOTP may be distinguished by use of the PCA-LDA model by Rijavec et al [240]. The Raman method by Moskowitz et al. offers identification of most individual plasticisers and includes non-phthalates [247]. However, none of the methods are ideal for collection objects, with ATR-FTIR spectroscopy requiring destructive sampling, and while the Raman method is non-destructive, the instrument used is known to induce burning for some samples.

No study has yet identified PVC additives using non-destructive IR spectroscopy alone. Recognising the heritage sector's preference for non-destructive analysis, it appears worthwhile to establish the extent to which additive peaks can be observed with ER-FTIR spectra.

1.6.4 Other techniques for additive analysis

Beyond point-based spectroscopy, hyperspectral scanners can be used for non-destructive surface analysis of 2D or 3D objects, although lower resolution images result from a larger field of view [248]. In some cases, plastics with low melting or glass transition temperatures may be affected by the heat from the high-intensity light sources used in some imaging techniques. Ultraviolet and near-infrared (NIR) scanners are commercially available, and NIR imaging is used to identify plastic types in the recycling industry [68,249,250]. Few studies demonstrate the distinction of specific formulations, but a hyperspectral NIR approach has been used to distinguish

plastics by the polymer, and the flame retardant used [251]. Additive migration is unlikely to be uniform across an object owing to the non-uniform ageing behaviour of plastics. Csefalyova et al. also demonstrated the use of NIR imaging and principal component analysis (PCA) to map the spatial distribution of phthalate plasticiser across a planar historic PVC sample [248].

Whether the location of damage is of relevance to conservation measures remains unknown; however, analysing the composition of a sample as a function of thickness/depth from the surface can be used to determine the loss mode for additives in plastics. Spatial resolution at the micrometre scale by coupling point-based vibrational spectroscopy to optical microscopes is useful for cut cross-section samples; infrared or Raman micro-spectroscopy offers spatial resolutions of between ~10-50 μm [252,253]. IR microscopy has been used to determine additive concentrations along cut cross-sections in diffusion and ageing studies of plastics [253,254]. Focal plane array detectors used for microscopic infrared imaging significantly enhance the speed of data collection, although at a higher cost. The narrower spectral range (typically >900 cm^{-1}) also limits interpretation using the 700-800 region which can be informative for some plastics such as PVC and CA, compared to point-to-point mapping systems [255]. Nano-scale resolution (~ 100 nm) has also been achieved using AFM probes coupled with infrared absorption spectroscopy to map chemical components in plastic samples [256].

For non-destructive depth profiling, vibrational spectroscopy is unsuitable due to the low penetration depths of the incident light. However, confocal Raman spectroscopy can achieve greater penetration depth [257,258]. Adams et al. successfully used terahertz time-domain spectroscopy (THz-TDS) for concentration-depth profiling of

known samples. However, the complexity of spectra means that it is only suited to samples of known history and formulation [259].

Single-sided NMR, a low-field technique, also enables non-destructive concentration-depth profiling of a plastic sample. Scans performed at various distances from the sample using an adjustable height stage allow profiling through the material in ~100 μm slices [249]. Adams et al. demonstrated the first use of proton relaxometry to measure the concentration profile through a plasticised PVC sample of a known formulation. A decrease in the concentration of plasticiser leads to a reduction in T1 and T2 relaxation times related to both the additive (long T2) and polymer components (short T2) and the proton fraction; therefore, signals from low concentration (<13%) samples could not be discriminated. However, they also observed different relaxation behaviour with different additives and suggested that the creation of a database recording two characteristic relaxation parameters and proton fractions from characterised samples could allow the identification of additives without the need for further spectroscopic analysis.

For 3D objects, the above methods will also be affected by non-planar surfaces as the penetration depth of incident light can vary. However, techniques such as terahertz pulsed imaging (THz) have been used to analyse 3D objects non-destructively, but they require expertise in operation and data analysis. For example, both THz-TDS and 3D THz pulsed imaging were used by Strlič et al. to distinguish plastic type in historic samples, as well as image features such as internal cracks and delamination. However, no spectral features differed between plasticised and non-plasticised PVC samples [260].

1.7 Magnetic resonance imaging

Finally, mid to high-field magnetic resonance systems are routinely used to image the distribution of mobile species within complex three-dimensional matrices, e.g. imaging water in human tissue in clinical research. High field MRI has been used in two examples to study plastics; O'Donnell et al. imaged the distribution of an organic lubricant within a solid polyethene pipe; blisters with a high concentration of lubricant were observed [261], and Wiesenberger et al. monitored the absorption of an organic solvent into PMMA rods [262].

The distinction of small molecules from larger polymeric components is reliant on differences in molecular mobility and the associated differences in longitudinal (T1) and transversal (T2) magnetisation decay rates. Magnetic resonance imaging (MRI) applies the principles of nuclear magnetic resonance for clinical imaging. The difference in relaxation behaviour of materials is exploited by using a spin-echo pulse sequence. Contrast images result from the difference in the T1 and T2 of abundant molecules such as water, fat, and bone within the subject. The proton density of different species may also be used to construct an image.

Instead of acquisition of the FID immediately after the 90 pulse, a delay followed by a second 'refocusing' pulse results in a 'spin-echo' (illustrated in Figure 15). The second 180 pulse comes halfway between the first pulse and the time at which the signal echo is sampled. The time difference between the initial pulse and signal acquisition at the peak of the echo is called the echo time and can be varied. The whole cycle is repeated after a user-defined repetition time (TR).

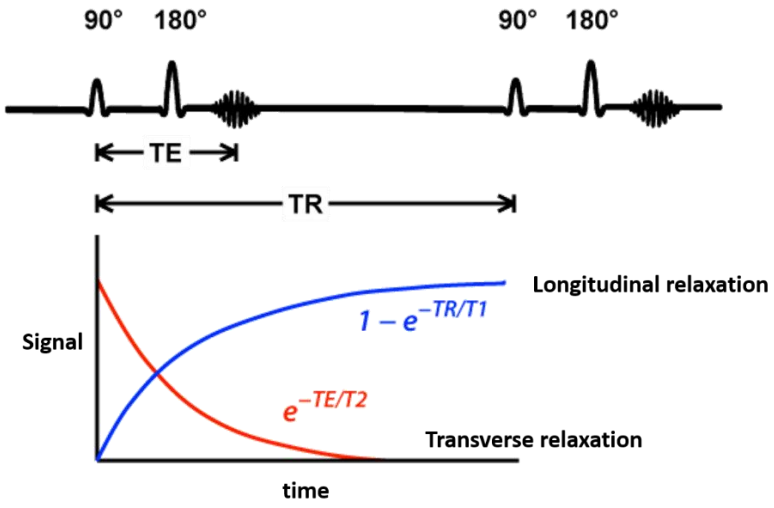

Figure 15: Typical spin-echo pulse sequence and evolution of T1 and T2 relaxation.

Sourced from: http://mriquestions.com/tr-and-te.html

By choosing a repetition time (TR) longer than T1, the magnetization in z for all components can recover to its steady-state and contribute to the signal. Choosing a shorter TR allows a greater contribution to the image from components with a shorter T1, whilst longer T1s are not fully recovered and thus have weaker signal intensity. Similarly, varying the echo time (TE) allows differentiation of components based on their long or short T2 values.

In general, solid structures such as cortical bone or some tissues have short T2 and T2* values and are invisible to MRI. Hardware limitations meant that switching between transmission and signal receiving modes of the coil could not occur quick enough to record the signal before decay was complete. Recently developed ultrashort echo (UTE) sequences allow signals to be acquired at ultrashort echo times (<100 us) before magnetization in the xy plan returns to zero. UTE sequences have therefore allowed imaging of previously invisible solid components such as bone.

Proton signals from bound protons, such as those in polymers, will decay more quickly (short T2) than those from more mobile species, such as additives or free water (long T2) [263]. Experimental parameters such as pulse echo (TE) and repetition times (TR), may be adjusted so that full recovery of the signal derived only from polymeric protons is achieved and therefore does not contribute to the image, unlike that from the additives.

It should be noted that the additive concentration required to achieve a sufficient signal-to-noise ratio will be system-dependent [264,265]. Furthermore, analysis is also expensive, and spectral interpretation is non-trivial, so the practicality of such methods is significantly limited for heritage applications currently.

1.8 Conclusion

Many studies have focused on two plasticized plastics; PVC and CA, which have been observed to degrade in museum collections over the past 50 years. Plastic conservation literature to date has included studies on environmental control for preventive conservation, conservation cleaning methods, and sampling and characterisation methods.

For CA, characterization methods that currently exist appear suited to condition monitoring by measuring deacetylation but are unable to measure the mechanism of plasticiser loss alongside deacetylation which limits understanding of how the two processes interact.

Other studies of CA have focused on its response to environmental change. Macro-scale environmental actions dominate preventive conservation with temperature and humidity control. Although efforts to study micro-environmental control with enclosures are promising, findings from indoor air literature illustrates the sink behavior of such materials can be significant in plasticiser migration dynamics. Micro-scale environmental control studies showed that adsorbents for CA and PVC can enhance plasticiser migration rates due to their behavior as a sink material, and external literature also suggests storage materials may be an overlooked sink material for plasticized objects.

Aside from preventive measures, cleaning is the only interventive method studied to date. Solvent cleaning has been found to be effective at surface removal of plasticiser exudates although changes to surface finishes should be considered.

Studies from outside the conservation literature have also been reviewed. Alongside extrinsic factors which are moderated by environmental control, intrinsic factors such as additive type can affect migration behaviour. An approach using molecular modelling to understand migration behaviour for different PVC plasticisers was not able to model the decade's long timescales relevant to museums. Therefore, identifying if certain PVC formulations translates to an elevated risk or timescale for deterioration in condition would benefit from the use of case studies and ongoing monitoring. Any findings could enable conservators to tailor or prioritize resources for more vulnerable objects. Furthermore, the existence of diffusion and evaporation-controlled migration regimes, the variable volatility of plasticisers, and the different storage environments used in museum collections, also brings into question whether degradation occurs without observation of the classic warning signs of bloom and sweating.

Considering the move to reduce phthalate use in favour of alternatives it is also clear that there is value in experiments which look to the future and include alternative plasticisers likely to be found in collection objects soon. For example, library matching on PVC has relied on spectra recorded for phthalate-plasticisers only. Will non-phthalate plasticised PVC be identifiable using the same method, and can we expect non-phthalate plasticised PVC to degrade on the same timescale and in the same manner as we expect for phthalate plasticised PVC?

Finally, the literature review illustrates ideal best practices and the outputs of fundamental research and highlights the challenges associated with plastic conservation, but the actual implementation of such methods is unknown. For example, much effort has gone into the development of plastics identification

methods and fairly robust methods for polymer identification by ATR-FTIR exist, but these are less likely to be accessible to non-scientific users and non-invasive sampling is preferred. A major limitation of this review is that it cannot answer how such research has translated into conservation practices. This will be explored in the next chapter.

In conclusion, the overarching aim of this thesis is to evaluate methods to identify degradation products, and support future efforts to explore if a more advanced understanding of plastic formulations can be used to tailor preventive conservation treatments.

2 Survey of professionals involved in plastics conservation

Chapter 1 illustrates how efforts to conserve plastic objects have rapidly developed due to observations of deteriorating plastics across collections. In the UK, collection surveys in the 1990s and more recent pan-European research identified vulnerable plastics and typical degradation patterns [266–269]. Anecdotally, plasticiser migration is a common observation and is problematic for conservation professionals. However, the conservation or scientific literature rarely addressed it at the start of this work in 2018, and published collection and condition surveys lacked detail on the extent of plasticiser migration and its impact. Four decades after research began to consider plasticiser loss in CA, it is interesting to consider what conservation measures are used and what challenges remain.

2.1 Research Questions

An anonymous online survey for curatorial and conservation professionals was produced to gather data for multiple projects within the author's research group. The practitioners survey detailed below is the first survey of conservation and curatorial professionals to record the challenges of conserving plastic objects by assessing:

- What proportion of heritage collections contain plastic objects, and in what form?
- What type of damage is observed?
- How objects are acquired, if materials are identified, and who is involved in the process?
- What are the recurring challenges in the conservation of plastic objects?
- Is plasticiser migration a significant challenge for conservation?

2.2 Methodology

Participants answered forty-four questions designed to understand acquisition, identification, and conservation strategies for plastic objects within heritage establishments and identify perceived concerns related to their conservation. Survey questions were a variety of single-choice, multiple-choice, and free-form text inputs. Appendix 0 includes a copy of the survey.

While an online survey relies on a self-selecting audience likely to have some knowledge or concerns regarding plastic degradation already, it allows a broad and global audience to be reached. The degree of a participant's familiarity with plastic objects may also influence their responses. Therefore, questions related to their experience and the general make-up of their collection were also included.

Most questions were initially planned alongside other researchers at UCL. Questions were edited, and all other aspects, including survey design, ethics approval, survey dissemination, and data analysis, were undertaken alone.

UCL's Research Ethics Board approved the survey. The survey was hosted on UCL's Opinio Survey Platform and was available to complete between 25th April and 31st August 2019. The survey was anonymous, and the collected data complied with GDPR regulations.

The survey was advertised to both curatorial and conservation professionals, with targeted questions for each group. Participants were recruited through professional membership bodies (ICON), personal contacts, professional network groups online (LinkedIn, Facebook), and at the Plastics Heritage Congress 2019 in Lisbon.

2.2.1 Data validation and cleaning

From an initial 105 form entries, five were judged to be duplicated or triplicated based on responses and timestamps; only the most complete response of each multiplet set was retained. A further ten entries showed no response, and an additional ten failed to respond after the first question.

Initial questions (questions 1 - 10) surveyed the participants' demographics, including job role, career length, expertise, experience, and quantity and type of objects in the collections they represented. Participants without experience working with plastics and those unwilling to answer question 11 were excluded from the dataset. Participants who progressed beyond question eleven (N = 71) stated they worked with plastic objects (question 2) and expressed their level of concern regarding plastics in their care (question 11).

2.2.2 Dropout rate

The overall survey dropout rate was calculated as the number of respondents to answer the last mandatory question (question 41) as a percentage of the 71 eligible participants.

2.3 Results and discussion

The survey used conditional logic to target specific questions based on previous answers; for example, those who identified as curators in question 2 were ineligible for questions 28-39. Therefore, the following results do not always represent all respondents who answered the screening questions 1 to 11 (N=71) but always represent those eligible to answer each question. The number of participants who answered each question is noted in brackets '(N=)'.

Figure 16 shows the dropout rate for respondents deemed eligible to take the survey was 19%. There is a lack of generalisable studies related to survey dropout rates; therefore, the absolute figure is of limited use. However, the most widely cited study by Hoerger et al. found a positive correlation between dropout rate and survey length [270].

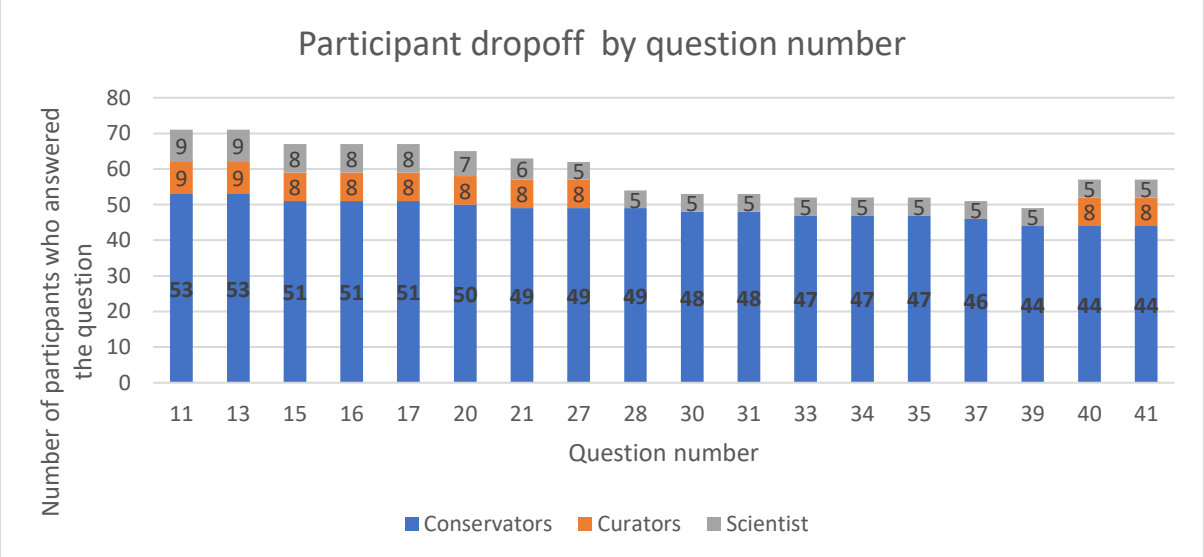

Figure 16: Participant dropout by question number. N.B. Curators were not eligible for questions 28-39.

2.3.1 Respondent demographics

75% of respondents identified as conservators, 13% as curators and 13% as scientists. One respondent identified as both a curator and scientist but followed the questions offered to curators. Thirty-seven respondents voluntarily shared their location. The majority represent UK museums, but practitioners from the United States, Canada, New Zealand, Italy, Denmark, Belgium, Austria, Tunisia, Germany, and Australia also participated.

All respondents were asked to consider the proportion of plastic objects in their collections by choosing from three statements; ‘plastics make up a minor/moderate/major proportion of our collection’. 86% of respondents represent organisations where plastics represent ‘minor’ or ‘moderate’ proportions of their collection. Examples of the fourteen organisations reporting ‘major’ plastics collections include Fondazione Plart, Naples, which includes a facility “committed to researching and developing appropriate methods for the conservation and restoration of synthetic materials used in art and design” [271], the Wimbledon Lawn Tennis Museum, which “collect clothing & shoes annually from players”, and the Museum of Design in Plastics, Bournemouth “the only accredited museum in the UK with a focus on plastic” which

aims to “increase understanding and appreciation of the use and significance of plastics in design”[272].

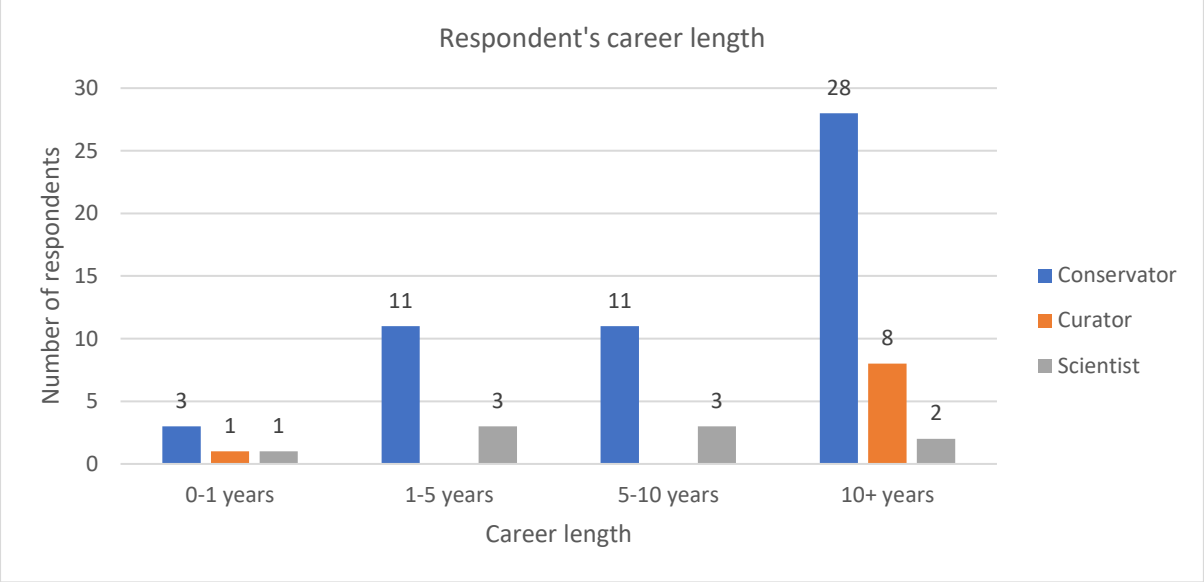

Figure 17: Career length of survey respondents

2.3.2 Education and professional experience

72% of conservators (N=53), 56% of curators (N=9), and 67% of scientist respondents (N=9) recorded their expertise or specialist knowledge of plastics in questions 4 and 5. Figure 18 shows that overall, informal ‘on-the-job’ training was the most common training type, but many also reported experience gained from degrees or short courses.

As with previous surveys of the conservation sector [273,274], the profession’s broad nature was hard to capture. When asked to state their area of expertise, many

respondents selected one or more areas of expertise, and five selected ‘other’ and self-identified as ‘general’ or ‘objects conservators’.

Conservator respondents (N=53) selected an average of 2.76 areas of expertise; 57% selected expertise in plastic materials, of which 63% (N=30) also selected preventive conservation. Question 5 asked conservator respondents who did not self-identify with plastic expertise if they have specialist knowledge of plastic materials; instead, 39% (N=23) of ‘non-experts’ reported specialist knowledge. Figure 18 shows that 39/53 conservators have some knowledge of plastics, gained through their conservation degree (49%), short courses (53%) and informal work experience (72%).

Of respondents who undertook a conservation degree, more recent graduates were more likely to gain knowledge of plastics conservation during their degree; 78% of respondents (N=18) who have less than 10 years of experience in the sector vs 43% of respondents(N=21) with more than 10 years experience. While plastic conservation is a newer topic in tertiary education courses, there is a wealth of practical plastics conservation knowledge retained in the conservation sector, with up to 30 years of experience reported.

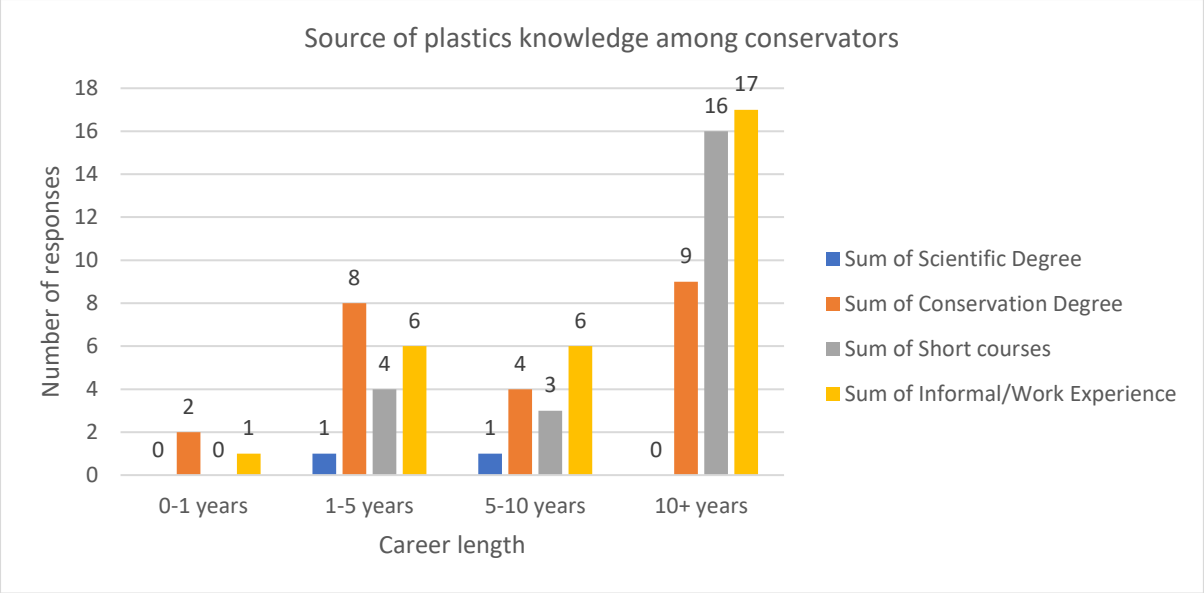

Figure 18: Educational history of plastic curation and care.

2.3.3 What type of collection objects contain plastic?

Objects made from plastic are found throughout collections, but Figure 19 illustrates that archival media, textiles, and 3D objects such as jewellery and toys are found in more than half of the respondents' collections.

The term archival media was chosen to encompass audio-visual media, such as cellulosic films or PET tape. The range of plastic media found within archives has been shown to include photographic film, mechanical objects such as gramophone disks, magnetic tapes, and visual artwork such as animation cels [266,275]. A survey by Chu et al. offers more detail on the presence and condition of plastics in archives, including that 90% of the Australian archives surveyed reported plastics in their collections, and 50% of respondents found at least some of their plastics are visually in 'poor condition' [276].

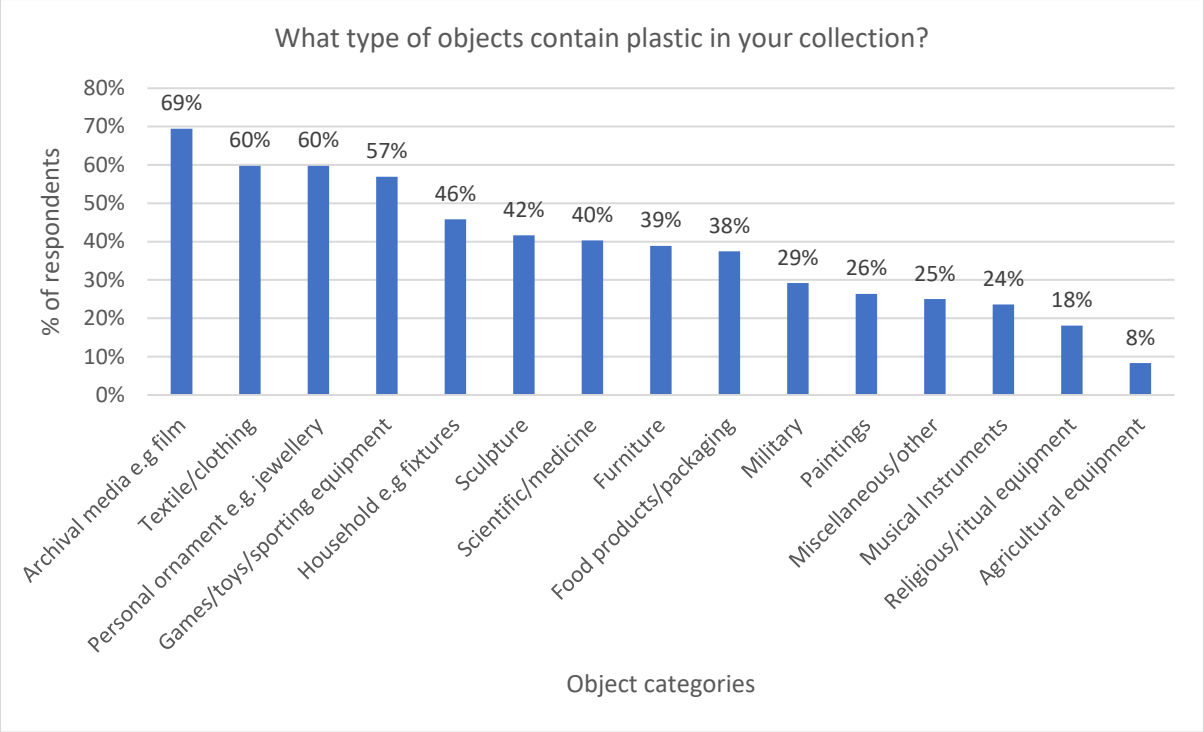

Figure 19: Plastic containing object types in a respondent's collection. Object types are adapted from the British Museum's Object Thesaurus [277]

2.3.4 What type of damage is observed for historic plastics?

The survey responses are also a valuable way to determine which plastics are considered the most vulnerable and identify any patterns in the types of damage.

Nine respondents shared their concerns regarding the instability of specific plastic types in their collections; CA (6) and, CN (6) and, PVC (4), PU (1), rubber (2), which are known to degrade and display signs of damage [6]. Two respondents highlighted the effects of visible damage such as discolouration and yellowing, with the following comments;

- *"some of which are already changing (embrittlement, yellowing!)"*

- *“Discolouration and deformation making artworks unexhibitable”*

Concerns around off-gassing and emission from plastics were related to health and safety issues, and the potential for damage to adjacent materials, and two respondents discussed plasticiser loss as a specific concern.

- *“CN, CA, PVC, PUR and rubber off-gassing poses risk to neighboring artefacts”*
- *“influence of plastics on other materials of the objects”*
- *“Loss of plasticisers, degradation products and their effect on other materials”*
- *“interaction of plastic deterioration products with other collection items and the storage and/or display materials.”*
- *“What potential hazards are being released as part of the degradation process.”*
- *“A further concern is health and safety (what kinds of additives have been used in historic plastics?)”*
- *“Evaporation of plasticisers”*
- *“storage (off-gassing, sticking to other collection items)”*
- *“the effect of degradation could have on the objects close by”*

These responses are supported by question 33; “Which of these [damage types] have you observed?” where 76% and 84% of respondents have seen evidence of additive migration by bloom and sweating, respectively. Figure 20 illustrates that the other indicators of additive loss, e.g., cracking, brittleness, and deformation, are also commonly observed. These results demonstrate the importance of additive migration as a damage type. The results are similar to Keneghan’s survey of objects at the British Museum, UK, where chemical damage, including cracking, discolouration, and bloom, were most commonly observed [266].

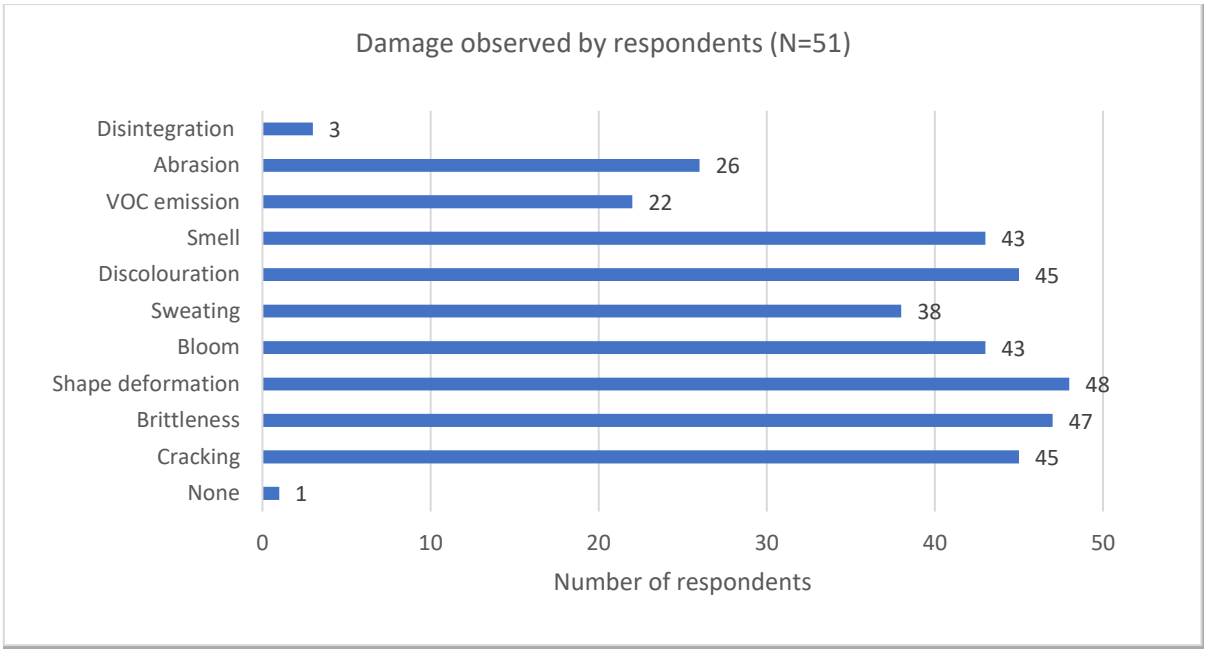

Figure 20: Damage observed on plastic objects by respondents. Sweating and bloom are generally associated with additive migration or loss. Deformation, brittleness, and cracking may also result from polymer degradation.

2.3.5 Recurring challenges in the conservation of plastic objects

In response to the question '*Are you concerned about plastics in your collection?',* 94% identified as very concerned or somewhat concerned (Figure 21). However, participation in the survey may be biased towards those with pre-existing concerns. Fifty-seven respondents recorded their thoughts as free-text responses to a follow-up question.

The most frequently mentioned concern was storage. 59% (N=57) had concerns about inadequate storage or a lack of knowledge on how best to store plastic objects. Respondents also referred to the varying storage needs of different plastic types and considered identification alongside storage, e.g., *"need for identification to determine*

best storage options", and "*We need more time, money and experienced staff to identify the least chemically stable objects in the existing collection and to provide the best possible storage conditions".*

- *Other than extreme cases, we make no special efforts to store plastics or composites objects with plastics in any different way than the rest of the collection*
- *Inadequate cold storage space for the number of plastics we have; storage in minimally-climate-controlled areas; identification of parts on objects; issues arising with mixed-material objects*
- *A lot of plastics are inappropriately housed. Many are showing signs of deterioration.*
- *Storing objects made of plastics, influence of plastics on other materials of the objects.*
- *Not adequate storage conditions*
- *Best methods of storage*
- *Storage conditions and physical support to retard degradation and support objects to limit physical stress and to keep objects in a display able form, say as they become brittle*
- *lack of knowledge on how to store properly to slow degradation*
- *almost total absence of appropriate storage*
- *Knowing how to best store different plastics in large mixed material collection stores.*
- *Effective storage and preservation.*
- *we need more time, money and experienced staff to evaluate our storage strategies.*

- *How they are being stored and the effect of degradation could have on the objects close by; we don't have an in depth survey of how much plastic we have let alone which types.*

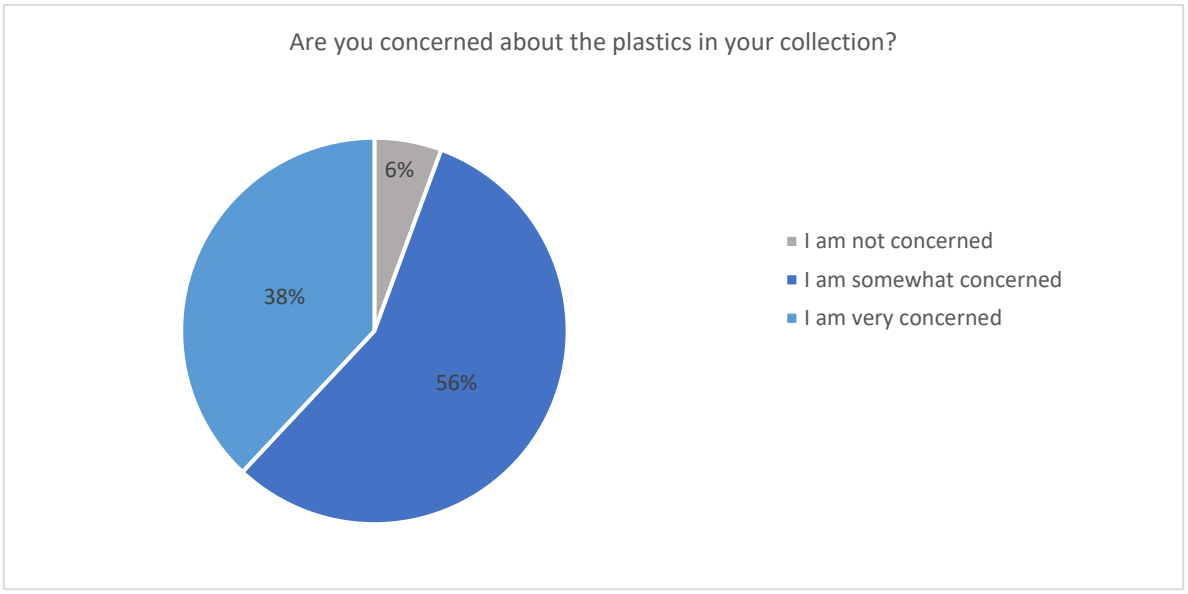

Figure 21: Degree of concern for plastics in respondents' collections

2.3.6 Identification of plastic type in objects

56% of all respondents report they are involved in identifying plastic materials, including 87% of conservator respondents. Identification is primarily an output from a post-acquisition condition assessment or is attempted to inform a conservation strategy. Identification at acquisition is not a common practice and is only a routine part of the acquisition process for 14% of respondents. Only two respondents reported that there was never any attempt to identify any materials used in a plastic object at their organisation. As such, 91% of respondents surveyed report that at least some of the polymers present in objects are identified in their organisation (Figure 22).

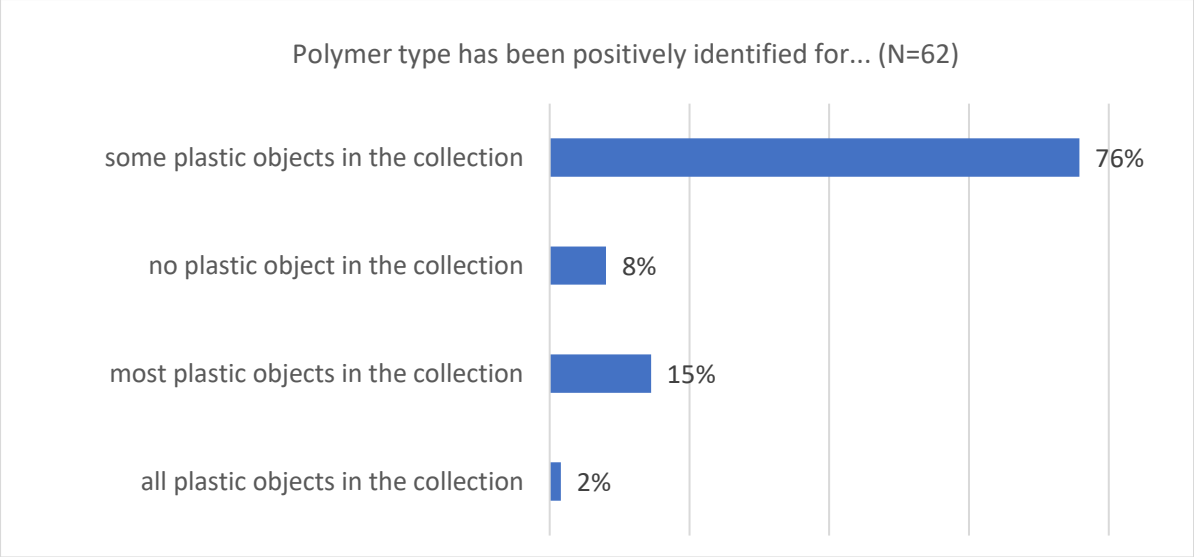

Figure 22: Extent of polymer identification in collections

At the start of the survey, 35% of all respondents described challenges in identifying plastic types in free-text responses. When asked later if there are any 'barriers to polymer identification at your organisation', 85% of conservators (N=49) reported barriers to identifying the plastic-type. The options of funding (78%), equipment (82%), and time (80%) were all selected as barriers, but expertise was the least significant barrier.

Figure 23 shows that non-scientific techniques are favoured. All practitioners rely to some extent on their knowledge of an object's history or use ID flow charts to narrow down polymer type by appearance, date, and tactile properties. Conservators and curators used non-scientific means as their primary method of polymer identification, whereas infrared spectroscopy is favoured by those identifying as scientists. Two of the specialist plastic museums, Fondazione Plart, Naples and Museum of Design in Plastic, Bournemouth, were among nine respondents to have identified most items in their collections. Still, methods without using scientific equipment were favoured among this group.

When scientific analysis using analytical equipment is preferred or required, ethics can restrict the sampling method; one respondent noted a policy of non-destructive sampling ("*Sampling techniques have to be non-destructive"*). However, another noted Bellstein's burning testing [6], a destructive method to identify halogenated compounds, e.g. PVC. *"I do use the diphenylamine spot test for help in identifying cellulose nitrate and the Beilstein test, for PVC (although the latter mostly for storage materials rather than artefacts), when a sample can be taken."*

Figure 23 demonstrates that if a plastic-type can be identified (), the majority of respondents (N=58) record the polymer by its chemical nomenclature (42) and/or common names (31); brand names are less widely used. However, one respondent also detailed how *"… records on our collections management system use specific terms like 'Bakelite' or 'Perspex' or 'cellulose nitrate' without any polymer identification…".*

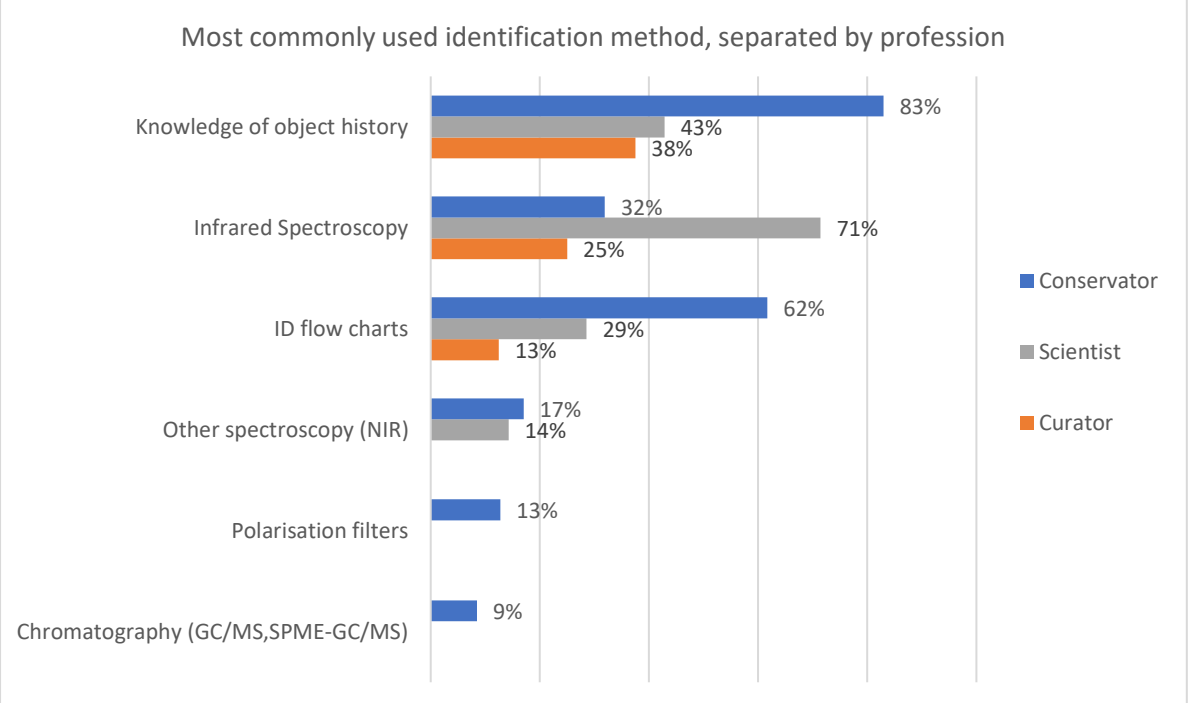

Figure 23: Identification methods favoured by all respondents; the percentages record the proportion of curators/scientists/conservators who use each method.

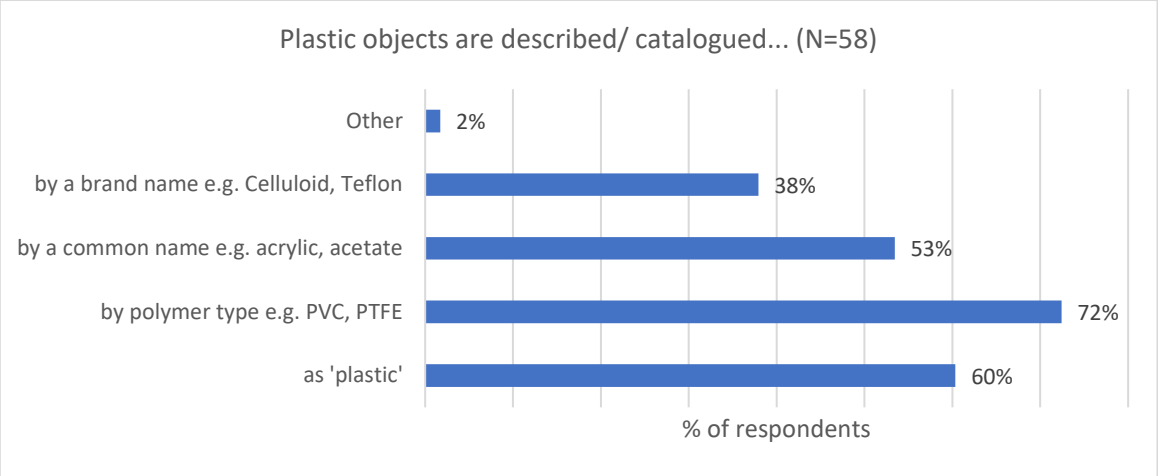

Figure 24: How respondents describe/catalogue plastic items in their collection management system

2.3.7 Conservation strategies

Setting a conservation strategy for plastics can be resource-intensive and is aided by knowledge of the variety of plastic types and appropriate preventive measures. As shown in , cconservators consult various sources, including conservation literature, and collaborate with academics and colleagues at conferences. To date, the conservation literature has set guidelines for environmental control with temperature and humidity level targets and recommended preventive measures such as isolation and monitoring for the most vulnerable plastics such as cellulosic films (Table 16). Restorative treatments have not been reported for the typical issues discussed in Chapter 1, such as deacetylation or additive migration.

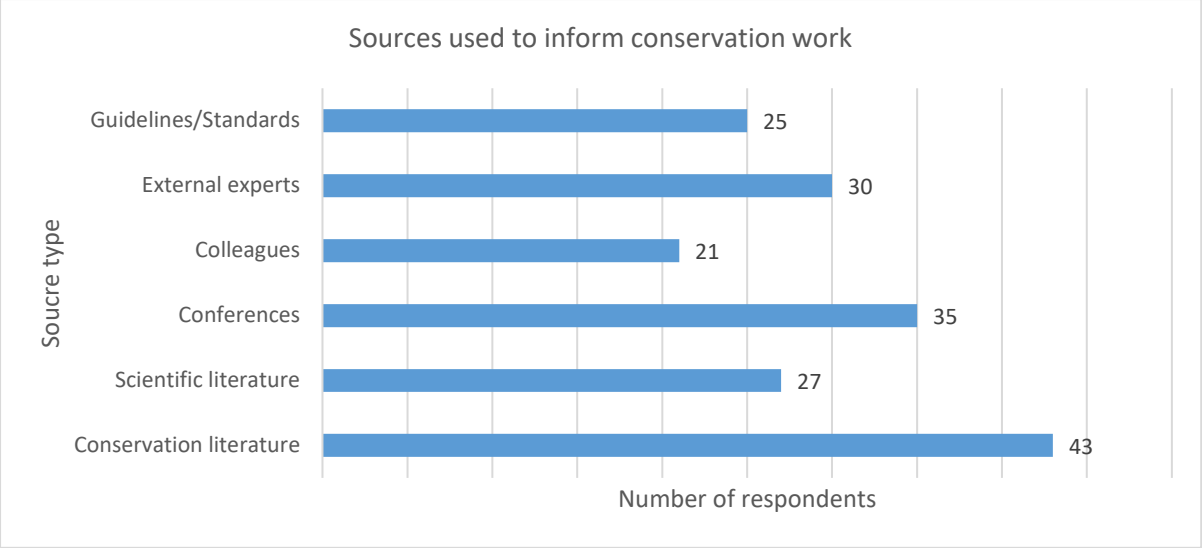

Figure 25: Sources used to inform conservation work

This has translated into standard procedures or guidelines specific to plastics conservation at 45% of respondents' organisations (N=48). Responses to Question 30 in Figure 26 show those with moderate (N=20) or major (N=9) plastics collections are more likely to have guidelines in place, whereas 67% of respondents with minor (N=24) amounts of plastics throughout their collection have no guidelines in place (.

Table 16: Example environmental guidelines for the conservation of cellulose acetate

Guideline & Author	**Temperature**	**Relative Humidity**	**Details**
BSI [278] PD5454:2012 Guide for the storage and exhibition of archival materials	5 °C - 18 °C (cool) or – 15 ±5 °C (cold)	30 -50% 50 %RH	CA-based material should have a permeable wrapping …. and a pollutant scavenger inside the outer packaging to absorb internally generated AA vapour.

Library of Congress [279] Care, Handling, and Storage of Motion Picture Film	<0°C	30-50%	Remove CA from non-ventilated storage containers; use ventilated storage containers; keep storage area well ventilated. Isolate from other collection items.
Canadian Conservation Institute [280] Care of Objects Made from Rubber and Plastic	<0°C	< 65%	Cold, dark, dry, and oxygen-free storage conditions.

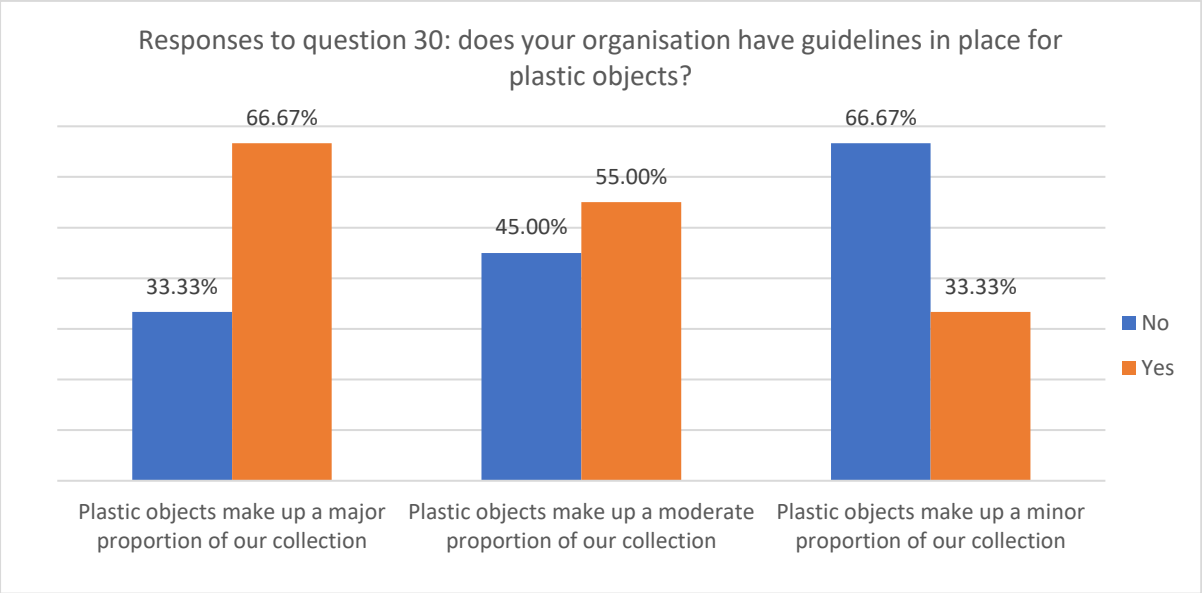

Figure 26: Responses to question 30; "Do you have any standard procedures or guidelines at your organization for conserving plastic objects incl. temperature, relative humidity, and lighting levels for display and/or storage?".

Questions 30-38 survey the use of four typical preventive conservation strategies (i) isolation (ii) low-temperature storage (iii) ventilation control and (iv) assessment & monitoring.

2.3.8 Isolation of objects

82% of respondents (N=40) isolate plastic objects. The free-text responses used to record 'what [is isolated] and why?' suggest degrading objects are most likely to be isolated rather than vulnerable objects before visible deterioration occurs; "*if they are showing significant signs of deterioration" and "If they have degraded so much they are a danger to themselves or other objects".*

Two-thirds of those who isolate objects (N=33) referred to actively degrading CA and the safety risk of CN objects, e.g., "*CN as it is flammable (goes into cold storage); CA if it is beginning to degrade"* and *"badly deteriorating CA when it has been decided the work can no longer be displayed".*

PVC was the next most common response and was discussed in terms of reducing the impact on other objects, such as the known softening due to plasticiser sorption or solvation [6], e.g., "*we have not yet identified PVC with loss of plasticiser, but we would isolate these if we did.", "We are starting to isolate PVC. Especially ones that are signs of deterioration.",* and *"stickiness or extreme degradation, especially if it will affect the rest of the composite object".*

Two respondents also discussed the isolating effect of anoxic storage of rubbers, latex, and polyurethane and the isolation of rubbers by freezing.

2.3.9 Temperature-controlled storage

Eighteen respondents recorded their use of temperature-controlled storage across questions 30-38 (N=48), including storage in a refrigerator (12) and freezer (8).

- *we have frozen, cold, cool and standard 70/50 temperature zones.*

- *all plastics are kept at 6'C and 32%RH in archive vault*
- *deteriorating PU stored in freezer.*
- *rubber is stored in fridge, if possible.*
- *CN as it is flammable (goes into cold storage); CA if it is beginning to degrade; soft rubber when possible (cold storage)*

2.3.10 Ventilation

Measures designed to control airflow are also used, either by increasing or decreasing ventilation. Two respondents use sealed environments with oxygen absorbers to inhibit the degradation of rubber and latex. Five respondents reported using well-ventilated storage for materials such as CN and CA to prevent the build-up of off-gassing acids.

- *Sealing into barrier foil with oxygen absorbers (rubber, latex);*
- *We have moved cellulose nitrate and acetate objects away from others into ventilated space, but they are not technically isolated*
- *We have a small cool room with separate ventilation for 'Unstable plastics' (if it can fit!)*

As demonstrated by the last comment, space is generally the limiting factor for isolation, cold storage, and ventilation.

- *hoping to move the cellulose nitrate and acetate film into cold storage.*
- *the museum hasn't got a special storage area with cooler temperatures*
- *I would like to freeze rubber objects but freezer capacity is a barrier to this.*
- *No, the right storage facilities/environment are lacking*
- *Composite/large objects are a problem.*

These comments echo Chu et al.'s finding that adoption of cold or cool storage guidelines is limited by '*high financial cost, inappropriate infrastructure or space, a small collection size, lacking manpower for preparation and lack of familiarity with cold storage or time to implement it'* [276].

2.3.11 Condition assessment & monitoring

Ad-hoc assessments of plastic objects are most common, prompted by loan or exhibition plans and in response to visual changes in the object. 29% of respondents carry out regular condition assessments, for instance, yearly. 18% of respondents reported the absence of any condition monitoring on plastic objects within their collection.

Some effort is dedicated to longer-term monitoring methods; for instance, 20% of respondents recorded their use of acid detection (A-D) strips to monitor degrading cellulose acetate objects. Initially developed by the Image Permanence Institute as a visual indicator, a colour change indicates the presence of gaseous acetic acid released by CA films [8]. The potential of monitoring volatile organic compounds (VOCs) as a non-destructive means of tracking degradation markers has been explored, for instance, by using solid-phase microextraction - gas chromatography/mass spectrometry (SPME-GC-MS) [281], but the monitoring of VOCs among respondent's institutions remains limited to the use of A-D strips.

2.4 Conclusion

There are considerable challenges in conserving plastic materials; in particular, CA, CN, PVC, rubbers, and PU remain the focus of a conservator's work with plastics. Most practitioners have observed discolouration, deformation, cracking, and

embrittlement as plastics degrade. Most have also observed sweating and blooming associated with additive migration.

Respondents focused on isolation and controlling environmental conditions during storage to slow degradation. Recommendations for temperature-controlled storage and isolation have developed over the last forty years and were initially proposed to slow the degradation of semi-synthetic cellulosic materials. It is evident that CA and CN are well studied and resourced relative to other plastics; most respondents adopt a similar conservation strategy; the use of cold storage and isolation is most commonly an interventive response to visible signs of degradation, and colourimetric sensors to monitor the extent of acidic emissions are used by around 20% of respondents. Established routines were not as evident for other plastics. As regular condition assessments are uncommon, conservation strategies develop in response to ad-hoc assessments in advance of an exhibit/loan. The interventive approach typically reflects the lack of storage space for temperature-controlled storage or isolation.

Preventive action for plastics also relies on knowledge of the material to plan the best storage environment; for example, according to Shashoua, plasticised PVC should not be stored in contact with PS, PE or metals, and CA should not be stored near metals [6]. As identification is most commonly performed during condition assessments and not at acquisition any preventive action taken from acquisition is not based on an identified plastic type. However, identifying polymers is challenging; practitioners typically rely on their knowledge of an object's history and recently developed flow charts. Only one-third of conservators have used infrared spectroscopy – the least invasive polymer identification method. The challenge of purchasing and running

expensive instrumental equipment is understandable for smaller museums; however, non-destructive analysis can also be preferred even when equipment is available.

Overall, conservators identified polymer identification and inadequate storage as their most significant challenges, which reflects the lack of resources available to plan, prioritise, and implement a conservation strategy before degradation is visibly occurring.

In the context of this thesis, the survey results show that plasticised objects are an acknowledged concern for some respondents, but it is unlikely that plasticised objects are identified. As discussed in chapter 1, isolation is beneficial for limiting migration to other objects, and cold storage reduces migration rate, but neither are routinely employed for the most plasticised material, PVC.

Conservation research to date has focused on external influences on ageing behaviour, whereas outside of the heritage sector, migration tests have confirmed that different plasticisers have different compatibility and, therefore, different expected migration behaviour. To understand the risk of degradation inherent in a material, it would be informative to understand how formulations varied over time and if they can be expected to exhibit different ageing behaviour. The conservation community would also benefit from sharing case studies to establish if patterns in damage type and object lifetime can be observed. To date, examples of plasticiser loss shared within the conservation community are sparse, and common causes are hard to confirm. As the nature of a formulation is currently unlikely to be identified using the most common polymer identification methods, scientific methods should be used to gain a deeper understanding of formulations and related degradation behaviour. There is scope to establish methodology for the analysis of degradation phenomena such as surface

deposits. Wider use of such analysis would aid the conservation community to establish if certain PVC formulations are inherently linked to the vulnerability of an object.

Comments detailing the lack of time, money, expertise, and analytical equipment available to conservators and conservation scientists, highlight room for an approach to additive identification, that is either not reliant on specialised analytical equipment or can be undertaken in a high-throughput fashion on a limited budget.

3 Analysis of plasticized objects by spectroscopic and magnetic resonance techniques

This chapter first details the analysis of PVC samples using infrared spectroscopy, GC-MS, and ^{1}H NMR spectroscopy, before discussing novel methods for cellulose acetate analysis. The work described in this chapter was used to aid the development of a TLC method for PVC plasticiser analysis in Chapter 0.

Qualitative and quantitative analysis of new and vintage PVC objects was performed with established GC-MS and 1H NMR spectroscopy methods for plasticiser analysis on 26 objects suspected to be PVC. Objects were purchased online as surrogates for those found in heritage collections including vintage toys to represent historic PVC formulations and more recently manufactured medical equipment to represent modern formulations.

A section on low-field NMR is not directly applicable in the heritage sector and arose due to limited access to high-field NMR and GC-MS analysis for initial additive analysis during the COVID-19 pandemic. Due to the lower spectral width of low-field systems, which can lead to peak overlap, the study aimed to determine if plasticisers could be distinguished rapidly with a lower-field spectrometer and multivariate data analysis techniques. During the development of the low-field NMR method, Duchowny et al. published a quantitative method for the determination of plasticisers (>3 wt.% DIBP, DEHP, DINCH, DINP or TOTM) by solvent extraction of PVC samples and analysis with a 40 MHz low-field spectrometer [213]. Therefore, the work in this chapter does not progress beyond a qualitative method but expands the range of plasticisers analysed to include DnBP, DIDP, DOTP, DEHA, and ATBC.

To confirm polymer type, samples were analysed using ATR-FTIR spectroscopy. Prior to this work, conclusive identification of PVC by ER-FTIR spectroscopy had proved challenging with established historic plastic libraries when analysing spectra recorded during a survey at Tate [1]. Identifying these PVC objects by ER-FTIR spectroscopy was also challenging due to the complexity of the spectra and poor matching to reference spectra.

Therefore, the chapter also includes a critical analysis of the limitations of the above methods. Some improvements to aid PVC and plasticiser identification are also proposed, for example, new ATR-FTIR spectroscopy libraries were evaluated for the determination of PVC as the polymer type. At the time of the Tate survey, the IRUG database contained three distinct ATR-FTIR spectra for 'phthalate-plasticised PVC', and the PolIRes database contained one downloadable total reflectance spectra of a PVC sample and a KKT-transformed version [282]. One image of an ER-FTIR spectra was available but could not be downloaded or manipulated for analysis with spectral matching software [223]. Since 2021, PVC samples had been included in three open-source ATR libraries for microplastics; the Primpke, FLOPP, and FLOPP-e libraries [283,284]. Using these methods 24 of the objects were identified as PVC and contained identifiable plasticisers of PVC.

CA analysis

The second part of the chapter describes the analysis of cellulose acetate using ^{1}H NMR spectroscopy and magnetic resonance imaging. As discussed in Chapter above1, FTIR spectroscopy can be used for CA identification and we previously demonstrated plasticized CA can be analysed by solution-state ^{1}H NMR. The polymer's degree of substitution, and DEP content can be measured using the two

methods described in Figure 27 and Figure 28, respectively. Two different sample preparation methods are required; hereafter referred to as the 'DS method' and 'qNMR-DEP method', respectively.

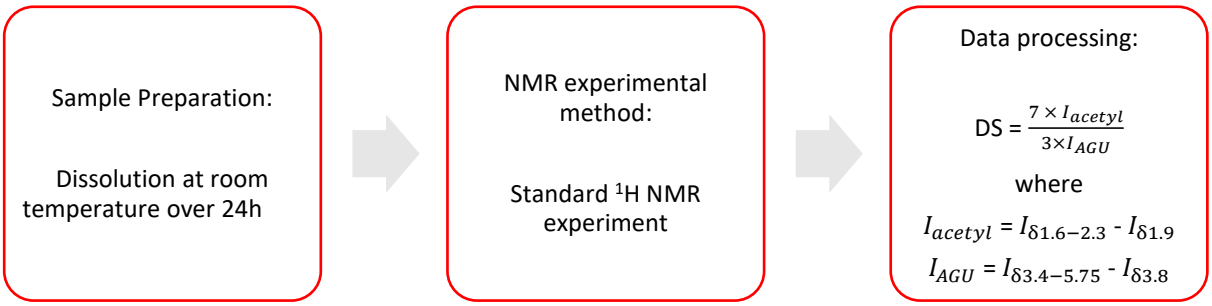

Figure 27: DS method reported in reference [158].

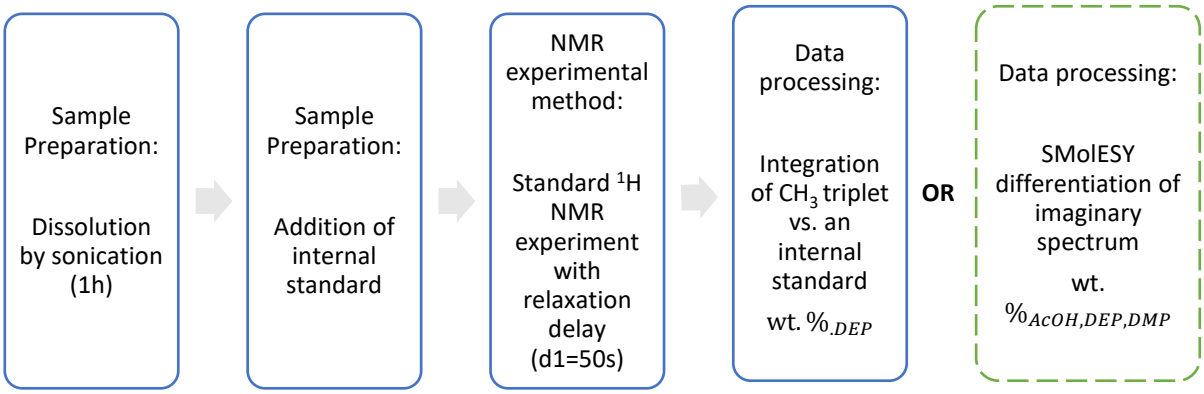

Figure 28: qNMR method to measure wt.% DEP is referred to as the 'qNMR-DEP method'. The dashed line denotes the proposed processing method using the SMolESY transformation ('qNMR-SMolESY method').

DS measurement relies on the analysis of peaks overlapped by aliphatic protons present in small molecules such as acetic acid and dimethyl phthalate; the method described in Figure 27 subtracts acetic acid and dimethyl phthalate integral regions between 2.3 and 1.6 ppm and 5.75 and 3.40 ppm, respectively. The DS method also

uses a short interscan delay, which is long enough for complete relaxation of polymeric protons but does not fulfil qNMR criteria for complete relaxation of phthalate protons.

Following the qNMR criteria for an interscan delay greater than 5 x T_1 for a 90° pulse, an interscan delay of d_1 = 50 s and 30° pulse allows an accurate quantification of DEP using the distinct methylene triplet resonance at 1.25 ppm (T_1 = 2.76 s) and an internal standard (T_1= 10 s). Theoretically, interaction with the polymer can affect the relaxation process, so the sample is sonicated to decrease the risk of matrix effects on the quantification. However, quantification of analytes other than DEP has not been attempted due to overlapping polymer signals. In an unpublished attempt to unify both methods, samples were prepared and analysed by the qNMR-DEP method but processed for DS measurement. However, more significant variability in calculated DS values resulted, potentially from sonication or thermally induced deacetylation.

CA spectra are characterized by broad polymer-derived resonances alongside observable but overlapped peaks for small-molecule additives and acetic acid. Consequently, spectra of plasticized cellulose acetate samples were processed using the recently published SMolESY method (qNMR-SMolESY method, Figure 28**)** which has been used to analyse complex spectra from biological samples. The principal aims were to assess if the derivative spectra could resolve non-polymeric species and allow quantitative analysis. Additionally, we report a further attempt at unifying the DS and qNMR methods into a single experiment ‘all-in-one’ method.

3.1 Research Questions

The work summarised above aimed to answer the following research questions for PVC:

- Can infrared spectroscopy be used to differentiate between plasticiser types?
- Is low-field NMR suitable for plasticiser identification?
- Can new ATR-FTIR spectroscopy libraries be used to the identify PVC?

For cellulose acetate, this work aimed to:

- Understand if small molecule peaks can be resolved from polymeric peaks using SMolESY-NMR for CA?
- Explore if one qNMR method can be used to analyse polymer degree of substitution and plasticiser content?

3.2 Methodology

3.2.1 FTIR spectroscopy

All spectra were collected on a Bruker Alpha II spectrometer equipped with a Diamond ATR or External Reflectance QuickSnap module using OPUS v7.5 software (Bruker Optik GmbH, Ettlingen, Germany). All spectra were recorded in the range of 4000 – 399 cm^{-1}, with a spectral resolution of 4 cm^{-1} and 16 co-added scans. Background spectra were recorded before analysis, and the ATR crystal was wiped with isopropanol to remove contamination between samples. No baseline correction or smoothing was undertaken.

Samples (~3 x 3 mm) were removed from the object with a scalpel for ATR-FTIR spectroscopy where necessary. For ER-FTIR spectroscopy, objects were held tight to the sampling aperture (3.5 x 1.5 cm). A similar small aperture used by Bell et al. for curved surfaces was not available. However, all samples aside from tubing contained an area large enough to cover the aperture. Where a spectrum is labelled ‘transflection’, a reflective gold mirror was held behind the sample during spectrum collection.

Spectragryph software (v. 1.2.13) was used for library matching. PCA was performed using the PCA for Spectroscopy package in Origin 8.0.

External reflectance spectra were transformed to pseudo-absorbance spectra using the Kramers-Kroning Transformation available in EssentialFTIR software (Operant LLC, Monona, WI, USA). Identification of peaks between 720 - 760 cm^{-1} was performed using the Peak Analyzer tool in Origin 8.0 (OriginLab, Northampton, Massachusetts, USA) without setting a baseline, and using a peak height threshold of 20.

The signal-to-noise ratio (SNR) was measured as the ratio of the intensity of peaks between 720 - 760 cm^{-1} and the root mean square of background noise between 760 - 800 cm^{-1}.

ATR-FTIR spectra were compared to two open-source ATR-FTIR spectroscopy reference libraries provided by Primpke et al. and the FLOPP and FLOPP-e libraries created by De Frond et al.[283,284]. The FLOPP-e library contains spectra from 'weathered' samples collected by outdoor environment sampling, compared to FLOPP's use of virgin plastics. The similarity between spectra was assessed from the measured Pearson correlation coefficient of the whole spectrum (ATR v. FLOPP & ATR v. FLOPP-e: 675 - 4000 cm^{-1}, ATR v. ER & ATR v. Primpke: 400 - 4000 cm^{-1}) using Origin 8.0 or Spectragryph software (v. 1.2.13).

Averaged spectra were produced for each aromatic plasticiser type (phthalate, terephthalate, trimellitate), as identified by ^{1}H NMR, and a mean average spectrum was calculated using the 'Average' function in Spectragryph software (v. 1.2.13).

3.2.2 Gas Chromatography – Mass Spectrometry (GC-MS)

GC-MS analysis was performed on a Thermo Scientific Trace 1310 Gas Chromatograph connected to an ISQ single quadrupole mass spectrometer using EI mode (70 eV), a 5% Phenyl Polysilphenylenesiloxane TR-5MS column (30 m x 0.25 mm (i.d.) x 0.25 µm film thickness), and a helium mobile phase. 0.2 µl of each extract is injected by the autosampler (TrisPlus RSH) in splitless mode.

The GC oven temperature was ramped from 100 °C to 200 °C at 30 °C $min^{-1,}$ then to 250 °C at 3 °C min^{-1}, held for 2.5 min, ramped to 270 °C at 40 °C min^{-1}, held for 2 min, ramped to 320 °C at 80 °C min−1 and held for 5 min. The injection port and

transfer line temperatures were both set at 300 °C. The ion source temperature was set to 230 °C, and the helium carrier gas flow rate was 1 mL min^{-1}. Mass spectra were recorded after a solvent delay of 2.5 min and a run time of 31.0 min. The acquisition was performed in full-scan mode (m/z = 40–350).

Retention times of each analytes were determined by injection of a standard solution (EPA Method 8061A Phthalate Esters Mixture, Restek, Bellefonte, Pennsylvania, United States) containing 15 phthalates (1000 µg/mL each in 80:20 hexane:acetone).

3.2.3 ^{1}H NMR Spectroscopy for PVC samples

^{1}H NMR analysis followed an adapted literature procedure [212]. Plasticized PVC (10 mg) was steeped in $CDCl_3$ (0.8 mL) for 2 hrs at room temperature. 0.5 mL of the extract was withdrawn and introduced into NMR tubes, followed by 0.15 mL of an internal standard solution (64 mM benzyl benzoate in $CDCl_3$).

Pure plasticiser samples were prepared at a concentration of 250 mM in NMR grade deuterated chloroform.

High field ^{1}H NMR spectra were acquired at 298 K on a Bruker Avance Neo 700 MHz NMR spectrometer equipped with a helium-cooled broadband cryoprobe, using a standard single pulse experiment with a 30° pulse and 16 scans. A relaxation delays of 50s was used to ensure complete relaxation for quantitation, the acquisition time was 4s.

Low field ^{1}H NMR spectra were acquired using a Nanalysis 60e benchtop NMR spectrometer at a 60.11 MHz proton frequency. Samples were pre-heated at 34 °C prior to placing them in the spectrometer. Chemical shifts are expressed in parts per

million (ppm, δ) and are referenced to the residual solvent signal of $CDCl_3$ (7.26 ppm for ^1H NMR). All coupling constants (J) are absolute values and are expressed in hertz (Hz).

Spectra were analysed using MestReNova (v.14.2.0, MestreLab Research S.L, Madrid) or TopSpin software (v. 3.6.2, Bruker BioSpin GmbH, Germany).

3.2.4 ^1H NMR spectroscopy for CA samples

Sample preparation followed the method described by Da Ros et al; for all NMR analyses, deuterated dimethyl sulfoxide (DMSO-d_6, 99.9 atom % D, Sigma Aldrich, London, United Kingdom) was used as solvent. ^1H NMR spectra were acquired at 298 K on a Bruker Avance Neo 700 MHz NMR spectrometer equipped with a helium-cooled broadband cryoprobe, using a standard single pulse experiment with a 30° pulse. Proton relaxation delays were set to 50 s, the acquisition time was 4s and the number of scans was equal to 32.

Phase and baseline correction were performed using the TopSpin software, version 4.0.3 or Mestrenova. All ^1H chemical shifts were referenced to the residual DMSO solvent signal at 2.50 ppm.

Samples analysed using the all-in-one method were prepared as follows. Cut samples (~15 mg) were dissolved in DMSO- d_6 (650 µL), followed by a 150 µL of 112 mM solution of 1,2,4,5-tetrachloro-3-nitrobenzene in DMSO- d_6 which was prepared immediately prior to use. 0.5 mL of this solution was transferred to an NMR tube immediately prior to analysis.

Spectra were analysed (peak picking and integration) using the SMOLESY package available for use in MATLAB (2019b).

3.2.5 Magnetic Resonance Imaging for CA samples

2 mm thick DEP plasticized cellulose acetate sheets (0, 10, and 20 wt.%) werre previously prepared and stored at 4°C from manufacture. 0 wt.% and 10 wt.% samples were prepared and donated by Dr Simoni da Ros and Isabella del Gaudio. Samples were removed from the refrigerator, placed in a petri dish, and allowed to condition in a silica gel desiccator for 1 hour at room temperature before being cut into squares (40 mm x 40 mm) and weighed (N=3).

3 ‘dry’ samples were placed in a desiccator post-weighing for 19 hours. Samples were re-weighed and replaced in a desiccator one hour before transfer to the scanner bed. 5 ‘wet’ samples were immersed in distilled water after weighing for a variable length of time (Table 17). As no scales were available at the MRI facility, samples were removed one hour before analysis, surface water was removed with a paper towel, samples were weighed, and then re-immersed. Immediately before analysis, samples were removed, and surface water was removed with a paper towel.

Both drying and immersion methods resulted in variable water contents between samples (Table 17). Samples with lower plasticiser content absorbed more water, an observation confirmed by the dynamic vapour sorption study reported by del Gaudio et al. [285]. For dried samples, mass loss was observed to decrease as initial plasticiser content increased. However, the origin of mass loss cannot be confirmed for samples 6- 8 as the plasticiser content was not monitored during drying.

Table 17: Experimental parameters, sample composition, and mass change upon immersion in water or placement in a silica gel desiccator.

Sample number	**Composition**	**Submersion time (h)**	**Drying time (h)**	**Mass change from immersion (%)**	**Mass change on drying (%)**
1	0 wt.% DEP CA	16	-	6.6	-
2	10 wt.% DEP CA	114	-	4.2	-
3	20 wt.% DEP CA	190	-	2.9	-
4	20 wt.% DEP CA	3	-	1.4	-
5	20 wt.% DEP CA	1	-	1.0	-
6	0 wt.% DEP CA	-	19	-	-3.7
7	10 wt.% DEP CA	-	19	-	-2.7
8	20 wt.% DEP CA	-	19	-	-1.5

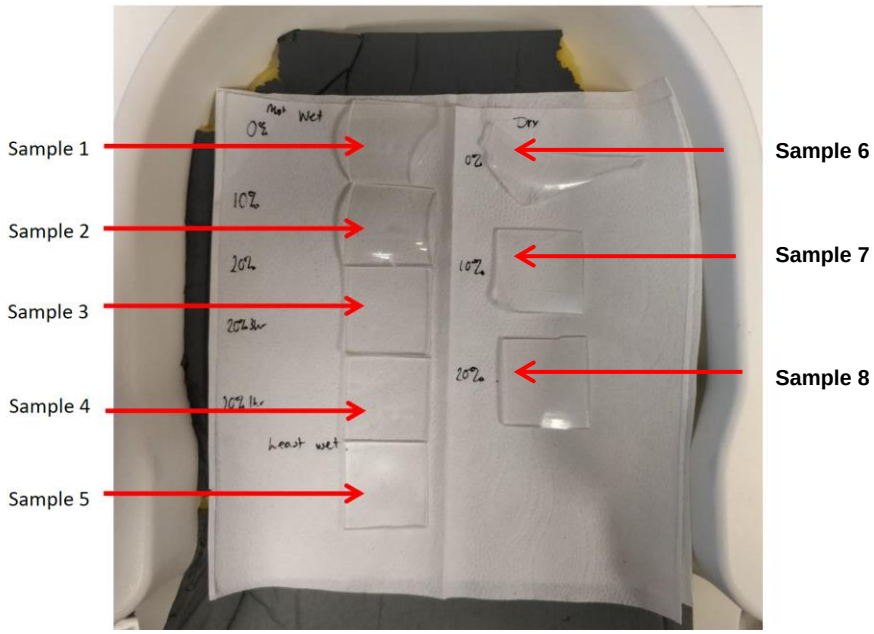

Figure 29: Placement of samples within the RF receiver head coil. Image courtesy of Dr S Wastling.

Dr Stephen Wastling performed image acquisition and data analysis at Queen Square Institute of Neurology, UCL, London. Image acquisition was performed on a 3Tesla Siemens PrismaFit clinical MR scanner (Siemens Healthineers AG, Munich, Germany).

A proprietary ultrashort-TE (UTE) pulse sequence ('PETRA') with radial k-space sampling was used with default parameters (Table 18). TE was varied between 0.07 ms and 0.1 ms in increments of 0.01 ms.

A saline bag was placed in the head coil to tune the ^{1}H frequency of the scanner before acquisition due to the absence of a sufficiently strong signal from the samples. Signal intensity was averaged across multiple 0.9 mm^3 voxels. No signal contamination from the polymeric head coil material or adjacent samples was observed.

Table 18: Default settings of PETRA UTE pulse sequence, sourced from [12]

Parameter	Default
Repetition Time (TR) 1	3.32 ms
Repetition Time (TR) 2	2250 ms
Echo Time (TE)	0.07 ms
Inversion Time (TI) 1	1300 ms
Inversion Time (TI) 2	900 ms
Slice Thickness	0.9 mm
Field of View	300 × 300
Matrix	320 × 320
Voxel Size	0.9 × 0.9 × 0.9 mm
Bandwidth	400
Flip Angle	6 degrees
Radial Views	60,000
Acquisition Time	5:57 minutes

3.3 Results

3.3.1 Quantitative sample analysis by ^{1}H NMR and GC-MS

Table 19 shows the plasticiser(s) identified and quantified by ^{1}H NMR spectroscopy and GC-MS for each object. There was no noticeable trend in plasticiser use with object age aside from the dominance of DEHP. The transition to non-phthalate plasticisers in consumer products and medical devices was clear in the most recently manufactured samples (FMO, ERA, BBI, HEI, NIP, VYG, FKB).

There is good agreement between the result from NMR and GC-MS analysis, although it is likely that incomplete precipitation of PVC during work-up occurred where there a lower concentration was measured by GC-MS (e.g. PIL). Only DEHP was quantified by GC-MS due to instrument downtime and the unavailability of a reference standard. Samples analysed later (FMO onwards) were not assessed by GC-MS as the NMR method proved reliable and quick without the multi-step preparation method or calibration curve required for GC-MS analysis.

Table 19: Plasticiser content per sample, as determined by ^{1}H NMR spectroscopy and GC-MS.

Sample	**Plasticiser identity and content (wt. %)**	
	^{1}H NMR	**GC-MS (largest m/z if RT varies vs standard)**
PIL	36 DEHP	27 DEHP
SNO	42 DINP	DINP
DOG	38 DINP	DINP
NOD	37 DEHP	38 DEHP

GRG	~28 DINP	DINP (418)
DOD	29 DEHP	13 DEHP
PNK	~40-43 Unknown phthalate	DIHpP (362)
WHD	~33 DINP	DINP (418)
PHC	Unknown	No analytes detected
BLC	14 DEHP 7 DBP	11 DEHP 11 DBP
RDC	14 DEHP, 7 DBP	Not analysed
MCS	27 DINP	DINP
TCS	6 DIUP + unknown	triphenyl phosphate (m/z 326, 327, 77) isopropyl phenyl diphenyl phosphate (m/z 368, 251, 118, 77) No phthalates (m/z 149)
PEN	21 Unknown phthalate + unknown	15 DEHP
YED	38 DEHP	41 DEHP
FMO	30 ATBC	Not analysed
ERA	39 pentaerythritol tetravalerate	Not analysed
BBI	17 TOTM	Not analysed
NIP	28 TOTM	Not analysed
VYG	28 DOTP	Not analysed
FKB	41 DEHP	Not analysed
SUC	25 DOTP	Not analysed
HEI	26 DOTP	Not analysed
TBW	30 DEHP	DEHP

By ^{1}H NMR spectroscopy, phthalate additives were confirmed by characteristic resonances at δ7.7- and δ 4-4.4 ppm but determining the exact nature of the alkyl chain was more challenging. If the alkyl chain could not be identified, the number of protons measured from δ 0.5 – 2 ppm was matched against the formula of known phthalates. The molecular weight of the matched phthalate was used to estimate the percentage composition by weight (wt. %). By GC-MS, matching to the NIST library was inconclusive, although a phthalate moiety with m/z = 149 was present in all three samples and the largest m/z ion were used to identify the phthalates in WHD, GRG and PNK.

Sample TCS was later confirmed to be a TPU plastic, similar in form to PVC and mistakeable using the PIK identification method. Interpretation of the ^{1}H NMR was likely erroneous as phthalates are not in use with TPU.

3.3.2 Qualitative analysis by ATR-FTIR spectroscopy and ER-FTIR spectroscopy

Table 20 uses the physical descriptors identified by Bell et al. to describe a sample's features of relevance and the recommended sampling method (ATR or ER). Figure 30 shows ATR-FTIR spectroscopy and Kramers-Kroning transformed (KKT-ER) spectra for each sample. Individual spectra are available in appendix 8.6 and 8.7.Only 3 objects were unable to be analysed using the ER setup; as most tubing did not cover the ER sampling aperture, and thin samples correlated with lower spectral quality in the objects studied. As shown, thin flat samples GOC, COC, BLC and RDC all produce distorted and noisy spectra, whereas thicker samples generally result in a higher quality spectrum.

Additional context was considered when interpreting spectra. All samples, excluding fabrics, were classed as ‘elastomers’ using the Plastic Identification Toolkit. According to the toolkit, prime candidates were therefore limited to natural rubber, flexible polyurethane, plasticized PVC, silicone rubber, and synthetic rubber. Library matches which were not PIT candidates were manually evaluated, and no additional elastomeric candidates were identified through this analysis.

Table 20: Sample characteristics and recommended sampling

Sample	Date mark or estimated decade	Indications of polymer from packaging and branding	Object descriptors (c.f. Bell et al.)							ER spectra recorded?
			Textured /Smooth	Matte/ Glossy	Curved/ Flat	Flexible/ Rigid	Soft/ Hard	Robust/ Fragile	Bell's recommended sampling method	
DOD	1960s	-	S	M	CF	FR (aged)	S	F	ATR	Y
GRG	1970s	-	S	M	CF	FR	S	R	ATR	Y
GOC	2021	'Oilcloth'	S	G	F	F	S	R	ER	Y
HEI	2021	-	S	G	C	F	S	R	ATR	Y
MCS	2021	-	S	G	F	F	S	R	ER	Y
NIP	2021	-	S	G	C	F	S	R	ATR	N
NOD	>1984	Playmakers Noddy Vinyl Squeaker	S	M	CF	F	S	R	ATR	Y

PEN	1960s	Sunshine Vinyl Toy (Mettoy)	S	M	CF	F	S	R	ATR	Y
PHC	2010s	-	S	M	F	F	H	R	ER	Y
PIL	>1972	-	S	M	CF	FR	S	R	ATR	Y
PNK	Unknown	-	S	G	CF	FR (solid)	H	R	ER	Y
SNO	>1974 by presence of a barcode	Vinyl Squeak Toy	S	M	CF	F	S	R	ATR	Y
SUC	2021	-	S	G	CF	F	S	R	ER	Y
DOG	1960s	Vinyl Squeeze Toy	S	M	CF	F	S	R	ATR	Y
WHD	1960s	-	S	G	CF	F	S	R	ER	Y
FMO	2021	-	S	M	F	F	H	R	ER	Y
ERA	2021	-	T	M	F	FR (solid)	H	R	ER	Y
FKI	2021	-	S	G	C	F	H	R	ATR	N
BBI	2021	-	S	G	C	F	S	R	ATR	Y

CLO	2021	‘Oilcloth’	S	G	F	F	S	R	ER	Y
BLC	1980s	-	T	M	F	F	S	R	ATR	Y
RDC	1980s	-	T	M	F	F	S	R	ATR	Y
VYG	2021	-	S	G	C	F	S	R	ATR	N
YED	1990s	Vinyl Toy	S	M	CF	F	S	R	ATR	Y

Attempts at sample collection without clamping objects to the ATR crystal or destructive sampling (c.f. Bell et al.) were unsuccessful aside from flat sheet/fabric material. When a suitable edge or corner of an object was identified, the geometry of the object frequently limited the use of the clamp, and manual pressure was not sufficient to record a spectrum. Instead, ATR-FTIR spectra were recorded by destructive sampling of a thin <0.5 mm slice from the surface with a scalpel. Clamping samples in a non-destructive manner was possible for all 2D sheet materials (PHC, TCS, MCS, COC), a 1 mm thick protrusion for PNK, and WHD as the shoe sole geometry was akin to a sheet material.

Usable ER spectra were not recorded for samples NIP and HEI as the transparent flexible tubes were unable to fill the sampling aperture and hence resulted in spectra dominated by noise. Transparent and thin materials generally gave poor results due to insufficient reflectance of the incident light, such that the contribution of the sample environment is clearly observed in samples BAL, RDC, and COC and VYG. The increasing sample thickness of two transparent PVC fabrics from COC to MCS confirms this observation; wherein the MCS spectra contains low-intensity but distinct peaks below 1800 cm^{-1}. Sample BBI, a similar but wider transparent tube, did provide a higher quality ER spectrum when coiled to maximize the sample amount within the aperture.

For spectra showing visible amounts of noise during acquisition, a mirrored surface was also held behind the sample to enhance reflection back to the detector. Figure

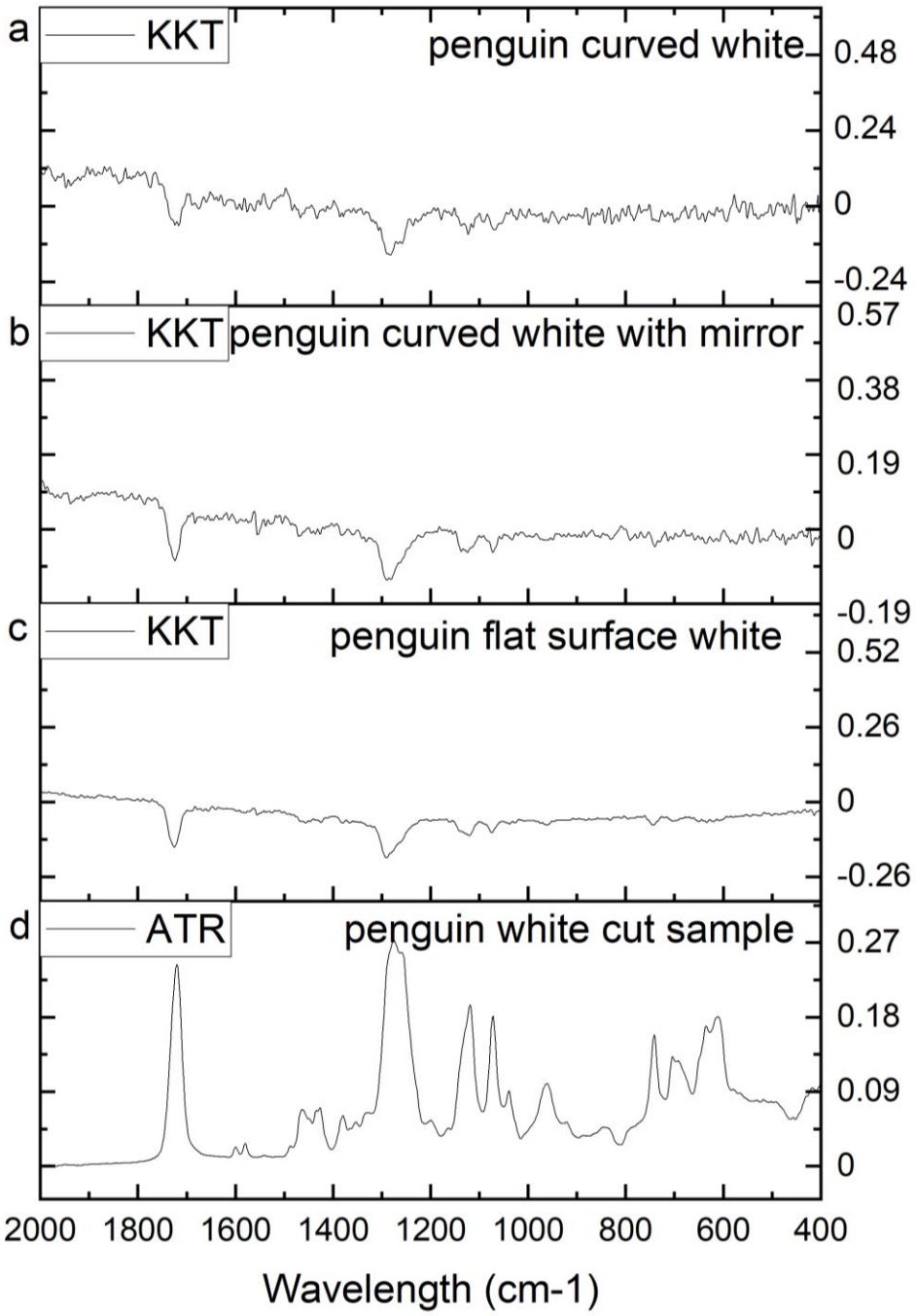

32 and

Figure 33 show multiple spectra for the PEN sample and illustrate how noise reduces with reflection from a mirrored surface (a vs b) and signal quality improved for flat versus non-flat surfaces (a vs c).

Distortion was evident in all external reflectance spectra in Figure 30, especially above 1800 cm^{-1}. Baseline correction by fitting a quintic function appeared suitable for some KKT-ER spectra, but no single method of baseline correction was suitable for all, so no further spectral pre-processing was applied to ATR-FTIR spectroscopy or KKT-ER spectra.

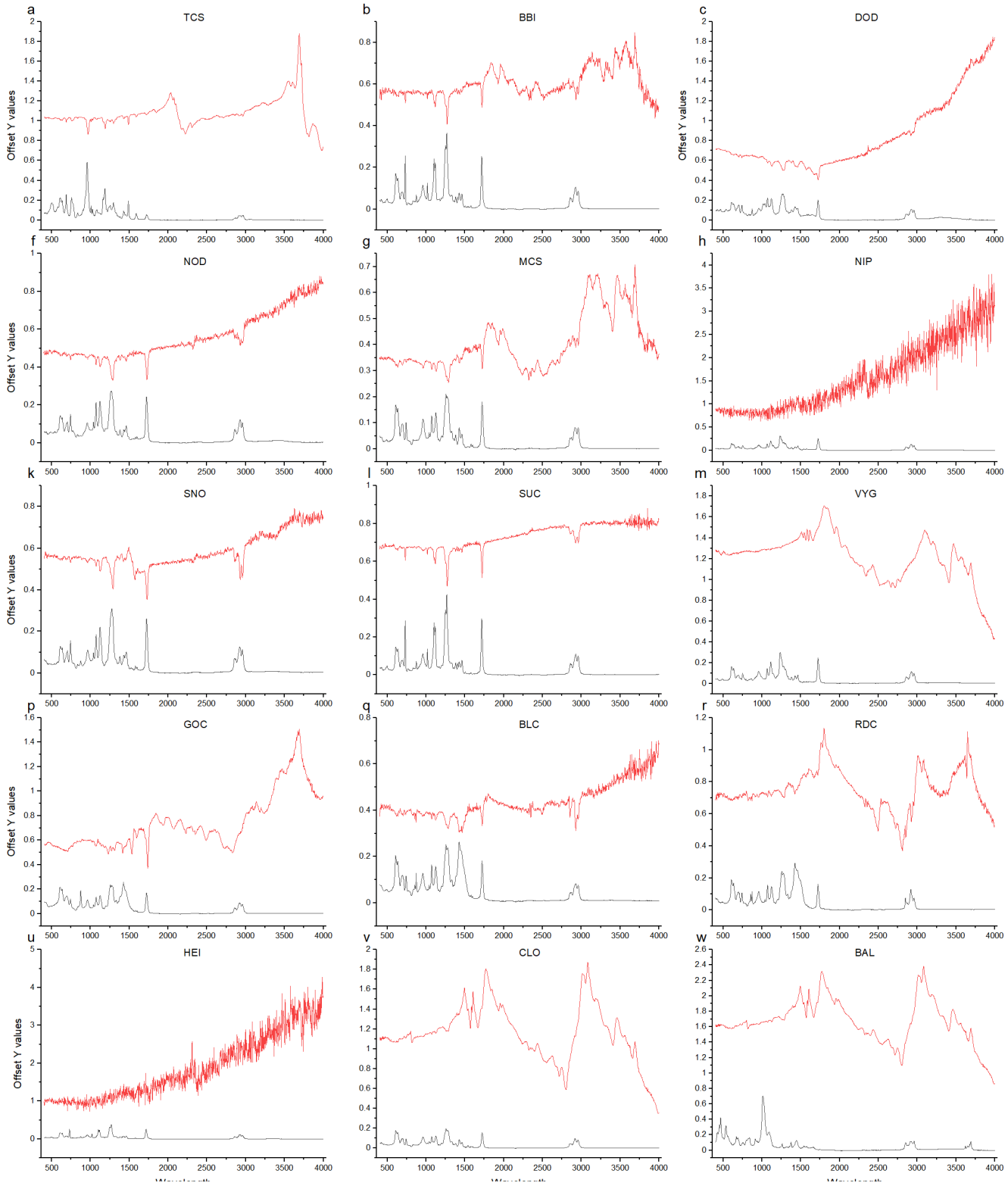

Figure 30*a*: Comparison between KKT-ER-FTIR spectra (red line) and ATR-FTIR spectra (black line) for each suspected PVC sample.

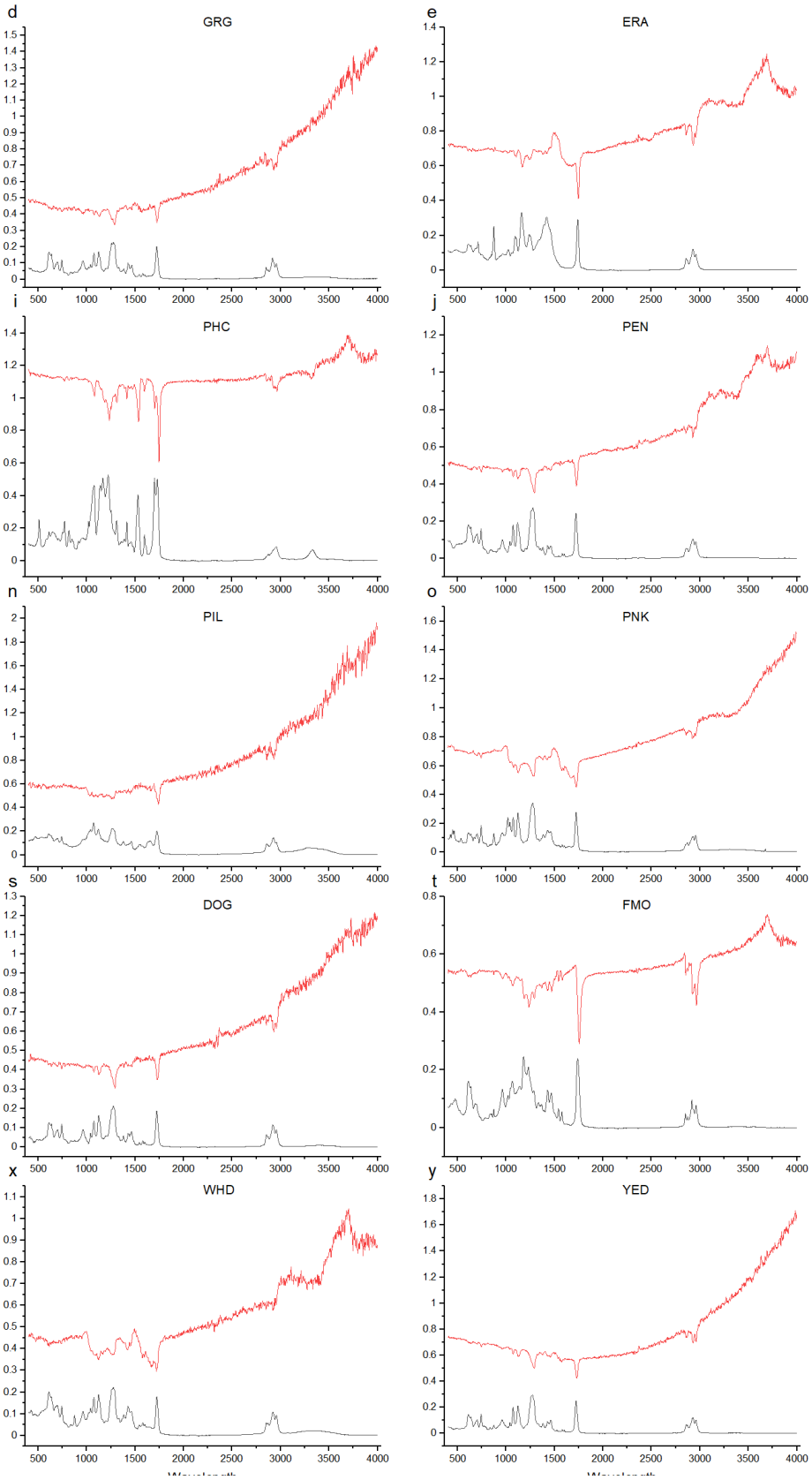

Figure 31*(contd):* Comparison between KKT-ER-FTIR spectra (red line) and ATR-FTIR spectra (black line) for each suspected PVC sample.

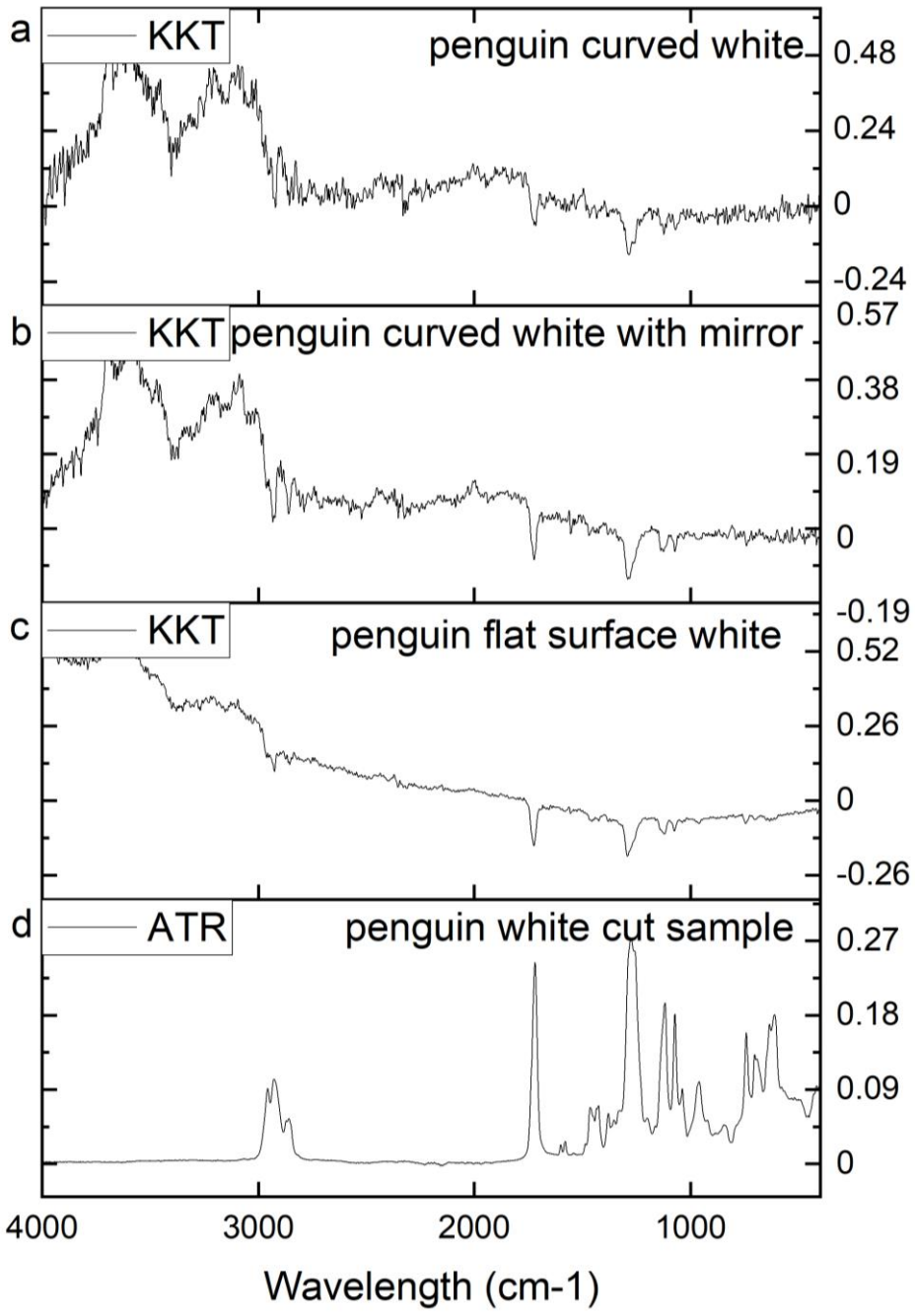

Figure 32: The quality and SNR of external reflectance spectra are impacted by specular reflectance from a curved surface (a) versus a flat surface (c). The signal-to-noise ratio improved when a mirrored background was placed behind the sample (transflection) (b).

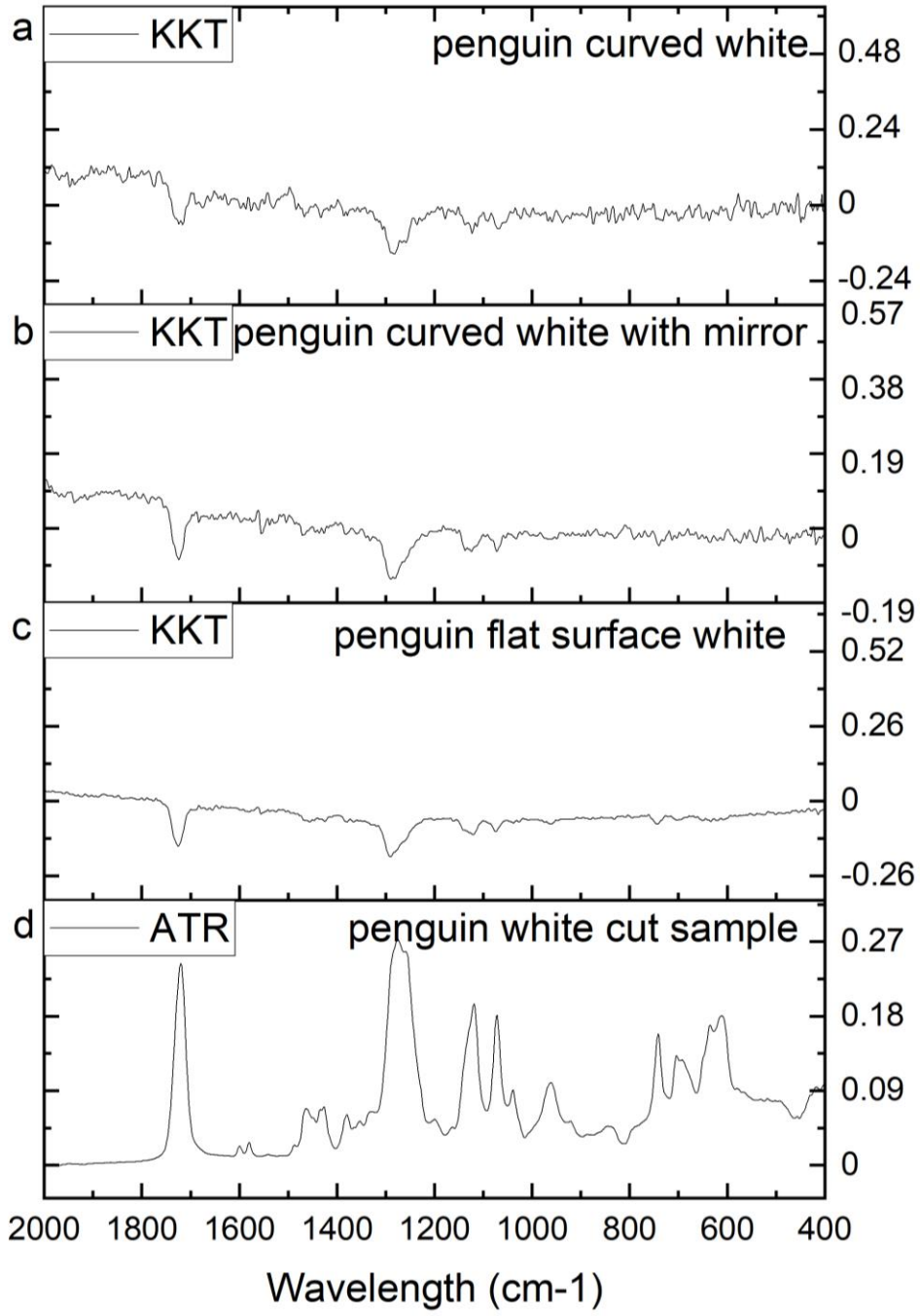

Figure 33: While Restrahlen bands appear at high wavelengths, they have no noticeable impact below 1800 cm^{-1} which is the region used for additive identification.

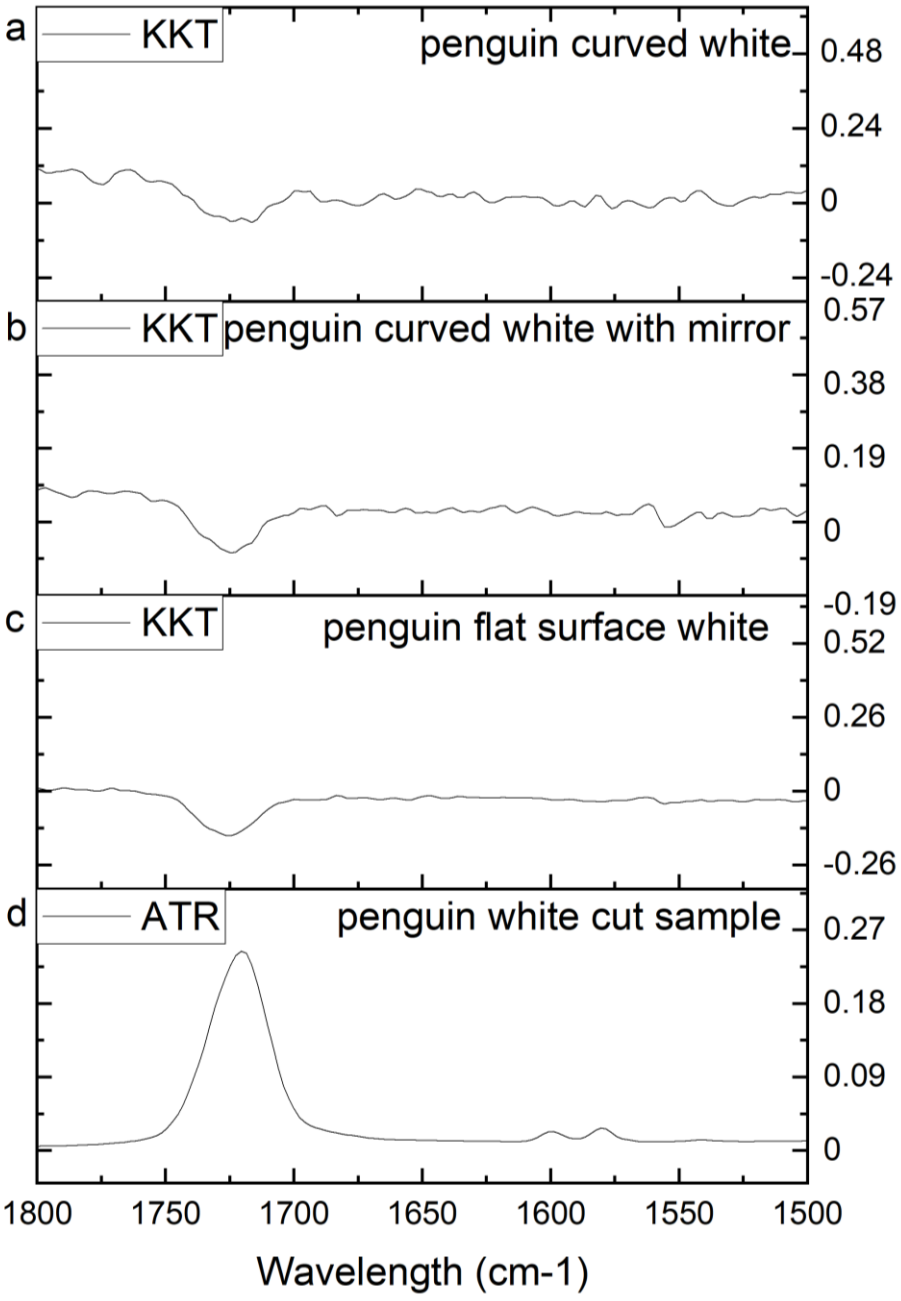

Figure 34: Weak intensity doublet peaks at 1580 and 1600 cm^{-1} can quickly identify phthalate plasticized PVC by ATR-FTIR spectroscopy, but the corresponding peaks are rarely recorded with external reflectance spectroscopy due to low intensity and significant baseline noise.

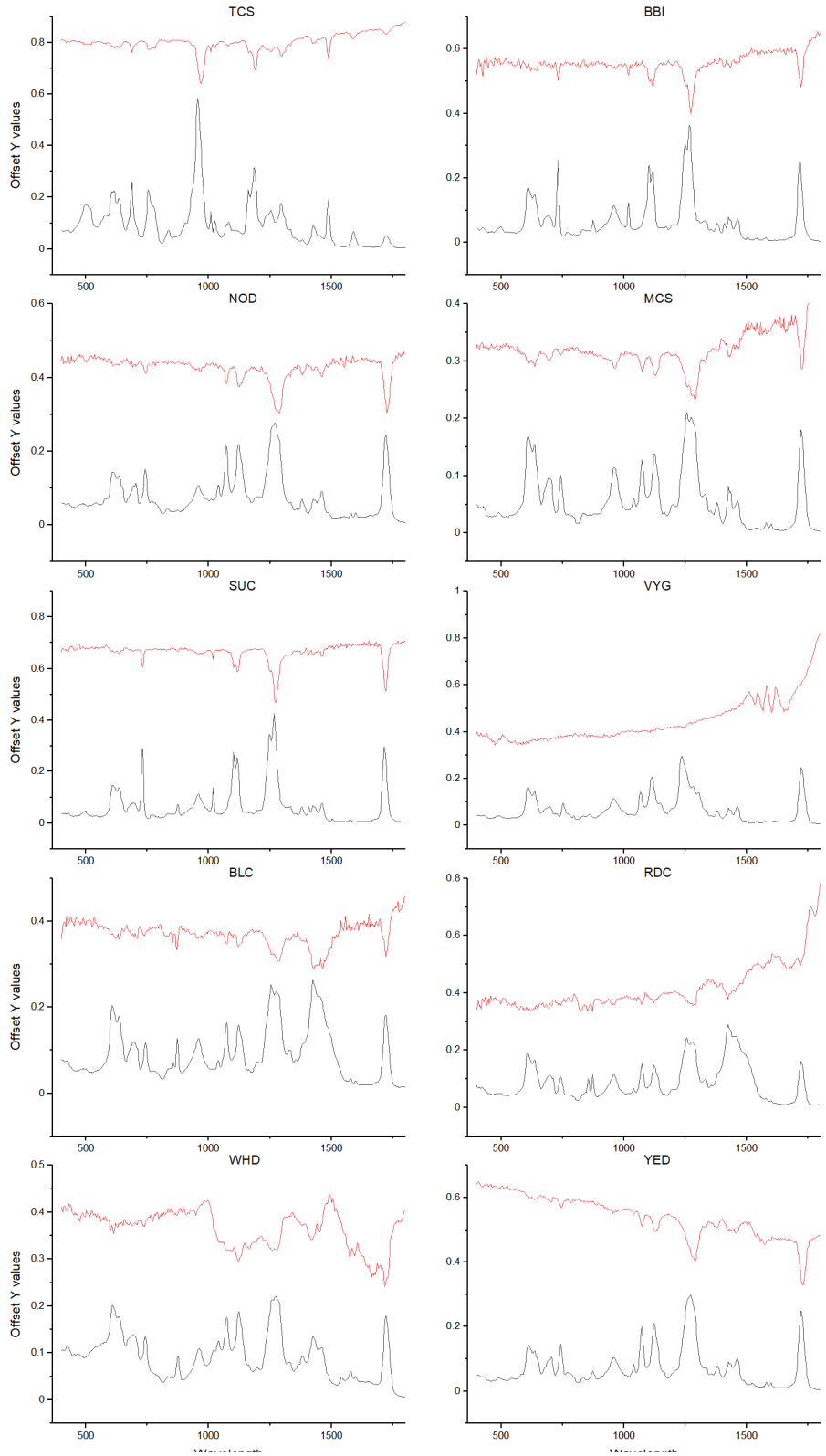

Figure 35: Expanded 400-1800 cm^{-1} region of KKT-ER-FTIR spectroscopy (red line) and ATR-FTIR spectra (black line) for each sample. N.B samples NIP and HEI are not shown due to noise-dominated ER-FTIR spectra.

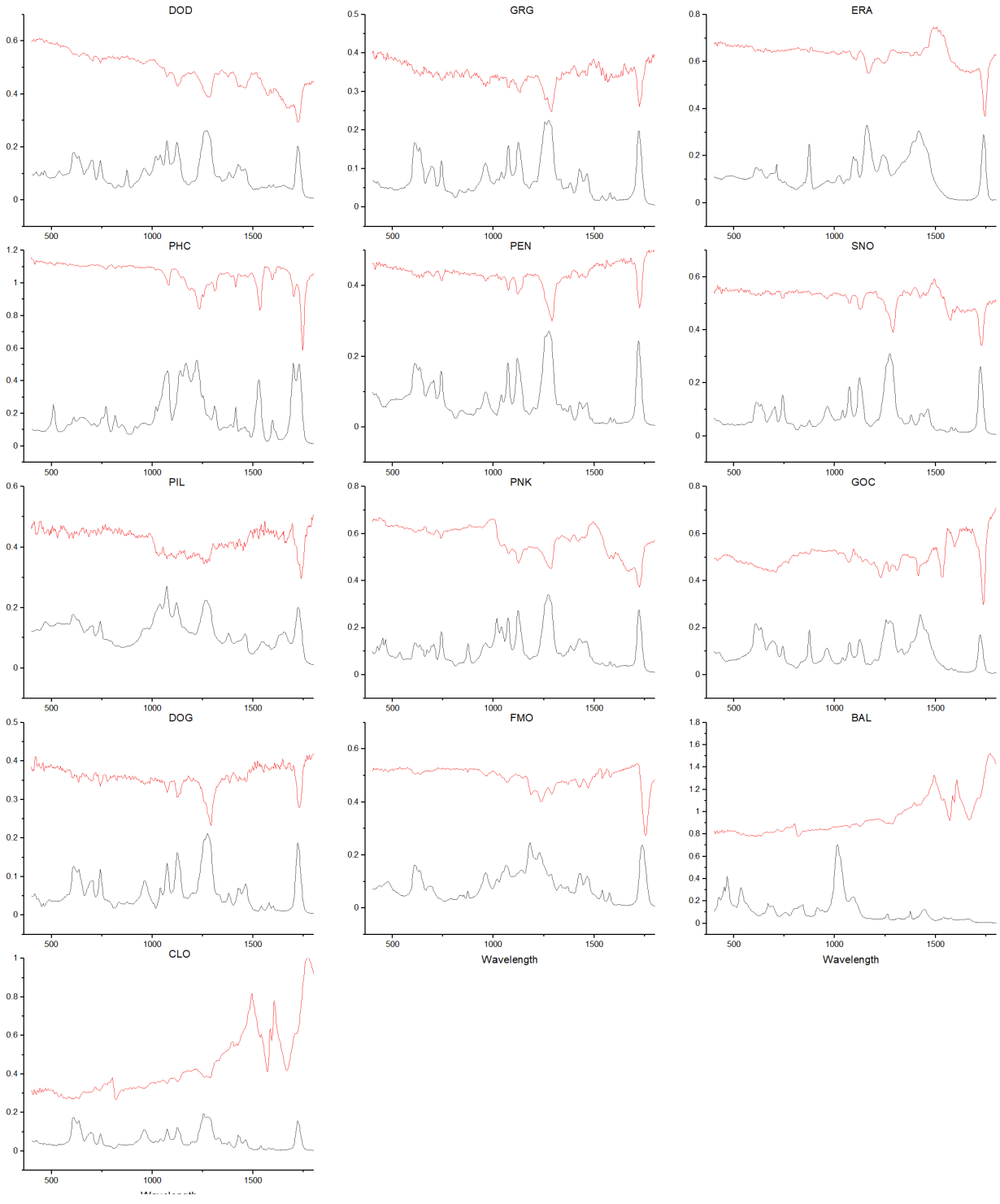

Figure 36(contd): Expanded 400-1800 cm^{-1} region of KKT-ER-FTIR spectroscopy (red line) and ATR-FTIR spectra (black line) for each sample. N.B samples NIP and HEI are not shown due to noise-dominated ER-FTIR spectra.

3.3.3 Principle Component Analysis of ATR-FTIR spectra for outlier detection

As in previous studies to differentiate microplastic spectra, PCA was used to rapidly identify outlier samples before library matching. The first two principal components explained a majority of the variance (76%) between spectra and highlighted outliers which were later confirmed by comparison to spectral libraries as a polyurethane phone case (PHC), a PVC/cloth composite oilcloth (GOC).

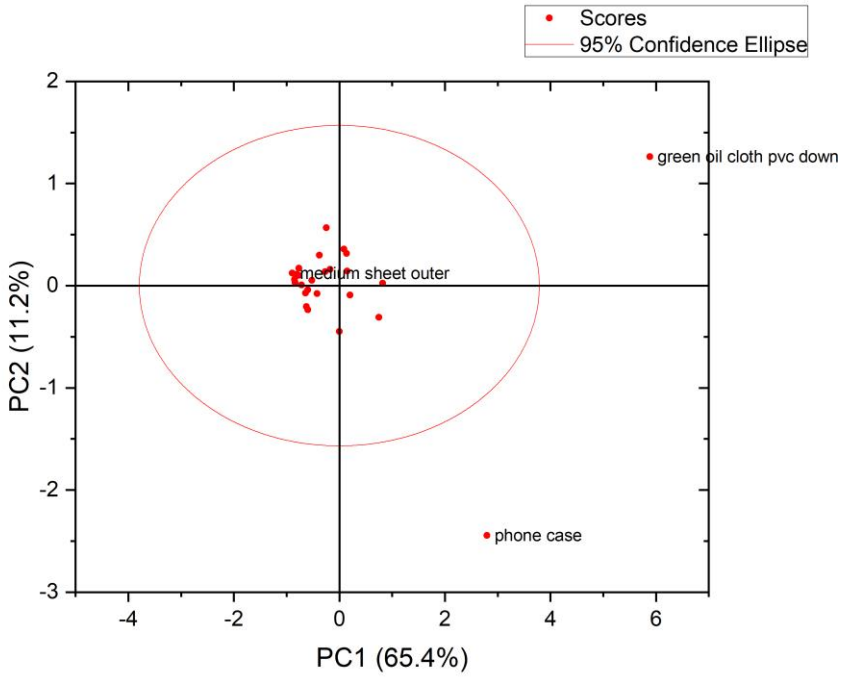

Figure 37: Covariance PCA, showing phone case and green oil cloth samples as outliers.

3.3.4 Spectral library matching for the identification of PVC by ATR-FTIR spectroscopy

Polymer identification was based on the highest Pearson's correlation coefficient when the sample spectra was compared to the full library spectra set. Individual spectra are detailed later in the chapter. To simplify interpretation and highlight the importance of representative libraries Table 21 shows how three spectra (representing the average of all spectra recorded per aromatic plasticiser class) matched to all 'PVC' labelled library spectra. The FLOPP-e and FLOPP library spectra consistently gave the highest correlation coefficients versus the Primpke library. Matches to PVC 5, 21, 27 (FLOPP) are similar across the averaged spectra, while the more intense phthalate peaks in PVC 24 and 25 lead to poor matches for TOTM and DOTP plasticised samples.

The results of matching between individual sample ATR spectra and the three open-source ATR-FTIR spectroscopy libraries are available in appendix 8.2. In general, the 'pronounced peaks, an uneven baseline, and increased spectral noise, indicative of environmental weathering' led to slightly lower correlation coefficients with FLOPP-e library spectra. 27/37 and 29/37 spectra were correctly identified as PVC using the FLOPP and FLOPP-e, respectively. Four individual samples were mischaracterised by FLOPP but were correctly identified with the FLOPP-e library. Two of those samples were DOTP and TOTM plasticised, but as seen in Table 21, correlation to TOTM and DOTP samples can be strong despite their lack of representation in the libraries.

*Table 21: The results of library matching for averaged sample spectra against FLOPP, FLOPP-e and Primpke libraries. Colour gradients indicate the highest (green) to lowest (red) match per averaged sample. *Visual inspection included identification of 741, 730 and 752 cm^{-1}peaks, and a lack of intense carbonyl peaks at 1720 cm^{-1} indicative of plasticised samples.*

Library	**Reference spectra in library**	**Plasticiser identified by visual inspection***	**Pearson's correlation coefficient spectra (%)**		
			DOTP plasticised - averaged	**Phthalate plasticised - averaged**	**TOTM plasticised - averaged**
FLOPP	PVC 5. Clear Clingwrap Film	Unknown	76.54	83.63	84.49
	PVC 21. Green Slinky Toy Fragment	phthalate	74.26	80.12	79.34
	PVC 23. Pink Yoga Mat Foam	phthalate	71.46	84.99	74.8
	PVC 24. Clear Cosmetics Bag Fragment	phthalate	84.09	95.29	88.76
	PVC 25. Green Yoga Mat Foam	phthalate	82.3	95.29	84.84
	PVC 27. Green Roof Sheet Fragment	phthalate	72.89	80.22	79.86

FLOPP-e	PVC 2. Blue Fragment	phthalate	83.31	93.48	88.28
	PVC 4. White Fragment	phthalate	81.75	92.57	85.95
	PVC 7. Green Film	Unknown	74.35	84.3	84.41
	PVC 1. Clear Fragment	Unknown	70.92	83.9	80.94
	PVC 9. White Fragment	Unknown	68.16	77.02	74.09
	PVC 3. Orange Foam	Unknown	68.13	76.15	77.2
Primpke	376 (SBR co-polymer)	Unknown	70.13	72.98	75.27
	527 (SBR co-polymer)	Unknown	68.54	70.79	73.2
	466 (uPVC)	Unplasticized	64.66	65.37	67.1
	591 (uPVC)	Unplasticized	64.4	65.27	66.98
	408	Unknown	50.52	61.38	55.75

Only 5/37 samples were correctly identified as PVC with the Primpke library and a further four samples matched to a known vinylic acetate co-polymer sample. PVAc and PVC do not afford identical FTIR spectra but literature showed acetate derived peaks at 1740 cm^{-1} and vinylic backbones were evident and C-C and CH_2 stretches are retained [286]. Manual inspection found no conclusive evidence of acetate co-polymers. However, it does illustrate that blends can be challenging to identify using library matching.

Despite the exclusion of non-polymeric samples from the Primpke library, accurate matching was poor due to the variety of materials included as solid polymers. For example, the most common incorrect matches; alkyd varnish, and poly(diallyl isophthalate) resin contain functional groups similar to plasticised PVC, including carbonyl esters, aromatic C-H bonds, and alkyl chains. As they are not formed into thick sheet materials or injection moulded they can be considered incompatible with the objects' forms. Furthermore, Figure 38 and the sample details recorded in

Table 21 illustrate why the five ‘PVC’ labelled Primpke reference samples were poor matches for many samples. By examination of the carbonyl region between 1720 - 1730 cm^{-1}, two reference spectra were found to contain no peaks and therefore are likely unplasticized PVC (Primpke 466 and 591). The remaining three references (Primpke 376, 408, and 527) showed clear peaks in the carbonyl region, but there was no evidence for aromatic plasticisers between 730-750 cm^{-1}. Additionally, Figure 39 showed low-intensity peaks at 3026, 1639, 1602, 1493, 965, 759, 699 cm-1 for Primpke 376 and 572. These peaks did not appear in any individual sample spectra and are consistent with an SBR co-polymer. Overall, the collected PVC samples are not well represented by the Primpke reference spectra although the vinylic character of the polymer was evident in many of the individual matches.

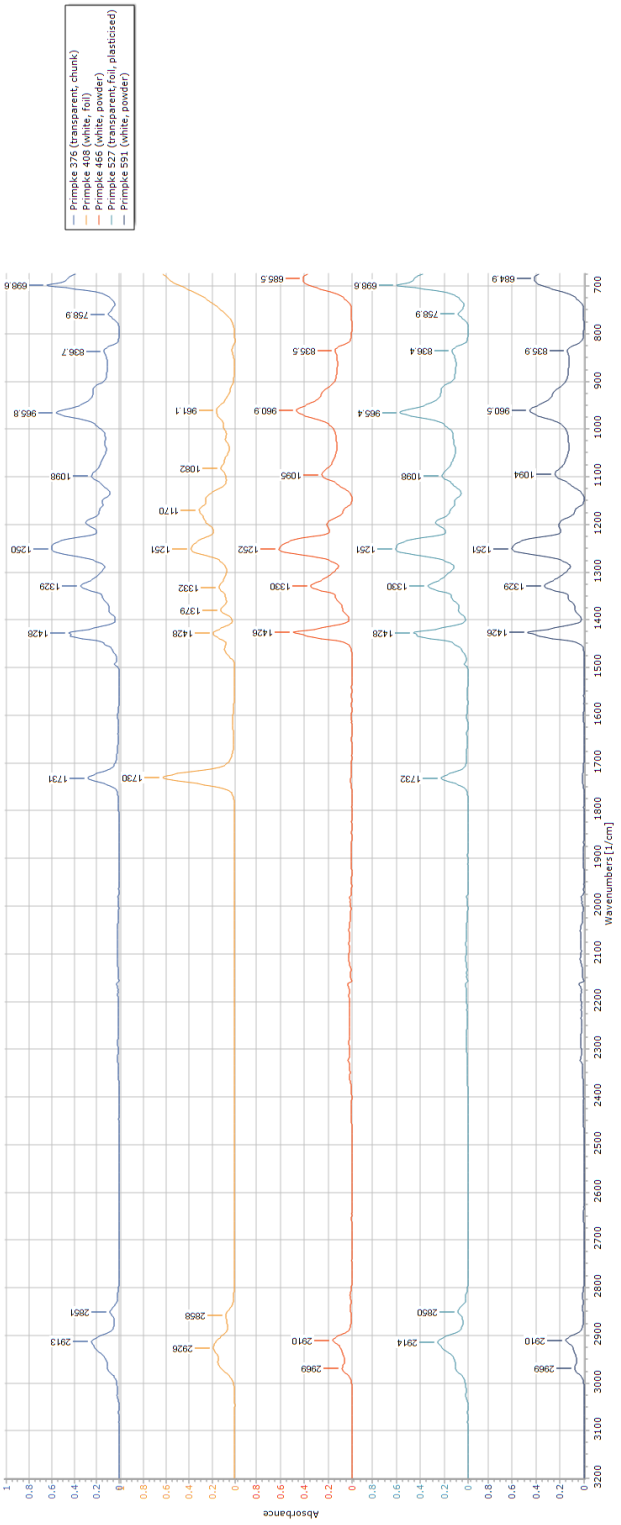

Figure 38: Reference spectra for PVC available in the Primpke library. Primpke 376 and 527 contain an SBR co-polymer, Primpke 591 and 466 are unplasticized PVC, Primpke 408 is plasticised by an unknown plasticiser.

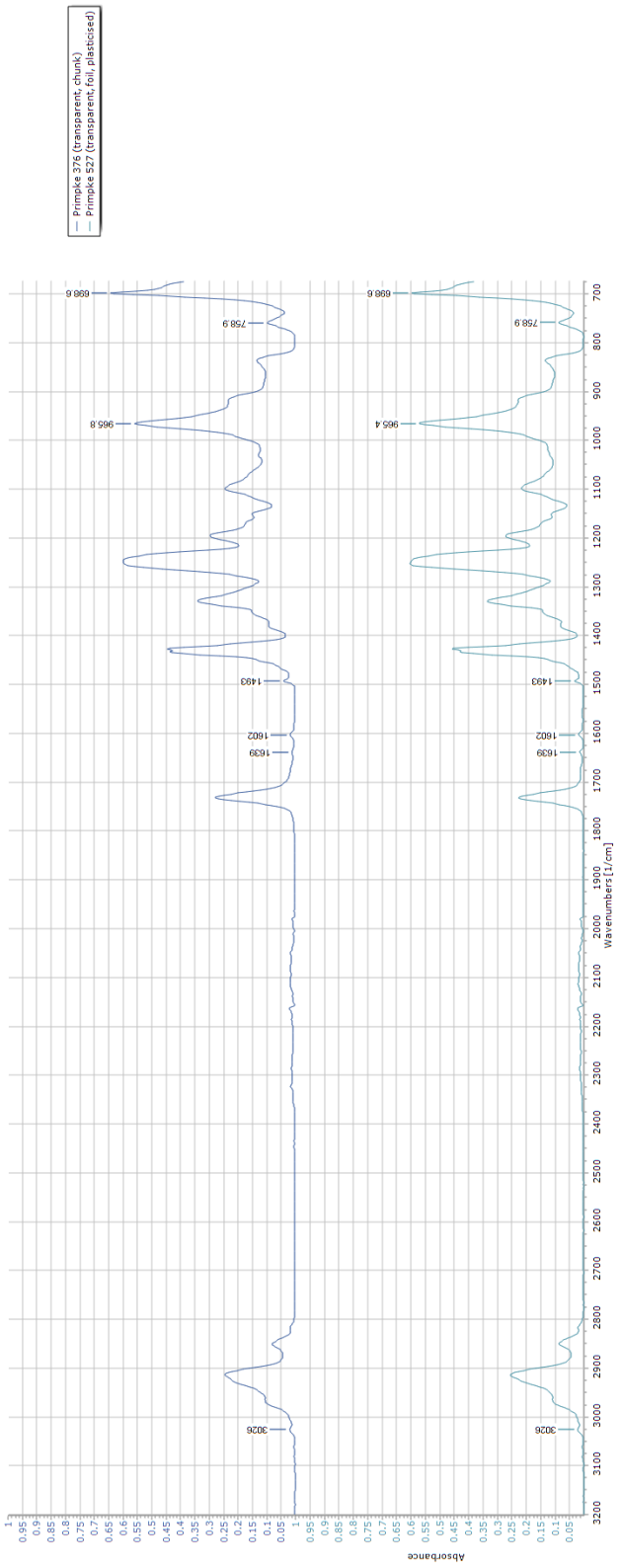

Figure 39: ATR-FTIR spectra of Primpke library samples 376 and 527, labelled peaks at 3026, 1639, 1602, 1493, 965, 759 and 699 derive from an SBR co-polymer.

3.3.5 Spectral library matching for the identification of PVC by ER-FTIR spectroscopy

Table 22 shows the results of library matching for raw and KKT-ER spectra to the PolIRes total reflectance spectra library. Full spectrum matching with the library's polymeric samples (excluding shellac and amber samples) was poor; only 7/42 samples were identified as PVC although a further 9 most closely matched a PVDC, the dichloride version of vinylic chloride derived polymers. Limiting the matching region below 1800 cm^{-1} gave higher correlation coefficients and a further 8 correct matches, including 6 previously identified as PVDC. Comparison of TR and TR-KKT matching below 1800 cm^{-1} highlighted the lower match coefficients with KKT spectra; likely due to the invalid application of KKT where volume reflectance contributes to the spectrum.

Finally, many of the incorrect matches do not fit with the form of the product and can therefore be considered unlikely with some prior knowledge of plastic types. However, other matches (TPE, TPU, SBR) from elastomers such as rubbers (natural, silicone, synthetic), and polyurethanes (PUR) have a similar flexible form and appearance. For example, a terephthalate-plasticised PVC sample (SUC) was misidentified as a thermoplastic elastomer polybutylene terephthalate (PBT) co-polymer, with a 2% higher correlation coefficient compared to PVC. In general, the interpretation of these spectra indicates the need for material insight when identifying PVC objects by spectroscopic analysis and the non-trivial effect of additives on the results with matching libraries. The Plastic Identification Toolkit seems particularly well suited to communicating the expected form of plastics when confirming library matches [287,288]. The polymer composition of the samples discussed here were

not independently verified, and the use of Py-GCMS would be recommended for future studies.

Table 22: Comparison of ER-FTIR spectra to the PolIRes Total Reflectance and KKT libraries. Matches were quantified using Pearson's correlation coefficient (r). NA denotes matches less than 60% or if a PVC match was recorded in the first round.

Object ID	**Spectra ID**	**Top match by spectral region with PolIRes TR library**				**2nd round: top match with PolIRes TR-KKT library**	
		4000-400 cm^{-1}	**r %**	**1800-400 cm^{-1}**	**r %**	**1800-400 cm^{-1}**	**r %**
BBI	bbraun w mir	PVDC	66.73	TPE(PBT)	79.71	PBR	70.38
CLK	black cape	**PVC**	81.9	PP	81.37	POM Resin	61.06
COC	clear oil cloth 2 layers	**PVC**	98.27	**PVC**	91.18	NA	
	clear oil cloth 4 layers	**PVC**	98.31	**PVC**	89.6	NA	
	clear oil cloth	**PVC**	95.24	**PVC**	78.59	NA	
DOD	donald flat blue hat	CF	82.21	LDPE	86.07	NA	
	donald flat foot	NA		PF	93.93	PF	83.44
	donald round tail	NA		CF	93.63	NA	73.77

ERA	eraser flat	SBR	76.97	PF	74.83	NA	65.2
FMO	fimo kids white flat	CA	79.37	CAB	81.04	CA	73.24
GRG	green giant flat foot	NA		PP	94.28	**PVC**	81.26
	green giant round face	CF	53.68	PP	78.44	NA	
GOC	green oil cloth aged with mirror	PUR	57.7	TPU	75.13	TPU	54.29
	green oil cloth aged	PPS	68.23	TPU	78.51	PUR	51.66
HEI	heidelberger with mirror	PVDC	78.78	PP	73.59	NA	
MCS	medium clear sheet flat with mirror	PVDC	91.12	**PVC**	95.15	PUR	85.13
	medium clear sheet flat with silver mirror	PVDC	89.52	**PVC**	92.57	PUR	73.16
	medium clear sheet flat	PVDC	66.03	**PVC**	91.54	NA	
NIP	nipro butterfly set	PVDC	93.21	PP	79.24	NA	
NOD	noddy flat base	TPU	91.33	**PVC**	90.31	**PVC**	94.77
PEN	penguin black round	TPU	95.88	TPU	89.36	Acrylic	79.46

	penguin white belly round w mirror	PVDC	70.27	**PVC**	87.33	**PVC**	67.91
	penguin white belly round w silver mirror	PVDC	71.3	**PVC**	85.95	NA	
	penguin white belly round	PVDC	67.84	**PVC**	77.97	**PVC**	62.35
	penguin white foot flat	CN	79.26	TPU	90.02	**PVC**	85.95
PIL	pilsbury hat flat	CF	58.02	TPU	93.15	CAB	83.29
PNK	pink pig base flat	NA		PF	89.23	PF	76.35
RDC	red cape	**PVC**	89.55	**PVC**	65.39	PUR	89.72
	red cape (with card inner)	PUR_ether	90.89	**PVC**	62.04	NA	
SNO	snoopy flat	**PVC**	84.62	**PVC**	79.84	PF	76.22
SUC	sucker pads without mirror	PET	75.04	TPE(PBT)	87.87	TPE(PBT)	93.22
	sucker pads with mirror	PTFE	77.06	TPE(PBT)	87.94	TPE(PBT)	94.38
TCS	thick clear sheet flat with mirror	Rubber	64.29	PPO	64.65	NA	
VYG	vygon	CF	57.69	**PVC**	65.71	NA	

DOG	white dog flat foot	**PVC**	86.99	**PVC**	84.04	UP	76.84
	white dog round head	TPU	92.11	PP	91.76	**PVC**	84.78
WDS	white doll shoe flat	TPU	89.52	PF	89.49	PF	75.15
YED	yellow dog flat base	TPU	95.63	TPU	93.59	PF	74.42
	yellow dog round	NA		SBR	58.42	SBR	65.23

3.3.6 Retention of spectral features between KKT-ER and ATR-FTIR spectra

The interpretation of ER spectra was aided by ATR spectra. The overall level of correlation between ATR-FTIR spectroscopy and ER-FTIR spectra was quantified with Pearson's correlation coefficient to expand on Picollo et al.'s finding that the spectra were highly similar. Table 23 shows that correlation coefficients increased when the comparison was limited to the 400-1800 cm^{-1} region. This relates to the visible reduction in atmospheric peaks, Restrahlen peaks, and volume reflectance bands at lower wavenumbers. An r^2 value above 0.6 also appeared to offer a reliable measure of visibly similar spectra in this sample set.

Table 23: Correlation between ATR-FTIR spectroscopy and KKT-ER spectra for each sample

Sample	**Pearson correlation coefficient (r) between ATR-FTIR spectroscopy and KKT-ER spectra by region**	
	400 - 4000 cm^{-1}	**400 - 1800 cm^{-1}**
DOD	0.42484	Not significant
GRG	0.47054	0.68945
GOC	0.51786	0.58372
HEI	No suitable ER-FTIR spectroscopy spectrum	
MCS	0.3992	0.73036
NIP	No suitable ER-FTIR spectroscopy spectrum	
NOD	0.55647	0.82564
PEN	0.52851	0.78416
PIL	0.5232	0.51945

PNK	0.46734	0.27901
SNO	0.47764	0.47296
SUC	0.69289	0.86655
TCS (Not PVC)	0.27013	0.83051
DOG	0.48822	0.82154
WHD	0.52948	0.17394
FIM	0.62407	0.58755
ERA	0.501	0.10607
FKB	No suitable ER-FTIR spectroscopy spectrum	
BBI	0.45731	0.79054
CLO	-0.06552	0.34467
BLC	0.58063	0.85039
RDC	0.08049	0.29185
VYG	-0.23553	0.18986
YED	0.34831	0.30753

For polymer identification, multiple studies have reported characteristic peaks for ATR-FTIR spectra of PVC which were used to aid the interpretation of ER-FTIR spectra and understand the low matching scores with KKT-ER reference spectra. As

shown in Figure 30 and

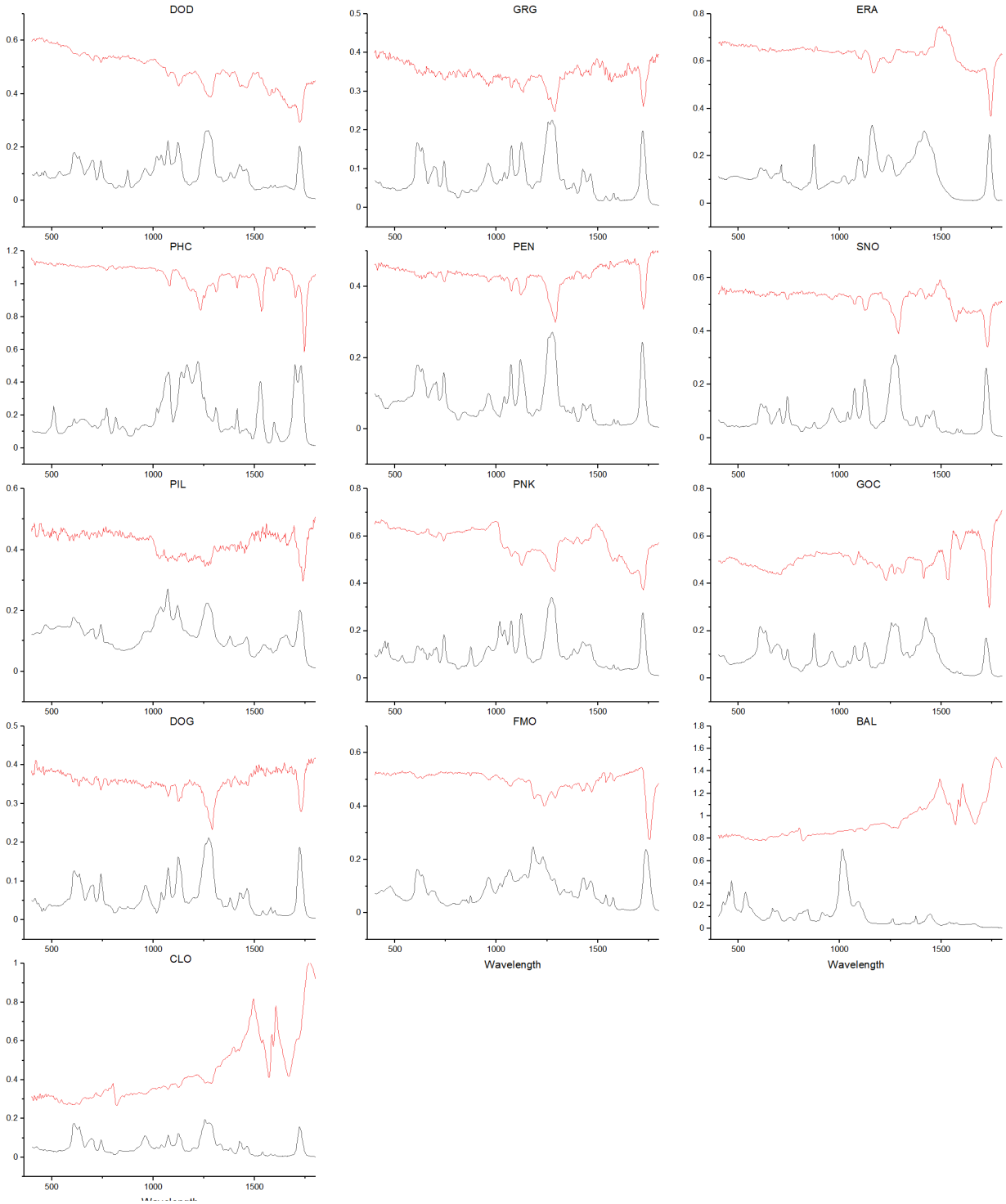

Figure 36, the most well-resolved peaks present in ER-FTIR spectroscopy are found below 1800 cm^{-1}. In general, the most intense peaks are found within 1200-1300 and 1100-1150 cm^{-1} ranges. Previous studies have reported peaks in these regions may

include C-Cl and C-H (aromatic) angular deformations, as well as vibrations derived from C-O-C, and O-C=O in DOTP.[229]. Peaks at 957 (broad), 609, and 635 cm^{-1} derived from the CH2 bending and C-Cl stretching modes of the vinyl chloride polymer are also retained across many of the collected ER-FTIR spectra, although peaks at 609 and 635 cm^{-1} are particularly hard to distinguish from baseline noise. A known peak for the angular deformation of CH2 – Cl at 1426 cm^{-1} was not reliably identified in the collected ER-FTIR spectra.

For additive identification, low-intensity peaks between 730-760 cm^{-1} are associated with C-H bending in aromatic groups, and were used to identify phthalate, terephthalate and trimellitate plasticisers.

Table 24 shows the ATR-FTIR spectroscopy peak maxima, ER-FTIR spectroscopy peak maxima, and ER-FTIR spectroscopy signal-to-noise ratios. The correct plasticiser class was identified by ER-FTIR spectroscopy for 12/19 samples, however, SNR ratios are routinely below 2 for phthalate-plasticised samples, and a peak was not observed in all spectra, for example sample GRG shown in Figure 40.

Peak shifts were observed in 7 KKT-ER spectra, with peaks shifted up to 4 cm^{-1} away from the corresponding ATR-FTIR spectra, which could confuse identification if used alone.

Discussion of other plasticiser-specific peaks in the literature is limited beyond doublet peaks characteristic of terephthalate and phthalates at 1580-1600 cm^{-1}, which are typically 5 to 10 times less intense than the related peaks at 730 and 760 cm^{-1} and they were not observable in any KKT-ER. Therefore, the origin of other more intense peaks present in the ER-FTIR spectra were studied to improve the reliability of plasticiser assignment from ER-FTIR spectra.

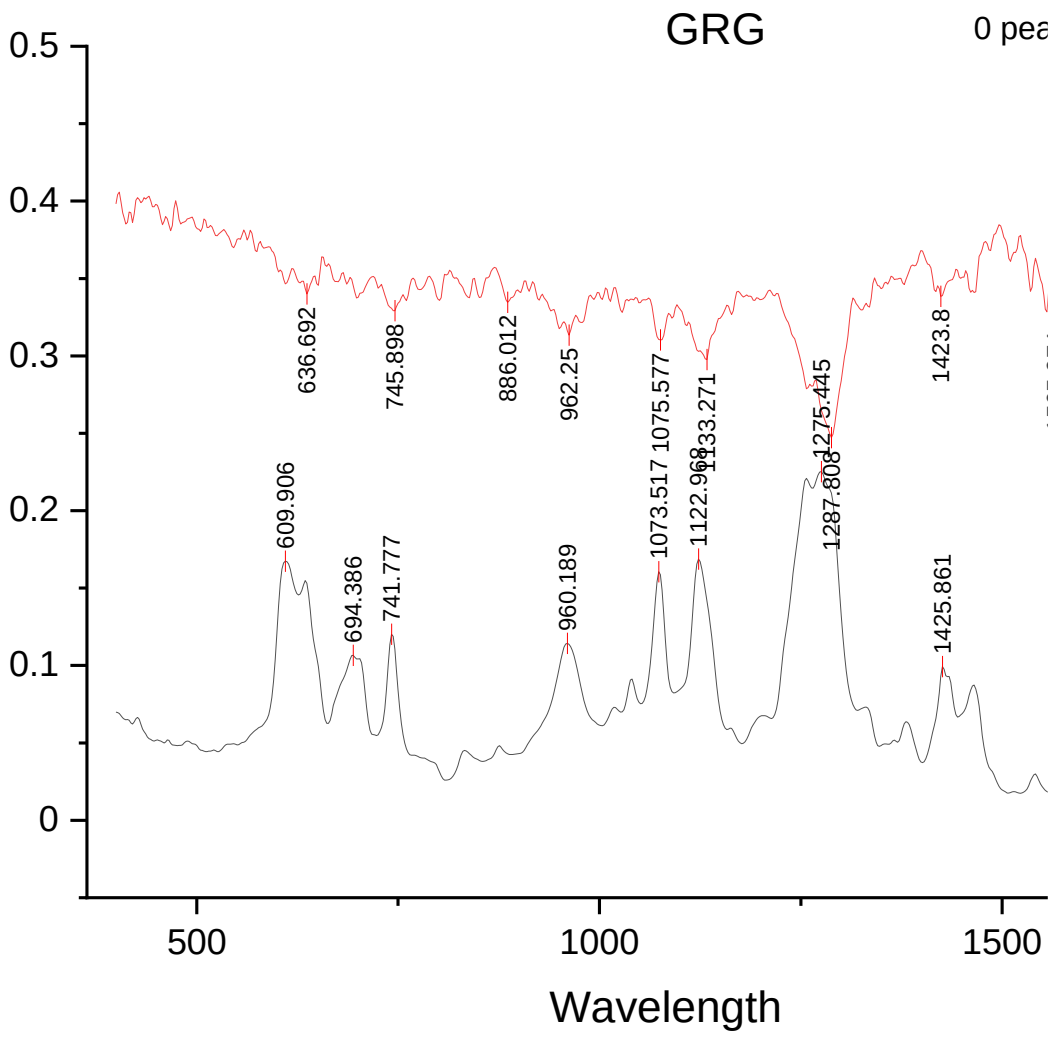

Figure 40: ER (red) and ATR (black) spectra of sample GRG. A phthalate derived peak at 741 cm^{-1} is clear, but a corresponding peak has shifted to 745 cm^{-1}in the corresponding ER spectra and the signal is barely distinguishable from the noise.

Table 24: Characteristic peaks for aromatic plasticisers were identified in both ATR-FTIR spectroscopy and KKT-ER spectra

Sample	Known plasticiser class	v (cm $^{-1}$) of peaks detected 725-755 cm^{-1}		
		ER	**ER SNR***	**ATR**
DOD	Phthalate	741	1.21	741
GRG	Phthalate	745	1.17	741
GOC	Phthalate	n.d.	-	730
HEI	Terephthalate	n.d.	-	731
MCS	Phthalate	743	2.06	741
NIP	Trimellitate	n.d.	-	752
NOD	Phthalate	743	1.77	741
PEN	Phthalate	743	1.48	741
PIL	Phthalate	n.d.	-	741
PNK	Phthalate	741	1.51	741
SNO	Phthalate	741	2.79	741
SUC	Terephthalate	731	7.37	729
TCS (Not PVC)	None	n.d.	-	754
DOG	Phthalate	741	1.26	741
WHD	Phthalate	737	1.57	741
FIM	Citrate	n.d.	-	n.d.
ERA	Valerate	n.d.	-	n.d.
BBI	Terephthalate	731	21.14	731
CLO	Phthalate	n.d.	-	741

BLC	Phthalate	n.d.	-	743
RDC	Phthalate	n.d.	-	743
VYG	Trimellitate	n.d.	-	752
YED	Phthalate	745	1.29	741

* SNR calculated from the root mean square of background noise between 765-800 cm^{-1}

3.3.7 Assignment of plasticiser peaks in ER-FTIR spectra of plasticised PVC

Figure 41 highlights the three most intense regions observed in the collected ATR-FTIR spectra. Peaks between 1230-1275 cm^{-1} (**O-C**=O), 1102-1122 cm^{-1} (C-**O-C**=O) and 1716-1723 cm^{-1} (**C=O**) are associated with vibrational modes of the ester functional groups [289]. They are features which are retained across most ER-FTIR spectra.

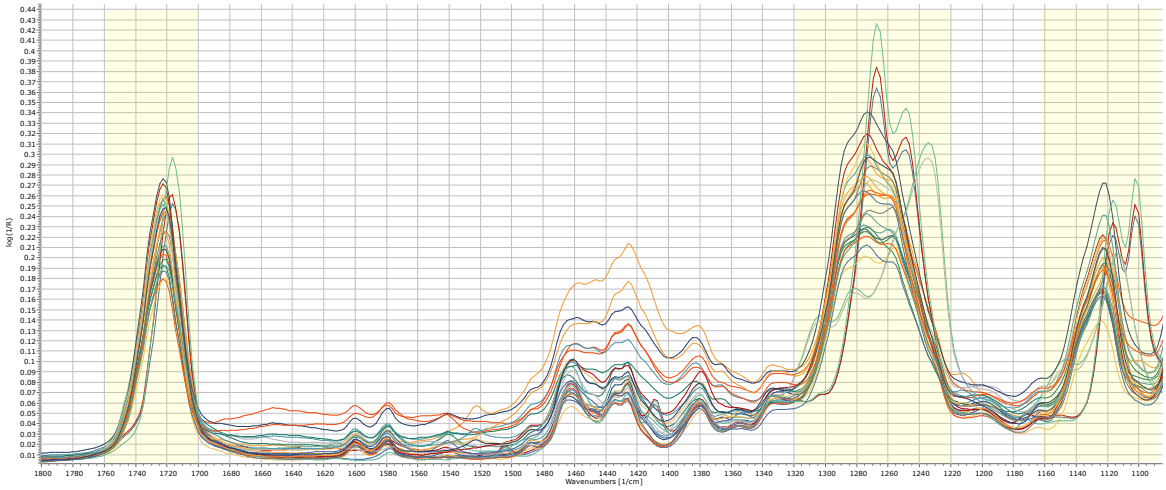

Figure 41: ATR-FTIR spectra of all plasticised PVC samples with the most intense peak regions highlighted, peaks between 1230-1275 cm^{-1} (O-C=O), 1102-1122 cm^{-1} (C-O-C=O) and 1716-1723 cm^{-1} are associated with the ester group of plasticisers.

Previous studies have reported a Cl-CH angular deformation is observed at 1255 cm^{-1}, which suggested PVC-derived peaks could contribute to the peaks observed in the 1230-1275 cm^{-1} region in Figure 41. However, Figure 42, Figure 43, and Figure 44 compare spectra of a pure ‘x’-class plasticiser with an averaged spectrum of ‘x’-plasticised PVC samples. As evidenced by the retained band shapes the peaks in

the two regions ~1200-1350 and ~1100-1170 cm^{-1} are influenced by the plasticiser. Slight shifts in peak maxima are due to interactions with the polymer and are well reported.

Figure 44 shows DINP compared to all ortho-phthalate plasticised samples. As expected, comparison of individual sample spectra to spectra of individual ortho-phthalates (DEHP, DBP, DINP) did not reveal any distinct differences by which the exact phthalate could be identified.

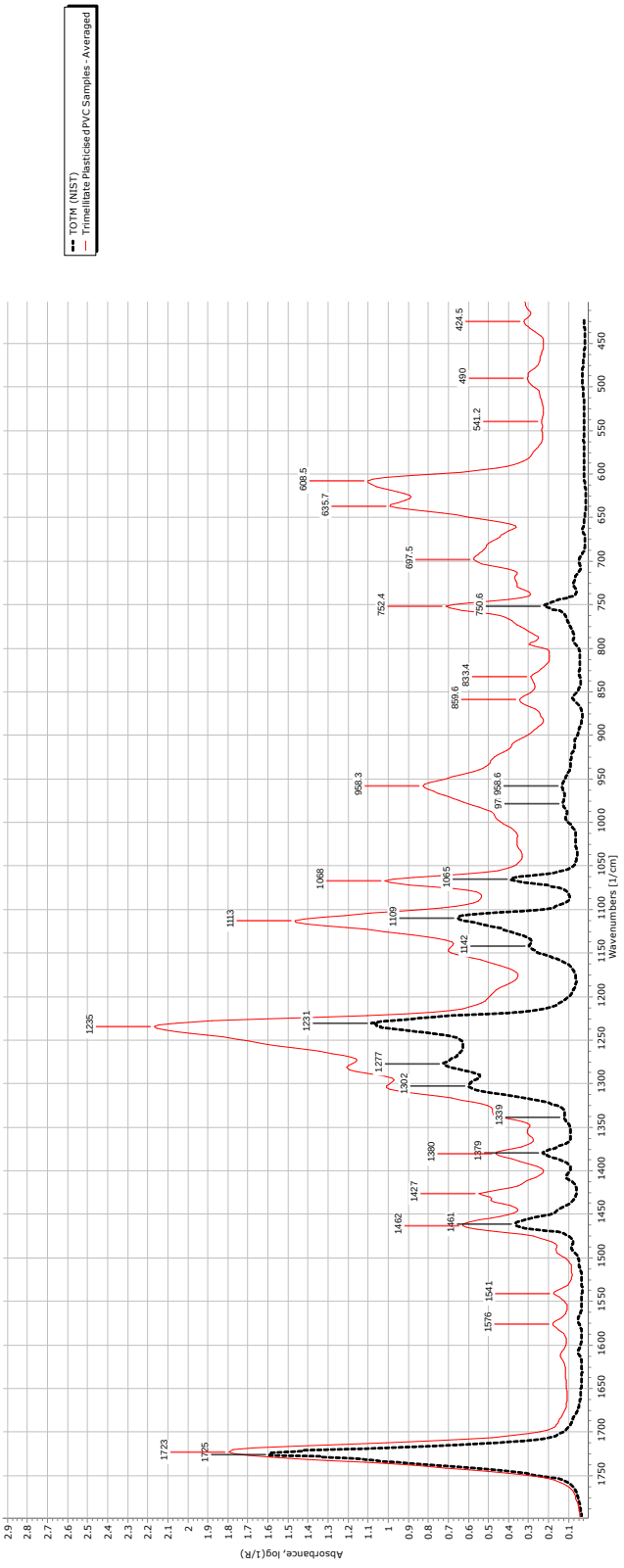

Figure 42: ATR-FTIR spectra of pure TOTM (black) and averaged spectra of TOTM-plasticised PVC samples (n=2)

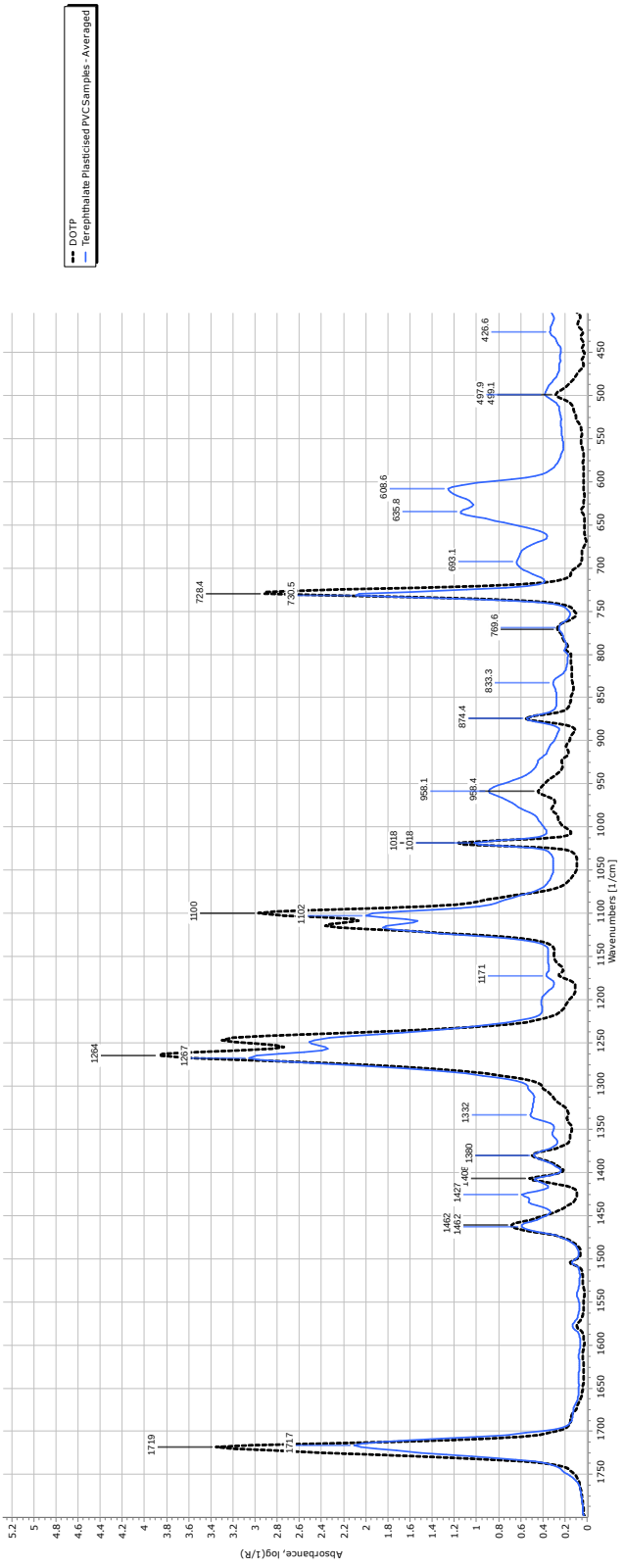

Figure 43: ATR-FTIR spectra of pure DOTP (black) and averaged spectra of DOTP-plasticised PVC samples (n=3)

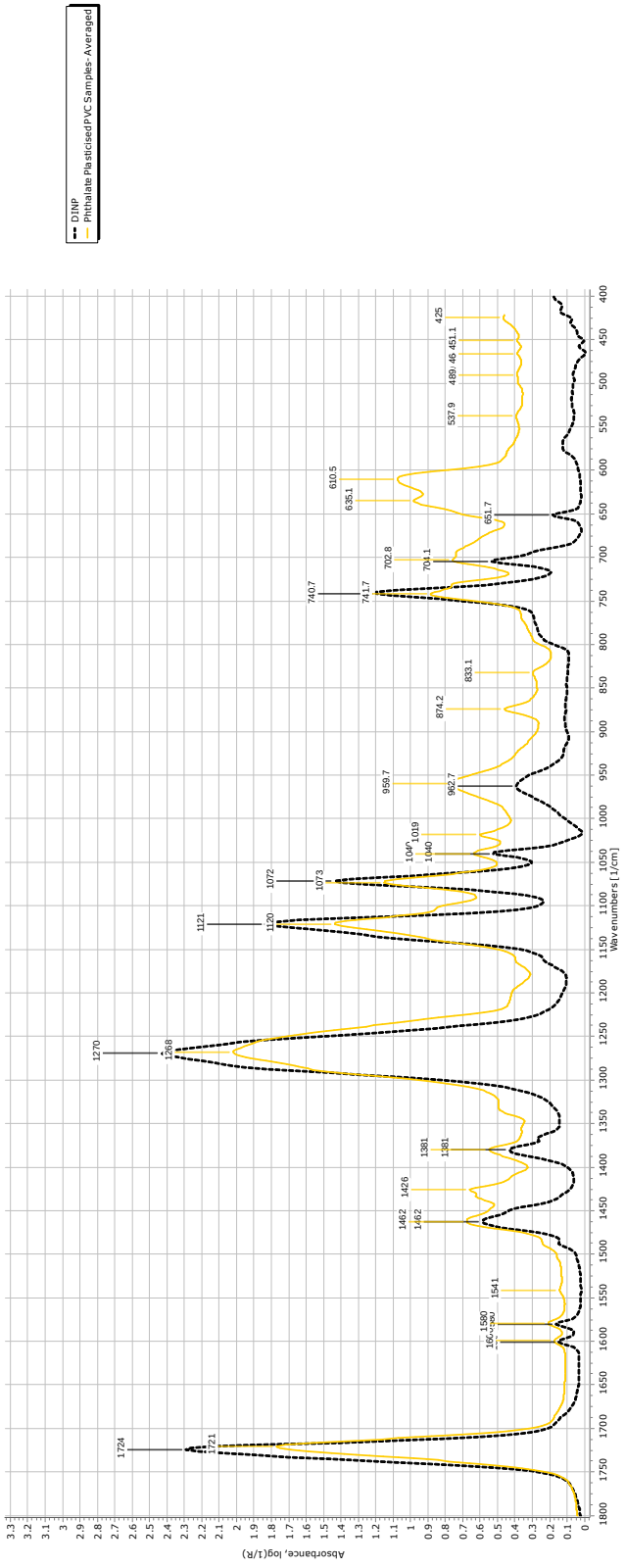

Figure 44: ATR-FTIR spectra of pure DINP (black) and averaged spectra of ortho-phthalate plasticised samples (n=22)

Figure 45 shows how peak maxima at 1235 & 1114 cm^{-1} can be attributed to the presence of TOTM (red traces), 1267 & 1102 cm^{-1} for DOTP (blue traces), and 1274 & 1122-1124 cm^{-1} for ortho-phthalate (orange traces) plasticised PVC.

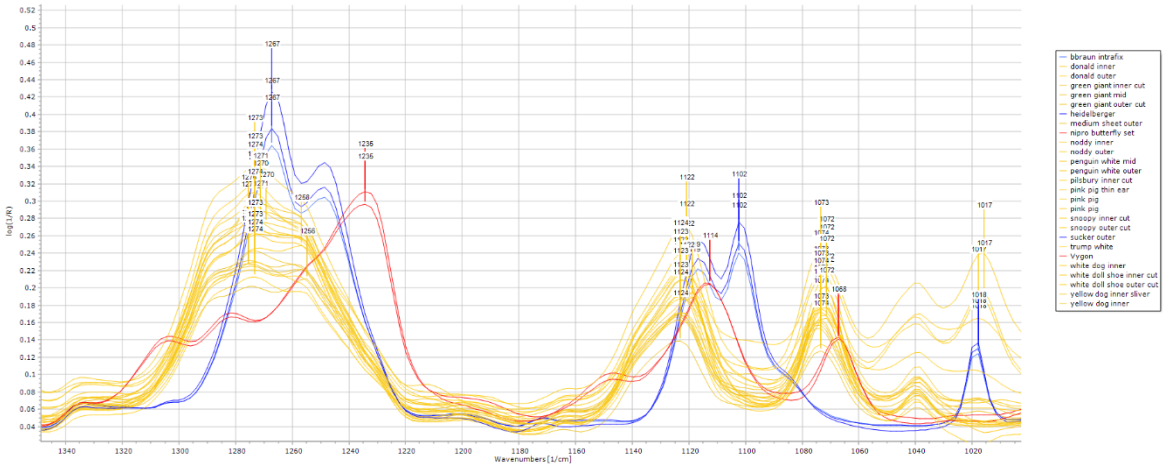

Figure 45: Differences in ATR-FTIR spectroscopy peak maxima between 1400-400 cm^{-1} (top) showing distinct differences (bottom) at 1270-1230 cm^{-1} and 1100-1125 cm^{-1} for PVC samples plasticised with DOTP – blue, ortho-phthalates – orange, and TOTM – red, as determined by the presence of peaks at 729, 741, and 752 cm^{-1}.

As with the ATR-FTIR spectra, Figure 46 illustrates how the most intense peaks in ER-FTIR spectra of phthalate-plasticised samples generally occur between 1073-1075, 1122-1131, and 1200-1350 cm^{-1}. Spectra were normalised to a value of 1 at 1127 cm^{-1} to ease their comparison. They are comparable to an averaged phthalate-plasticised ATR-FTIR spectroscopy spectrum and clearly differ from DOTP- and TOTM-plasticised samples.

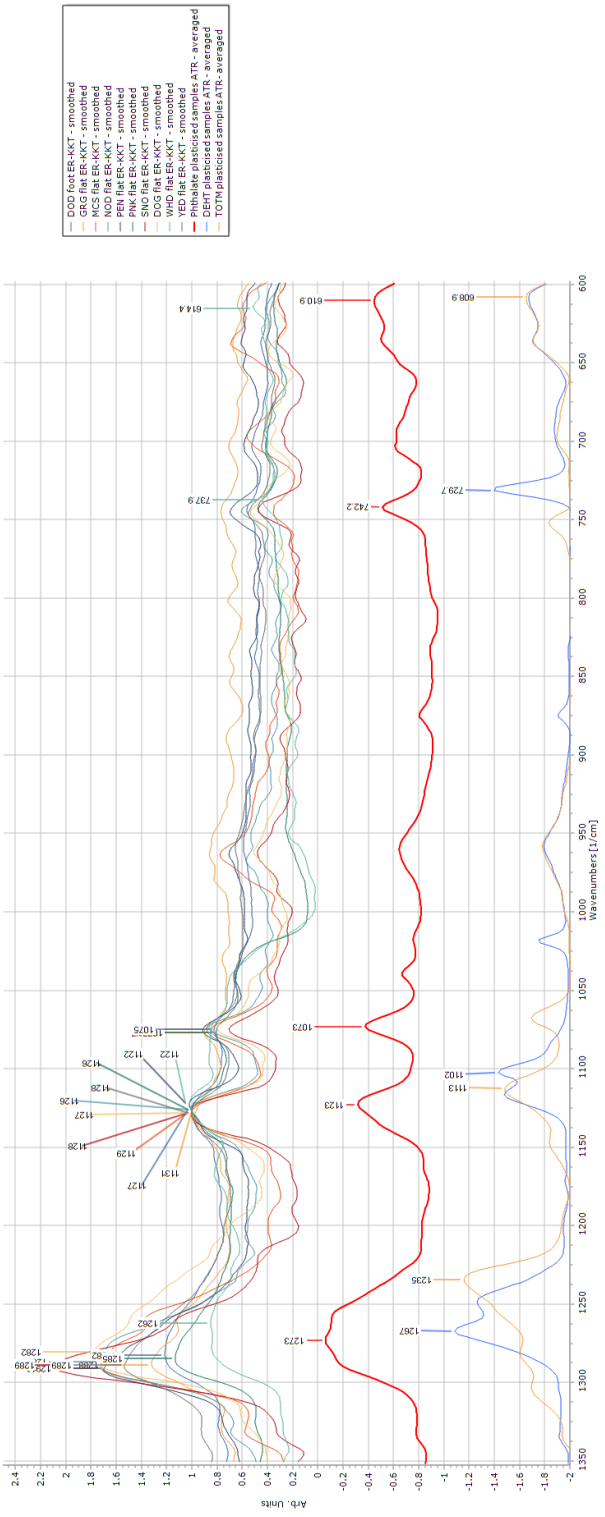

Figure 46: ER-FTIR spectra of phthalate-plasticised samples, highlighting peaks at 1125, 1280, and 1075 cm^{-1} which are also visible in phthalate-plasticised PVC ATR-FTIR spectra, and do not occur in DOTP or TOTM-plasticised samples.

Some spectra such as WHD showed low SNR, but peaks in these three regions could still be distinguished. For samples BLC, GOC, CLO, PIL and RDC there was no distinguishable peak at 741 cm^{-1}, despite the known presence of phthalates by GC-MS and NMR. Figure 47 illustrates how three of the five samples (BLC, RDC, and CLO), could still be identified as phthalate-plasticised samples due to the bands centred at 1073-1076, 1123-1128, and 1285-1287 cm^{-1}, whereas expected peaks at 741 cm^{-1} are missing due to the low signal to noise ratios. Comparison to the ER spectra shown in Figure 48 for DOTP samples discounts the presence of DOTP.

While the ER-FTIR spectra of two DOTP-plasticised samples (BBI, SUC) showed a much higher SNR ratio (SNR = 7 and SNR = 20) for the characteristic ~729 cm^{-1} peak (now shifted to 733 cm^{-1}), the most intense plasticiser bands identified in Figure 45 are retained. Figure 48 shows that peaks found at 1017, 1105, 1109 and 1274 cm^{-1} in ER-FTIR spectra of samples BBI and SUC are comparable to peaks at 1019, 1102, 1116 and 1267 in the averaged ATR-FTIR spectra from three DOTP-plasticised samples. Although contributions from C-C backbones in PVC are expected in this region, the same peaks (also shifted) were observed in ATR-FTIR spectra of pure DOTP and were not apparent in an averaged ATR-FTIR spectra of unplasticized PVC samples, which confirms the peaks result from the inclusion of DOTP.

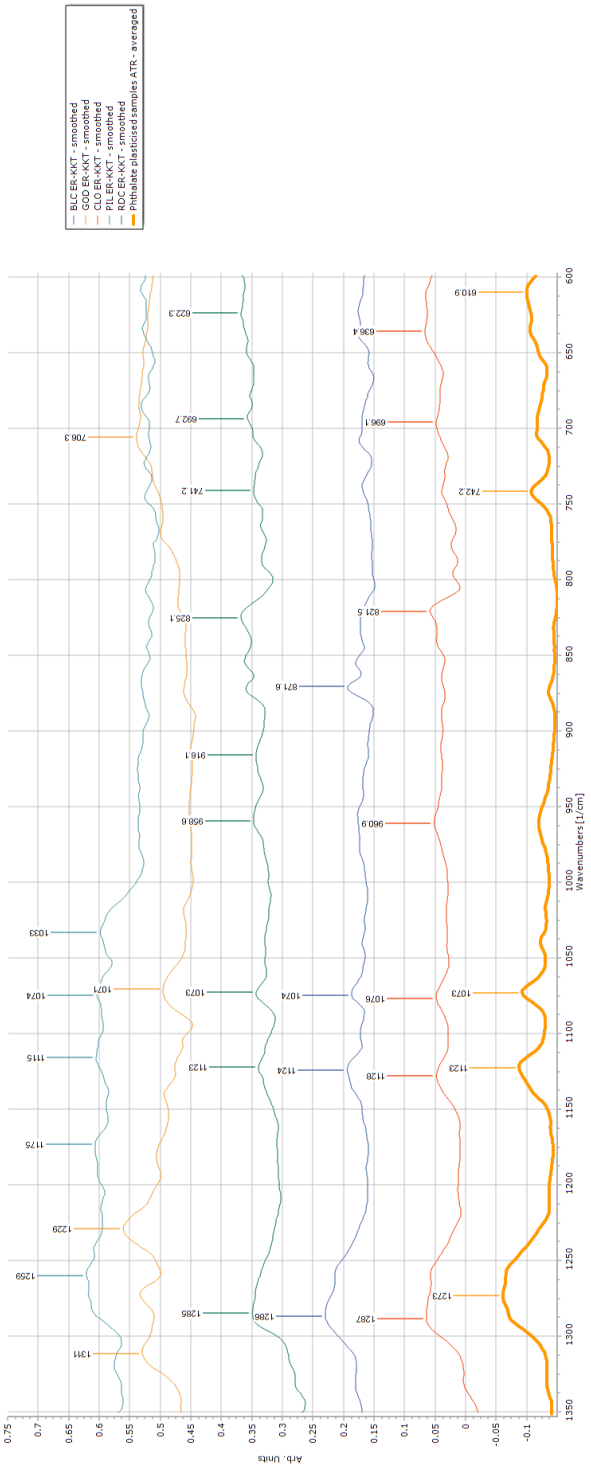

Figure 47: ER-FTIR spectra of known phthalate-plasticised samples which do not show a peak at 741 cm^{-1}, compared to an averaged phthalate-plasticised PVC ATR-FTIR spectroscopy spectrum. Peaks centred at 1073-1076, 1123-1128 and 1273-1287 cm^{-1} are evident in samples CLO, BLC, and RDC.

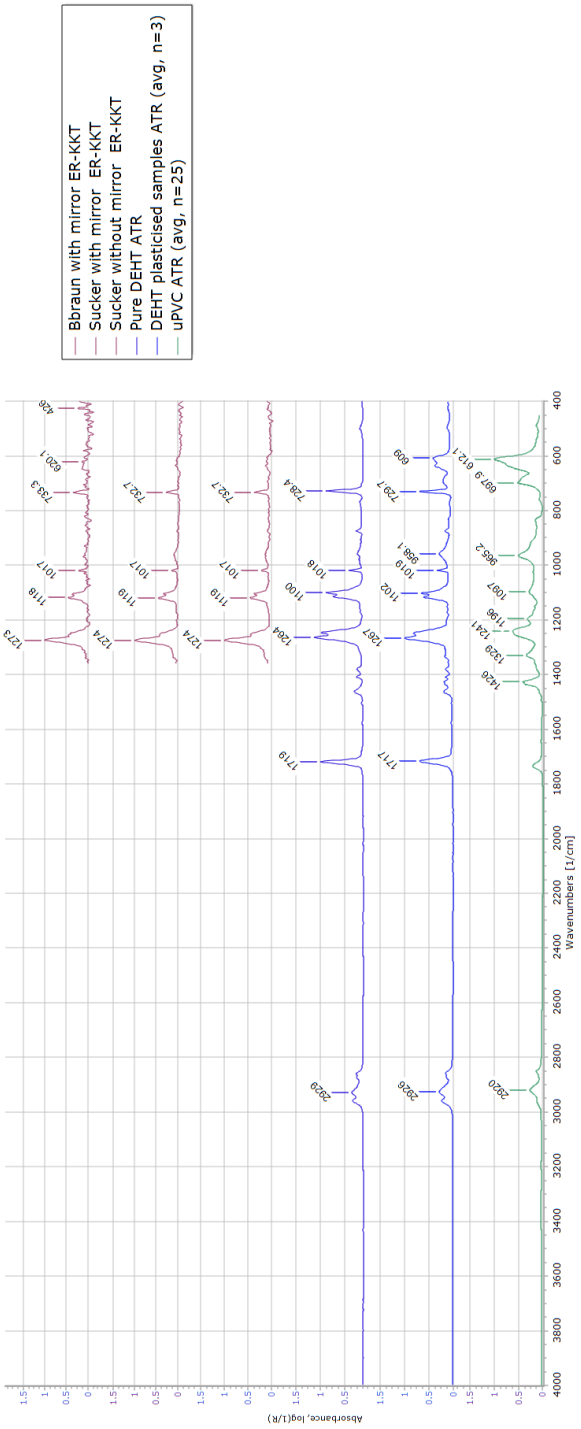

Figure 48: Comparison between DOTP-plasticised sample (BBI and SUC) ER-FTIR spectra, a pure DOTP ATR-FTIR spectroscopy spectrum, an averaged DOTP-plasticised sample ATR-FTIR spectra, and an averaged uPVC ATR-FTIR spectra.

The applicability of a model such as Rijavec et al.'s was considered to classify plasticiser type from these observations, therefore, as a first step principal component analysis was used to explore the sample set. Figure 49 illustrates that a lack of correlation between spectra taken from the same samples was observable, and thus identification of key variables related to additive content was not possible. Therefore, variance with respect to plasticiser content could not be distinguished with raw ER-FTIR spectra or with a reduced region of KKT-ER spectra (400-1800 cm^{-1}). This can be explained by the high noise levels observed.

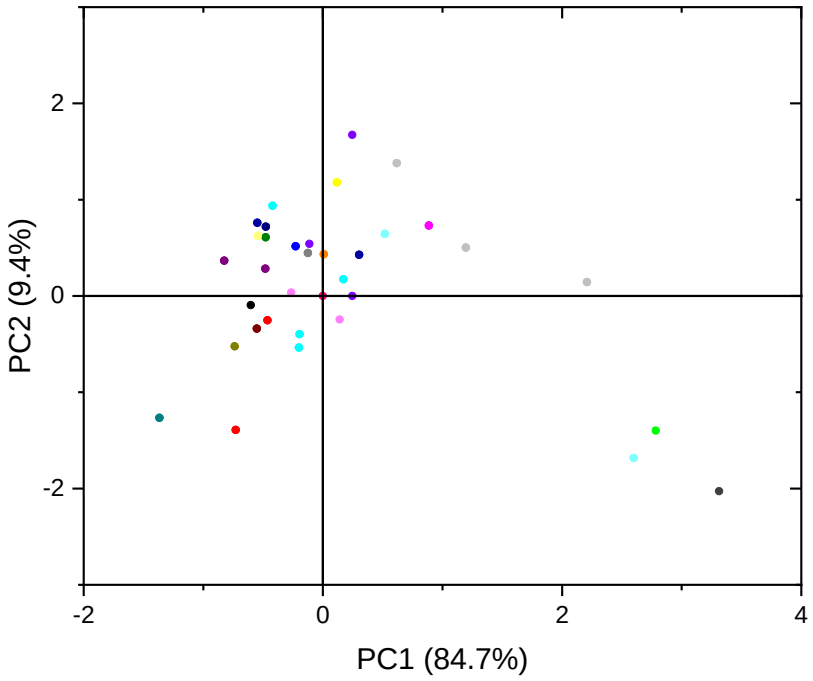

Figure 49: Points represent single KKT-ER spectra containing peaks between 400-1800 cm^{-1}; colours denote different spectra from the same sample

3.3.8 Identification of aliphatic plasticisers by IR spectroscopy

Finally, in addition to the FTIR spectra of pure aromatic plasticisers shown above, ATR spectra of five aliphatic plasticisers were recorded (or collected from NIST) for reference. Spectra were colorised with respect to their aliphatic or aromatic nature, to aid visualisation of differences between the two types. Figure 50 shows the 1160-1210 cm^{-1} region; the only part of the spectra where peaks are observed for aliphatic plasticisers only. No aliphatic-plasticised PVC samples were found in the study; therefore, it was not possible to confirm if these peaks are retained when incorporated into PVC. However, the lack of peaks in this region for all aromatic-plasticised samples analysed in this study suggests there is likely no interference from PVC derived peaks. While peaks are observed in this region for uPVC (see Figure 48), there appears to be minimal correlation between peaks in uPVC and plasticised PVC samples.

As shown in Figure 51, the peaks in this region are also some of the most intense, and therefore may also be distinct and observable in ER-FTIR spectra, as with aromatic plasticisers. Each plasticiser also shows distinct peak maxima which may enable further distinction.

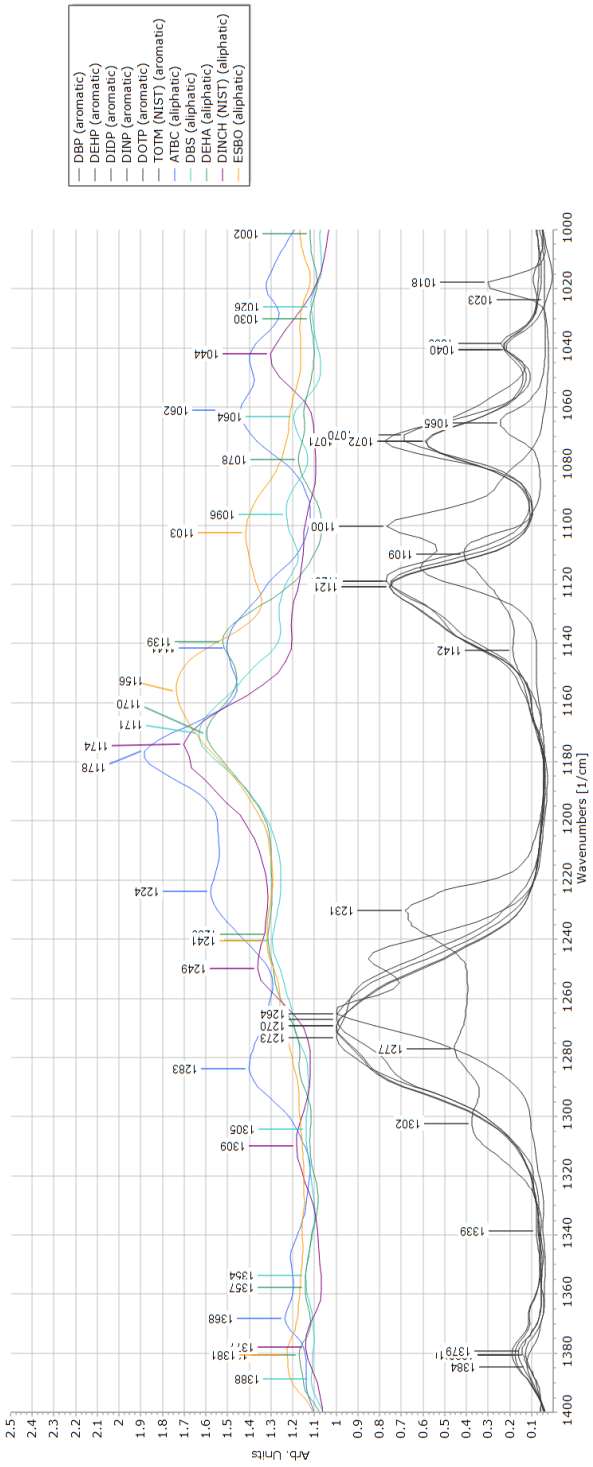

Figure 50: ATR-FTIR spectra of aliphatic (coloured) and aromatic (black) plasticisers, showing the presence of intense peaks between 1160-1210 cm^{-1} for all aliphatic plasticisers and their absense in aromatic plasticisers. The baseline value of aliphatic plasticisers is adjusted to 1.

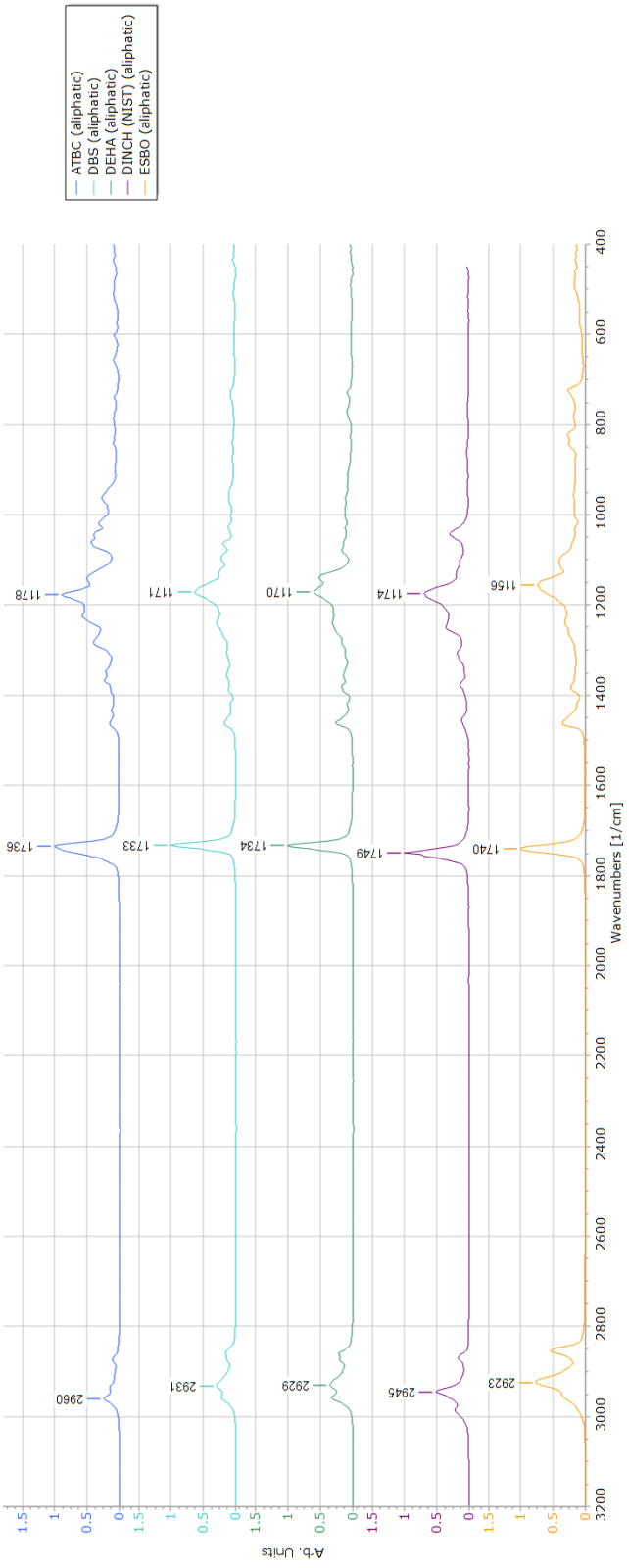

Figure 51: ATR-FTIR spectra of aliphatic plasticisers (ATBC, DBS, DEHA, DINCH, and ESBO). The three most intense peaks per plasticiser are labelled.

3.3.9 Low-field NMR for plasticiser identification

Figure 53 shows the ^{1}H NMR spectra acquired at 60 MHz for 0.25 M solutions of phthalate and alternate plasticisers (DBP, DEHP, DIDP, DOTP, ATBC, DBS and DEHA) in deuterated chloroform. Spectra from plasticisers reference solutions were recorded over 16 scans. Peak assignments and coupling constants are recorded in Table 25.

A high concentration (~0.25 M) is recommended to reduce the length of time and number of scans required to record a spectrum. 0.25 M is equivalent to the complete extraction of plasticisers from a 160 mg PVC sample, assuming the sample contains at least 30 wt.% plasticisers. The recommended concentration is, therefore, impractical for heritage purposes where micro-sampling is required. However, extracts from 10 mg samples are shown in Figure 52 and were suitable for identification if scan numbers were increased four-fold.

Figure 54 shows significant differences remain observable in the splitting patterns of the methylene multiplet across a phthalate series, such that they can be used for identification. 64 scans were required to achieve the observed resolution of the characteristic multiplet at 4 ppm from the low concentration samples. In all samples and known standards multiplet peaks are most clearly resolved at ~3.75 to 4 ppm for the methylene group adjacent to the ester group. The poorly resolved methylene resonance for DIDP is representative of its manufacture from isomeric C10 alcohols and thus small changes in chemical shift across the isomers are observed. A similar and largely indistinguishable spectrum was observed for DINP in Figure 52 (second from top), and DiHpP from sample PNK (bottom). By comparison to Figure 54 and Figure 53 all samples can be qualitatively identified as phthalate plasticisers,

although the use of benzyl benzoate as a reference standard obscured the aromatic peaks. Due to the low SNR no quantitative analysis was attempted.

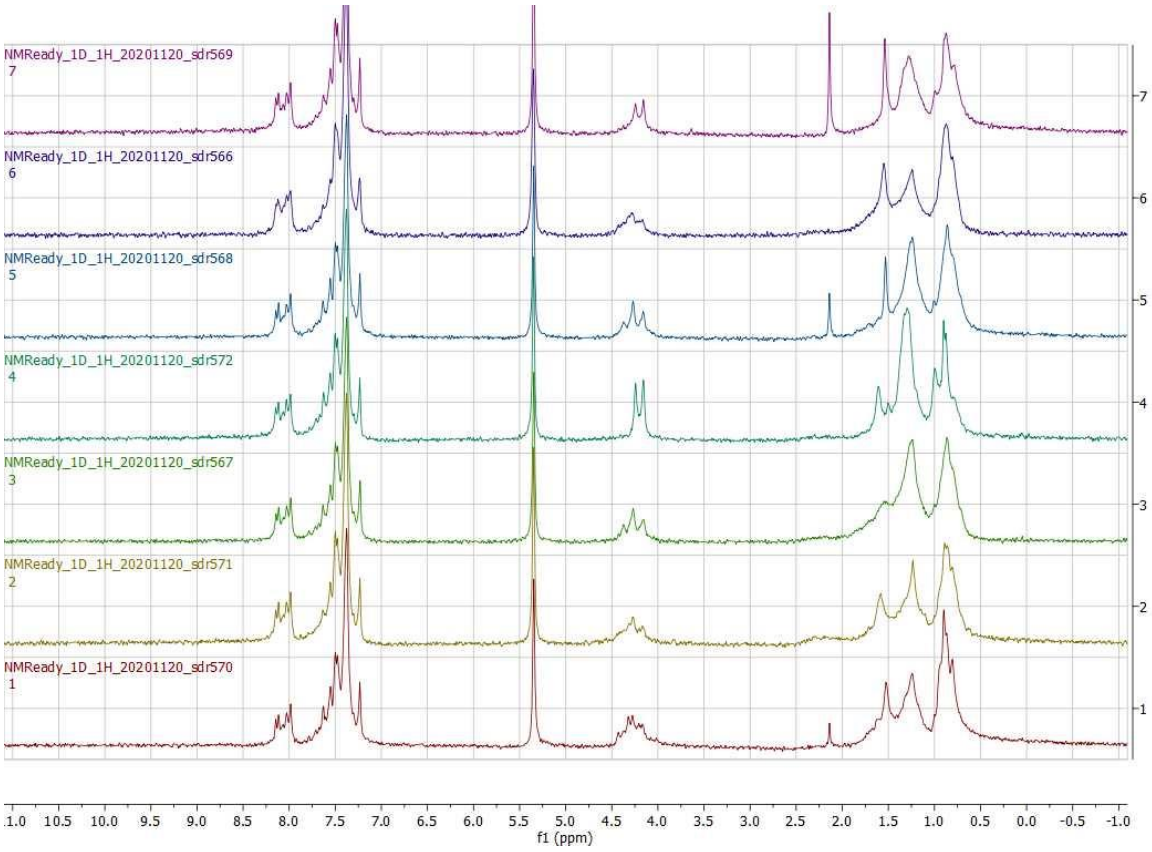

Figure 52: 60 MHz ^{1}H NMR spectra of sample extracts (10 mg in 800 ul CDCl3 with benzyl benzoate internal standard).

Table 25: ^{1}H NMR peak assignments for various plasticisers

Plasticiser	**^{1}H NMR chemical shifts, multiplicity and coupling constants at 60 MHz**
DOTP	δ 8.07 (s, 1H), 4.25 (d, J = 4.9 Hz, 1H), 1.34 (s, 3H), 1.17 – 0.73 (m, 3H).
DBS	δ 4.04 (t, J = 6.2 Hz, 1H), 2.26 (t, J = 6.6 Hz, 1H), 1.71 – 1.39 (m, 2H), 1.28 (s, 3H), 0.95 (d, J = 5.8 Hz, 2H).
DEHA	δ 3.94 (d, J = 4.5 Hz, 1H), 2.23 (d, J = 6.0 Hz, 1H), 2.00 – 0.60 (m, 9H).
ATBC	δ 4.39 – 3.82 (m, 1H), 3.22 (s, 1H), 1.84 – 0.64 (m, 4H)
DIDP	δ 7.48 (qd, J = 5.9, 3.3 Hz, 1H), 4.10 (q, J = 6.7 Hz, 1H), 1.11 (s, 3H), 0.70 (d, J = 4.6 Hz, 5H).
DEHP	δ 7.49 (dq, J = 6.8, 4.6 Hz, 1H), 4.09 (d, J = 5.1 Hz, 1H), 1.20 (s, 3H), 1.03 – 0.51 (m, 3H).
DBP	δ 7.93 – 7.24 (m, 1H), 4.29 (t, J = 6.4 Hz, 1H), 2.12 – 0.62 (m, 4H).

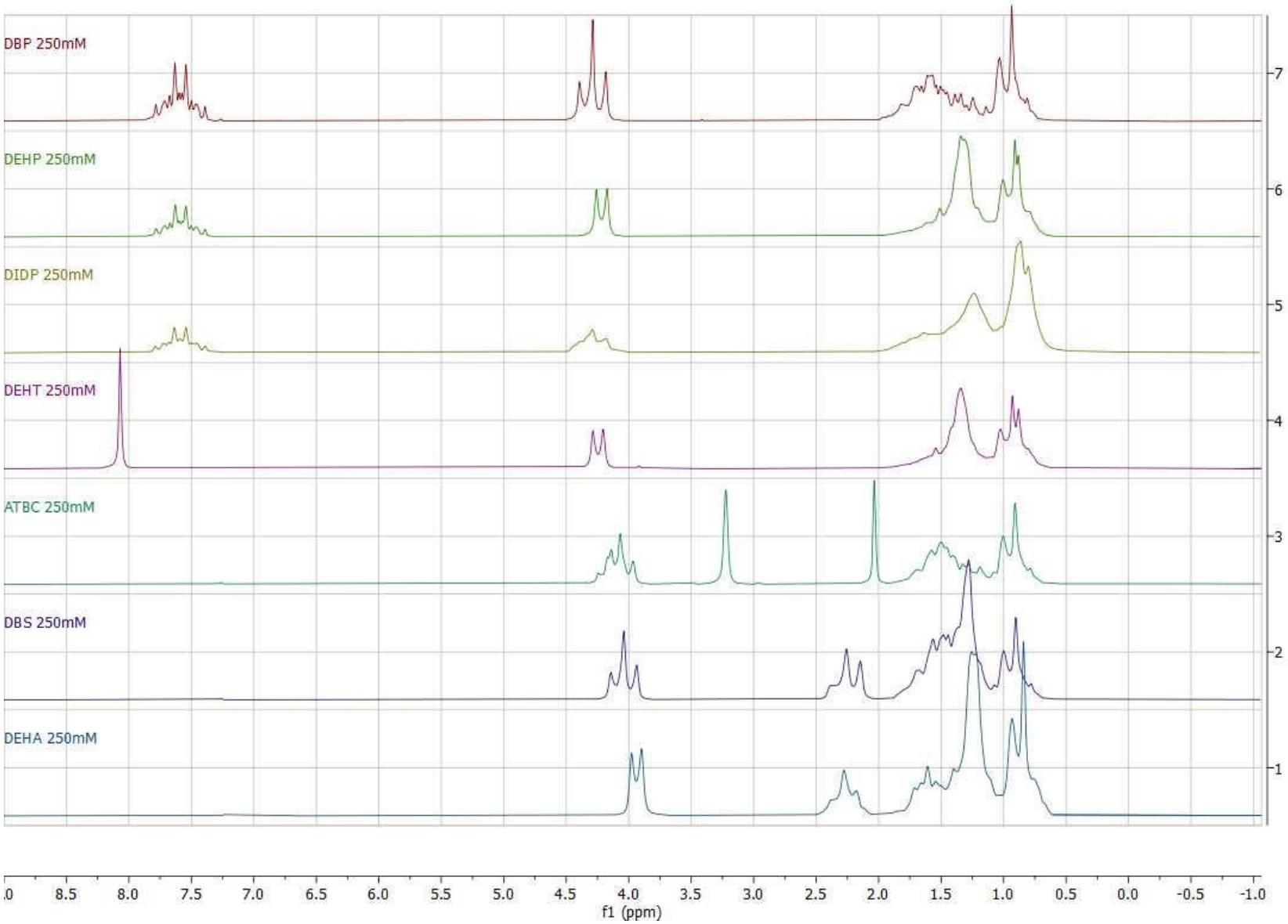
DBP 250mM
DEHP 250mM
DIDP 250mM
DEHT 250mM
ATBC 250mM
DBS 250mM
DEHA 250mM
7
6
5
4
3
2
1
.0 8.5 8.0 7.5 7.0 6.5 6.0 5.5 5.0 4.5 4.0 3.5 3.0 2.5 2.0 1.5 1.0 0.5 0.0 -0.5 -1.0
f1 (ppm)

Figure 53: 60 MHz ^{1}H NMR spectra of 250mM solutions of DBP, DEHP, DIDP, DOTP, ATBC, ATBC, DBS, and DEHA in $CDCl_3$, recorded with 16 scans.

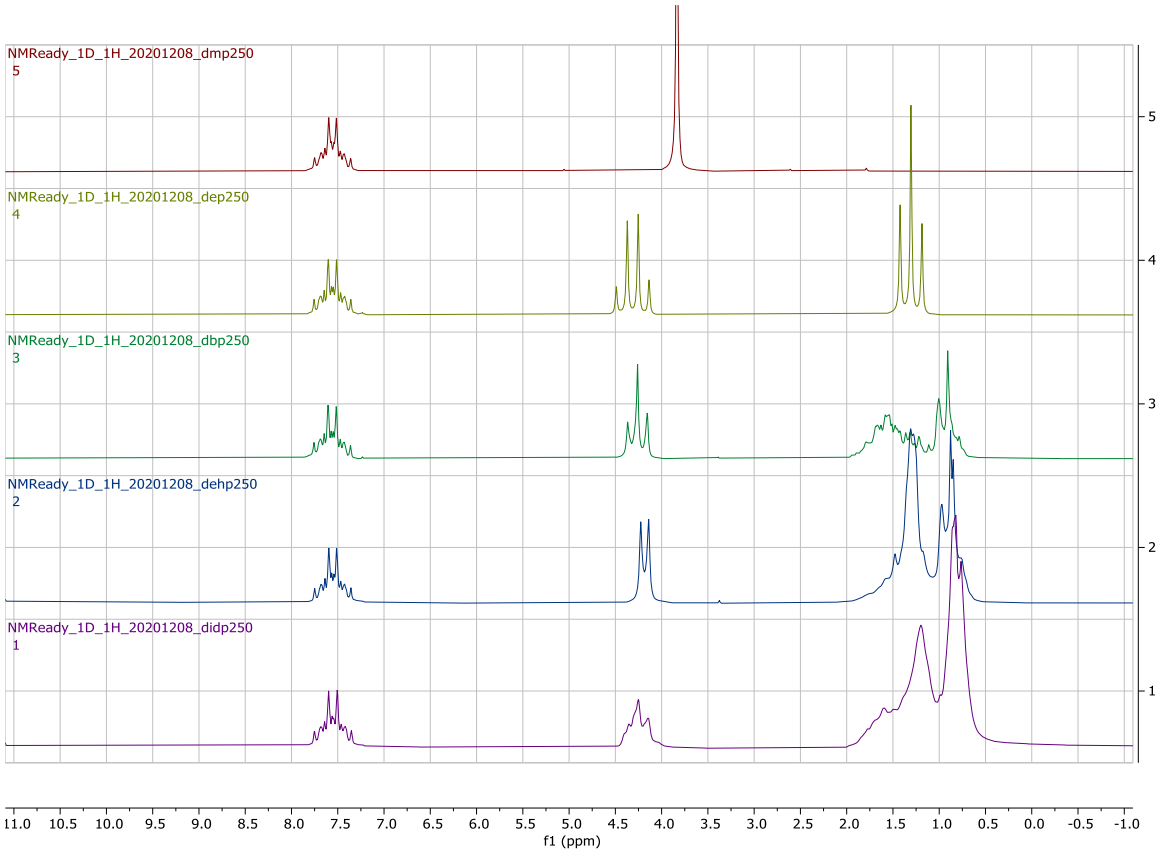

Figure 54 ^{1}H NMR spectra of 0.25M solutions of single phthalates in $CDCl_3$, showing variations in splitting patterns for homologous phthalates. From the top; dimethyl phthalate, diethyl phthalate, dibutyl phthalate, diethylhexyl phthalate, diisodecyl phthalate.

As discussed later in Chapter 4, a combination of two plasticisers is not uncommon in plasticised PVC. For illustration purposes; individual and summed spectra for an equimolar DEHP/DIDP combination are shown in Figure 55. As demonstrated with the arithmetically summed spectra; the broader resonance from DIDP is hard to distinguish beneath the doublet resonance afforded by the branched DEHP, and

detection of both phthalates is not trivial, any development of the method to include mixtures analysis would likely require deconvolution.

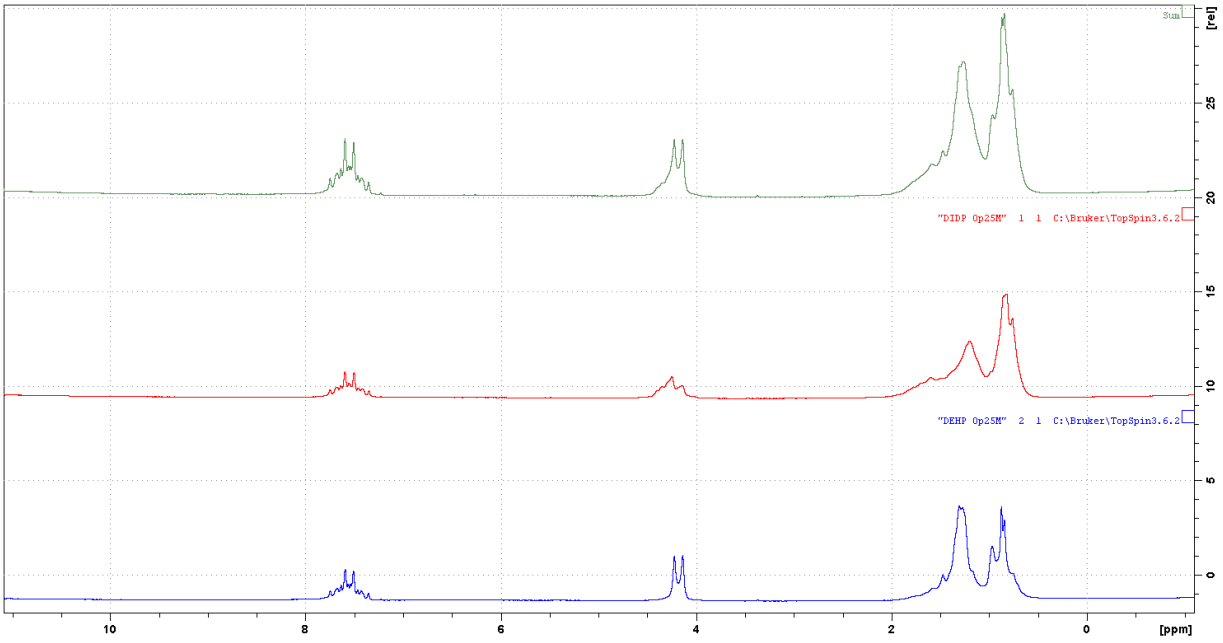

Figure 55 ^{1}H NMR of 0.25M DIDP in $CDCl_3$ and 0.25M DEHP in $CDCl_3$, and the combined (arithmetically summed) spectra.

At this point no further work was undertaken using low-field NMR spectroscopy due to the publication of an improved method which allowed quantification for aromatic plasticisers by Duchowny et al.

The following sections discusses magnetic resonance spectroscopy (NMR) and magnetic resonance imaging (MRI) methods developed to study CA.

3.3.10 ^{1}H NMR analysis of CA using SMolESY data processing

Figure 56 demonstrates a typical ^{1}H NMR spectrum for a plasticized CA sample in DMSO-d_6 recorded at 600 MHz using the DS method. Both phthalate and CA resonances are visible; phthalate resonances are observed at 3.8 ppm (DMP), 4.2 ppm (DEP), and 7.5 ppm (common to all phthalates), and broad peaks between 3-5 ppm represent cellulose acetate.

The singlet peak of acetic acid is also observable at 1.9 ppm. There is evidence that acetic acid concentrations within a sample can be an informative marker for CA's degradation state; Littlejohn et al. used ion chromatography to measure salt levels in historic CA objects and found that *'[acetate] concentrations reflect the state of degradation of the whole material'.*

The result of the SMolESY transformation on spectra recorded using the DS method (where polymer chains are supposed most intact) can be seen in Figure 56. The derivative filter removes polymer signals, and additive resonances are resolved, as exemplified by DMP's singlet resonance at 3.8 ppm and DEP's quartet at 4.2 ppm.

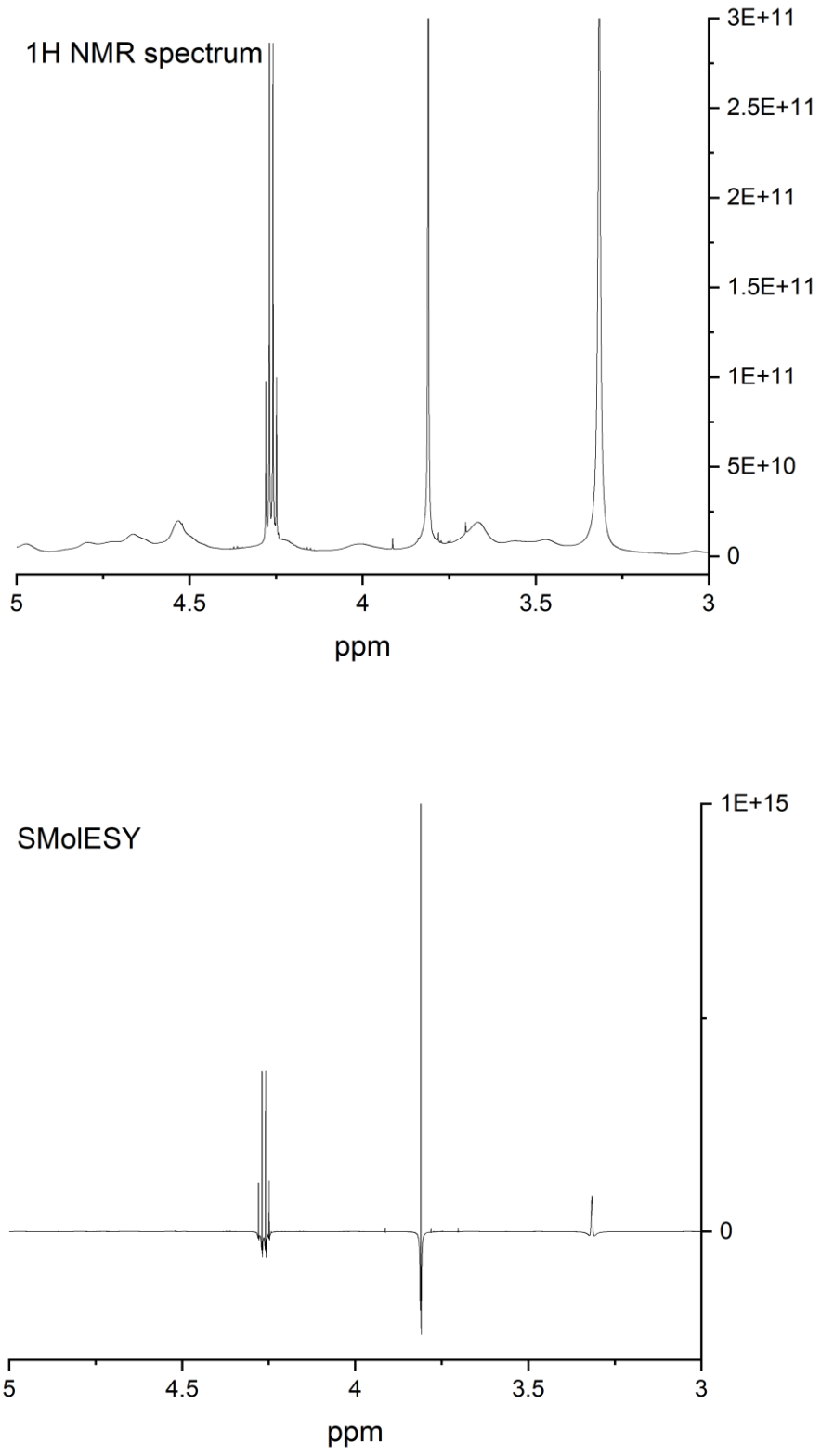

Figure 56: Comparative ^{1}H NMR spectra of sample HS91 (CA plasticized with DEP and DMP) before and after SMolESY processing.

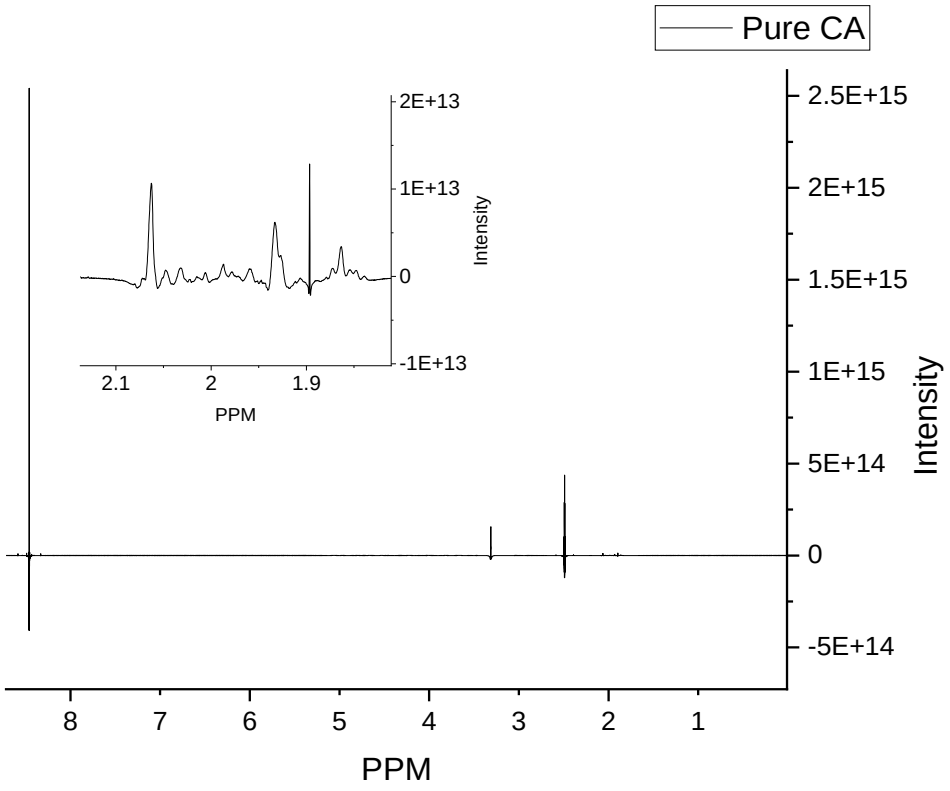

Figure 57: SMolESY spectrum of an unplasticized CA sample. Resonances remain for water (3.3 ppm), DMSO solvent (2.5 ppm), and the internal standard (8.5 ppm). Inset depicts low-level residual signals from CA (1.8-2.1 ppm) and acetic acid (1.9 ppm).

When the sample contains no small molecules of interest, the spectrum in Figure 57 is dominated by water and solvent signals. Small residual peaks can also be observed between 1.8-2.1 ppm and include a characteristic peak at 1.89 ppm for acetic acid (see inset).

Validation of ^{1}H qNMR with SMolESY processing for quantitative analysis of CA

Table 26 shows that spin-lattice relaxation (T_1 values) were found to be independent of concentration over the range studied by comparison with the relaxation data reported by Da Ros et al. The longest relaxation time remains that of the internal standard; therefore, all experiments continued to use the relaxation delay of 50 s in addition to a 4 s acquisition time.

Table 26: T_1 values measured for analytes of interest, chemical shifts denote the specific resonances used for all qNMR data

Analyte	**Peak centre, δ (ppm)**	**T1 (s)**
DEP	1.286	2.76
DMP	3.80	
AcOH	1.915	3.17
Internal Standard	8.47	10.64

Limits of detection and quantification

LOD and LOQs for each analyte (Table 27) are given as molar concentrations. A molar concentration is most appropriate as ^{1}H NMR spectroscopy strictly reflects the number of spins in the solution, but conversion to a percentage by weight (mass of additive/mass of host sample) is used routinely in polymer science.

Table 27: SMolESY spectra limits of detection and quantification for each analyte

Analyte (splitting pattern)	**Chemical shift (ppm)**	**SNR**	**LOD (mM)**	**LOQ (mM)**	**LOD (equivalent wt.%)**	**LOQ (equivalent wt.%)**
DEP (t)	1.25	313	1.27	1.27	0.49	0.49
DEP (q)	4.2	144	1.27	1.27	0.49	0.49
DMP (s)	3.8	3010	1.44	1.44	0.55	0.55
AcOH (s)	1.91	1935	0.94	2.05	0.10	0.22

All analytes in the lowest concentration sample were visibly distinct from the baseline of the spectra. As LOD is influenced by peak shape, width, and intensity, multiplet resonances of DEP were harder to distinguish versus singlet DMP and AcOH peaks which remained distinct from the baseline at the lowest molar concentration. As previously defined (Page 2) limits of quantification were determined as the sample with the lowest concentration for which the signal-to-noise (SNR) ratio exceeded 86 for all component peaks of a split resonance.

Validity of DEP, DMP and acetic acid quantification

For the overlapped peaks (DEP quartet, DMP, acetic acid), the deconvolution method returned average values within 111-120% of the spiked concentration, whereas those measured from SMolESY spectra gave more accurate measurements at 93-109% of the spiked value. In all cases, the residuals are random about zero, confirming the linearity of the SMolESY response for the peaks of interest.

The graphs shown in Figure 58 compared the qNMR-SMolESY method for quantitative analysis, against standard integration of the processed real spectra (for the non-overlapped DEP triplet) or against the integrals measured using the 'global spectral deconvolution' (GSD) fitting method in MNova software (all overlapped analyte peaks). The results from linear regression between measured and spiked concentrations are supportive of the SMolESY method's quantitative accuracy for the analytes of interest.

All results indicate a linear working range with $R^2 > 0.99$ under the experimental conditions of 0.5 – 30 wt.% DEP and DMP, and 0.1 - 6 wt.% acetic acid. Errors in the spiked analyte concentration derived from sample preparation were estimated and found to be up to 5%, despite efforts to minimize systematic errors. Conversely, in common with the majority of quantitative NMR studies, errors from spectral processing were assumed to derive from integration, and a maximum error of 1% was estimated as in the original SMolESY study. Analysis of blank samples containing only internal standard and polymer gave a background reading in the regions where DMP and acetic acid protons resonate (<0.1 wt.%); therefore, fitting through the origin was not undertaken.

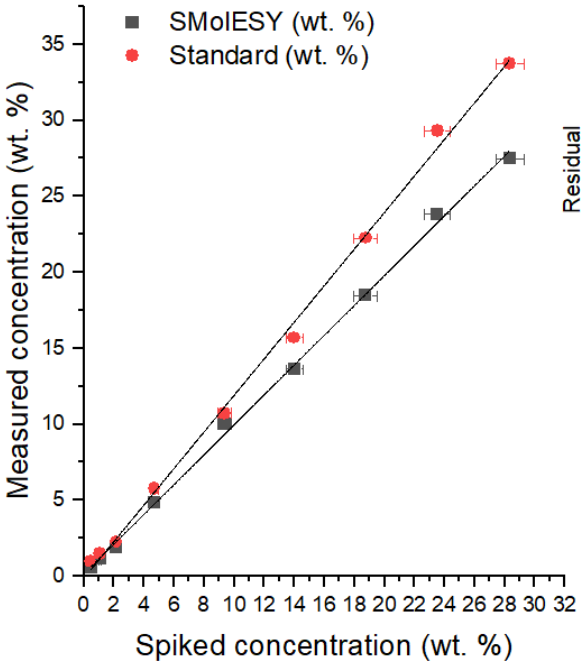

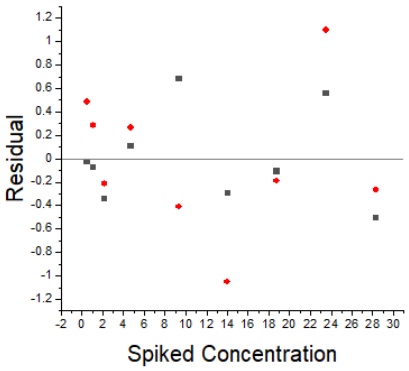

Analyte	diethyl phthalate, 1.25 ppm	
Equation	y = a + b*x	
Plot	SMolESY	Standard
Intercept	0.15034 ± 2.93462E-5	-0.11679 ± 3.59397E-5
Slope	0.98254 ± 1.95853E-6	1.2033 ± 2.39857E-6

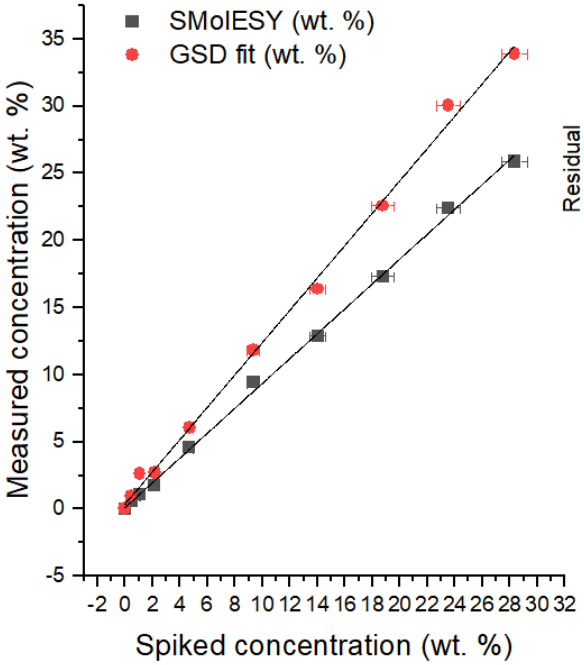

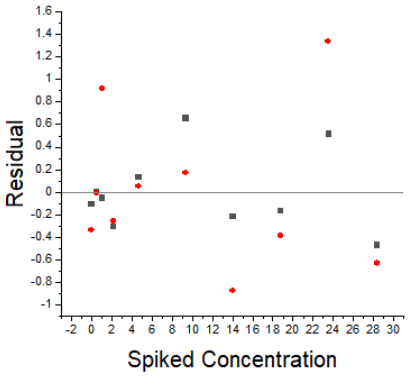

Analyte	diethyl phthalate, 4.2 ppm	
Equation	y = a + b*x	
Plot	SMolESY	GSD fit
Intercept	0.10462 ± 2.46148E-5	0.37096 ± 3.20139E-5
Slope	0.92599 ± 1.73163E-6	1.20434 ± 2.25214E-6

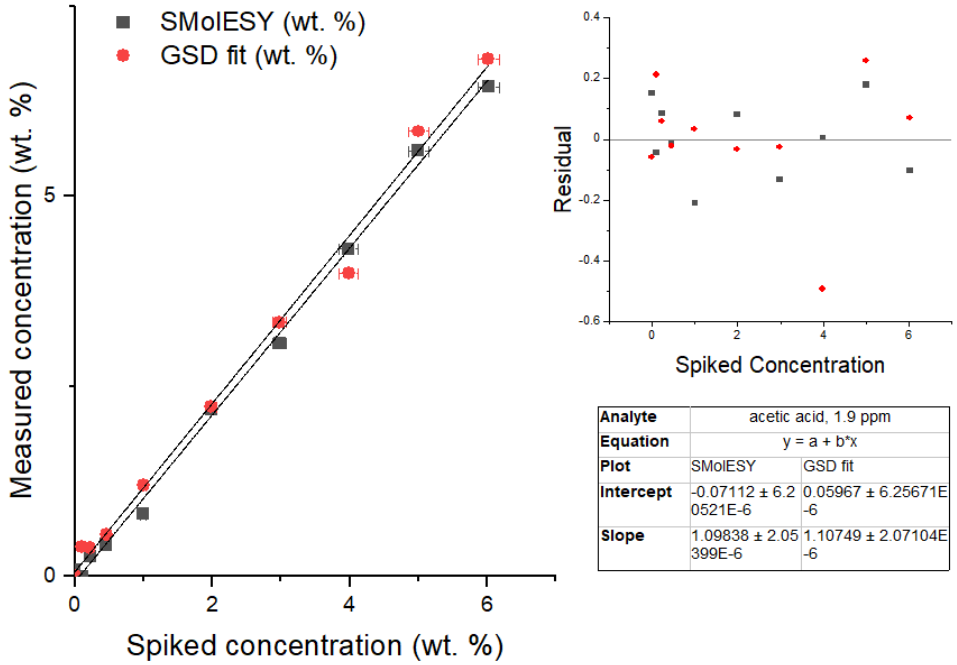

Analyte	acetic acid, 1.9 ppm	
Equation	y = a + b*x	
Plot	SMolESY	GSD fit
Intercept	-0.07112 ± 6.20521E-6	0.05967 ± 6.25671E-6
Slope	1.09838 ± 2.05399E-6	1.10749 ± 2.07104E-6

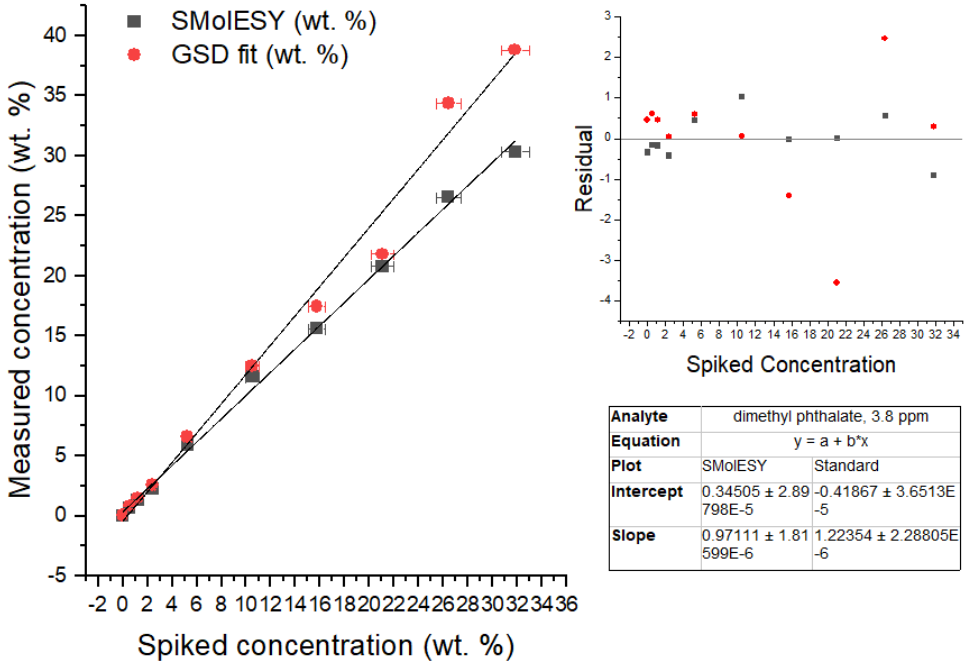

Analyte	dimethyl phthalate, 3.8 ppm	
Equation	y = a + b*x	
Plot	SMolESY	Standard
Intercept	0.34505 ± 2.89798E-5	-0.41867 ± 3.6513E-5
Slope	0.97111 ± 1.81599E-6	1.22354 ± 2.28805E-6

Figure 58: Comparison of spectra analysis methods (integration of phase-corrected spectra, integration of phase-corrected spectra with GSD, and integration of

SMolESY spectra) for absolute quantification of additives in a CA plastic sample. Spiked samples containing unplasticized CA, 0.5 – 30 wt.% DEP and DMP, and 0.10 – 6 wt.% AcOH were prepared, and the spiked concentration was compared to the measured concentration. Error bars represent the uncertainty derived from serial dilution of the spiked solutions.

Application to real samples

Assessment of 6 qNMR spectra previously recorded by Da Ros et al. confirmed that concentrations measured using the qNMR-SMolESY method are comparable to those measured from Da Ros et al.'s FTIR and qNMR-DEP analysis (Table 28). Positive correlation between both NMR methods is observed. The qNMR-SMolESY method underestimates the wt.% DEP versus the standard qNMR method; a trend which appears to increase with increasing concentration but cannot be explained by differences in line width.

Table 28: Total and individual concentrations of small-molecule components (incl. DEP, DMP and AcOH) measured by ATR-FTIR spectroscopy and ^{1}H NMR spectroscopy (processed with qNMR-DEP and qNMR-SMolESY methods).

Sample	**^{1}H qNMR-DEP[a] (phased spectrum)**	**^{1}H qNMR-SMolESY (imaginary spectrum)**				**ATR-FTIR spectroscopy[a]**
	wt.% DEP CH3	wt.% DEP CH3	wt.% DMP	wt.% AcOH	Total Phthalate wt.%	Total Phthalate wt.%
SDR392	11.8	11.5	11.4	1.0	22.9	23.30
SDR391	21.4	21.2	6.5	0.2	27.7	27.07
SDR390	24.73	23.1	0.2	0.0	23.3	23.58
SDR389	26.0	23.1	0.5	0.1	23.6	24.38
SDR388	28.1	23.2	0.0	0.2	23.2	25.32
SDR387	28.1	24.8	0.4	0.0	25.2	26.91

[A]Values reproduced from Da Ros et. al.

All-in-one method for DS measurement and small molecule quantification

Accurate quantification of small molecules using the qNMR-SMOLESY method offered the possibility that the measurements made by Da Ros et al. could be achieved with only one ^{1}H NMR experiment and one sample using the workflow outlined in Figure 59.

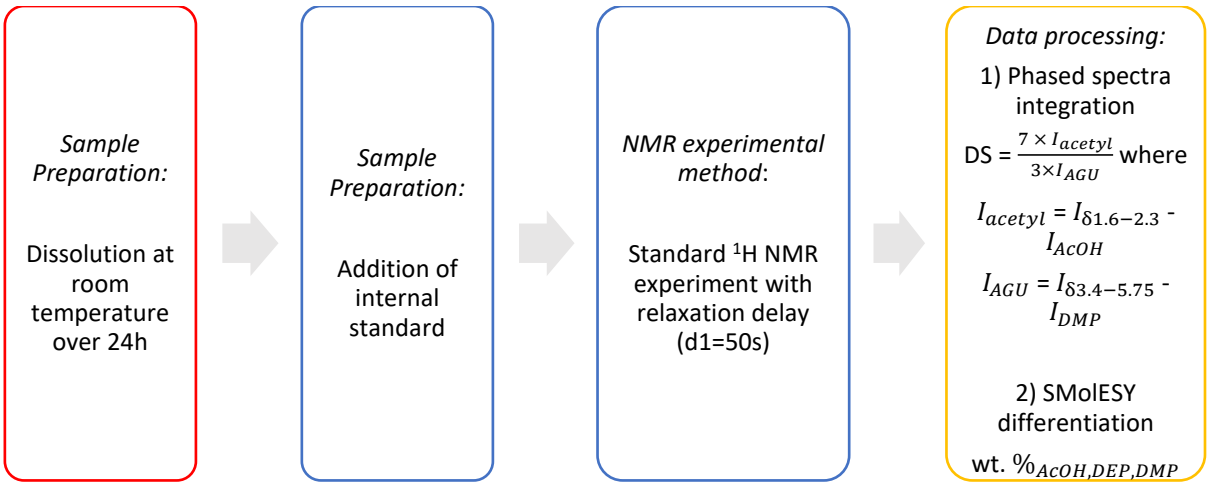

Figure 59: A proposed method for the measurement of DS and small molecule concentrations.

The experimental method used unaided dissolution to minimize polymer chains scission (c.f. DS method). Sample preparation also included the addition of an internal standard, and spectra were acquired after a relaxation delay to meet qNMR guidelines (c.f. qNMR method). For data analysis, DS measurement was performed on the phased spectrum, and transformation of the imaginary spectrum using the SMolESY method allowed small molecule quantification.

Table 29: Comparison of DS measured using ATR-FTIR spectroscopy, and ^{1}H NMR DS and all-in-one methods. [a] values published in Da Ros et. al.

Sample	**ATR-FTIR spectroscopy[a]**	**^{1}H NMR[a]**	**All-in-one method (incl. relaxation delay d_1 = 50s)**
HS91 doll head	2.440 ± 0.017	2.219	2.014
CW-red	2.452 ± 0.013	2.307 ± 0.026	0.36
CW-black	2.454 ± 0.012	2.268 ± 0.023	0.08
CW-green	2.457 ± 0.010	2.313 ± 0.016	2.018

Table 30: Comparison of concentrations measured from ^{1}H NMR recorded using the qNMR-SMolESY and all-in-one methods.

Sample	**All-in-one-SMolESY**			**^{1}H qNMR-SMolESY (imaginary spectrum)**			**^{1}H qNMR-DEP (phased spectrum)**
	DEP CH3 wt.%	DMP wt.%	AcOH wt.%	DEP CH3 wt.%	DMP wt.%	AcOH wt.%	DEP CH3 wt.%
HS91 doll head	11.8	14.8	0.9	9.3	12.8	0.8	10.8
CW-red	22.3	8.9	1.5	16.0	7.2	0.1	19.7
CW-black	21.4	0.9	0	19.7	0.8	0.1	23.4
CW-green	22.9	0.6	0.1	20.0	0.5	0.1	23.5

Additive concentrations are in broad agreement between the two SMOLESY methods, the discrepancy can be ascribed to the lack of pre-processing such as phase and baseline correction. The all-in-one method overestimates the concentration versus underestimation by the qNMR-SMOLESY method, but there is no current value in knowing an absolute plasticiser concentration for conservation practice. The values for DS and acetic acid concentration are relevant parameters in lifetime predictions. The low value for DS in two samples (CW-red and CW-black) cannot be fully explained but the overestimation of acetic acid and underestimate of DS in sample CW-red suggests deconvolution of the acetic acid peak from the glycosidic ring peaks was not successful and requires additional evaluation.

3.3.11 MRI analysis of solid CA samples

Figure 60 shows the magnetic resonance image produced using the instrument's shortest available echo time TE = 0.07 ms. The brightest parts of the image correspond to pixels with the highest proton density.

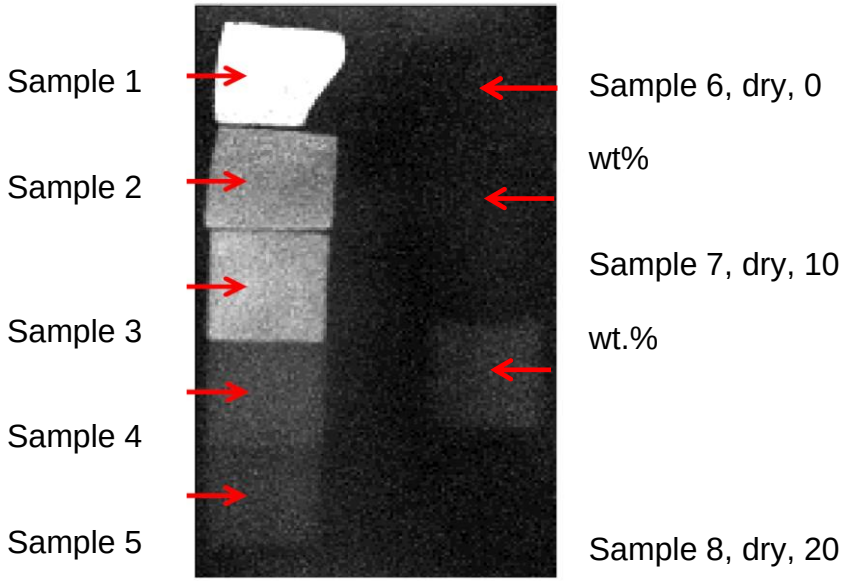

Figure 60: MRI image of saturated 'wet' samples (left) adjacent to 'dry' samples (right), images acquired with TE=0.07 ms

Polymer visibility

The lack of observable signal in Figure 60 for a dried and unplasticized sample (sample 6) suggests that complete relaxation of CA protons occurred before signal acquisition could begin. Signal acquisition is limited by the instrument setup; the RF coil is used initially to excite the sample, and then receives the MR signal in return. Such 'ultrafast relaxation' is consistent with other literature studies, for example, ultrafast relaxation has previously been observed for three solid polymers (PEEK, PA6, PET) using a similar UTE pulse sequence and a comparable 3T scanner [13].

A range of T2* values was observed for various plastics; a PE sample with an ultrashort T2* of 94 μs was just detectable by clinical scanners, whereas much larger values for PUR and PVC were measured; a TE of 4.82 ms was required to observe total signal decay for a PVC sample (T2*=0.7 ms).

Visibility of hydrated samples

As no signal is expected from CA protons, the visible signals from samples 1-5 are likely to result from the water within the plastic sample. All wet samples (1-5) were visible when using an ultrashort echo time (TE) of 0.07 ms and remained visible at the longest TE of 1 ms. Relaxation of the excited species was not complete at the longest echo time of 1 ms, therefore it was impossible to measure T2* from the non-decayed signal.

Figure 61 shows the mean signal intensity across each sample. When comparing signal intensity between wet samples, the results suggest a general trend of increased signal intensity with the mass of water absorbed. Sample 1 gave the highest signal intensity, which is consistent with it being the most saturated sample. Correlation is also observable between increasing water content and signal intensity for samples 3 to 5. Sample 2 does not follow the trend; however, it may show low intensity due to its curved shape; measurement of an averaged signal from the whole sample was impossible, so fewer voxels were sampled and contributed to the average signal intensity.

No equilibrium moisture contents for CA samples have been found in the literature, however, greater than 1% mass increases were observed during Dynamic Vapour Sorption studies of thin-film samples at room temperature and greater than 10% relative humidity. Under environmental conditions similar to those recommended for

museums [14,15], del Gaudio et al. found that aged samples ‘showed greater water affinity than non-aged samples for those containing plasticiser’ [285].

In a best-case scenario, a non-destructive MRI method would enable the dynamics of polymer aging behaviour to be captured in a spatially-resolved manner (concentration profiles) and holistically to ensure all degradation products are observed. For cellulose acetate this would include hydrolysis product formation and plasticiser loss and would require resolution of signals from acetic acid and plasticisers. However, as there is evidence of incomplete relaxation of both plasticiser and water at all echo times, the distinction between additive and water signals would also be required. Due to the non-ideal sample thickness and shape for voxel analysis, attempts at signal resolution by bi- or multi-component fitting of the decay curves could not be explored [290]. If this were achievable, MRI could be a useful tool to further study the degradation of CA due to water absorption and its interplay with plasticiser migration.

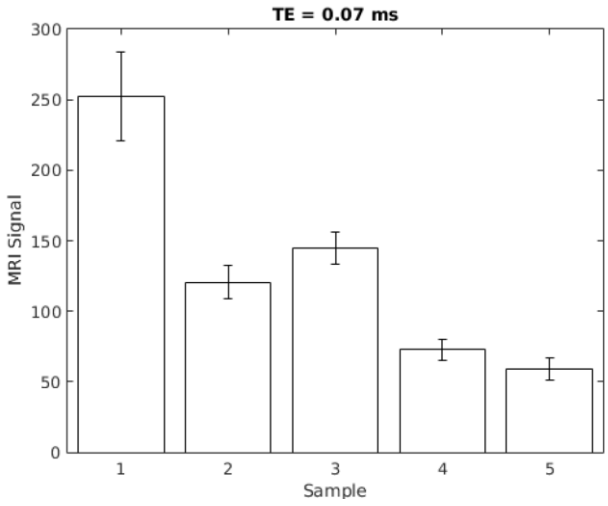

Figure 61: Mean signal intensity of 'wet' samples 1-5

Visibility of plasticised samples

Comparisons between dry plasticized samples 6-8 are less clear as the weak resonance observable in the most highly plasticized sample 8 could be due to the relaxation of DEP molecules comprising 20 wt.% of the sample mass. Despite sample 7 comprising half the amount of DEP molecules no signal was detectable. A lower proton density would reduce the signal intensity, however, the extent to which this accounts for the complete absence of a recordable signal is unknown. Furthermore, given the weakly visible signal from the dry but highly plasticized sample 8, it should also be considered that plasticiser molecules may contribute to the signal observed in 'wet' samples 3-5.

Relaxation parameters (T_1, T_2*) for the species responsible (DEP or water) for the signal in CA were not measurable due to the incomplete signal decay at the longest echo time, and no relevant data could be found in the literature. However, many factors including the surrounding matrix and molecular mobility will influence spin-spin relaxation. A similar hydrogen-bonding network akin to the biological examples of water in bone is probable for polymer-plasticiser and polymer-water interactions, which would be expected to quicken relaxation versus unbound species. Therefore, short T2* values (<10 ms) would not be unexpected.

Limitations

An inherent limitation of using a clinical instrument is the resolution afforded by 0.9 mm^3 voxel sizes. Pre-clinical scanners designed for rodent MRI offer greater resolution with smaller samples, however, UTE pulse sequences are not yet possible using pre-clinical hardware. As image slice thickness (0.9 mm) was comparable to sample thickness (1 mm), and not all samples were perfectly flat, the analysed slice did not always represent the entire sample. Thicker samples would be required to

determine if concentration gradients across three dimensions can be observed with the resolution offered.

3.4 Conclusion

In terms of improving polymer identification for PVC, matching ATR-FTIR spectra to open-source ATR-FTIR spectroscopy libraries was especially effective, although non-phthalate formulated samples were poorly matched. The diversification of PVC library spectra is required to improve matching for PVC identification which was limited by the dominance of phthalate-plasticised reference spectra. Confusion with other thermoplastics was common when matching ER-FTIR spectra to the only pre-existing PolIRes library. All ER-FTIR spectra measured here are noisy, but using a smaller aperture would likely improve the quality of observations made on non-flat samples, which account for four of the samples unsuited to analysis by ER-FTIR spectroscopy. Furthermore, the example of an unlabelled SBR co-polymer in a Primpke library PVC spectrum demonstrates that co-polymer blends may be present and could lead to a lower match score versus more common formulations. For the analysed samples, no peaks which could be related to other co-polymers such as vinyl acetates were observed, although more extensive polymer analysis by NMR spectroscopy would be the most conclusive way of ruling out a blended plastic containing co-polymers.

For plasticiser identification, ER-FTIR spectroscopy & ATR-FTIR spectra for each object were used to establish that ER-FTIR spectroscopy is suitable for the classification of phthalate, terephthalate, and trimellitate-plasticised samples. This was achieved using different peaks to those traditionally used for plasticiser identification and offers the advantage of high peak intensities in generally noisy ER-

FTIR spectra. The shapes and peak maxima of the three most intense peaks (between ~1300-1000 cm^{-1}) across all ATR-FTIR spectra were observed to depend on the plasticiser class for trimellitate, phthalate and terephthalate plasticised samples. Analysis of these peaks offer a more robust method for plasticiser identification versus the previously reported use of low intensity peaks within the 730-50 cm^{-1} region for ATR spectra. The suggested peaks are easily identifiable in KKT transformed ER spectra and can be compared to ATR-FTIR spectra for identification. All samples showed similarly high plasticiser concentrations (>20 wt.%), therefore a limit of detection using the ER-FTIR spectroscopy method could not be calculated, although the low SNR values measured suggest concentrations below 20 wt. % seen here would be challenging to observe with the traditional 730-750 cm^{-1} region. A lower detection limit may be achievable using the suggested peaks. While the identifiable plasticisers are limited in scope, ER-FTIR spectroscopy offers a rapid screening tool before destructive methods such a GC-MS and NMR are required.

For additive quantification, the established ^{1}H NMR spectroscopy method proved the easiest, quickest, and most conclusive method to identify and quantify plasticisers. But a combination of GC-MS and NMR was required to identify some sample additives; NMR spectroscopy of extracts offered the simplest way to assess sample additives quantitatively and qualitatively. Low field NMR required higher sample mass than the established GC-MS and NMR methods but offered suitable resolution for qualitative identification of most plasticisers. The method requires 10 mg of sample, which limits its use in conservation settings. No aliphatic plasticisers such as ATBC, DEHA or DINCH were identified in the purchased objects, but their inclusion would be a useful extension of the work considering their use in modern

formulations. As such spectra of a variety of pure plasticisers and peaks of interest for PVC analysis are reported here for future reference.

For cellulose acetate samples, the recently developed SMolESY method to derivatize ^{1}H NMR spectra successfully resolved resonances from cellulose acetate containing phthalate plasticisers and acetic acid, with low limits of detection <0.5 wt.%. It is the first demonstration of how derivative NMR spectra can aid the analysis of cellulosic plastic samples where the overlap of broad polymer resonances impedes the analysis of small molecule additives in the sample matrix.

Studies to date suggest there is a range of small molecules which may be present in degraded CA. During this study sufficient historic or degraded samples were not available, so the experiments were not performed in an untargeted manner which would enable the method to be evaluated for the detection and analysis of non-phthalate additives. However, expected chemical shifts which have limited overlap with CA polymer peaks suggest our method would not hinder their identification or quantification.

In comparison to our previous work, the validity of the ‘all-in-one method’ is perhaps the most useful aspect, where analysis of the polymer’s degree of substitution, additives quantification, and free acetic acid concentration can now be performed and uses only one sample and one qNMR experiment. However, the method was only successful for two of four samples tested here. Further samples are needed to understand if the method can be considered accurate for all CA samples.

When compared to previously published methods in the conservation literature, it offers a more detailed analysis of a sample versus ATR-FTIR spectroscopy,

particularly in the distinction of species with common functional groups (e.g. carbonyls in phthalates and acetates), which typically requires chromatographic resolution by time-consuming and solvent intensive GC-MS. However, access to the infrastructure is rare outside academia. Additionally, like the sampling method required for liquid injection or pyrolysis GC-MS, solution-state NMR is also a destructive technique. However, sampling the bulk material is more closely representative of the whole object versus the point-based sampling and surface analysis offered by ATR-FTIR spectroscopy. Furthermore, while ATR-FTIR spectroscopy may be performed non-destructively for planar samples, it is known that the non-planar geometries of real objects can severely hinder analysis.

Regarding the MRI experiments for CA analysis, the initial results from saturated samples suggest that the ultrashort echo time sequences are suitable for imaging hydrated CA samples in the range 1-6 wt.%. Highly plasticized samples may also be visible although further work is required to conclude. Comparison to an unplasticized and dry sample suggests that the relaxation decay of protons from CA does not contribute to any of the images captured using the clinical imaging system where 0.07 ms is the shortest echo time achievable. To understand the relaxation behaviour of water and other non-polymeric species within the polymer matrix, the experiment could be repeated over a broader TE range (>1 ms). This would allow complete relaxation to be observed, and T2* to be measured. Ultimately, the method trialled here would not be routinely applicable for heritage objects; the voxel size and resolution of a clinical scale scanner are unsuitable for studying distributions or gradients in small objects, where the microscopic resolution would be required, and the cost is prohibitive. However, the visibility of both water and plasticiser-derived

signals leaves scope for future research into the degradation mechanism of CA by magnetic resonance imaging techniques.

4 The development of a Thin Layer Chromatography method for plasticiser identification

A significant limitation of the methods described in Chapter 4 is the inaccessibility of the instrumentation, as discussed in Chapter 2. This chapter details efforts to develop a TLC method to enable a rapid assessment of plasticised PVC during large-scale condition and collection surveys. Compared to the techniques evaluated in the previous chapter, TLC is amenable to heritage settings due to its simple and high-throughput nature while requiring <1 mg of a sample.

The method development builds upon prior knowledge, including extraction efficiency tests and mobile phase combinations discussed in section 1.5.5. The chapter next details a case study used to develop a surface swabbing method. As evidenced by at least one respondent in the practitioner's survey, sampling ethics in the heritage sector can preclude the destructive collection of samples. As seen in chapter 1, it is well known from indoor air chemistry studies, that SVOCs are abundant on surfaces in households and two studies have found significant concentrations of plasticisers on PVC surfaces and adjacent surfaces, by collecting samples with solvent-wetted swabs. As conservators routinely use swabs to clean objects, the potential to combine the two processes for the collection of degradation products was investigated, i.e., to use the cleaning process for sample collection.

During this work, a PVC object was under conservation at UCL Culture and provided the opportunity to trial swabbing methods with the aid of a professional conservator. The aim of the conservator was to understand what was present on the surface to inform their conservation treatment. The work became a case study within the chapter, with an aim to collect and identify plasticisers from PVC surfaces in a non-

destructive manner using conservation-approved cleaning methods and compare the results to destructive sampling.

Finally, once a new method was developed and limits of detection measured, efforts turned to augmenting data interpretation beyond checking the similarity of Rf values and UV responses. A meta-analysis of literature data was used to assess what plasticiser combinations made sense as judged by their use in commercial products. A frequent itemset mining (FIM) algorithm was used to identify combinations and assess the likelihood of two or more plasticiser occurring together versus individually or in combination with other components. Frequent itemset mining was developed initially for consumer purchase data where it was used to find typical combinations of items per transactions, defined as an ‘association rule’; for example, 60% of people purchasing coffee also purchase milk. For this application a transaction is equivalent to an individual PVC sample, an item is an analyte found within that object, and an association rule is for example ‘DINP is combined with DIDP in 5% of cases’. The use of FIM is relatively novel; it has recently been used to assess chemical exposure risk from consumer product and purchasing data and is more fully explained elsewhere [291].

4.1 Research Goals

In summary, the research goals of this chapter are as follows:

- To identify a simple and cheap method, including a TLC stain for visualisation.
- To determine the limits of detection so that sample amounts may be minimised.
- To evaluate the suitability of swab sampling for historical objects.

- To evaluate the method’s suitability against typical samples discussed in the literature.

4.2 Methodology

4.2.1 Stain preparation

All solutions were stored in amber glassware or foil-wrapped glassware to exclude light. Stains were used within 1 week of preparation.

Vanillin-H_2SO_4

Vanillin stain (35 ml) was prepared by dissolving 6.9 g of vanillin in absolute ethanol (35 mL) under stirring. A 2M solution of sulfuric acid was prepared from concentrated sulfuric acid (11 mL) and distilled water (100 mL).

Sulfone phthalein dye solutions

Dye indicator solutions are typically prepared by dissolving the solid free acid in a solvent system containing a weak aqueous sodium hydroxide solution with ethanol, water, or both. Alternatively, the dyes' sodium salt may be dissolved in an ethanol and water mixture.

0.04% Bromocresol green stains

Bromocresol green (BCG), free acid (40 mg, Merck KGaA, Darmstadt, Germany) was dissolved in 100 mL absolute ethanol, and 0.1 M aqueous sodium hydroxide (Atom Scientific, Hyde, Cheshire, UK) was added dropwise with stirring until a blue colour appeared.

A BCG solution was also used as purchased (Atom Scientific, Hyde, Cheshire, UK). The blue stain contained 0.04 w/v% bromocresol green sodium salt in industrial methylated spirits (95 % ethanol in methanol).

Bromothymol blue indicator solution

A bromothymol blue indicator solution was used as purchased (Honeywell Specialty Chemicals Seelze GmbH, Seelze, Germany). The green stain contained 0.05 w/v% bromothymol blue in a 20% aqueous ethanol solution.

4.2.2 Sample preparation

Extraction from solid plastic samples

1 mg of sample was removed from an object's surface by a scalpel and extracted in hexane (20-50 µL) for at least 5 minutes at room temperature. Aliquots of extract solutions were taken immediately to avoid evaporation of the solvent.

Extraction from cleaning swabs

A cotton swab wetted with a 50% isopropanol/water solution was moved across the object surface in a lift-and-roll motion. The swab was removed from the wooden support and extracted in hexane (100 µL per swab) for at least 20 mins.

Reference solution preparation

To a vial containing bromocresol green, free acid (10 mg) and benzyl benzoate (10 mg) was added hexane (10 mL), producing a yellow solution (1 ug/µL).

Standard solutions preparation

During method optimisation, mixed solutions were prepared as above to give a concentration of 1 ug/µL per individual analyte in the sample. Acidic analytes were dissolved in ethanol or ethyl acetate; all others were prepared in hexane.

Case study - Direct sampling of objects

Discrete beads (< 1 µL) of the orange liquid were sampled directly from the surface with a microcapillary pipette.

Solid particles were removed by scraping with tweezers and placed in a vial before analysis by NMR.

Surfactant cleaning solutions of Orvus Paste and Dehypon 54 were prepared by dissolution in deionised water to give 1 w/w% solutions. A hand-rolled cotton wool swab on a bamboo stick was briefly dipped into the cleaning solution and applied to an inconspicuous trial area (approx. 2 cm^2) of the object using a 'roll-and-s' motion by the Conservator. A new dry swab was used to remove any excess cleaning solution when necessary. For each trial spot, the used cotton wool swab(s) was removed from the bamboo stick, sealed in a scintillation vial, and refrigerated.

A pre-soaked non-woven IPA wipe (Cutisoft Pre-Injection Wipes) akin to those used in the environmental and forensic analysis was also tested. The wipe was held in forceps and moved across a small area (approx. 2 cm^2) of the surface, and the used wipe was placed in a scintillation vial.

For the phthalate extraction trial, DEHP (13.5 mg), DEP (12.6mg) and DBP (10.3 mg) were added to 11.4 mL of R0 grade water. 50 mg of the surfactant was added to 2 x 20 scintillation vials, followed by 5 mL of the aqueous phthalate solution. The solutions were vortexed and left to settle for 18 hours before n-hexane (1 mL) was added, the vials vortexed, and left to settle. The top layers were sampled twice with a micropipette (1 µL and 5 µL) and the aliquots applied to a F254 Silica gel TLC plate.

The Dehypon solution was then heated above the cloud point to 40 °C for 10 mins, before cooling to room temperature. Sodium carbonate (500 mg) was added to the Dehypon solution and sodium carbonate (1 g) was added to the Orvus paste solution. Both solutions showed two distinct phases, and a light foam in the Orvus paste solution collapsed. The solutions were left to settle for 24 hours, after which time both Dehypon

layers were clear, the lower aqueous layer was clear for Orvus paste, but the upper layer was cloudy. The top layer of each solution was sampled as before and applied to a TLC plate which was immediately visualised under 254nm light.

Swab sampling of samples DOD, TCS and TWB

A cotton swab wetted with 1:1 isopropanol: water and the excess solvent was removed before it was rolled over the surface (TCS = 36 cm^2, DOD = 4 cm^2, TWB = 63 cm^2), removed from the wooden stick, placed in a vial, hexane (100 µL) added and the vial agitated. A 5 µl aliquot of the hexane solution was removed after 10 minutes. As the swab absorbed the hexane, the aliquot was collected by squeezing the swab against the vial or pressing the micropipette into the swab.

4.2.3 Plate preparation

Normal phase TLC plates (POLYGRAM SIL G UV254, silica gel layer, 5 x 20 cm, Macherey-Nagel, Duren, Germany, or HPTLC Silica gel 60 F_{254}, Merck KGaA, Darmstadt, Germany) were cut to 5 x 10 cm, wrapped in foil, heated at 110 °C for 30 minutes, and allowed to cool in a desiccator before use.

The mobile phase (10 mL) was added to a CAMAG Twin Trough Chamber (10 x 10 x 2 cm) containing a Whatman Filter Paper to aid saturation of the chamber environment over 30 minutes before adding the prepared TLC plate.

Solutions were applied using a microcapillary pipette (1-5 µL Hirschmann Microcapillary Pipette, Merck KGaA, Darmstadt, Germany). 1-2 µL of analyte solutions were applied to the plate alongside a 1 µL aliquot of the reference solution. Aliquots were applied evenly across a pre-marked pencil line drawn lightly 1 cm above the base of the plate, and aliquots were applied 0.5 cm away from plate edges.

4.2.4 Plate elution

The aliquot solvent was allowed to evaporate before the dried plate was lowered into the elution solvent, ensuring no contact with the filter paper or adjacent plates. The solvent front was developed over 8 cm (typically 8-10 minutes) before the plate was removed, and the solvent was allowed to evaporate for 5 minutes.

All experiments were performed under ambient conditions, and the temperature ranged between 15-20 °C and 30-60 % relative humidity.

Pre-concentration

If individual aliquots were applied unevenly, for example, if applied in multiple stages, plates may be placed in a flat-bottomed beaker and eluted in 100% methanol or acetone (1 ml) until the solvent front reaches the predefined pencil line.

Plate development, visualisation, and recording

A photographic lightbox was constructed from a cardboard box and black fabric. A UV lamp (254 nm, UVC) was suspended 9.5 cm above and to the right of the plate. Two LED strips were attached to the underside of the box lid (12 cm above the plate). A small aperture for the smartphone camera lens was cut in the centre of the box lid. TLC plates were placed on a black background inside the base of the box.

All plates were first visualised and photographed at 254 nm. The plate was then exposed to the stain in a sealed chamber (Iodine stain for 30 mins) or dipped in a solution (BCG, BTB, and vanillin). Iodine-stained plates were observed immediately; otherwise, excess liquid was blotted on absorbent paper, and the plate was allowed to develop at room temperature.

The vanillin-stained plate was first heated at 80 °C for 10 minutes before spraying with sulfuric acid and heating at 110 °C for 30 minutes. Secondary alkaline or acid stains were applied using a spray bottle at 20 cm from the plate.

Plates were monitored for the appearance of coloured spots, typically around 5 - 10 minutes after staining and were photographed under visible illumination.

4.2.5 Image analysis

R_f values and the resolution (R_s) between adjacent spots were measured using ImageJ or JustTLC software and Microsoft Excel.

$$R_f = \frac{distance\ from\ baseline\ to\ spot\ centre\ (X)}{solvent\ front\ distance}$$

$$R_s = \frac{2(X_2 - X_1)}{W_1 + W_2}$$

Where W1 and W2 represent spot width, and X is the distance from the baseline to spot centre.

4.2.6 Meta analysis of literature data

Relevant publications were identified by combinations of search terms “plasticiser”, “quantification”, and/or “survey” using the Web of Science platform.

Table 31 lists nine publications which provided quantitative analysis of plasticisers with quoted wt. % and quoted detection limits or documented the non-detection of a targeted analyte.

Table 31: Publications meeting search criteria

Publication	**Number of samples**	**Overview of study**
Al-Natsheh, 2015 [292]	17	GC–MS determination of eight phthalates in polymeric toys and childcare articles
Bernard, 2015 [293]	7	Migrated substances from medical devices
Bernard, 2017 [294]	9	Consumer goods & Toys
Danish Environmental Protection Agency, 2015 [295]	37	Consumer goods & Toys
Kawakami, 2011 [296]	34	Medical devices
McCombie, 2017 [297]	120	PVC Toys
Rijavec, 2022 [240]	77	Consumer goods
US CPSC, 2010 [298]	35	Consumer goods
Xie, 2016 [151]	13	Consumer goods & Toys

Where possible, analytes common to multiple samples were identified according to a quoted CAS number and name (N.B DINCH is reported under two CAS numbers). Every effort was made to identify the correct analyte. However, DnOP/DEHP are isomeric, and the latter has been referred to as DOP.

Data cleaning

If a sample was tested for an analyte, its value was recorded as the quoted % wt. If the target analyte was not detected (i.e. wt.% = 0 or below the LOD), the value was set to 0 (numerical) or nd (non-numerical), dependent on each algorithm's requirements. If a sample was not targeted for an analyte, it was labelled ‘NA’. This

process reduced the number of numerical data points from 4006 to 750 across 369 samples.

For association rule mining, 0 values were set to ‘FALSE’ and all remaining numeric values set to ‘TRUE’. NA values remained unchanged.

Data filtering

As discussed in Chapter 1**,** the limit of detection for TLC is much higher than the GC-MS and NMR techniques used to generate the data points of the dataset. The association mining algorithm used requires a binary dataset and does not consider the concentration value (wt%). Therefore, association rules were likely to include minor or trace analytes not relevant to TLC. For example, DEHP is a common artefact in GC analysis of phthalates, and its actual value must be corrected by blanks.

For TLC, a LOD of 0.5 ug/spot is typically quoted; therefore, basic scenario modelling was used to explore the effect of proposed experimental variables on analyte detection by TLC. The resulting minimal analyte concentration (wt. %) was used to filter the dataset.

Scenario modelling to estimate minimal detectable analyte concentration for TLC.

The extract concentration (ratio of sample mass to extraction solvent volume) was fixed at 50 µL per mg of sample. Factors modelled include analyte concentration in the sample, extraction efficiency of the analyte in the solvent, and aliquot dosage.

Association analysis

Instead, the *apriori* algorithm via the arules packages was to perform for association analysis. Frequent itemset mining was used to identify combinations of additives that exist within one or more rows of a dataset.

As the different studies targeted different analytes the dataset is incomplete. For each pairwise plasticiser combination mined the dataset was first subset to include only samples where the method tested for both additives. “Support”, shown in Equation 5 was therefore calculated relative to the number of samples tested for both analytes and not the whole dataset.

Equation 5:

$$Support = \frac{number\ of\ samples\ containing\ A\ \&\ B}{number\ of\ samples\ \ tested\ for\ samples\ A\ and\ B}$$

Some of the measures which are used to assess the mined rules are ‘support’, ’confidence’, ‘coverage’, and ‘lift’ as defined in Table 32. Higher values of support, confidence and lift provide stronger evidence of the association rules’ validity.

Table 32: Measures of interest for evaluation of mined association rules

Interest Measure	**Definition**	**Interpretation**
Support	Support(A=>B) = P(A U B)	the probability of A & B occurring together in a sample
Confidence	Confidence(A=>B) = P(B|A)	the % of cases where A is present which also contain B. a value of 1 shows that B is always present if A is present
Coverage	Coverage(A=>B) = P(A)	the probability for the antecedent (A) alone in the subset
Lift	P(A U B) / P(A)P(B)	a value greater than 1 indicates a combination occurs more frequently than expected if they were independent
Count		Number of samples where A & B were observed together
Total samples		Number of samples tested for A & B

Association rules for >2 combinations

The process was repeated to incorporate combinations of >2 additives with a maximum number of combinations = 2^n-1 where n= number of additives.

The dataset was subset to include only the 120 samples analysed using McCombie et al's method. It is the most comprehensive method for plasticiser analysis, targets 18 analytes including the three most common additives. Rules were mined using the apriori algorithm, with a confidence limit of 0.5 (50%) and a support of 0.01 (1%).

Scatter and balloon plots were created using Python (version: 3.10.12), plotly (5.15.0), and pandas (1.5.3).

4.3 Results

Scenario modelling was used to evaluate the impact of experimental parameters; by calculating the on-plate concentration of an extracted analyte under given conditions. Table 33 demonstrates the effects of solvent extraction efficiency between 10-100% (>50% is likely, c.f. page 58), and sample mass. The calculations assume a 1 ul aliquot volume which minimises the need to repeatedly apply the solution on to the TLC plate, which can cause the analyte solution to the spread and give an uneven baseline. Additionally, a 50-fold extraction solvent volume (50 µL) represents the minimal amount to fully cover a typical 1 mg sample. Finally, a 0.5 ug per spot limit of detection (LOD) was targeted following the work of Fhionnlaoich et al. for aromatic analytes visualised under UV light [299].

Shaded cells in Table 33 indicate conditions where the on-plate concentration of the analyte would be above the LOD. For example, a 1 mg sample of a plasticised object containing >5 wt.% aromatic plasticiser is theoretically suitable for investigation if the solvent extraction efficiency is greater than 50%. Plasticiser concentrations are generally between 20-40 wt.% for PVC, so a 5 wt.% detection limit would represent the majority of objects. Table 33 also shows that reducing the sample mass by 50%

could be used with more highly plasticised samples. Alternatively, the extraction solvent volume could be decreased to visualise components above 1 wt.%.

Table 33: The effect of extraction efficiency, aliquot volume, sample mass, and plasticiser concentration on TLC spot concentration.. The values highlighted are above a typical 0.5 ug/spot LOD for UV-active analytes by TLC.

Analyte concentration (ug/spot) as a function of extraction yield and plasticiser concentration (assuming a 1 mg sample mass and 1 µL of solvent extract)					
	Plasticiser concentration (wt%)				
Solvent extraction efficiency (%)	**0.1**	**1**	**2**	**5**	**10**
10	0.002	0.02	0.04	0.1	0.2
20	0.004	0.04	0.08	0.2	0.4
30	0.006	0.06	0.12	0.3	0.6
40	0.008	0.08	0.16	0.4	0.8
50	0.01	0.1	0.2	0.5	1
60	0.012	0.12	0.24	0.6	1.2
70	0.014	0.14	0.28	0.7	1.4
80	0.016	0.16	0.32	0.8	1.6
90	0.018	0.18	0.36	0.9	1.8
100	0.02	0.2	0.4	1	2
Analyte concentration (ug/spot) as a function of sample mass and plasticiser concentration with a 50% extraction efficiency, and 1 µL aliquot					
	Plasticiser concentration (wt%)				
Sample mass (mg)	0.1	1	2	5	10
0.1	0.001	0.01	0.02	0.05	0.1
0.5	0.005	0.05	0.1	0.25	0.5
1	0.01	0.1	0.2	0.5	1
2	0.02	0.2	0.4	1	2

The next step was to test visualization methods for expected analytes. The plasticisers used were informed by Chapter 1 and included non-phthalate plasticisers. Dibutyl sebacate appears uncommon in recent literature but was discussed in older TLC methods (see Table 9), which may be useful for older PVC objects in heritage collections.

Benzyl benzoate is not a known plasticiser but is included as a surrogate reference standard. To improve the accuracy of identification, analytes are typically compared against known reference standards spotted in an adjacent band to reduce the reliance on variable R_f values. However, in this study, phthalates are unsuitable standards due to availability; they are regulated chemicals and require a license to purchase in the U.K. Instead, benzyl benzoate was trialed as a surrogate reference. It is frequently used as an internal quantitative standard in GC-MS analysis of phthalates, is cheap, and its purchase is not restricted. The retention behavior of a substance on the TLC stationary phase is affected by intrinsic chemical structure but also environmental factors, whereas the closed column system removes these factors for GC-MS. Therefore, there is no empirical relationship between R_f values of analytes, however, the inclusion of benzyl benzoate does serve to check consistency over time and between different experiments.

Table 34 shows the suitability of various visualization methods (UV, vanillin, BCG, BTB and resorcinol) for each plasticiser ester, their potential dicarboxylic acid hydrolysis products, and benzyl benzoate. The majority of analytes were distinguishable to the naked eye after staining at a minimum of 1 ug/spot concentration. The merits and limitations of each method are discussed below.

Table 34: Suitability of staining solutions and visualisation methods for the detection of each analyte

Analyte	**Visualization method**				
	U.V. (254 nm)	**Vanillin**	**BCG[a]**	**BTB**	**Resorcinol stain[d]**
Plate background colour	*Green*	*None*	*Blue*	*Yellow*	*Brown/pink*
Dimethyl phthalate (DMP)*	+	-	+[ab]	NA	NA
Diethyl phthalate (DEP)*	+	-	+[ab]	+	+
Dibutyl phthalate (DBP)*	+	-	+[a]	+	+
Diethylhexyl phthalate (DEHP)*	+	+	+[a]	+	+
Diisononyl phthalate (DINP)*	+	+	+[a]	+	+
Diisodecyl phthalate (DIDP)*	+	+	+[a]	+	+
Dioctyl terephthalate (DOTP)*	+	+	+[a]	+	+
Diethylhexyl adipate (DEHA)	-	+	+[a]	+	+
Acetyl tributyl citrate (ATBC)	-	-	+[a]	+	+
Dibutyl sebacate (DBS)	-	-	+[a]	+	+
Epoxidised soybean soil (ESBO)	-	+	+[a]	+	+
Adipic Acid (A.A.)	-	NA	+[c]	+	NA
Citric Acid (CA)	-	NA	+[c]	+	NA
Phthalic Acid (PA)*	+[b]	NA	+[c]	+	+
Trimellitic Acid (TA)*	+[b]	NA	+[c]	+	+
Stearic Acid (S.A.)	-	NA	+[c]	+	-
Benzyl benzoate (BzOBn)*	+	-	+[ab]	-	NA

*All analytes were loaded on a Silica G F254 plate at 1 ug/spot concentration without elution. + indicates a visible spot, – indicates no visible spot, N.A. indicates the combination was not tested. [a] yellow after 8 minutes, transition to blue at 10 minutes, [b] faint, [c] yellow, immediate appearance. * indicates aromatic analytes.*

Iodine was also trialled but gave poor contrast after ~0.5 hr in a sealed chamber. Most analytes were visible as faint orange spots (2 ug/spot), but the contrast to the plate background was poor.

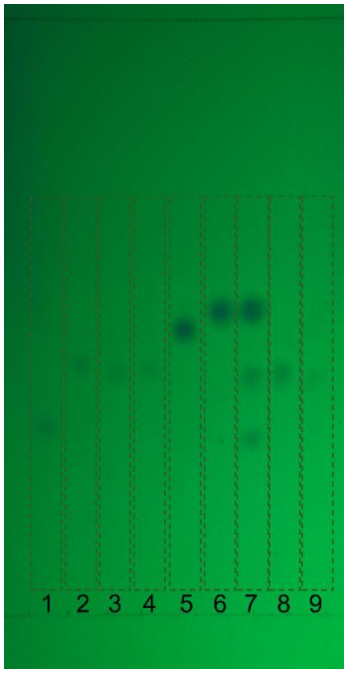

Figure 62: Aromatic plasticisers at 1 ug/ul concentration, visualised under UV 254 nm light, eluted with a 9:1 hexane: ethyl acetate mobile phase. 1.DBP, 2. DEHP, 3. DINP, 4. DIDP, 5. TOTM, 6. DOTP, 7. Phthalate Mix 1, 8. DINP + DIDP, 9. Benzyl benzoate

Illumination with a UVC lamp (254 nm)

As seen in Figure 62, aromatic compounds (phthalates, terephthalate, trimellitate) were visible under ultraviolet light at 254 nm at 0.5 ug/spot. Benzyl benzoate is visible at >1 ug/spot concentration. As expected, aliphatic components were not visible.

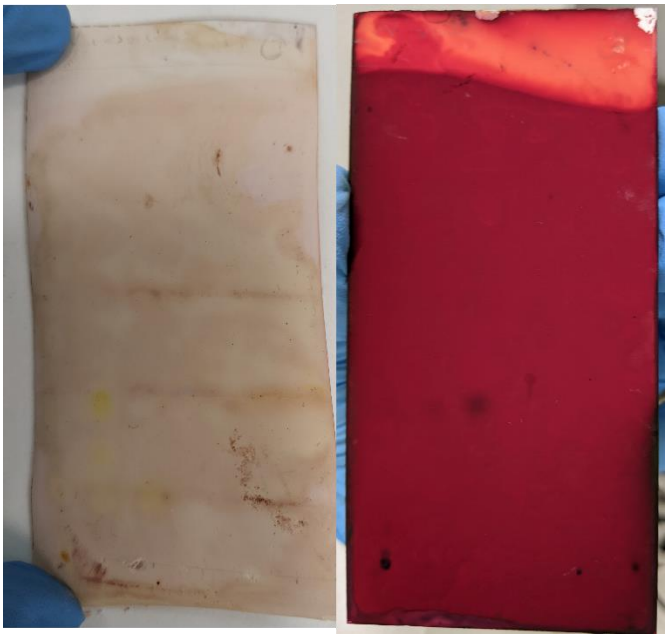

Figure 63: Resorcinol-stained plate at 150 °C (left), at 120 °C (right).

Staining with Resorcinol

Yellow spots are visible in Figure 63 but are indistinct against a light pink/red background, due to the requirement to heat the stained plate as 150 °C which was incompatible with polymer-backed plates. Lowering the temperature to the maximum recommended temperature for the plates, 120 °C, gave a burgundy-coloured plate with few analytes visible as dark spots.

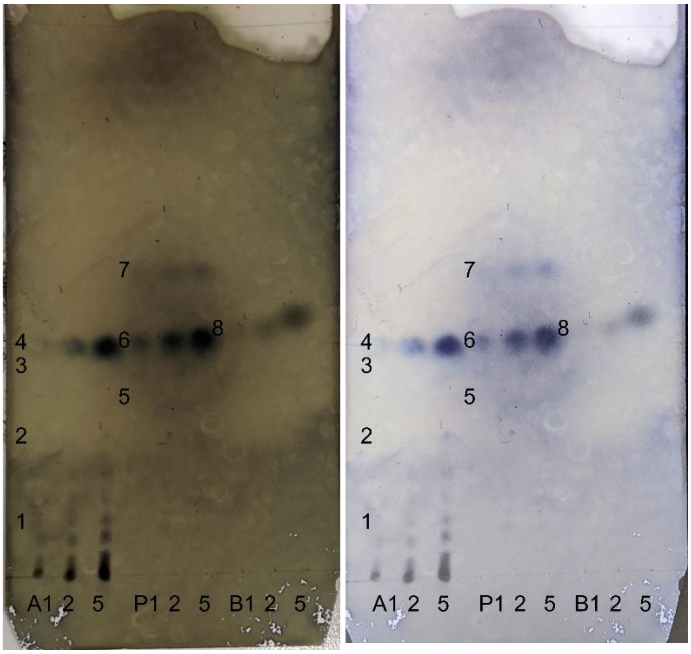

Figure 64: Visualisation of plasticisers with Vanillin-H2SO4 stain. Analytes are numbered as 1. ESBO , 2. ATBC, 3. DBS, 4. DEHA, 5. DBP, 6. DEHP/DINP/DIDP, 7. DOTP, 8. Benzyl Benzoate.

Staining with Vanillin-H_2SO_4

No analytes were visible after the first alcoholic vanillin stain. However, Figure 64 shows dark spots on a dark yellow background after the subsequent acid stain for ESBO, DOTP, C8+ phthalates, and DEHA (1 ug/spot), DBS (2ug/spot), and benzyl benzoate (5 ug/spot). Benzyl benzoate was visible at 1 ug/spot in the initial 5 mins of heating but then faded, and after 30 minutes, only the 5 ug/spot was visible. The plate colour evolved to purple over time. DBS and DBP remained invisible throughout plate development.

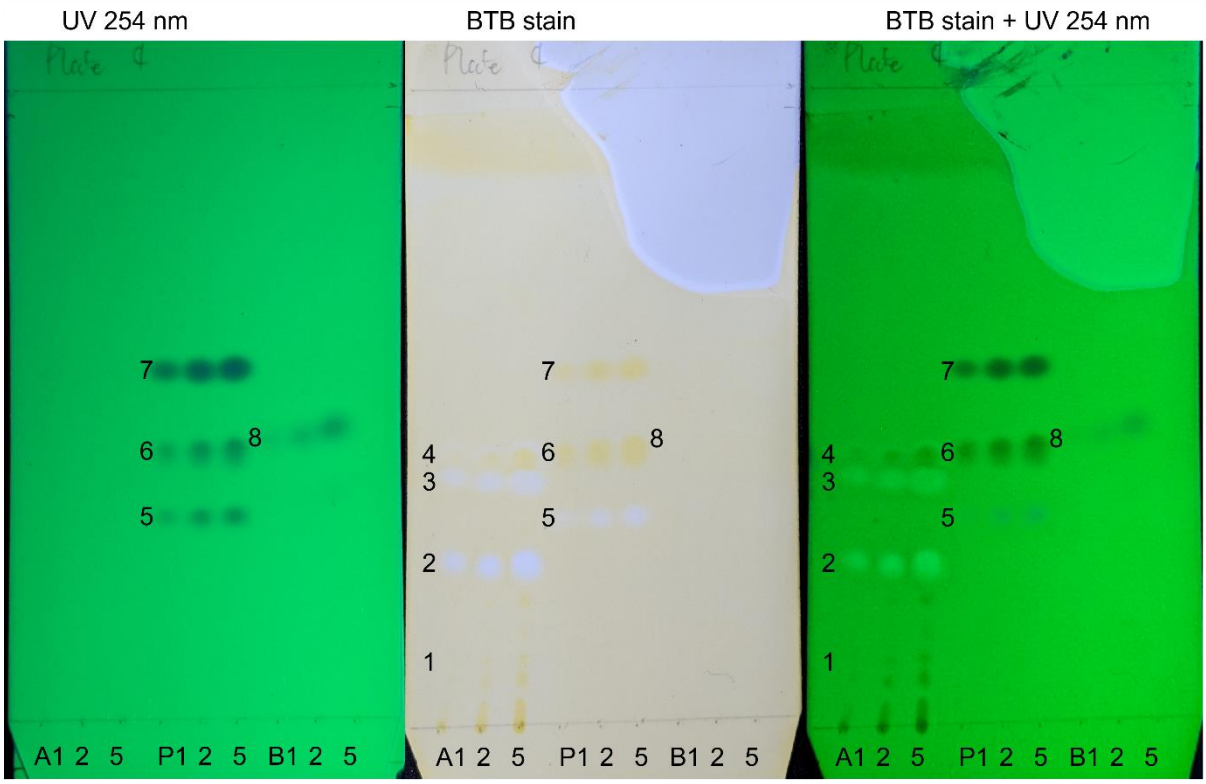

Figure 65: Visualisation of plasticiser analyte mixtures by BTB stain. Labels indicate mixture (A/P/B) and concentrations of 1, 2, and 5 ug/spot, A = aliphatic mix, P= phthalate mix, B = benzyl benzoate. 1. ESBO , 2. ATBC, 3. DBS, 4. DEHA, 5. DBP, 6. DEHP/DINP/DIDP, 7. DOTP, 8. Benzyl Benzoate.

Staining with bromothymol blue (BTB)

Figure 65 (centre & right) shows typical responses after staining with a BTB stain. Dark yellow and white spots appeared against a light-yellow background 5 minutes after dipping. Dark yellow spots appeared for DEHA, DEHP, DINP, DIDP, and DOTP (1 ug/spot LOV). At least five smaller spots were clearly observed at 5 ug/spot for ESBO. Otherwise, baseline components were observed at 2 ug/spot. ATBC, DBS, and DBP all produced distinct white spots from a 1 ug/spot aliquot. The white colour

is comparable to the unstained section of the plate and suggests a localised discolouration of the dye by ATBC, DBS, DBP and faintly by DEHA.

Benzyl benzoate was not visible by staining at any concentration. BTB itself is UV active at 254 nm, but this did not hinder UV visualisation of the plate post-staining ('BTB + UV 254 nm', Figure 65). Interestingly, the location of the aliphatic analytes (ATBC and DBS) was distinct under UV illumination post-staining; and the lack of UV activity due to BTB in these locations reinforces the suggestion that intact dye molecules are not present and BTB's aromaticity is lost.

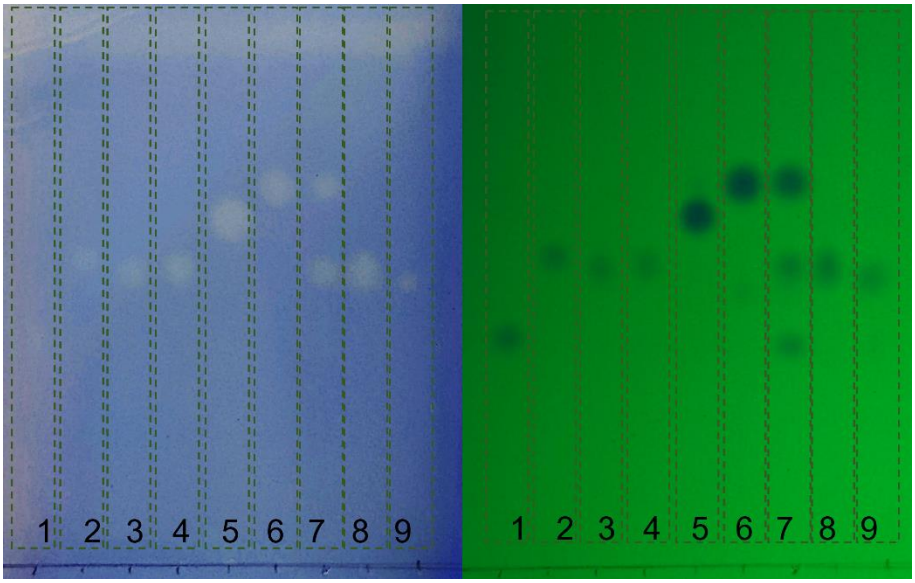

Figure 66: Visualisation of aromatic plasticisers at 1 ug/spot concentration with BCG stain(left) and UV 254 nm light (right). 1. DBP, 2. DEHP, 3. DINP, 4.DIDP, 5. TOTM, 6. DOTP, 7. Phthalate Mix 1, 8. DINP + DIDP, 9. Benzyl benzoate. Image brightness (+40%) and contrast (+40%) adjusted for clarity.

Staining with Bromocresol Green (BCG)

Figure 66 shows a typical plate developed with BCG stain where analytes are stained yellow/light blue against a blue background. The contrast observed by BCG

is more apparent to the naked eye than that reproduced here under artificial lighting. Results were comparable between a commercial and freshly prepared solution.

Acidic analytes caused an immediate colour change to yellow, whereas a slower evolution to yellow around 8 mins after dipping at room temperature (~18-20 C) was characteristic for all esters. Yellow spots marking the location of ester analytes were transient; in the case of the C8+ phthalates, TOTM and DOTP, the colour transitions to light blue around 10 mins after dipping. For all other analytes, the yellow colour faded quickly and typically within 2 mins of appearance (c.f DBP, ln 1,Figure 66). The colour responses are shown in Table 35.

LOVs were 1 ug/spot for aromatic analytes; however, the aliphatic plasticisers appeared best resolved above 2 ug/spot. Only the baseline component of ESBO was visible at 5 ug/spot, and no minor components were visible. All UV-active analytes remained visible under UV light post-staining.

Summary of stain methods

Table 35: Characteristic responses for analytes with BCG and BTB stains

Analyte	**BCG**	**BTB**
Plate background	*Blue*	*Yellow*
Diethyl phthalate (DEP)*	Yellow -> Colourless	White
Dibutyl phthalate (DBP)*	Yellow -> Colourless	White
Diethylhexyl phthalate (DEHP)*	Yellow -> Light Blue	Dark Yellow
Diisononyl phthalate (DINP)*	Yellow -> Light Blue	Dark Yellow

Diisodecyl phthalate (DIDP)*	Yellow -> Light Blue	Dark Yellow
Dioctyl terephthalate (DOTP)*[a]	Yellow -> Light Blue	Dark Yellow
Trioctyltrimellitate (TOTM)*	Yellow -> Light Blue	Dark Yellow
Diethylhexyl adipate (DEHA)	Yellow -> Colourless	Dark Yellow + White
Acetyl tributyl citrate (ATBC)	Yellow -> Colourless	White
Dibutyl sebacate (DBS)	Yellow -> Colourless	White
Epoxidised soybean soil (ESBO)	Yellow -> Colourless	Dark Yellow
Adipic Acid (A.A.)	Yellow	Dark Yellow
Citric Acid (CA)	Yellow	Dark Yellow
Phthalic Acid (PA)*	Yellow	Dark Yellow
Trimellitic Acid (TA)*	Yellow	Dark Yellow
Stearic Acid (S.A.)	Yellow	Dark Yellow
Benzyl benzoate (BzOBn)*	Yellow -> Light Blue	Colourless

[a] contains DEHP and DEP impurities from manufacture.

In summary, two sulfanophathalein dye solutions were found to allow the visualisation of acid and ester analytes, with limits of visualisation at 1 ug/spot loading (2 ug/spot for ESBO). Neither iodine nor vanillin stains allowed complete analysis of all plasticiser analytes tested, and resorcinol's variability and heating requirements were incompatible with the proposed method.

The main distinctions between the BCG and BTB stains were.

- The proposed reference, benzyl benzoate, was visible with BCG but not BTB staining
- ESBO's components were visible with BTB but not BCG
- No fading was observed with BTB stained plates during development or after 24 hrs, unlike BCG
- BTB allows the differentiation of ATBC, DBS, and DBP analytes versus all others by colour (white versus dark yellow) under the conditions studied (9:1 hexane: ethyl acetate, 1 ug/spot).

In practical terms, BCG and BTB are both ideal for the proposed application in the heritage sector; they are compatible with economical polymer-backed plates, can be developed at room temperature, and can be purchased as pre-prepared pH indicator solutions from commercial vendors. Most importantly for ease of interpretation of most analytes they give discernible coloured spots against a coloured background, without requiring UV light.

BCG is a documented TLC stain, but BTB does not appear to have been used for TLC previously, so a standard preparation method is unavailable. Contact with the manufacturer suggested the solution is 0.05 wt.% bromothymol blue in an unspecified 10-20% ethanol/water mix [300,301], but repeats with freshly prepared or other commercial BTB stains were not performed due to time constraints. Furthermore, as the proposed benzyl benzoate standard is visible with BCG, subsequent work attempted to optimize and understand the BCG stain. BCG's performance was found to be repeatable between commercial and prepared formulations, but efforts were made to increase the longevity of the stained analytes spots.

BCG stain optimisation

A proposed mechanism of action for BCG's interaction with ester analytes is the on-plate hydrolysis of the analyte ester to the conjugate acid or mono-acidic product. The subsequent reaction of the acid with the pH adjusted BCG solution would be expected to induce the BCG's blue to yellow colour change, akin to its use as a pH indicator. The delayed appearance of the colour change (after 8 minutes) suggested the acid production was a rate limiting step.

However, the rate of appearance of the analytes were unchanged when either the sodium hydroxide concentration in the BCG stain was increased, or the plate was pre-dipped with a sodium hydroxide solution before BCG staining. No further attempts at optimization were undertaken.

Optimisation of the mobile phase

Finally, in order to target an R_f range between 0.2-0.8, ensure solvent availability and avoid too volatile solvents which can introduce variability in elution rates, mobile phase selection was limited to combinations of solvents shown in

Table 36, which are also known solvents for additive extraction from PVC (Table 8). Polar solvents (acetone, alcohols) are generally available from conservation suppliers, whereas hexane, chloroform and ethyl acetate would be less common in conservation settings. Petroleum ether was included due to its use in UCL Culture's conservation lab, alongside isopropanol.

*Table 36: Solvents used for mobile phase optimization. *N.B. included due to use in UCL Culture Conservation Lab.*

Solvent	**U.V. cut off (nm)**	**Boiling point (°C)**	**Eluotropic polarity on silica** [302]	**Notes on use**
Hexane	195	69	0.01	Immiscible with methanol.
Chloroform	245	61.2	0.26	Restrictions on purchase
Acetone	330	56.2	0.43	Most volatile
Ethyl acetate	256	77	0.45	-
Isopropanol	205	82.4	0.63	-
Methanol	205	64.6	0.73	-
Petroleum Ether (40-60)*	-	40-60	Expected similar to hexane	-

The eluotropic series can be used to guide mobile phase selection by providing an estimate of a mixture's polarity on silica [302]. Figure 67 shows a 1% mix of methanol in chloroform was too polar (0.26), leading to poor separation for esters close to the solvent front, whereas reducing the solvent polarity with only 5-10% polar solvents in hexane enabled a greater spread of retained analytes across the plate. There was no advantage in terms of resolution or R_f values when using petroleum ether as the non-polar component versus hexane.

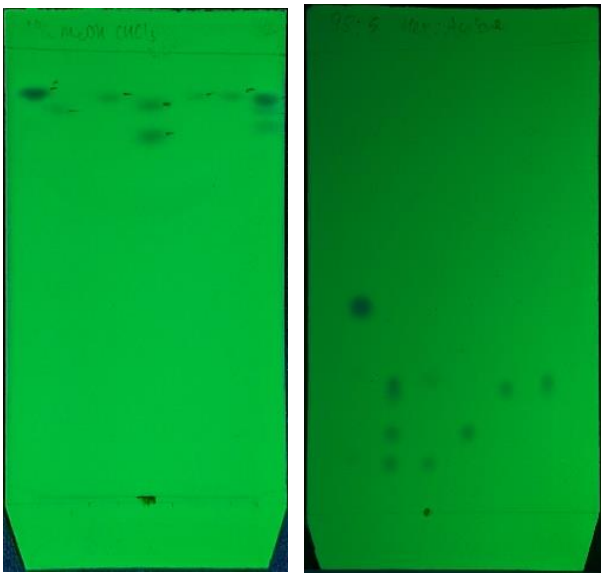

Figure 67: Poor separation between analytes eluted with 1% chloroform/methanol (left), versus 5% acetone/hexane (right).

Figure 68 shows R_f values for combinations of 5-30% polar solvent with n-hexane. The use of 10% acetone or ethyl acetate was compatible with target R_f values between ~0.2 and 0.8; whereas 5% polar solvents gave too low R_f values.

High polarity mixtures were not used due to the lower resolution offered between the DOTP/C8+ phthalates, and DBP/C8+ phthalates (e.g. 20% acetone/hexane). The resolution between analytes is reported in

Table 37. DEHP/DIDP/DINP co-elute for all solvent systems tested and are therefore referred to as C8+ phthalates in this work. However, with a commercial phthalate reference solution in methanol, 10% hexane: ethyl acetate mobile phase was able to resolve all six components (DMP, DEP, DnBP, BnBzP, DEHP, DnOP), including the isomeric pair DEHP and DNOP (not tested above). In comparison 10% hexane: acetone only resolved four out of six analytes. As such, 10% ethyl acetate with hexane was chosen as the mobile phase. A minor advantage of using ethyl acetate versus acetone is the lower volatility versus acetone, which theoretically ensures a more consistent mobile phase over time.

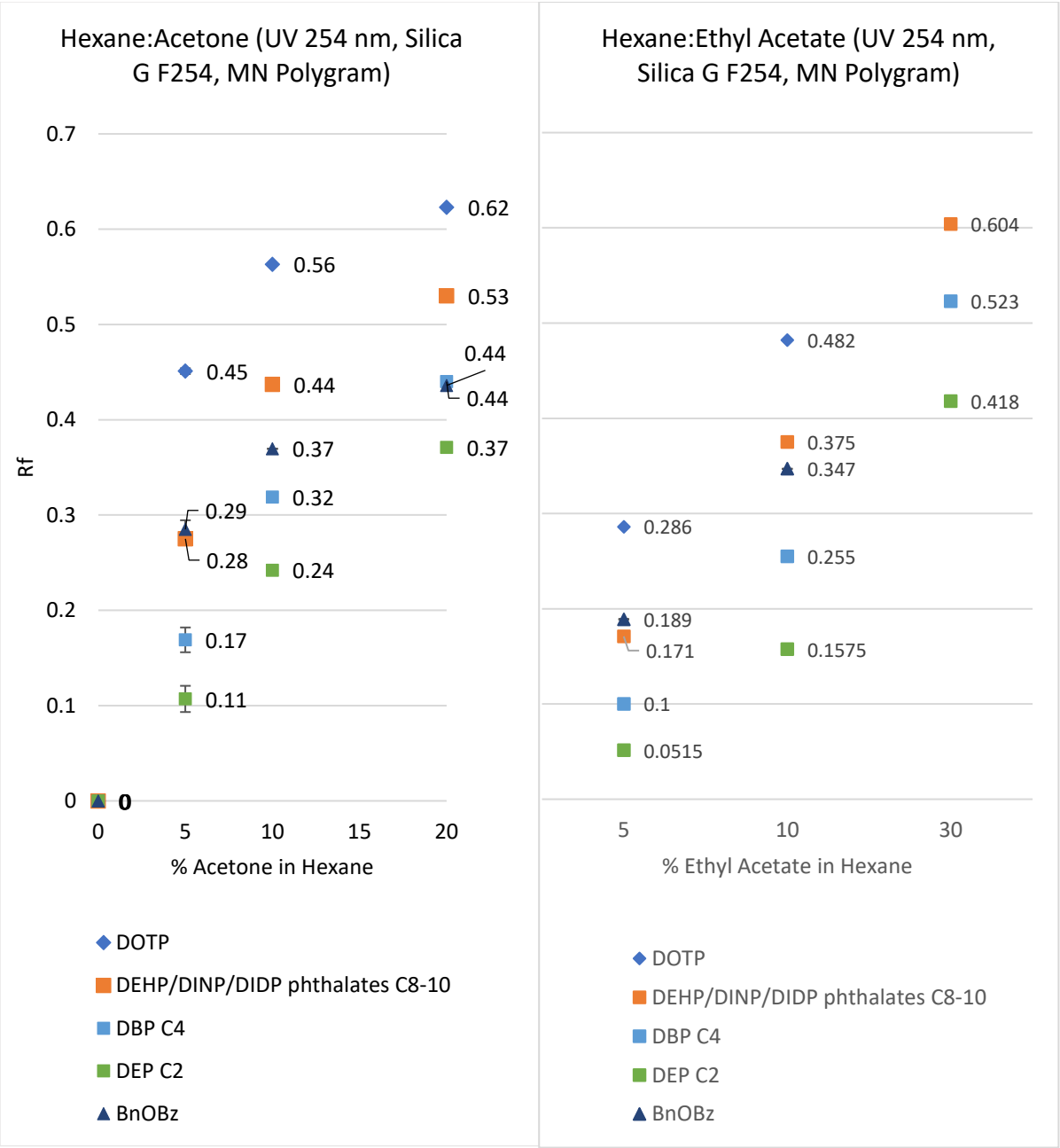

Figure 68: Optimisation of acetone/ethyl acetate in hexane mobile phases showing R_f values

Table 37: Resolution between aromatic plasticisers with different mobile phases

Polar component (% in hexane)	**Resolution between adjacent spots (Rs)***			**Rf (N=1)**		
	DOTP/ C8-10 phthalate	**C8-10 phthalate /DBP**	**DBP/DEP**	**DOTP**	**DEP**	**C8-10 phthalate**
5% acetone	2.6	2.16	1.56	0.45	0.11	0.28
10% acetone	2.31, 1.96	2.46, 2.64	1.95. 1.83	0.56	0.24	0.44
20% acetone	1.2	1.62	1.60	0.62	0.37	0.53
5% ethyl acetate	2	1.5	1.4	0.29	0.05	0.17
10% ethyl acetate	1.98, 1.88	2.16	2.0	0.48	0.16	0.38
30% ethyl acetate	-	1.86	2.66	-	0.42	0.60

* $Rs = \frac{2(X_2 - X_1)}{W_1 + W_2}$, W_1 and W_2 = spot width, X = distance from the baseline to spot centre.

However, Figure 69 shows the most significant issue with the proposed method. There is substantial overlap between DEHA and C8-10 phthalates, so identification with BCG or BTB is not possible and would require 254 nm UV light to distinguish them. While not analysed here, the homologous DINA (diisononyl adipate) plasticiser is also likely to be overlapped.

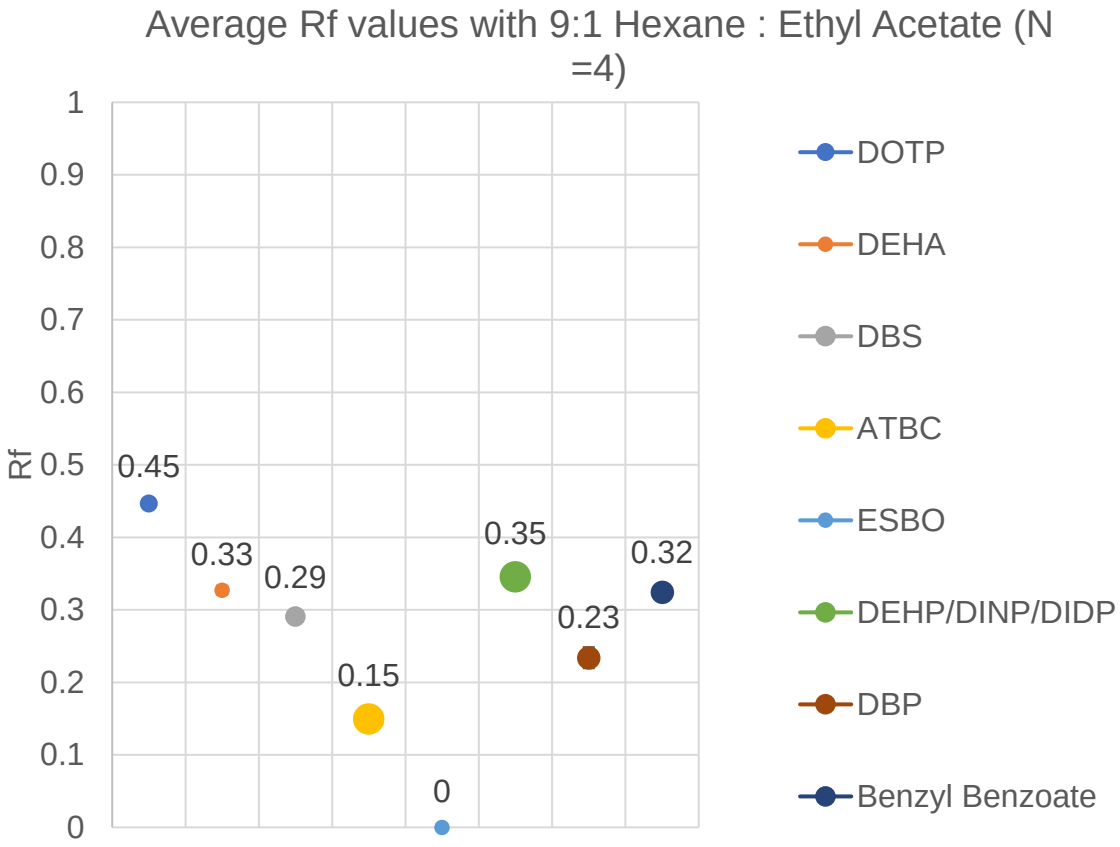

Figure 69: Average R_f values recorded for plasticisers. Spots are scaled to cover the calculated standard deviation values, to highlight the potential error and overlap between analytes, and R_f variability across different runs.

4.3.1 Practical considerations

Several factors can influence the R_f value. During these experiments repeats could be variable as factors such as chamber temperature and humidity were not controlled although the room was. The spotting solvent can also influence spread (page 62) which depends on its volatility and ability to wet silica. For example, in the example of DnOP and DEHP separation using the commercial reference mix, using methanol may concentrate the analyte at the baseline sufficiently to improve the resolution across the 8 cm elution distance.

So, when using an R_f value to identify a component, samples must be applied carefully to ensure that the analyte is concentrated into a narrow band or spot and that the baseline is level and equal between analytes and reference standards. Applying a sample in bands (—) versus spots (●) is one method used to narrow the analyte's width when applied to the plate. Commercial pre-concentrating plates allow broad or uneven spotted samples to concentrate during the initial stages of elution and form narrow bands at their junction between two stationary phases with different activity toward analytes.

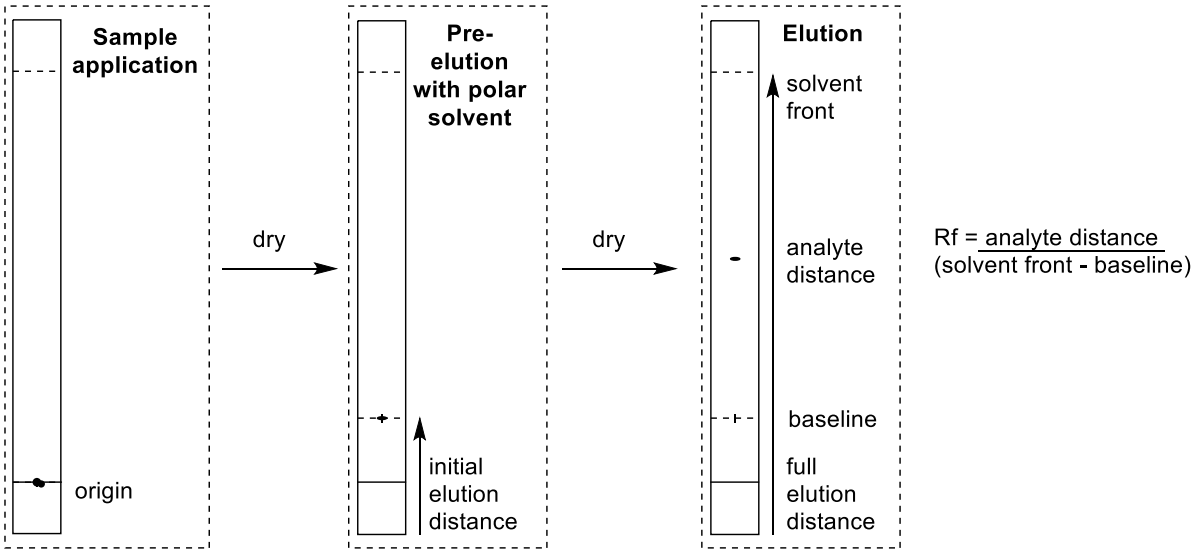

Figure 70: Band narrowing by pre-concentration with a polar solvent front

Figure 70 also shows a similar outcome by pre-eluting the plate for a short distance in a polar solvent such as methanol or acetone as analytes concentrate in the polar solvent front [303]. The plate is then dried before eluting with the desired mobile phase. Addition of colored BCG to the benzyl benzoate reference standard solution aided pre-elution with 100% methanol or 100% acetone. The BCG travelled with the polar solvent front forming a visible narrow band in the pre-concentration step but remained stationary on the baseline when eluted with all hexane-based mobile

phases. Therefore, BCG can act as a visual guide to pre-elution distance and as a marker for the baseline during data analysis. Figure 71 illustrates that both BCG and benzyl benzoate can be combined to provide one reference solution.

Figure 71: Pre-concentration with a polar solvent and BCG solution. From left to right: 1. BCG is visible after spotting in both plates. 2. Same plates as 1 under UV light. 3. Plates after pre-elution with methanol (left) and acetone (right). 4. After development with 9:1 hexane: ethyl acetate, the central lane contains BCG (baseline) and benzyl benzoate (top spot).

Other analytes of interest

A previous study identified solid deposits on museum objects as stearic acid, which is used as a lubricant alongside metal stearates as heat stabilisers in the manufacture of PVC (Table 5). Phthalic acid was also found on a PVC surface by Shashoua, has been observed in light ageing experiments, and is proposed to result from the hydrolysis of phthalate esters [132]. Evidence of plasticiser hydrolysis has also been observed with CA. Therefore, the activity of potential hydrolysis products from the plasticisers studied was also assessed. There is little literature on the environmental breakdown products of plasticisers so Figure 72 shows the complete hydrolysis products, however, monoesters such as mono-ethylhexyl phthalate or anhydrides are known degradation products in biological studies.

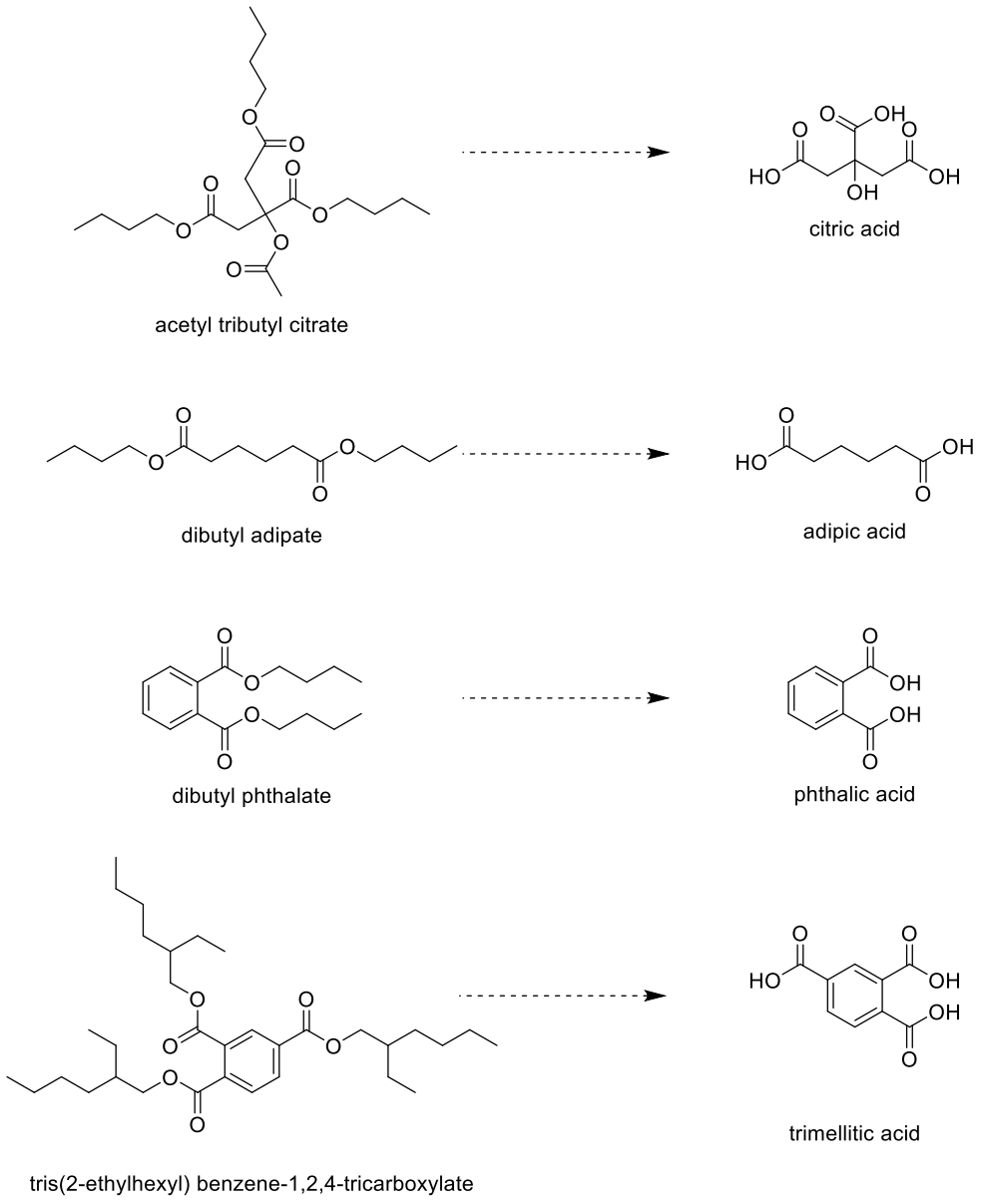

Figure 72: Potential acidic hydrolysis products of various plasticisers

As previously noted, adipic, trimellitic, citric, and phthalic acid were visible immediately after BCG staining and remained at the baseline when eluted with 9:1 hexane: ethyl acetate. Whereas elution in 100% ethyl acetate led to distinct behavior between stearic acid and the plasticiser derived acids. Stearic acid gave a discrete R_f value of 0.59, whereas the others streaked from the baseline due to their multi-protic character versus the monoprotic stearic acid.

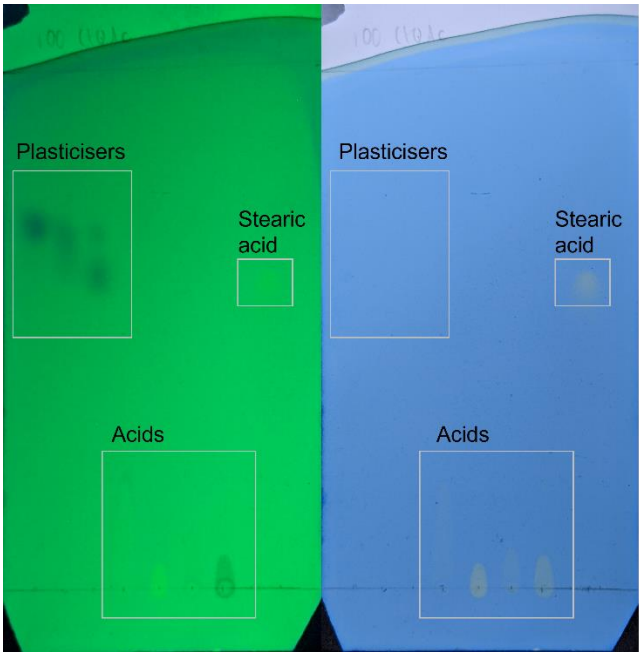

Figure 73: Differentiation between stearic acid, other acids, and plasticisers after elution with 100% ethyl acetate by UV and BCG. The BCG image is taken immediately <2 mins after staining to ensure no confusion with co-eluting plasticisers.

For comparison, all plasticisers were eluted in 100% ethyl acetate with R_f values between 0.59 and 0.77 and were not distinguishable immediately post-staining. Assuming a plate is first eluted with 9:1 hexane: ethyl acetate, any plasticisers shown in Figure 8 and Figure 9 would be at the solvent front with a second elution in 100% ethyl acetate, having travelled up the plate in the first elution, whereas the monoprotic and thus less polar stearic acid would elute to the middle of the plate, as observed here.

Therefore, if an acidic analyte was suspected due to a rapid reaction with BCG, a second elution with 100% ethyl acetate should enable identification of stearic acid vs phthalic acid. With further trials it may be possible to distinguish between the other acids, but this was not attempted.

Finally, polymeric plasticisers have not been analyzed but if extraction were achieved, polymeric analytes would likely be evident as multiple spots like ESBO or elongated streaks by TLC.

4.3.2 Data interpretation

Figure 74 to Figure 76 shows a flow chart created to aid identification of analytes, alongside known R_f values and expected for various analytes after BCG staining.

Identification guide flow charts:

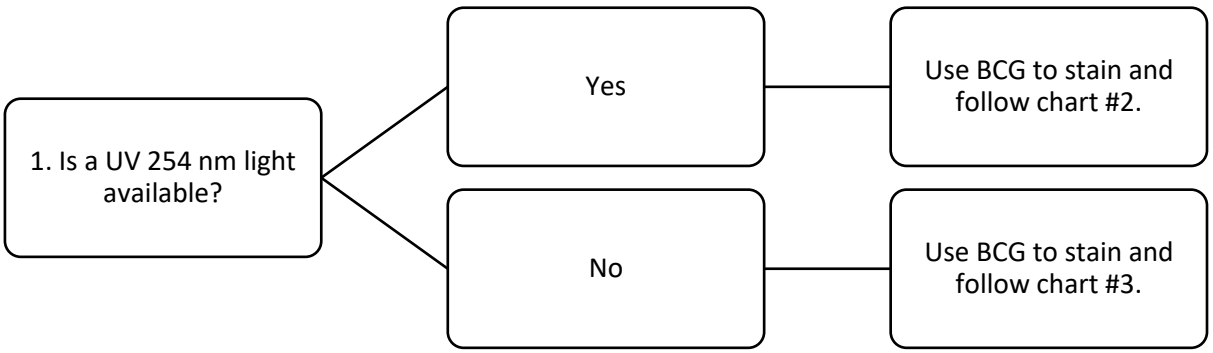

Figure 74: Initial flow chart selection

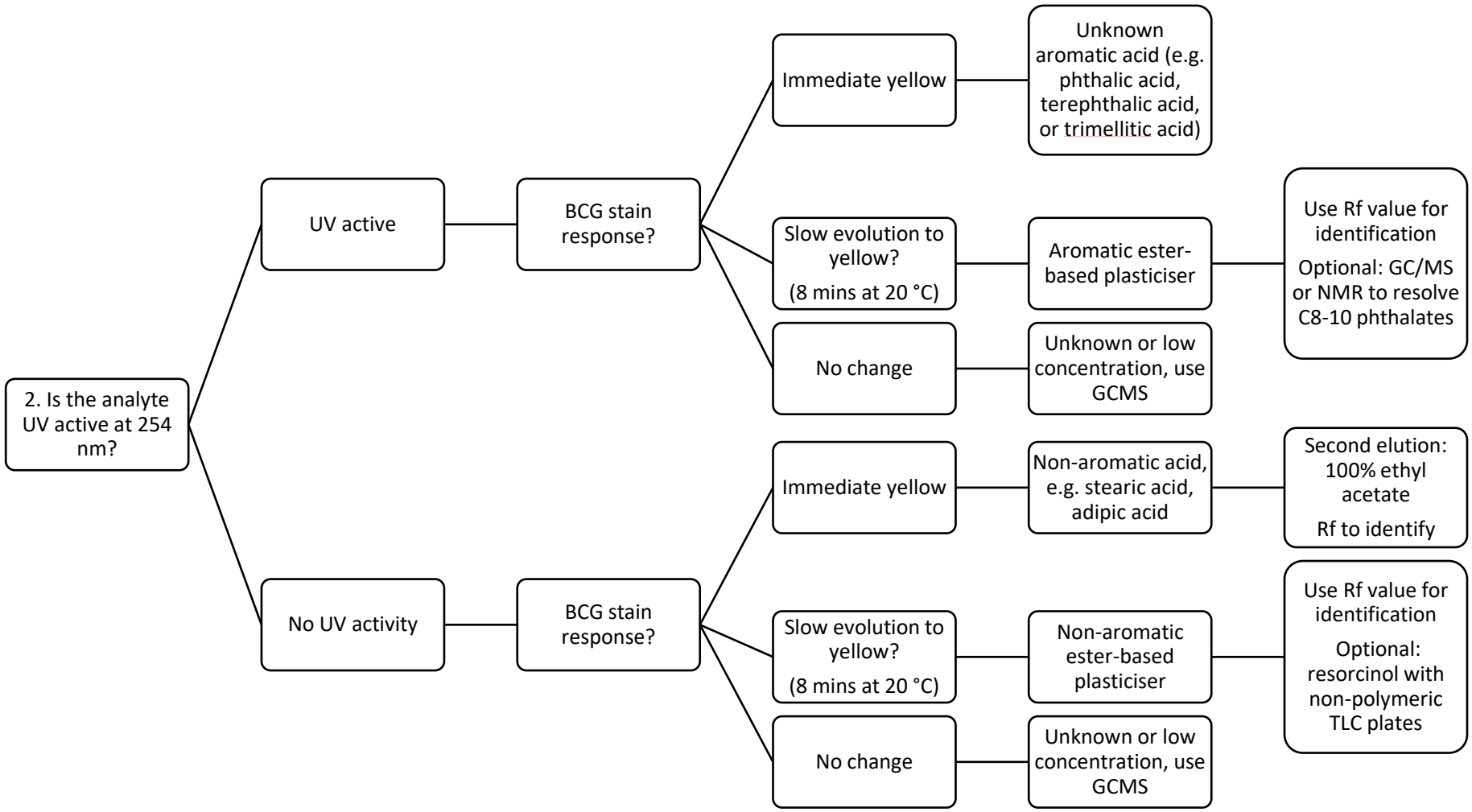

Figure 75: Analyte identification with BCG and UVC light

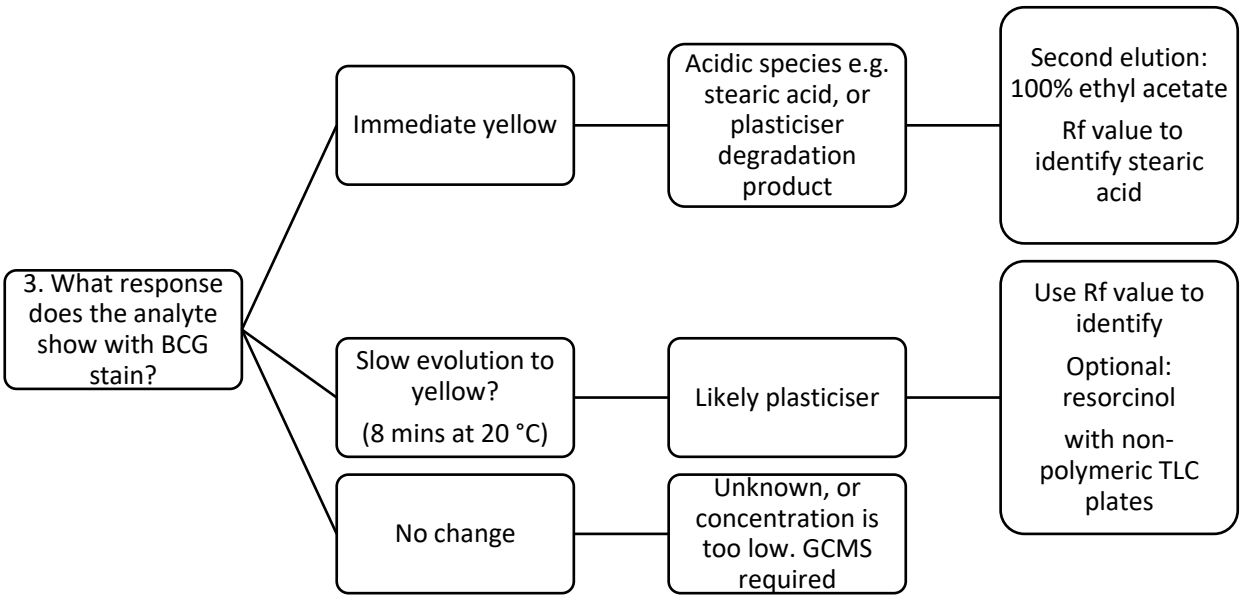

Figure 76: Analyte identification with BCG/BTB and UVC light

Evaluation of TLC methods with PVC samples

The samples previously analyzed by GC-MS, NMR and FTIR spectroscopy in Chapter 3 were used to evaluate the proposed method. Initially, sample HEI (38 wt% DOTP) was used to test the extraction method with 9:1 hexane:ethyl acetate by varying the solvent-to-mass ratio between 2.5 and 50 (e.g. a solvent-to-mass ratio of 50 corresponds to 1 mg sample, extracted with 50 µl solvent).

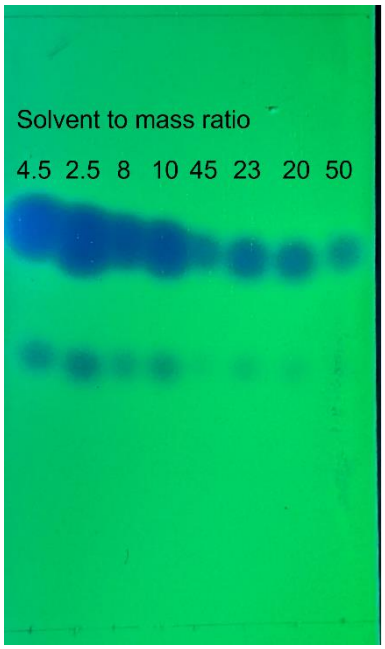

Figure 77: Solvent-to-mass ratio trials for extracting a 40% DOTP/PVC sample in 9:1 hexane: ethyl acetate after 5 minutes. Aliquot = 1 µL. N.B The plate was overexposed, therefore R_f values are not consistent with previous findings.

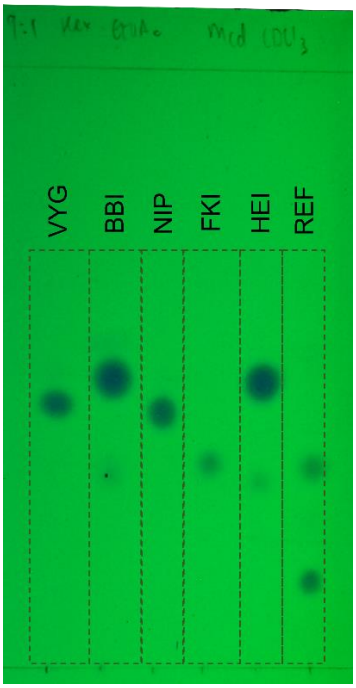

Figure 78: Examples of PVC medical device extracts in $CDCl_3$ after 2 hours. Solvent-to-mass ratio: 80.

Figure 77 shows that the highly concentrated extracts (ratio 2.5 to 10) oversaturate the plate, but there is also clear evidence of another analyte. Samples extracted with a ratio of 25-50 were less saturated and thus would offer more consistent R_f values. Furthermore, the other analyte (DEHP) remained detectable with a solvent-to-mass ratio of 20 but was not evident at higher dilutions. As 38% plasticization is towards the upper range of expected samples, a solvent-to-mass ratio of 20 was used to ensure adequate concentration of less plasticized samples, including minor components if present.

Using only 20 µL of solvent does not cover the whole extraction vial base but is sufficient to cover the 1 mg sample if placed carefully or if the vial is angled, whereas 50 µL is sufficient to cover the sample and the 12 mm base of a typical 12mm

chromatography vial. Extraction time can be elongated if initial aliquots are not concentrated enough for visualization, and dilution is also possible. Visualisation with UV light should be checked before elution if available.

Finally, chloroform extracts used for NMR analysis were also suitable for TLC analysis. However, the R_f values of samples which contained either TOTM or DOTP (VYG, BBI, NIP and HEI) were lower than expected, as the spots were oversaturated with a 2-hour extraction despite the higher solvent-to-mass ratio of 80 (800 µL per 10 mg). R_f values were as expected for the reference (benzyl benzoate) and FKI (C8-10 phthalates) samples, which were visibly less concentrated in Figure 78.

4.3.3 Plasticiser identification by TLC and comparison to GC-MS and NMR

In an effort to minimize oversaturation while observing lower concentration analytes, ~1 mg of a cut sample (0.42 – 1.85 mg) was extracted in 20 µL of 9:1 hexane: ethyl acetate for 5-10 minutes. A 1 µL aliquot was then applied to the plate. Plates were analyzed blind, using the method shown in Flowchart 2 (Figure 75).

Table 38 shows the results compared to the previous analysis by GC-MS and NMR spectroscopy. The developed method (Flowchart 2) correctly identified plasticisers in 10/25 available PVC samples. Identification was based on the closest R_f value among the analysed reference plasticisers. However, when comparing the R_f of the assigned plasticiser and the R_f of the analyte spot shown in Figure 79, the majority of measured R_f values are not within the standard deviation of the reference plasticiser R_f values; this was also true for the benzyl benzoate reference.

*Table 38: Comparison of plasticiser identification by TLC (Flowchart 2 method) with GC-MS and NMR analysis. *Samples are not PVC. 'C8-10. refers to DEHP/DINP/DIDP as single plasticisers or in a mixture.*

Sample	**Plasticiser and wt% determined by**		**TLC identified plasticiser (Flowchart 2)**	**Notes**
	^{1}H NMR	**GC-MS**		
PIL	36% DEHP	27% DEHP	C8-10	
SNO	42% DINP	DINP	C8-10	
DOG	38% DINP	DINP	C8-10	
NOD	37% DEHP	38% DEHP	C8-10	
GRG	~28% DINP	DINP	C8-10, + DBP	
DOD	29% DEHP	13% DEHP	DOTP + C8-10	
PNK	~40-43% DiHpP	DiHpP	DBP	
WHD	~33% DINP	DINP	C8-10	
PHC*	Unknown	Unknown	DBP	
BLC	14% DEHP 7% DBP	11% DEHP 11% DBP	C8-10 + DBP	
RDC	14% DEHP, 7% DBP	NA	C8-10 + DBP	

MCS	27% DINP	DINP	C8-10	
TCS*	5.82% DIUP + unknown aromatic	Phosphate	C8-10	
PEN	21% Unknown phthalate + unknown	15% DEHP + unknown	C8-10 + DBP	
YED	38% DEHP	41% DEHP	C8-10	
FMO	30% ATBC	NA	ATBC	
ERA	39% pentaerythritol tetravalerate	NA	ATBC	+ unknown polymeric/ESBO?
BBI	17% TOTM	NA	TOTM, DBP, ESBO	
NIP	25% TOTM	NA	TOTM	
VYG	28% DOTP	NA	C8-10	
FKB	41% DEHP	NA	C8-10	
HEI	26% DOTP	NA	DOTP + C8-10	
TBW	30% DEHP	DEHP	C8-10	
BAL*	Unknown	NA	C8-10	

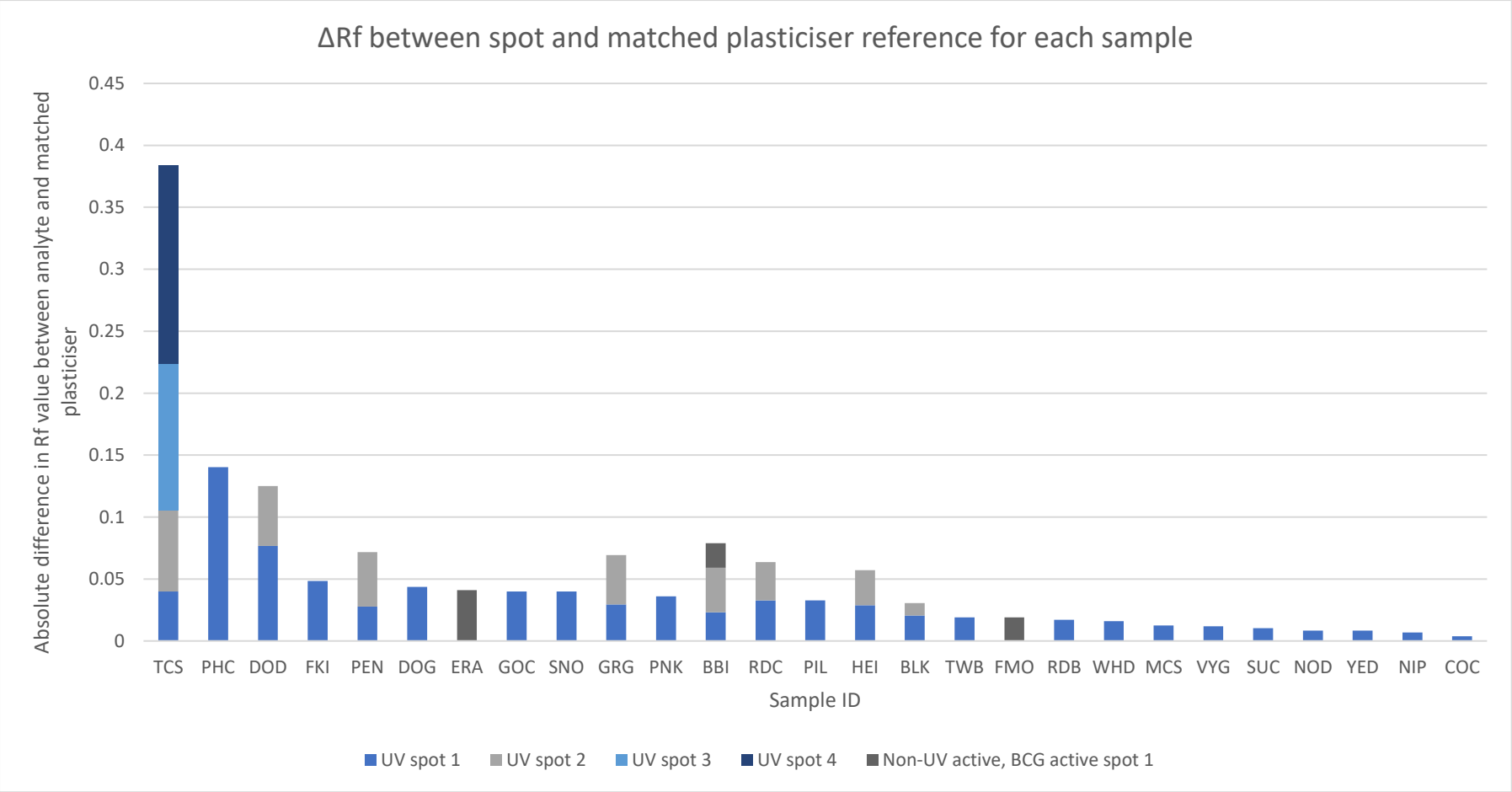

Figure 79: Difference in R_f between assigned plasticiser R_f and measured R_f for each spot (some samples showed multiple spots) detected using the Flowchart 2 method and closest R_f matching for each individual spot. Differences are generally larger than the standard deviation

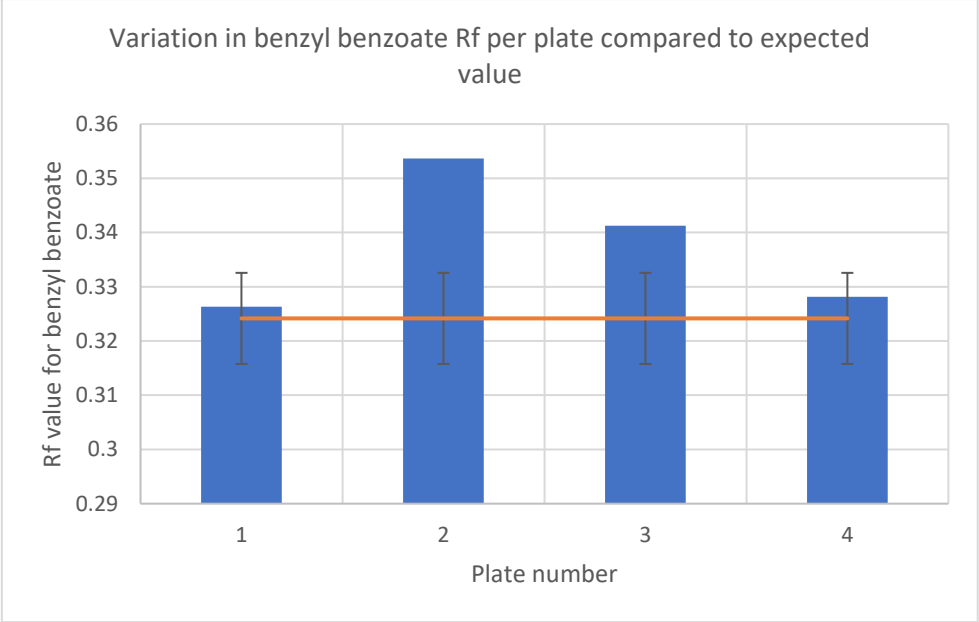

Figure 80: A representative example of R_f variation; benzyl benzoate R_f compared to the average value.

Variation can be ascribed to oversaturation of some analytes (in samples BBI, HEI, SUC, WHD and PIL) or variable environmental conditions in the chamber. Furthermore, the intensity and contrast of the BCG stain spot was clearly correlated to the analyte concentration. Therefore, a tendency towards oversaturation is preferred to aid visualisation, with the option of further dilution.

Individual samples can be used to illustrate the benefits or limitations of the method. For example, the TCS, PHC, and BAL samples all illustrate that non-PVC samples may contain UV-active additives which could be wrongly identified as plasticisers, therefore, where possible positive identification of PVC is recommended before TLC.

Mixed plasticisers appear well resolved, especially DEHP and DBP in both the BLC and RDC samples. By GC-MS and NMR the GRG and PEN samples were both

similar to C8-10 phthalates by GC-MS and NMR but did not closely match known phthalates, the same conclusion is drawn from TLC. Both show two closely eluted but distinct UV-active additives with retention times comparable to C8-10 phthalates. On the other hand two unidentifiable analytes were seen by GC-MS for PEN, but the presence of two aromatic plasticisers was not apparent by either NMR or GC-MS for GRG.

Both BBI & ERA contain polar analytes which streak from the baseline; the trace is like that expected of ESBO for BBI, but no resolution between oligomeric components is observable for ERA, which suggests that the methodology is not optimised for polymeric or ESBO plasticisers. Extending the extraction time would be recommended for low concentration analytes before a repeated analysis.

A valerate plasticiser identified by NMR in sample ERA was not included in the reference set, and a non-polar analyte spot was identified as ATBC by the R_f matching method. Assuming the spot is PEV, the difference between the R_f of PEV and ATBC is only 0.04, which would limit their separation.

Ultimately, the limitations of this method have the greatest impact if attempting to identify specific additives in a sample. However, in a survey setting, the specificity of R_f values would be less important, and instead analysis of multiple samples at once under the same conditions would enable clustering of similar samples. This could act is a pre-screening tool prior to targeted analysis for a subset of samples by GC-MS or NMR spectroscopy.

4.3.4 Case study & surface sampling

Figure 81: An 'AmbuBag' bag valve mask exhibit (RCA/UCL Culture), with bloom (left) and orange liquid on polyethene bag wrapper (right).

As shown in Figure 81, a medical AmbuVac device manufactured circa 2000 displayed signs of bloom while on display at the Association of Anaesthetists of Great Britain and Ireland (London Medical Museums of Health and Medicine). It was removed from display, transferred to a polyethene bag, and taken for conservation cleaning at UCL Culture's Conservation Laboratory by a conservator. Between the removal of the object from the display case and arrival in the laboratory, the curators observed that the crystals were less evident. However, Figure 81 (right) shows the surface was now observed to be 'sweating', and the clear polythene bag was also coated with an orange liquid.

As discussed in section 1.4, there is a potential to cause surface damage when swab cleaning; however, it is the only current cleaning method for visibly degraded objects, including those with surface accretions. In advance of planned wet cleaning, the conservator trialled several cleaning solutions, and 1-2 trial swabs per solution were available for analysis. As conservation professionals consider a range of factors

when deciding the optimum cleaning method, the Conservator's general observations on the object's condition and during test cleaning were also recorded.

4.3.5 Plastic identification and surface analysis

The AmbuVac contained at least three plastic materials; transparent yellow/orange-tinged hard plastic valves, black rigid plastic connections, and flexible black PVC was confirmed by ATR-FTIR spectroscopy. The object smelled strongly and induced a lachrymatory response when nearby. The surface of the PVC fabric appeared pitted, and the white solid deposits could not be removed in sufficient quantities for NMR analysis without risking scraping or catching the PVC fabric.

Spectra could not effectively be recorded by ER due to geometry and folds in the bag’s fabric, but the hand strap was confirmed as PVC by ATR-FTIR spectroscopy. Droplets of liquid were found across the object on both plastic components, whereas the solid deposit was observed at either end of the flexible PVC balloon. TLC of the liquid deposit was inconclusive as the sample was poorly soluble in hexane. However, a commercial 50% isopropanol/water swab was wiped across the surface and extracted in hexane before GC-MS analysis confirmed a DEHP plasticised object. The amount of collected crystals was too low for analysis by NMR spectroscopy and were not soluble in hexane.

4.3.6 Evaluation of solutions for surface cleaning and sample collection

Table 39: Conservator's observations from test cleaning

Cleaning solution	**Application method**	**Observation from test spot cleaning**
50:50 Ethanol: Water (Figure 82)	Hand-rolled cotton swab	Left a tide mark Dulled the surface
Pre-wetted 70:30 Isopropanol: Water non-woven wipe ('Cutisoft Pre-Injection Wipes')	Wipe held in forceps	No tide mark left. Poor control over the cleaned area. General unease with using non-conservation grade products.
1% Orvus Paste aqueous solution	Hand-rolled cotton swab	Surface wetting was less well-controlled but acceptable
1% Dehypon 54 aqueous solution	Hand-rolled cotton swab	Well-controlled wetting and removal of surface
Ecosurf EH9 microemulsion (Figure 82)	Hand-rolled cotton swab	Well-controlled wetting and removal of surface

When considering the efficiency of cleaning, all solutions allowed a visible reduction in the shine associated with the assumed exuded plasticiser, and all cotton swabs became orange in colour. In terms of controlled application, the microemulsion and Dehypon 54 non-ionic surfactant solution could be applied in a controlled manner, unlike the Orvus Paste solution, which spread further across the PVC surface.

Figure 82: Swab cleaning of AmbuBag surface, showing controlled application with a microemulsion solution (left) before cleaning with ethanol/water mix (centre) and after with dull and tide-marked surface (right).

The ethanol-water solution was unique in that it left a visible tide mark when dry. As cleaning is ideally only performed where necessary, solutions that do not leave tide marks are preferred. The area swabbed with the pre-wetted IPA wipe did not show any tide marks when dried and was effective in removing the exuded plasticiser. However, the wipe was more challenging to manipulate and apply to a defined area than a cotton swab. The conservator cleaned the whole object with the 1% Dehypon 54 solution, rinsed it with deionised water, and replaced the AmbuBag into the cardboard box with new Plastazote supports. However, the crystals appeared again a week after cleaning.

4.3.7 Extraction trials from surfactant cleaning solutions

Following conservation practice, a dry swab sampling of the exuded liquid was not permitted. Therefore, trials were used to assess if the extraction of plasticisers doped into the favoured Dehypon and Orvus paste surfactant solutions could be separated

by liquid-liquid extraction with n-hexane. Phthalate-doped Dehypon 54 and Orvus Paste solutions both visibly formed a separate phase to hexane, although foaming was observed. Phthalates were confirmed to have partitioned into the hexane phase in both solutions by the observation of UV activity shown in Figure 83. The upper layer of the hexane / Orvus Paste solution was excessively viscous suggesting incomplete phase separation. The addition of sodium carbonate reduced foaming and clarified phases, but Figure 83 shows the addition of the salt also reduced the UV activity in both solutions.

Figure 83: UV activity of hexane extracts from phthalate doped - Orvus paste and Dehypon cleaning solutions, showing a reduction of UV activity after sodium carbonate addition. N.B Dehypon's results are reversed by error.

Following the confirmation under UV light that phthalates partitioned from Dehypon into hexane, the two Dehypon 54 swabs were extracted in hexane. However, no phase separation was visible, either due to the large excess of solvent versus the swab or potential partial solubility of the surfactant in hexane at low concentrations. The TLC of the extract included assumed surfactant molecules characterised by streaked spot, as well as a single UV- active spot hypothesised to be the plasticiser. However, the R_f was not consistent with expected values. Previous studies have found surfactants can be effective mobile phases or modifiers in TLC [304], this was

assumed to affect the R_f value, and no additional surfactant TLC optimisation took place. Attempts at developing a cloud-point extraction method were similarly unsuccessful. After further discussion with the conservator, the small amount of surfactant solution which could be recovered from the use of swabs was expected to limit the ability to observe phase separation and take an aliquot.

4.3.8 Swab sampling with alcohol: water mixtures

The single ethanol/water AmbuBag swab provided by the conservator showed no evidence of plasticiser analyte by TLC using UV illumination, which may have been caused by a too high dilution volume (0.5 mL). Therefore, to test the suitability of non-destructive sampling and analysis by TLC, swabbed samples were acquired from two other samples. DOD (38% DEHP) was visibly soiled with brown spots on the surface, while TWB (30% DEHP) a recently manufactured vinyl fabric showed no visible accretions on the surface; the TCS sample showed visible amounts of dust but no significant deposits.

Figure 84: The dirtied surface of sample DOD. The surface was cleaned effectively (top left area) by localised application of a cotton swab wetted with isopropanol: water mixture (50%)

Figure 85 shows aliquots from the swab extracts run alongside a solvent extract of each sample. While DOD and TBW swab extracts were less concentrated, they were clearly visible and identifiable as a C8-10 phthalate when viewed under UV light, with BCG, and compared to the benzyl benzoate reference. The cleaning solution successfully removed the surface dirt without any noticeable discolouration or excess liquid forming on the surface.

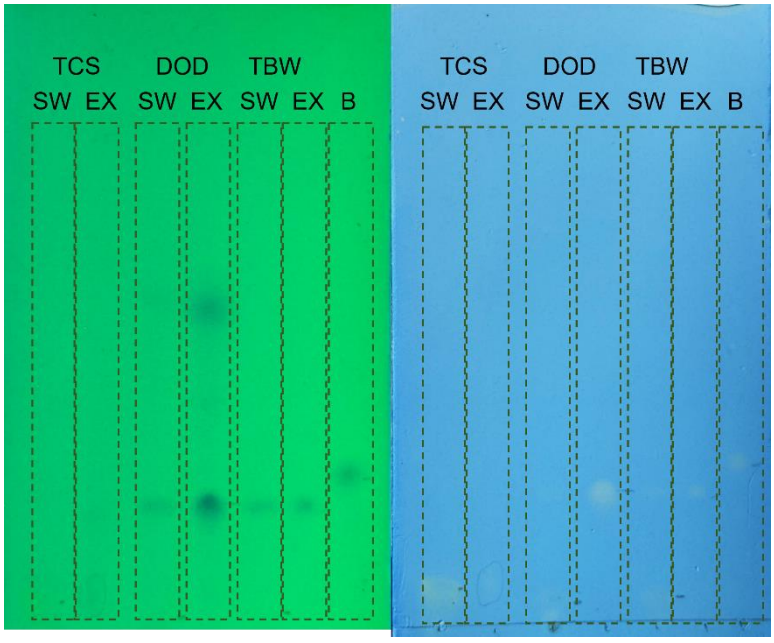

Figure 85: TLC of samples collected by direct extraction (EX) and swab sampling (SW) for samples TCS, DOD, TBW. Extract aliquot = 1 µL, Swab aliquots = 5 µL. B = benzyl benzoate standard.

The two examples shown were promising in demonstrating sample collection from both visibly dirty and visibly ‘clean’ objects. However, the methodology requires further work; for example, the swab size and sampling area was not standardised;

therefore, the volume of hexane was minimal to ensure an aliquot could be collected but may vary with different swabs. A longer extraction time or larger sampling area may also improve visibility. In terms of future work, the potential for discolouration by the solvent mixture was also not assessed with the two examples. The methodology should also be repeated for samples formulated with other known plasticisers.

While not performed on the same sample, microscopic analysis of another sample (RDC) showed no evidence of scratches after swabbing with the commercial 70:30 isopropanol: water swab. Therefore, it would be worthwhile to trial if the non-woven cloth also causes scratches like cotton swabs are expected to. Additionally, no discolouration was observed for the red RDC sample.

Swab sampling appears to be a suitable method for non-destructive plasticiser analysis, and the extraction procedure described is well suited for analysis by GC-MS or TLC. Reflecting the concerns noted in section 1.4.1, future consideration should be given to the invasive nature of the method, including discolouration over a wider variety of PVC objects, and scratching by microscopy.

4.3.9 Evaluation of TLC method against literature data

The samples studied here show that most objects contain only one additive, but formulations can contain multiple plasticisers. As few items with more than one plasticiser were sourced, examples of PVC additive analysis from literature were collated to identify typical concentration ranges and common plasticiser combinations. An overview of the nine publications are described in Table 31, but are all concerned with regulatory GC-MS testing for banned plasticisers in consumer goods like toys, flooring, food contact materials, and medical devices, so are broadly representative of PVC items observable in a museum.

Knowledge of potential combinations can aid the interpretation of TLC results, but the data collected is also used here to evaluate if known combinations may be observed using the proposed TLC method.

4.3.10 Itemset characteristics and plasticiser combinations

As shown in Table 40, the number and type of plasticiser analytes targeted by publications vary and largely reflect the high interest in phthalate plasticisers. Therefore, the data cannot be considered as representative of the population of all variations of PVC formulation but offers the most comprehensive assessment to date.

As such, a non-observed association rule is not indicative of an unused combination in PVC formulations but is a consequence of incomplete data. For example, while 49% of all samples in Figure 86 are single-component systems, McCombie et al.'s methodology offered the most comprehensive analysis of available plasticisers, and 95% of those samples contained more than one plasticiser.

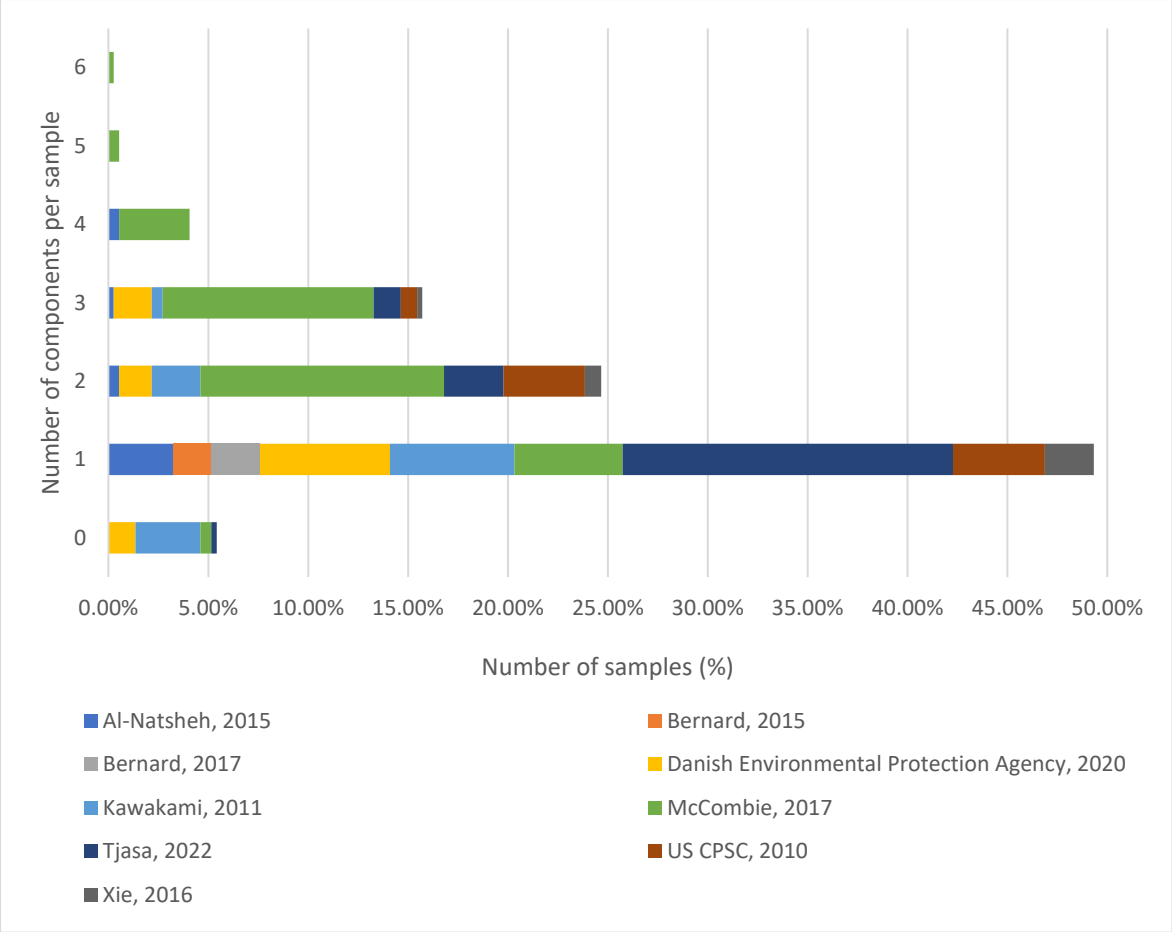

Figure 86: Overview of samples and number of analytes detected per sample by publication, >50% of samples contain more than one plasticiser.

Table 40: Number of analytes targeted per publication and frequency of analyte occurrence by publication after data cleaning.

Shading is used to denote which analytes were targeted by each publication.

Publication	No of analytes targeted per publication	ESBO	DOTP	TXIB	ATBC	TBC	DEHA	DINCH	TOTM	DHEH	BS_NPG_EHS	Me-Ester	PA	DEHP	DPHP	DBP	DIBP	DINP	DIDP	BBP	DNOP
Al-Natsheh, 2015	**7**													12		1	7	3	0	0	4
Bernard, 2015	**5**		0					4	3					0						0	
Bernard, 2017	**7**		1		1		0	1	5									1			
Danish Environmental Protection Agency, 2015	**6**		16											19		7	4	11		0	
Kawakami, 2011	**8**			0			0							33		3		9	2	0	0
McCombie, 2017	**19**	94	63	34	36	7	1	37	2	2	1	2	0	11	3	0		2	0		0
Rijavec, 2022	**7**		15					1						40	1	4	1	21	15		
US CPSC, 2010	**5**		14	9	20			13										0			
Xie, 2016	**11**		9		1		2	2						1			0	2	1	0	0
Total samples containing >1 wt% analyte		94	118	43	58	7	3	58	10	2	1	2	0	116	4	15	12	49	18	0	4

When combining and filtering data sets, the concept of missing data cannot be ignored. The data is mixed here; different analytes were targeted, and detection limits vary between techniques. The sample selection in each publication is biased towards the specific research aim, e.g., toys versus flooring or those initially screened to contain banned substances. The data was also filtered after collation. All these factors lead to skewed data. In typical applications of association analysis such as basket or market analysis, missing data is uncommon and avoided mainly due to the large datasets considered but can occur, e.g., when an item is out of stock. However, the data provides key insights into the characteristics of samples including typical concentration ranges, and which combinations exist in real items. For example, a conservator could identify a non-phthalate plasticiser and may also expect and seek to check if the item contains ESBO as a secondary plasticiser or stabiliser.

Sample characteristics

The first step in data analysis was to filter the collated data set of 369 samples and 4006 analytes. An individual analyte data points is a numeric concentration value which confirms that for a given sample a specific analyte was targeted by the analysis method, and either measured above the method's limit of detection (concentration >LOD), or it was not identified (concentration = 0). Non-targeted screening studies were not included unless concentrations were measured using known standards.

The prevalence of low concentration data points was evident and invalid for comparison to TLC methods with a much higher limit of detection versus the GC-MS

studies used. As the limits of detection and quantification varied between studies, various filtering methods were trialed to increase the commonality between datasets.

Figure 87 shows that 17% of analytes in the original dataset had a concentration below 1 wt. % and were excluded, but the number of samples decreased by only 5% post-filtering. This suggests a high representation of trace analytes in the dataset that were detected in samples alongside >1 wt. % analytes; a consequence of the high sensitivity of GC-MS analysis where trace samples are easily detected.

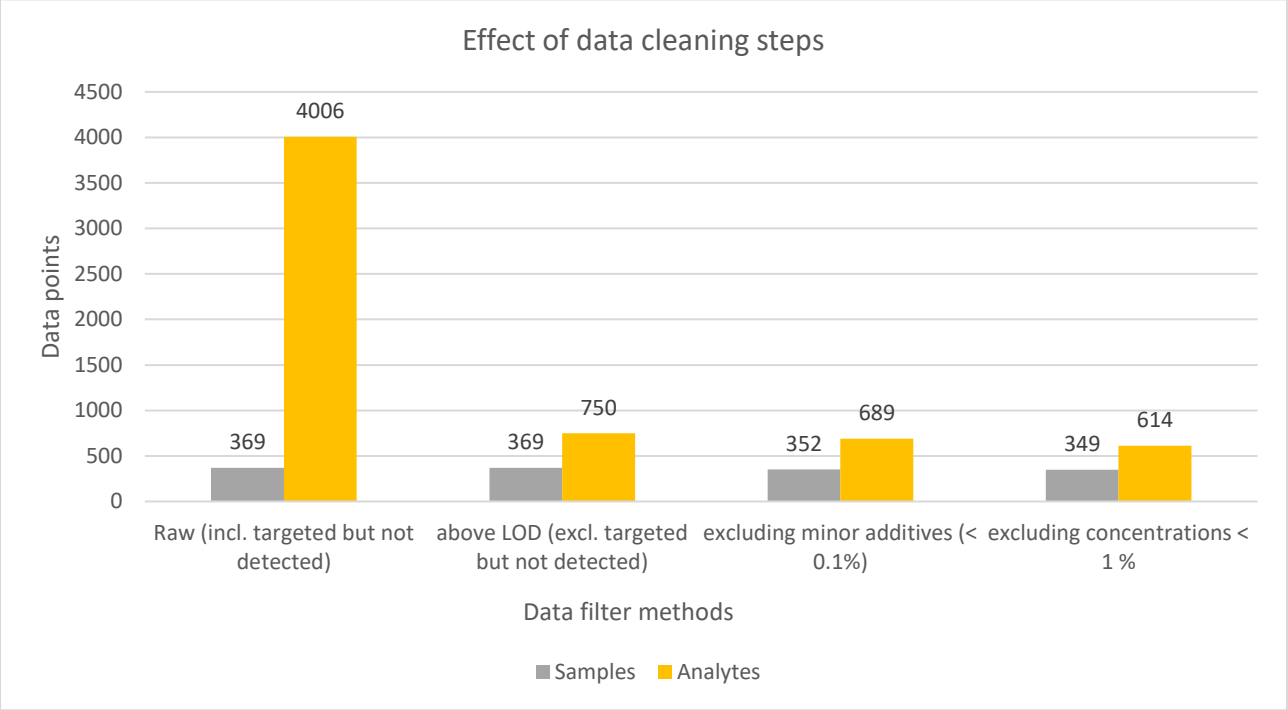

Figure 87: Effect of filtering steps on itemset characteristics (sample and analytes).

Therefore, a threshold of ~1 wt.% was used to filter trace analytes by assigning a non-numerical value to non-zero data points. Comparing the mined rules of the non-filtered vs filtered data (plasticiser >1 wt.%) set could also allow awareness of likely trace analytes missed by TLC but this is beyond the scope of this work.

Figure 88 shows the average, minimum, and maximum concentrations of individual analytes detected in the final dataset of 614 items (analytes) and 349 transactions (samples). Most additives are present in the 5-30 wt.% range but there are multiple examples of highly plasticized articles in the dataset. No patterns between the presence of an additive and its concentration range are apparent. In general, phthalates appear to be used in lower concentrations than TOTM or DOTP, but the small number of data points limits further analysis.

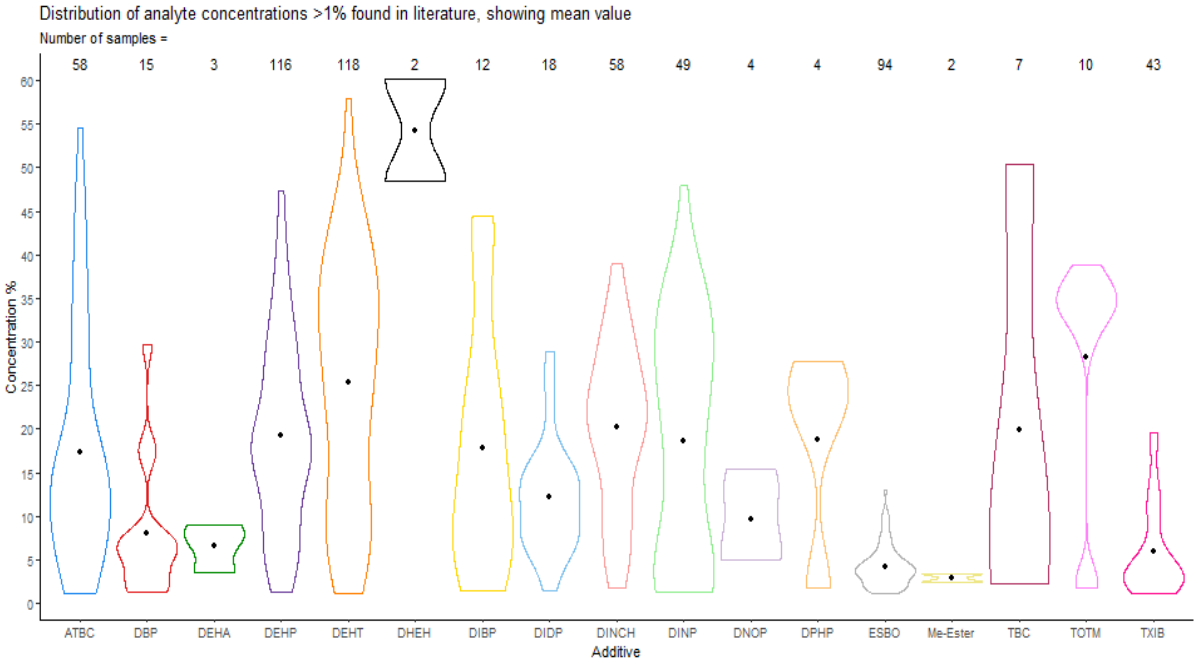

Figure 88: Concentration distribution of analytes found in the literature. Bar width is normalized to 1 for all analytes. The number of samples and mean value (●) are shown.

4.3.11 Mined association rules

An overview of combinations between two additives is shown in the balloon plot in Figure 89Figure 88. The spot size indicates how frequently the combination was observed as a percentage of samples tested for both additives.

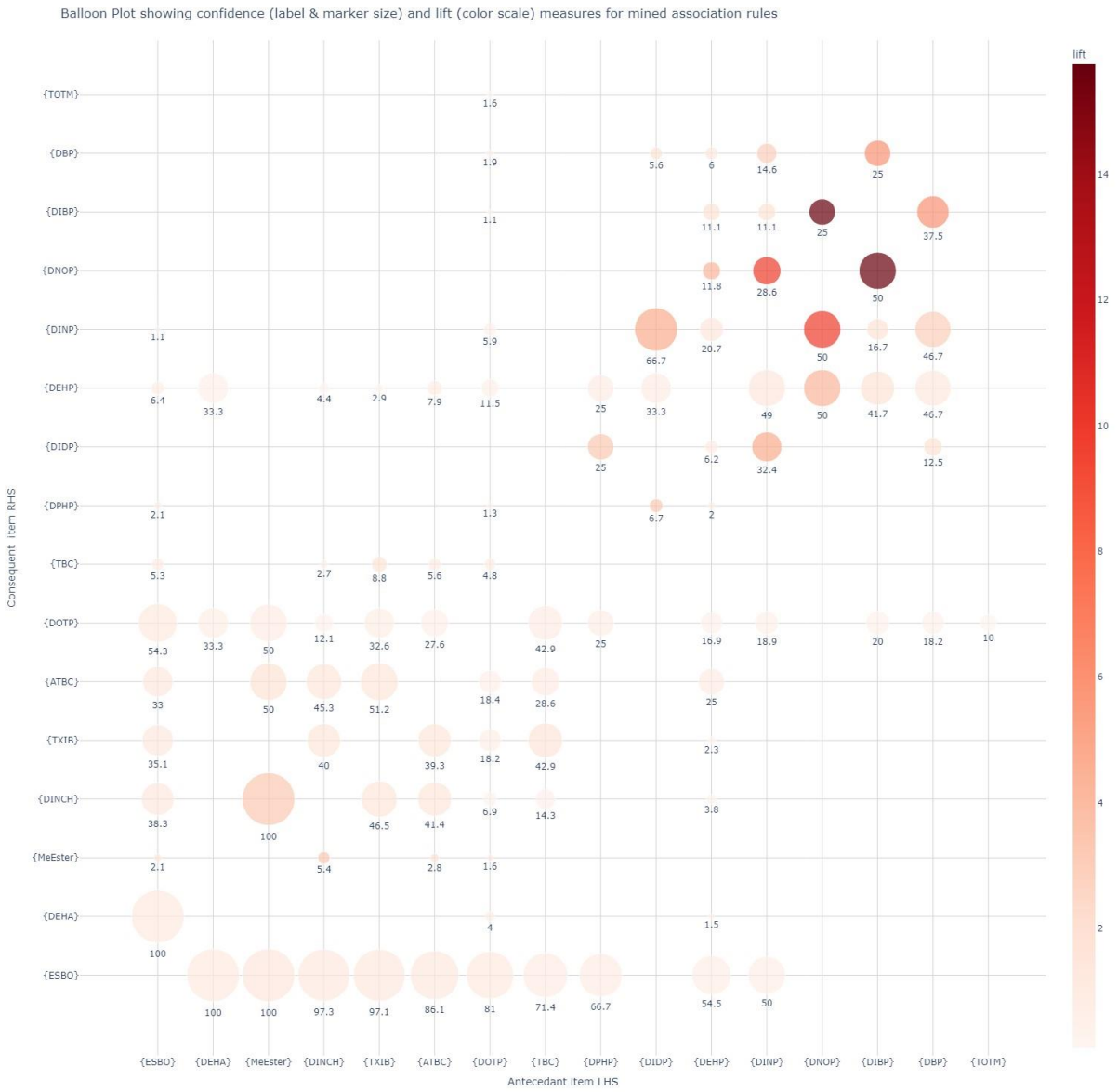

Figure 89: The balloon plot illustrates the mined association rules (combinations) between pairs of individual plasticisers. Spot size & labels indicates the confidence, and the colour scale represents the lift associated with a rule. The plot is read as "if {antecedent LHS} then {consequent RHS}".

By way of example, Table 41 shows the association results mined using the *apriori* algorithm for a combination of DINP and DIDP.

Table 41: Mined association rules between DINP and DIDP.

ID	Rules	Support	Confidence	Coverage	Lift	Count	Samples
67	{DIDP} => {DINP}	5%	67%	7%	4.70	12	261
683	{DINP} => {DIDP}	5%	32%	14%	4.70	12	261

The combination of DIDP and DINP is covered in rules #67 and #683 and can be summarised as follows:

- A subset of 261 samples were tested for DINP and DIDP.
- DINP and DIDP were both identified (above trace levels) in 12 / 261 samples (5% support).
- DINP was identified in 37 of 261 samples tested (14% coverage).
- DIDP was identified in 18 of 261 samples tested (7% coverage).
- DIDP was more often observed in combination with DINP than without DINP (12/18, 67% confidence).
- DINP was more commonly observed without DIDP (12/37, 32% confidence).

A lift value greater than 1 suggests that DIDP and DINP are identified together more frequently than would be expected if they followed their independent distributions in the dataset. They are both commercially available as C_9-C_{11} and C_8-C_{10} isomeric mixtures which is known to lead to non-trivial identification by mass spectrometry and could lead to the conclusion that both are present.

Given the limited dataset, overinterpretation of the measures of interest should be cautioned against. One challenge in using a combined dataset such as this one is the varied coverage of analytes tested. McCombie et al's method tested for the most additives per sample, but accounts for only 30% of the whole dataset. Consequently, while association rule #67 {DIDP} => {DINP} suggested an observable association due to the high confidence and lift scores, its general applicability is uncertain due to the low number of examples in the dataset.

Overall, a cluster in the bottom left quarter of Figure 89 illustrates that combinations of two 'non-phthalate' plasticisers are more common than combinations of two phthalates, or of phthalates mixed with non-phthalates. ESBO is the most common consequent item with high confidence values between 70-100%, reflecting its dual use as a secondary plasticiser and stabiliser (page 43) and its compatibility with a variety of primary plasticisers. This suggests that if an alternate plasticiser is identified, ESBO is also likely to be present.

To assess how the developed TLC method would work with the majority of samples in the dataset Figure 90 shows all additive pairs and their ability to be resolved by the proposed TLC method. The complete tabulated association rules and measures of interest are available in appendix 8.4.

16 of the 48 additive pair combinations identified in the literature dataset are easily distinguished by the proposed TLC method. None of the C_8 and C_{10} phthalates (DEHP/DIDP/DINP) combinations are detected by TLC. However, it was sometimes possible to distinguish an elongated spot from two analytes. The remaining combinations are all unstudied by TLC due to at least one analyte being unavailable during method development (TBC, TXIB and DINCH).

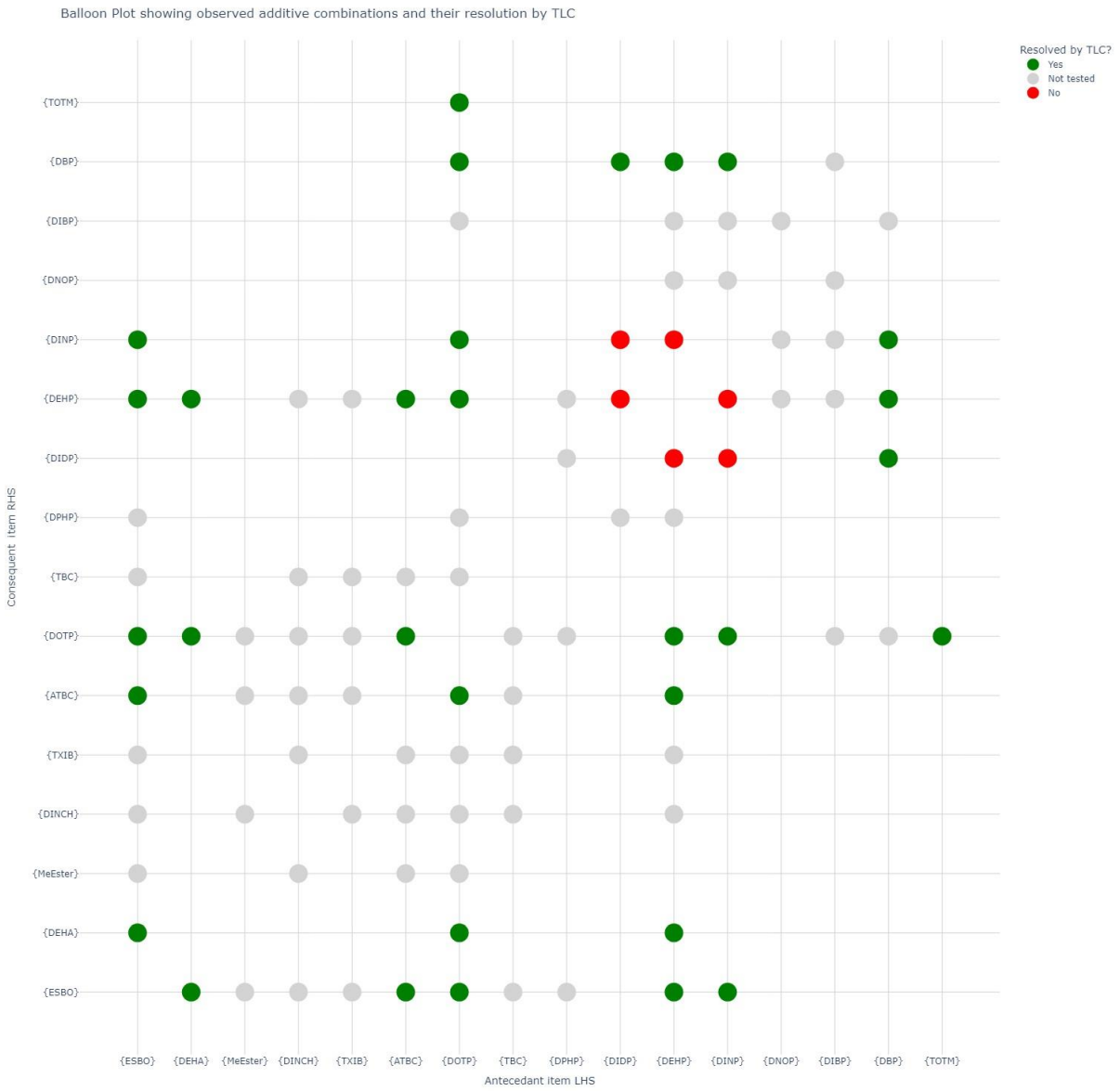

Figure 90: Scatter plot showing all plasticiser combinations observed in the literature dataset, colours indicate if the combination has been tested by TLC and can be resolved (green), cannot be resolved (red) or have not been tested (grey) using the proposed TLC method.

To illustrate how the association rules may be used to aid interpretation of TLC results,

Table 42 shows selected rules used to interpret five samples (BLC, RDC, GRG, DOD, HEI) which showed evidence of two plasticisers upon analysis by TLC.

Only two samples (BLC, RDC) were found to contain more than 1 plasticiser in Chapter 3, with both containing DEHP and DBP. By TLC, DBP can be clearly distinguished, but DEHP could be confused with DINP or DIDP. The association rules # 602, 581 and 51 suggest that if DBP is present either DEHP or DINP are more likely versus DIDP which showed the lowest support.

In another example, while sample DOD was clearly identified as containing only DEHP by GC-MS and ^{1}H NMR spectroscopy, a second UV active spot was evident by TLC. The higher spot was matched with the DOTP reference, and the more intense spot was matched to DEHP/DINP/DIDP. However, the weak intensity of the response appeared uncharacteristic compared to known DOTP samples which appear bright and blue tinged versus other aromatic plasticisers. No association rule for DIDP and DOTP was mined which makes the combination unlikely. Relatively few examples were found for DEHP and DINP (#82, 641). While the results cannot rule out its presence, in most cases where DEHP or DINP were found, DOTP was not detected. Considering that the spot appearance did not match DOTPs characteristics this adds weight to the interpretation that it is not DOTP.

Sample HEI showed a clear spot for DOTP which was confirmed by NMR, and another spot for a C8-10 phthalate. As before a combination of DOTP and DIDP can be considered highly unlikely, and while relatively rare DEHP and DINP (#82, 83, 65) have been observed with DOTP. Where other evidence is not available such as with sample DOD, any confirmation would rely on NMR or GCMS analysis.

Table 42: Selected association rules for combinations of 2 additives

ID	rules (x => y)	support	confidence	coverage	lift	count	number of samples

							in dataset
82	{DEHP} => {DOTP}	5%	17%	27%	0.43	12	263
641	{DINP} => {DOTP}	2%	19%	13%	0.47	7	291
611	{DEHP} => {DBP}	2%	6%	39%	1.20	7	298
602	{DBP} => {DEHP}	2%	47%	5%	1.20	7	298
581	{DBP} => {DINP}	2%	47%	5%	2.90	7	298
51	{DBP} => {DIDP}	0%	13%	3%	1.81	1	261
83	{DOTP} => {DEHP}	5%	12%	40%	0.43	12	263
65	{DOTP} => {DINP}	2%	6%	41%	0.47	7	291

Finally, combinations of more than 2 additives were also mined using a subset of the dataset containing only McCombie et al's targeted analysis of 18 plasticisers in plastic toys. Figure 91 shows the support, confidence, and lift measures for each mined rule, the rules are also available in appendix 8.5. Combinations of alternative plasticisers TXIB, DINCH, and ATBC, with ESBO were the most common. Once again ESBO is the most common consequent item which can be explained by its use as both a plasticiser and stabiliser. All rules have lift values greater than 1, and high confidence values, but no strong associations can be concluded due to the relatively low support measures and a small dataset. TXIB and DINCH were not analysed by TLC so the suitability of the TLC method could not be assessed for these combinations.

Figure 91: Support, confidence, and lift measures of association rules mined from McCombie et al's dataset. All rules contain more than two additives, with a confidence above 50%, and a support value >10%.

Sample BBI was the only sample that showed three analytes by TLC, but only TOTM by NMR. The TLC spots were attributed to TOTM, ESBO and DBP. Unfortunately, the dataset contained no examples of pairwise combinations of any of these plasticisers, and only 10 samples containing TOTM were observed across the whole dataset. Impurities of DEHP and DOTP are known to occur with TOTM, although the

Rf values did not indicate their presence in the sample [305]. Rule #351 associating DOTP and TOTM was mined, although with low measures of interest.

4.4 Conclusion

The developed TLC method including a newly proposed visualization stain was effective for the identification of plasticisers in real PVC samples. The successful use of surface swabbing to collect a sample in a minimally invasive manner highlights the methods utility for the analysis of surface bound degradation products. Indeed, the proposed methodology is optimized for potential application in heritage settings such as surveys, and with non-routine users in mind. A pre-concentration step allows the analytes to concentrate at the starting line without requiring perfect accuracy by the analyst when spotting the plate, and a reference standard is included to aid identification.

The predominant strength in proposing a TLC method for application to plasticiser analysis lies in its simplicity, high-throughput nature, the small sample size, and the ready availability of required chemicals including the visualization method which is commercially available and does not require heating. Wherever possible, the practitioner's survey findings in Chapter 1 have been considered, so the variety, quantity, and cost of chemicals and equipment required have been minimized as shown in appendix section 8.1. The main expense is the upfront cost of £50-100 for TLC plates and microcapillary pipettes, which are harder to source in small quantities. Some equipment is reusable, and some such as solvents and UVC light may not require purchase due to their use for other conservation and imaging tasks.

At a minimum, the method requires a 0.5-1 mg of a PVC sample and a hexane-ethyl acetate solvent mix as a dual-purpose mobile phase and extraction solvent. The

sampled amount could be collected in a discrete manner for all samples, and is also large enough for polymer analysis using ATR-FTIR spectroscopy, but is larger than a sample required for alternatives like pyrolysis GC-MS. Furthermore, due to the ubiquity of DEHP on multiple surfaces detailed in the literature, it is perhaps advantageous for the method to be insensitive to low amounts of DEHP. DEHP was only identified by TLC in samples where a high concentration was also observed by GCMS and ^{1}H NMR.

When compared to traditional methods, TLC is more involved than ATR-FTIR spectroscopy, and the quality of information is lower than extracts analyzed by GC-MS analysis, although was largely in agreement for these samples.

For data analysis and identification, a flow chart is provided to guide identification, with additional context provided by the results from studying combinations present in 349 samples analyzed in the wider scientific literature. The limit dataset limited extensive interpretation of additive combinations, but 3 samples illustrated how additional knowledge of plasticiser formulations could aid interpretation.

While not as extensive as either the GC-MS or NMR methods tested, the method would work best as a pre-screening method for example during a survey, and if sufficient equipment is available, further analysis by GC-MS or NMR could be used to confirm or aid identification for select samples. Compared to the GC-MS methods discussed in the literature which take 15-30 minutes per sample after extraction, the TLC method and plate development is complete within 20 minutes, and up to 16 samples were run contiguously.

Above all, previous studies show that conservators have used the visible presence of deposits and stickiness on an object as evidence of ongoing change or instability

and to inform their conservation strategies. An understanding of the migration capability and volatility of the deposit could be used to inform storage strategies but to date a methodology by which to explore those relationships is not available. This work shows that swab sampling and TLC or GC-MS analysis are appropriate tools to begin such work, without the need for destructive sampling. Furthermore, it remains unclear if plasticiser loss is always an observable process. In future, a swabbing method could be used to explore if the more volatile plasticisers, e.g., ATBC, DBP, etc. behave in the same way to the heavier phthalates which are known to visibly accrete on object surfaces and further inform our understanding of how plastic formulations influence aging behaviour.

5 Conclusion

In summary, this thesis reports methods for the identification of plasticiser additives in PVC and CA, within the ethical sampling constraints encountered in the conservation sector. The TLC and ER-FTIR spectroscopy methods proposed for PVC may both be performed in a non-destructive manner, while for CA, a new data analysis method allows quantitative assessments of additive concentrations, in addition to acetic acid and the degree of substitution of the polymer, and thus enables a holistic understanding of an objects condition. Two experiments are unlikely to find application in the conservation sector; low-field NMR spectroscopy was used for additive identification, and the first exploratory attempt at non-destructive analysis of plasticised CA by Magnetic Resonance Imaging is also described.

Chapter 1 shows that most reports of PVC conservation are proactive interventions after degradation is observed, and the research performed to date has not addressed the effect of additives on expected aging behaviour. It is clear from indoor air quality studies that different emissions behaviour occurs with different plasticisers. Experiments which consider this from the perspective of material stability would be valuable for the heritage sector and it is likely that differences in stability or aging behaviour may be noticeable for both PVC and CA objects over the long term and can be related to their formulation.

From Chapter 2 it was clear that the resources for polymer and additive identification are limited, but their identification can be used to prioritise conservation actions such as moves to temperature-controlled storage or isolation. A focus on non-destructive analysis led to Chapter 3 which found new ATR-FTIR spectroscopy libraries could be

used to identify PVC samples, and ER-FTIR spectroscopy can be used for identification of aromatic plasticisers in PVC. Due to the lack of available samples, non-aromatic plasticisers were not included, but method development with appropriate samples would improve the utility of the method.

The TLC methods developed in Chapter 4, are suitable for plasticiser identification, and can be performed with a small sample or via surface swabbing for example during cleaning. The later method is non-destructive, was successfully applied to samples which showed no signs of degradation and is an obvious candidate for surveying and to preventive conservation planning. The method is especially useful a screening step before more advanced analysis to overcome the non-specificity of the method. It is also a quicker and less invasive method compared to the traditional GC-MS methods. There remains scope to identify additional degradation products and stabilising additives such as ESBO and metal stearate and understand their influence on objects degradation. Interpretation of the results are made easier by flow charts and a fuller understanding of likely additive combinations use in formulations.

6 Bibliography

[1] J. Lee, L. Ireland, J.H. Townsend, B. Ormsby, A. Bartoletti, D. Cane, S. Da Ros, R. King, I. del Gaudio, K. Curran, Exploring the Materials and Condition of 20th-Century Dolls in Zoe Leonard's Mouth Open, Teeth Showing 2000, Polymers (Basel) 15 (2023) 34. https://doi.org/10.3390/POLYM15010034/S1.

[2] Michael. Bolgar, Jack. Hubball, J. Groeger, Susan. Meronek, Handbook for the chemical analysis of plastic and polymer additives, second edition, 2nd ed., CRC Press, 2015. https://doi.org/10.1201/b19124.

[3] J. Pospíšil, S. Nešpůrek, Polymer Additives, Plastic Packaging (2008) 63–88. https://doi.org/doi:10.1002/9783527621422.ch3.

[4] U.S. Patent Office, Official gazette of the United States Patent Office, 1933. https://www.google.com/books/edition/Official_Gazette_of_the_United_States_Pa/UJ1XQ5riRM0C?hl=en&gbpv=0 (accessed June 28, 2023).

[5] W.L. Semon, Synthetic rubber-like composition and method of making same, US1929453A, 1932. https://patents.google.com/patent/US1929453A/en (accessed June 28, 2023).

[6] Y. Shashoua, Conservation of Plastics, 1st ed., Routledge, London, 2012. https://doi.org/10.4324/9780080878782.

[7] Y. Shashoua, Inhibiting the deterioration of plasticized poly (vinyl chloride), Denmark's Technical University, 2001.

[8] N.S. Allen, M. Edge, J.H. Appleyard, T.S. Jewitt, C. V Horie, D. Francis, Degradation of historic cellulose triacetate cinematographic film: The vinegar

syndrome, Polym Degrad Stab 19 (1987) 379–387. https://doi.org/10.1016/0141-3910(87)90038-3.

[9] O. Madden, T. Learner, Preserving Plastics: An Evolving Material, a Maturing Profession, Conservation Perspectives: The Getty Conservation Institute Newsletter (2014).

[10] A. Pokorska, Understanding light sensitivity of plastics in heritage collections, UCL, 2021. https://discovery.ucl.ac.uk/id/eprint/10127953/ (accessed March 6, 2024).

[11] N. Balcar, G. Barabant, C. Bollard, S. Kuperholc, B. Keneghan, A. Lagana, T. van Oosten, K. Segel, Y. Shashoua, Studies in cleaning plastics, in: C. des travaux historiques et scientifiques (Ed.), Preservation of Plastic Artefacts in Museum Collections, 1st ed., Paris, 2012: p. 325.

[12] K. Curran, M. Strlič, Polymers and volatiles: Using VOC analysis for the conservation of plastic and rubber objects, Studies in Conservation 60 (2015) 1–14. https://doi.org/10.1179/2047058413Y.0000000125.

[13] R. Geyer, J.R. Jambeck, K.L. Law, Production, use, and fate of all plastics ever made, Sci Adv 3 (2017). https://doi.org/10.1126/sciadv.1700782.

[14] G. Wypych, Handbook of Plasticisers, Elsevier Science, 2017.

[15] L. Kyrides, Plastic compositions and method of making the same, US2035270A, 1933.

[16] M. Schilling, M. Bouchard, H. Khanjian, T. Learner, A. Phenix, R. Rivenc, Application of chemical and thermal analysis methods for studying cellulose

ester plastics., Acc Chem Res 43 (2010) 888–96. https://doi.org/10.1021/ar1000132.

[17] M. Rahman, C.S. Brazel, The plasticizer market: An assessment of traditional plasticizers and research trends to meet new challenges, Progress in Polymer Science (Oxford) 29 (2004) 1223–1248. https://doi.org/10.1016/j.progpolymsci.2004.10.001.

[18] M. Nouman, J. Saunier, E. Jubeli, N. Yagoubi, Additive blooming in polymer materials: Consequences in the pharmaceutical and medical field, Polym Degrad Stab 143 (2017) 239–252. https://doi.org/10.1016/j.polymdegradstab.2017.07.021.

[19] J.N. Hahladakis, C.A. Velis, R. Weber, E. Iacovidou, P. Purnell, An overview of chemical additives present in plastics: Migration, release, fate and environmental impact during their use, disposal and recycling, J Hazard Mater 344 (2018) 179–199. https://doi.org/10.1016/j.jhazmat.2017.10.014.

[20] U. Heudorf, V. Mersch-Sundermann, J. Angerer, Phthalates: Toxicology and exposure, Int J Hyg Environ Health 210 (2007) 623–634. https://doi.org/10.1016/j.ijheh.2007.07.011.

[21] M. Ji, S. Li, J. Zhang, H. Di, F. Li, T. Feng, The human health assessment to phthalate acid esters (PAEs) and potential probability prediction by chromophoric dissolved organic matter EEM-FRI fluorescence in Erlong lake, Int J Environ Res Public Health 15 (2018) 1–18. https://doi.org/10.3390/ijerph15061109.

[22] R. Hauser, A.M. Calafat, Phthalates and human health, Occup Environ Med 62 (2005) 806–818. https://doi.org/10.1136/oem.2004.017590.

[23] J.S. Tsang, O. Madden, M. Coughlin, A. Maiorana, J. Watson, N.C. Little, R.J. Speakman, Degradation of “Lumarith” Cellulose Acetate: EXAMINATION AND CHEMICAL ANALYSIS OF A SALESMAN’S SAMPLE KIT, Studies in Conservation 54 (2009) 90–105. https://doi.org/10.2307/27867074.

[24] B. Ayrey, L. Hewes, Advanced Materials Used in Space Suit Construction, in: O. Madden, A.E. Charola, K.C. Cobb, P.T. DePriest, R.J. Koestler (Eds.), The Age of Plastic : Ingenuity and Responsibility, Smithsonian Institution Scholarly Press, Washington D.C, 2012: pp. 61–76. https://doi.org/10.5479/si.19492367.7.

[25] W.J. Work, K. Horie, M. Hess, R.F.T. Stepto, Definition of terms related to polymer blends, composites, and multiphase polymeric materials (IUPAC Recommendations 2004), Pure and Applied Chemistry 76 (2004) 1985–2007. https://doi.org/10.1351/pac200476111985.

[26] T. Krieg, C. Mazzon, E. Gómez-Sánchez, Material analysis and a visual guide of degradation phenomena in historical synthetic polymers as tools to follow ageing processes in industrial heritage collections, Polymers (Basel) 14 (2022). https://doi.org/10.3390/polym14010121.

[27] K. Sanderson, Plastics for posterity, Nature (2007). https://doi.org/10.1038/news070521-12.

[28] B. Keneghan, A Survey of Synthetic Plastic and Rubber Objects in the Collections of the Victoria and Albert Museum, Museum Management and

Curatorship 7775 (2007) 321–331. https://doi.org/10.1080/09647770101001903.

[29] G. Barabant, Degradation associated with plastics found in surveys, in: B. Lavédrine, A. Fournier, G. Martin (Eds.), Preservation of Plastic Artefacts in Museum Collections, 1st ed., Scientifiques, Comité des travaux historiques et, 2012: pp. 298–301.

[30] N.S. Allen, M. Edge, J.H. Appleyard, T.S. Jewitt, C.V. Horie, D. Francis, Degradation of historic cellulose triacetate cinematographic film: The vinegar syndrome, Polym Degrad Stab 19 (1987) 379–387. https://doi.org/10.1016/0141-3910(87)90038-3.

[31] J.-L. Bigourdan, J. Reilly, Effectiveness of Storage Conditions in Controlling the Vinegar Syndrome: Preservation Strategies for Acetate Base Motion-Picture Film Collections, in: M. Aubert, R. Billeaud (Eds.), Image and Sound Archiving and Access: The Challenges of the 3rd Millennium, Proceedings of the Joint Technical Symposium Paris 2000, Paris, 2000: pp. 14–34.

[32] Care, Handling, and Storage of Motion Picture Film - Collections Care (Preservation, Library of Congress), (n.d.). https://www.loc.gov/preservation/care/film.html#Acetate (accessed August 20, 2020).

[33] S. Williams, Care of Objects Made from Rubber and Plastic, CCI Notes 15 (1997) 1–6.

[34] I.R. Ahmad, D. Cane, J.H. Townsend, C. Triana, L. Mazzei, K. Curran, Are we overestimating the permanence of cellulose triacetate cinematographic films?

A mathematical model for the vinegar syndrome, Polym Degrad Stab (2020). https://doi.org/10.1016/j.polymdegradstab.2019.109050.

[35] J.L. Gardette, J. Lemaire, Photothermal and thermal oxidations of rigid, plasticized, and pigmented poly(vinyl chloride), Polym Degrad Stab (1991). https://doi.org/10.1016/0141-3910(91)90117-A.

[36] W.H.H. Starnes, Structural and mechanistic aspects of the thermal degradation of poly(vinyl chloride), Pergamon, 2002. https://doi.org/10.1016/S0079-6700(02)00063-1.

[37] J. Lemaire, R. Arnaud, J.L. Gardette, Low temperature thermo-oxidation of thermoplastics in the solid state, Polym Degrad Stab (1991). https://doi.org/10.1016/0141-3910(91)90021-I.

[38] G. Wypych, PRINCIPLES OF THERMAL DEGRADATION, in: PVC Degradation & Stabilization /, Third edit, Toronto :, 2015: pp. 79–165. https://doi.org/10.1016/B978-1-895198-85-0.50006-6.

[39] Y. Shashoua, Inhibiting the deterioration of plasticized poly (vinyl chloride), 2001.

[40] A. Royaux, I. Fabre-Francke, N. Balcar, G. Barabant, C. Bollard, B. Lavédrine, S. Cantin, Aging of plasticized polyvinyl chloride in heritage collections: The impact of conditioning and cleaning treatments, Polym Degrad Stab 137 (2017) 109–121. https://doi.org/10.1016/j.polymdegradstab.2017.01.011.

[41] A. Royaux, I. Fabre-Francke, N. Balcar, G. Barabant, C. Bollard, B. Lavédrine, S. Cantin, Long-term effect of silk paper used for wrapping of plasticized PVC

objects: Comparison between ancient and model PVC, Polym Degrad Stab 155 (2018) 183–193. https://doi.org/10.1016/j.polymdegradstab.2018.07.016.

[42] A. Royaux, E. Apchain, I. Fabre-Francke, N. Balcar, G. Barabant, C. Bollard, B. Lavédrine, O. Fichet, S. Cantin, Conservation of plasticized PVC artifacts in museums: Influence of wrapping materials, J Cult Herit (2020). https://doi.org/10.1016/j.culher.2020.07.002.

[43] P. Pourmand, M.S. Hedenqvist, I. Furó, U.W. Gedde, Deterioration of highly filled EPDM rubber by thermal ageing in air: Kinetics and non-destructive monitoring, Polym Test 64 (2017) 267–276. https://doi.org/10.1016/j.polymertesting.2017.10.019.

[44] X.-F. Wei, K.J. Kallio, S. Bruder, M. Bellander, M.S. Hedenqvist, Plasticizer loss in a complex system (polyamide 12): Kinetics, prediction and its effects on mechanical properties, Polym Degrad Stab 169 (2019) 108985.

[45] X.-F. Wei, E. Linde, M.S. Hedenqvist, Plasticiser loss from plastic or rubber products through diffusion and evaporation, Npj Mater Degrad 3 (2019) 18. https://doi.org/10.1038/s41529-019-0080-7.

[46] Y. Liang, X. Liu, M.R. Allen, Measurements of Parameters Controlling the Emissions of Organophosphate Flame Retardants in Indoor Environments, Environ Sci Technol 52 (2018) 5821–5829. https://doi.org/10.1021/acs.est.8b00224.

[47] Y. Xu, Y. Zhang, An improved mass transfer based model for analyzing VOC emissions from building materials, Atmos Environ 37 (2003) 2497–2505. https://doi.org/10.1016/S1352-2310(03)00160-2.

[48] C.J. Weschler, W.W. Nazaroff, Semivolatile organic compounds in indoor environments, Atmos Environ 42 (2008) 9018–9040. https://doi.org/10.1016/j.atmosenv.2008.09.052.

[49] Z. Liu, W. Ye, J.C. Little, Predicting emissions of volatile and semivolatile organic compounds from building materials: A review, Build Environ 64 (2013) 7–25. https://doi.org/10.1016/j.buildenv.2013.02.012.

[50] Z. Liu, W. Ye, J.C. Little, Y. Xu, J.C. Little, Z. Liu, W. Ye, J.C. Little, Y. Xu, J.C. Little, Predicting emissions of SVOCs from polymeric materials and their interaction with airborne particles, Environ Sci Technol 40 (2006) 456–461. https://doi.org/10.1021/es051517j.

[51] Y. Wu, M. Xie, S.S. Cox, L.C. Marr, J.C. Little, A simple method to measure the gas-phase SVOC concentration adjacent to a material surface, Indoor Air 26 (2016) 903–912. https://doi.org/10.1111/ina.12270.

[52] Y. Liang, Y. Xu, An improved method for measuring and characterizing phthalate emissions from building materials and its application to exposure assessment, in: Indoor Air 2014 - 13th International Conference on Indoor Air Quality and Climate, 2014.

[53] C.M.A. Eichler, Y. Wu, J. Cao, S. Shi, J.C. Little, Equilibrium Relationship between SVOCs in PVC Products and the Air in Contact with the Product, Environ Sci Technol 52 (2018) 2918–2925. https://doi.org/10.1021/acs.est.7b06253.

[54] W. Wei, C. Mandin, O. Ramalho, Influence of indoor environmental factors on mass transfer parameters and concentrations of semi-volatile organic

compounds, Chemosphere 195 (2018) 223–235. https://doi.org/10.1016/j.chemosphere.2017.12.072.

[55] Y.-F. Mao, Z. Li, Y.-P. Zhang, Y.-L. He, W.-Q. Tao, A review of mass-transfer models and mechanistic studies of semi-volatile organic compounds in indoor environments, Indoor and Built Environment 27 (2018) 1307–1321. https://doi.org/10.1177/1420326X17704275.

[56] J. Cao, X. Zhang, J.C. Little, Y. Zhang, A SPME-based method for rapidly and accurately measuring the characteristic parameter for DEHP emitted from PVC floorings, Indoor Air 27 (2017) 417–426. https://doi.org/10.1111/ina.12312.

[57] W. Wei, O. Ramalho, C. Mandin, A long-term dynamic model for predicting the concentration of semivolatile organic compounds in indoor environments: Application to phthalates, Build Environ 148 (2019) 11–19. https://doi.org/10.1016/J.BUILDENV.2018.10.044.

[58] C. Bi, Y. Liang, Y. Xu, Fate and Transport of Phthalates in Indoor Environments and the Influence of Temperature: A Case Study in a Test House, Environ Sci Technol (2015). https://doi.org/10.1021/acs.est.5b02787.

[59] Y. Liang, X. Liu, M.R. Allen, The influence of temperature on the emissions of organophosphate ester flame retardants from polyisocyanurate foam: Measurement and modeling (supporting information), Chemosphere 233 (2019) 347–354. https://doi.org/10.1016/j.chemosphere.2019.05.289.

[60] Q. Deng, X. Yang, J. Zhang, Study on a new correlation between diffusion coefficient and temperature in porous building materials, Atmos Environ 43 (2009) 2080–2083. https://doi.org/10.1016/j.atmosenv.2008.12.052.

[61] C.B. Lauridsen, L.W. Hansen, T. Brock-Nannestad, J. Bendix, K.P. Simonsen, A study of stearyl alcohol bloom on Dan Hill PVC dolls and the influence of temperature, Studies in Conservation 62 (2017) 445–455. https://doi.org/10.1080/00393630.2016.1206651.

[62] E. Richardson, M. Truffa Giachet, M. Schilling, T. Learner, Assessing the physical stability of archival cellulose acetate films by monitoring plasticizer loss, Polym Degrad Stab 107 (2014) 231–236. https://doi.org/10.1016/j.polymdegradstab.2013.12.001.

[63] D. Littlejohn, R.A. Pethrick, A. Quye, J.M. Ballany, Investigation of the degradation of cellulose acetate museum artefacts, Polym Degrad Stab 98 (2013) 416–424. https://doi.org/10.1016/j.polymdegradstab.2012.08.023.

[64] D.C. Rambaldi, C. Suryawanshi, C. Eng, F.D. Preusser, Effect of thermal and photochemical degradation strategies on the deterioration of cellulose diacetate, Polym Degrad Stab 107 (2014) 237–245. https://doi.org/10.1016/j.polymdegradstab.2013.12.004.

[65] E. Linde, U.W.W. Gedde, Plasticizer migration from PVC cable insulation - The challenges of extrapolation methods, Polym Degrad Stab 101 (2014) 24–31. https://doi.org/10.1016/j.polymdegradstab.2014.01.021.

[66] M. Celina, K.T. Gillen, R.A. Assink, Accelerated aging and lifetime prediction: Review of non-Arrhenius behaviour due to two competing processes, Polym Degrad Stab 90 (2005) 395–404. https://doi.org/10.1016/j.polymdegradstab.2005.05.004.

[67] Y.R. Shashoua, Effect of indoor climate on the rate and degradation mechanism of plasticized poly (vinyl chloride), Polym Degrad Stab 81 (2003) 29–36. https://doi.org/10.1016/S0141-3910(03)00059-4.

[68] M.T. Giachet, M. Schilling, K. McCormick, J. Mazurek, E. Richardson, H. Khanjian, T. Learner, Assessment of the composition and condition of animation cels made from cellulose acetate, Polym Degrad Stab 107 (2014) 223–230. https://doi.org/10.1016/j.polymdegradstab.2014.03.009.

[69] B. Kemper, Influence of relative humidity and acetic acid concentration in the air to the loss of plasticizers from cellulose acetate material of the Transparent Figures of the Deutsches Hygiene-Museum Dresden, in: Plastics Heritage Congress, Lisbon, 2019.

[70] Y. Shashoua, Conservation of plastics: Materials science, degradation and preservation, 1st ed., Routledge, London, 2012. https://doi.org/10.4324/9780080878782.

[71] C.J. Weschler, Chemical reactions among indoor pollutants: What we've learned in the new millennium, Indoor Air, Supplement 14 (2004) 184–194. https://doi.org/10.1111/j.1600-0668.2004.00287.x.

[72] A. Rackes, M.S. Waring, Do time-averaged, whole-building, effective volatile organic compound (VOC) emissions depend on the air exchange rate? A statistical analysis of trends for 46 VOCs in U.S. offices, Indoor Air 26 (2016) 642–659. https://doi.org/10.1111/ina.12224.

[73] C. Liu, Y. Zhang, J.L. Benning, J.C. Little, The effect of ventilation on indoor exposure to semivolatile organic compounds, Indoor Air 25 (2015) 285–296. https://doi.org/10.1111/ina.12139.

[74] Y. Liang, Y. Xu, The influence of surface sorption and air flow rate on phthalate emissions from vinyl flooring: Measurement and modeling, Atmos Environ 103 (2015) 147–155. https://doi.org/10.1016/j.atmosenv.2014.12.029.

[75] M. Ekelund, B. Azhdar, M.S. Hedenqvist, U.W. Gedde, Long-term performance of poly(vinyl chloride) cables, Part 2: Migration of plasticizer, Polym Degrad Stab 93 (2008) 1704–1710. https://doi.org/10.1016/j.polymdegradstab.2008.05.030.

[76] M. Ekelund, B. Azhdar, U.W. Gedde, Evaporative loss kinetics of di(2-ethylhexyl)phthalate (DEHP) from pristine DEHP and plasticized PVC, Polym Degrad Stab 95 (2010) 1789–1793. https://doi.org/10.1016/j.polymdegradstab.2010.05.007.

[77] H. Wilson, S. VanSnick, The effectiveness of dust mitigation and cleaning strategies at The National Archives, UK, J Cult Herit 24 (2017) 100–107. https://doi.org/10.1016/j.culher.2016.09.004.

[78] C. Bergh, R. Torgrip, G. Emenius, C. Östman, Organophosphate and phthalate esters in air and settled dust - a multi-location indoor study, Indoor Air 21 (2011) 67–76. https://doi.org/10.1111/j.1600-0668.2010.00684.x.

[79] D.M. Lunderberg, K. Kristensen, Y. Liu, P.K. Misztal, Y. Tian, C. Arata, R. Wernis, N. Kreisberg, W.W. Nazaroff, A.H. Goldstein, Characterizing Airborne

Phthalate Concentrations and Dynamics in a Normally Occupied Residence, Environ Sci Technol (2019). https://doi.org/10.1021/acs.est.9b02123.

[80] Y. Wu, C.M.A. Eichler, J. Cao, J. Benning, A. Olson, S. Chen, C. Liu, E.P. Vejerano, L.C. Marr, J.C. Little, Particle/Gas Partitioning of Phthalates to Organic and Inorganic Airborne Particles in the Indoor Environment, Environ Sci Technol 52 (2018) 3583–3590. https://doi.org/10.1021/acs.est.7b05982.

[81] J.L. Benning, Z. Liu, A. Tiwari, J.C. Little, L.C. Marr, Characterizing gas-particle interactions of phthalate plasticizer emitted from vinyl flooring, Environ Sci Technol 47 (2013) 2696–2703. https://doi.org/10.1021/es304725b.

[82] N.R. Lee, Y.J. Chung, Study on Degradation Characteristics and Chemical Cleaning Methods of Plasticized PVC for Conservation of Plastic Artifact, Journal of Conservation Science 35 (2019) 159–168. https://doi.org/10.12654/JCS.2019.35.2.06.

[83] I.S. Biggin, D.L. Gerrard, G.E. Williams, The effect of aromatic plasticisers on the photo-dehydrochlorination of poly(vinyl chloride), Journal of Vinyl Technology 4 (1982). https://doi.org/10.1002/vnl.730040407.

[84] S. Hollande, J.L. Laurent, Study of discolouring change in PVC, plasticizer and plasticized PVC films, Polym Degrad Stab 55 (1997). https://doi.org/10.1016/S0141-3910(96)00165-6.

[85] J.M. Hankett, W.R. Collin, Z. Chen, Molecular Structural Changes of Plasticized PVC after UV Light Exposure, J Phys Chem B 117 (2013) 16336–16344. https://doi.org/10.1021/jp409254y.

[86] C. Wang, D.B. Collins, C. Arata, A.H. Goldstein, J.M. Mattila, D.K. Farmer, L. Ampollini, P.F. DeCarlo, A. Novoselac, M.E. Vance, W.W. Nazaroff, J.P.D. Abbatt, Surface reservoirs dominate dynamic gas-surface partitioning of many indoor air constituents, Sci Adv 6 (2020) eaay8973. https://doi.org/10.1126/sciadv.aay8973.

[87] L.B. Algrim, D. Pagonis, J.A. de Gouw, J.L. Jimenez, P.J. Ziemann, Measurements and modeling of absorptive partitioning of volatile organic compounds to painted surfaces, Indoor Air 30 (2020) 745–756. https://doi.org/10.1111/ina.12654.

[88] Y. Wu, C.M.A. Eichler, W. Leng, S.S. Cox, L.C. Marr, J.C. Little, Adsorption of Phthalates on Impervious Indoor Surfaces, Environ Sci Technol (2017). https://doi.org/10.1021/acs.est.6b05853.

[89] K. Curran, A. Možir, M. Underhill, L.T. Gibson, T. Fearn, M. Strlič, Cross-infection effect of polymers of historic and heritage significance on the degradation of a cellulose reference test material, Polym Degrad Stab 107 (2014) 294–306. https://doi.org/10.1016/j.polymdegradstab.2013.12.019.

[90] S.E. O'Rourke, Stress-cracking resistance of polycarbonate in contact with plasticized PVC compounds, Journal of Vinyl Technology 9 (1987) 147–150. https://doi.org/10.1002/VNL.730090404.

[91] V. Papakonstantinou, C.D. Papaspyrides, Plasticizer migration from plasticized into unplasticized poly(vinyl chloride), Journal of Vinyl Technology 16 (1994) 192–196. https://doi.org/10.1002/VNL.730160404.

[92] J.A. Jansen, ENVIRONMENTAL STRESS CRACKING-EXAMPLES FROM THE AUTOMOTIVE INDUSTRY, (n.d.). https://madisongroup.com/environmental-stress-cracking-examples-from-the-automotive-industry/ (accessed July 8, 2022).

[93] J.A. Jansen, Characterization of Plastics in Failure Analysis, in: Characterization and Failure Analysis of Plastics, ASM International, 2022: pp. 499–520. https://doi.org/10.31399/asm.hb.v11B.a0006933.

[94] E. Lacatus, J.W. Summers, Stress cracking of rigid polyvinyl chloride by plasticizer migration, Journal of Vinyl Technology 6 (1984) 157–161. https://doi.org/10.1002/VNL.730060407.

[95] Plasticizer-Induced Stress Cracking of Rigid PVC and Polycarbonate - Medical Design Briefs, (n.d.). https://www.medicaldesignbriefs.com/component/content/article/mdb/features/technology-leaders/24145 (accessed July 8, 2022).

[96] Hallstar, Stress-Cracking Resistance of Polycarbonate in Contact With Plasticized PVC Compounds, (n.d.). https://www.hallstarindustrial.com/webfoo/wp-content/uploads/hallstar-stresscracking-resistance-of-polycarbonate.pdf (accessed July 8, 2022).

[97] What is the best alternative to DEHP for medical-grade PVC?, (n.d.). https://www.plasticstoday.com/medical/what-best-alternative-dehp-medical-gradepvc-depends (accessed July 8, 2022).

[98] US4640819A - Stress crack reduction in polycarbonate parts, 1985. https://patents.google.com/patent/US4640819 (accessed July 8, 2022).

[99] J.M. Fischer, Handbook of Molded Part Shrinkage and Warpage: Second Edition, William Andrew, 2012. https://doi.org/10.1016/C2011-0-06800-X.

[100] A. Benazzouz, E. Dudognon, N.T. Correia, V. Molinier, J.M. Aubry, M. Descamps, Interactions underpinning the plasticization of a polymer matrix: a dynamic and structural analysis of DMP-plasticized cellulose acetate, Cellulose 24 (2017) 487–503. https://doi.org/10.1007/s10570-016-1148-y.

[101] S. Biedermann-Brem, M. Biedermann, S. Pfenninger, M. Bauer, W. Altkofer, K. Rieger, U. Hauri, C. Droz, K. Grob, Plasticizers in PVC toys and childcare products: What succeeds the phthalates? Market survey 2007, Chromatographia 68 (2008) 227–234. https://doi.org/10.1365/S10337-008-0672-9/TABLES/4.

[102] M. Rahman, C.S. Brazel, The plasticizer market: An assessment of traditional plasticizers and research trends to meet new challenges, Progress in Polymer Science (Oxford) 29 (2004) 1223–1248. https://doi.org/10.1016/j.progpolymsci.2004.10.001.

[103] P. Karmalm, T. Hjertberg, A. Jansson, R. Dahl, Thermal stability of poly(vinyl chloride) with epoxidised soybean oil as primary plasticizer, Polym Degrad Stab 94 (2009). https://doi.org/10.1016/j.polymdegradstab.2009.07.019.

[104] D. Li, K. Panchal, R. Mafi, L. Xi, An Atomistic Evaluation of the Compatibility and Plasticization Efficacy of Phthalates in Poly(vinyl chloride), Macromolecules 51 (2018) 6997–7012. https://doi.org/10.1021/ACS.MACROMOL.8B00756/ASSET/IMAGES/LARGE/MA-2018-00756R_0015.JPEG.

[105] M.S. Hedenqvist, U.W. Gedde, Parameters affecting the determination of transport kinetics data in highly swelling polymers above T(g), Polymer (Guildf) 40 (1999) 2381–2393. https://doi.org/10.1016/S0032-3861(98)00453-4.

[106] J.C. Huang, H. Liu, Y. Liu, Diffusion in polymers with concentration dependent diffusivity, International Journal of Polymeric Materials and Polymeric Biomaterials 49 (2001) 15–24. https://doi.org/10.1080/00914030108035864.

[107] L. Audouin, A. Andre, J. Verdu, Concentration and temperature dependence of plasticizer diffusion into plasticized PVC, Journal of Vinyl Technology 16 (1994) 57–61. https://doi.org/10.1002/vnl.730160114.

[108] B. Yang, Y. Bai, Y. Cao, Effects of inorganic nano-particles on plasticizers migration of flexible PVC, J Appl Polym Sci 115 (2010). https://doi.org/10.1002/app.31310.

[109] C. Morales Muñoz, Limpieza del PVC plastificado: metodología aplicable a obras de arte y objetos de museo, Universidad Complutense de Madrid, 2017. https://hdl.handle.net/20.500.14352/22163 (accessed March 10, 2024).

[110] A.L. Fricker, The conservation of polymeric materials in museum collections using advanced surface science and surface analysis techniques, Imperial College London, 2016. http://spiral.imperial.ac.uk/handle/10044/1/44079%0Ahttp://files/53141/Fricker - 2016 - The conservation of polymeric materials in museum .pdf.

[111] L. v. Angelova, G. Sofer, A. Bartoletti, B. Ormsby, A Comparative Surface Cleaning Study of Op Structure, an Op Art PMMA Sculpture by Michael Dillon,

Https://Doi.Org/10.1080/01971360.2022.2031459 (2022) 1–20. https://doi.org/10.1080/01971360.2022.2031459.

[112] A.L. Fricker, D.S. McPhail, B. Keneghan, B. Pretzel, Investigating the impact of cleaning treatments on polystyrene using SEM, AFM and ToF–SIMS, Herit Sci 5 (2017) 28. https://doi.org/10.1186/s40494-017-0142-5.

[113] Y. Shashoua, M. Alterini, G. Pastorelli, L. Cone, From microfibre cloths to poly(vinyl alcohol) hydrogels – conservation cleaning of plastics heritage, J Cult Herit 52 (2021) 38–43. https://doi.org/10.1016/j.culher.2021.08.009.

[114] J. Hackett, Cleaning PVC with Microemulsions - Victoria and Albert Museum, V&A Conservation Journal (2014). http://www.vam.ac.uk/content/journals/conservation-journal/autumn-2014-issue-62/cleaning-pvc-with-microemulsions-joanne-hackett/ (accessed April 14, 2022).

[115] L.M. Robeson, Environmental stress cracking: A review, Polym Eng Sci 53 (2013) 453–467. https://doi.org/10.1002/PEN.23284.

[116] S. Kavda, N. Dhopatkar, L. V. Angelova, E. Richardson, S. Golfomitsou, A. Dhinojwala, Surface behaviour of PMMA: Is gel cleaning the way to go?, Studies in Conservation 61 (2016) 297–299. https://doi.org/10.1080/00393630.2016.1200858.

[117] S. Kavda, S. Golfomitsou, E. Richardson, The effect of gelling agents and solvents on poly(methyl methacrylate) surfaces: a comparative study, n.d. https://discovery.ucl.ac.uk/10034059/1/GELs%2065%20Kavda_128dpi.pdf (accessed June 20, 2022).

[118] C.M. MUÑOZ, Spectrocolorimetric and microscopic techniques for the evaluation of plasticized PVC cleaning: a case study applicable to three-dimensional objects at museums, J Microsc 243 (2011) 257–266. https://doi.org/10.1111/j.1365-2818.2011.03499.x.

[119] C. Morales Muñoz, Surface modification of plasticized PVC by dry cleaning methods: Consequences for artworks, Appl Surf Sci 256 (2010) 3567–3572. https://doi.org/10.1016/j.apsusc.2009.12.156.

[120] C.M. Muñoz, H. Egsgaard, J.S. Landaluze, C. Dietz, A MODEL APPROACH FOR FINDING CLEANING SOLUTIONS FOR PLASTICIZED POLY(VINYL CHLORIDE) SURFACES OF COLLECTIONS OBJECTS, Journal of the American Institute for Conservation 53 (2014) 236–251. https://doi.org/10.1179/0197136014Z.00000000040.

[121] L. Bernard, D. Bourdeaux, B. Pereira, N. Azaroual, C. Barthélémy, C. Breysse, P. Chennell, R. Cueff, T. Dine, T. Eljezi, F. Feutry, S. Genay, N. Kambia, M. Lecoeur, M. Masse, P. Odou, T. Radaniel, N. Simon, C. Vaccher, C. Verlhac, M. Yessad, B. Décaudin, V. Sautou, Analysis of plasticizers in PVC medical devices: Performance comparison of eight analytical methods, Talanta 162 (2017) 604–611. https://doi.org/10.1016/J.TALANTA.2016.10.033.

[122] G.C. Whitnack, E.St.C. Gantz, Extraction and Determination of Plasticizers from Cellulose Acetate Plastics, Anal Chem 24 (1952) 1060–1061. https://doi.org/10.1021/ac60066a054.

[123] L. Bernard, R. Cueff, D. Bourdeaux, C. Breysse, V. Sautou, Analysis of plasticizers in poly(vinyl chloride) medical devices for infusion and artificial

nutrition: comparison and optimization of the extraction procedures, a pre-migration test step, Analytical and Bioanalytical Chemistry 2015 407:6 407 (2015) 1651–1659. https://doi.org/10.1007/S00216-014-8426-Z.

[124] C.H. Dong, Y.F. Liu, W.F. Yang, X.L. Sun, G.Q. Wang, Simultaneous determination of phthalate plasticizers in PVC packaging materials using homogeneous-ultrasonic extraction-GC-MS assisted with continuous wavelet transform, Analytical Methods 5 (2013) 4513–4517. https://doi.org/10.1039/c3ay40574e.

[125] M. Bonini, E. Errani, G. Zerbinati, E. Ferri, S. Girotti, Extraction and gas chromatographic evaluation of plasticizers content in food packaging films, Microchemical Journal 90 (2008) 31–36. https://doi.org/10.1016/J.MICROC.2008.03.002.

[126] F.D. Foster, J.R. Stuff, J.A. Whitecavage, E.A. Pfannkoch, Automated Extraction and GC/MS Determination of Phthalates in Consumer Products, 2013. https://gerstel.com/en/Automated_Extraction_and_GC-MS_Determination (accessed October 12, 2020).

[127] M. Gawlik-Jędrysiak, Determination of phthalate esters content in plastic articles: Comparison of extraction methods, Journal of Analytical Chemistry 68 (2013) 959–960. https://doi.org/10.1134/S1061934813090104.

[128] K. Sutherland, M. Kokkori, Investigating formulations of cellulose acetate plastics in the collections of the Art Institute of Chicago using pyrolysis gas chromatography mass spectrometry, J Anal Appl Pyrolysis 163 (2022) 105484. https://doi.org/10.1016/j.jaap.2022.105484.

[129] A. Pereira, A. Candeias, A. Cardoso, D. Rodrigues, P. Vandenabeele, A.T. Caldeira, Non-invasive methodology for the identification of plastic pieces in museum environment — a novel approach, Microchemical Journal 124 (2016) 846–855. https://doi.org/10.1016/j.microc.2015.07.027.

[130] J.S. Tsang, O. Madden, M. Coughlin, A. Maiorana, J. Watson, N.C. Little, R.J. Speakman, Degradation of “Lumarith” Cellulose Acetate: EXAMINATION AND CHEMICAL ANALYSIS OF A SALESMAN’S SAMPLE KIT, Studies in Conservation 54 (2009) 90–105. https://doi.org/10.2307/27867074.

[131] C.B. Lauridsen, L.W. Hansen, T. Brock-Nannestad, J. Bendix, K.P. Simonsen, A study of stearyl alcohol bloom on Dan Hill PVC dolls and the influence of temperature, Studies in Conservation 62 (2017) 445–455. https://doi.org/10.1080/00393630.2016.1206651.

[132] Y. Shashoua, U. Schnell, L. Young, Deterioration of plasticized PVC components in Apollo spacesuits — The Ministry of Culture Research Portal, in: Y. Shashoua, F. Waentig (Eds.), Lastics in Art - History, Technology, Preservation , Siegl, Munich, 2002: pp. 69–79. https://pure.kb.dk/en/publications/deterioration-of-plasticized-pvc-components-in-apollo-spacesuits (accessed April 14, 2022).

[133] N. Ledoux, G. Rayner, S. Costello, A. Chang, Preventive Conservation, Treatment, and Technical Study of Plasticized Poly(vinyl chloride) Multiples by Joseph Beuys, Studies in Conservation 68 (2023) 343–356. https://doi.org/10.1080/00393630.2022.2033520.

[134] K. Curran, M. Underhill, L.T. Gibson, M. Strlic, The development of a SPME-GC/MS method for the analysis of VOC emissions from historic plastic and rubber materials, Microchemical Journal 124 (2016) 909–918. https://doi.org/10.1016/J.MICROC.2015.08.027.

[135] G. Mitchell, C. Higgitt, L.T. Gibson, Emissions from polymeric materials: Characterised by thermal desorption-gas chromatography, Polym Degrad Stab 107 (2014) 328–340. https://doi.org/10.1016/J.POLYMDEGRADSTAB.2013.12.003.

[136] S. Hackney, Colour measurement of acid-detector strips for the quantification of volatile organic acids in storage conditions, Studies in Conservation 61 (2016) 55–69. https://doi.org/10.1080/00393630.2016.1140935.

[137] M. Kearney, I. Parkin, J.H. Townsend, M. Hidalgo, K. Curran, Characterisation of VOCs Surrounding Naum Gabo's Construction in Space 'Two Cones ', (Tate) by in situ SPME GC-MS Monitoring, Studies in Conservation 63 (2018) 369–371. https://doi.org/10.1080/00393630.2018.1486530.

[138] M. Kearney, J.H. Townsend, I.P. Parkin, M. Hidalgo, K. Curran, Factors affecting the practicality of solid-phase microextraction VOC analysis of artworks featuring polymeric materials in open environments, Microchemical Journal 155 (2020) 104711. https://doi.org/10.1016/j.microc.2020.104711.

[139] J. Cao, C.J. Weschler, J. Luo, Y. Zhang, Cm-History Method, a Novel Approach to Simultaneously Measure Source and Sink Parameters Important for Estimating Indoor Exposures to Phthalates, Environ Sci Technol 50 (2016) 825–834. https://doi.org/10.1021/acs.est.5b04404.

[140] F. Portoni, J. Grau-Bové, M. Strlič, Application of a non-invasive, non-destructive technique to quantify naphthalene emission rates from museum objects, Herit Sci 7 (2019) 58. https://doi.org/10.1186/s40494-019-0299-1.

[141] A. Pereira, A. Candeias, A. Cardoso, D. Rodrigues, P. Vandenabeele, A.T. Caldeira, Non-invasive methodology for the identification of plastic pieces in museum environment — a novel approach, Microchemical Journal 124 (2016) 846–855. https://doi.org/10.1016/j.microc.2015.07.027.

[142] B. Kemper, D.A. Lichtblau, Extraction of plasticizers: An entire and reproducible quantification method for historical cellulose acetate material, Polym Test 80 (2019) 106096. https://doi.org/10.1016/j.polymertesting.2019.106096.

[143] D. Saviello, L. Toniolo, S. Goidanich, F. Casadio, Non-invasive identification of plastic materials in museum collections with portable FTIR reflectance spectroscopy: Reference database and practical applications, Microchemical Journal 124 (2016) 868–877. https://doi.org/10.1016/j.microc.2015.07.016.

[144] M. Himmelsbach, W. Buchberger, E. Reingruber, Determination of polymer additives by liquid chromatography coupled with mass spectrometry. A comparison of atmospheric pressure photoionization (APPI), atmospheric pressure chemical ionization (APCI), and electrospray ionization (ESI), Polym Degrad Stab 94 (2009) 1213–1219. https://doi.org/10.1016/j.polymdegradstab.2009.04.021.

[145] V.P. Sica, K.L. Krivos, D.E. Kiehl, C.J. Pulliam, I.D. Henry, T.R. Baker, The role of mass spectrometry and related techniques in the analysis of extractable

and leachable chemicals, Mass Spectrom Rev 39 (2020) 212–226. https://doi.org/10.1002/mas.21591.

[146] C.E. Bernard, M.R. Berry, L.J. Wymer, L.J. Melnyk, Sampling household surfaces for pesticide residues: Comparison between a Press Sampler and solvent-moistened wipes, Science of the Total Environment 389 (2008). https://doi.org/10.1016/j.scitotenv.2007.08.044.

[147] H.V. Andersen, L. Gunnarsen, L.E. Knudsen, M. Frederiksen, PCB in air, dust and surface wipes in 73 Danish homes, Int J Hyg Environ Health 229 (2020). https://doi.org/10.1016/j.ijheh.2019.113429.

[148] S. Billets, A Literature Review of Wipe Sampling Methods for Chemical Warfare Agents and Toxic, U.S. Environmental Protection Agency, Washington DC. (2007) 56.

[149] J. Cettier, M.L. Bayle, R. Béranger, E. Billoir, J.R. Nuckols, B. Combourieu, B. Fervers, Efficiency of wipe sampling on hard surfaces for pesticides and PCB residues in dust, Science of the Total Environment 505 (2015). https://doi.org/10.1016/j.scitotenv.2014.09.086.

[150] S.A. Willison, I.I. Daniel Stout, A. Mysz, J. Starr, D. Tabor, B. Wyrzykowska-Ceradini, J. Nardin, E. Morris, E.G. Snyder, The impact of wipe sampling variables on method performance associated with indoor pesticide misuse and highly contaminated areas, Science of the Total Environment 655 (2019) 539–546. https://doi.org/10.1016/j.scitotenv.2018.11.128.

[151] M. Xie, Y. Wu, J.C. Little, L.C. Marr, Phthalates and alternative plasticizers and potential for contact exposure from children's backpacks and toys, J Expo Sci Environ Epidemiol 26 (2016) 119–124. https://doi.org/10.1038/jes.2015.71.

[152] P.A. Clausen, S. Spaan, D.H. Brouwer, H. Marquart, M. Le Feber, R. Engel, L. Geerts, K.A. Jensen, V. Kofoed-Sørensen, B. Hansen, K. De Brouwere, Experimental estimation of migration and transfer of organic substances from consumer articles to cotton wipes: Evaluation of underlying mechanisms, J Expo Sci Environ Epidemiol 26 (2016) 104–112. https://doi.org/10.1038/jes.2015.35.

[153] Q. Wang, B.K. Storm, Separation and analysis of low molecular weight plasticizers in poly(vinyl chloride) tubes, Polym Test 24 (2005) 290–300. https://doi.org/10.1016/J.POLYMERTESTING.2004.12.002.

[154] S. Genay, F. Feutry, M. Masse, C. Barthélémy, V. Sautou, P. Odou, B. Décaudin, N. Azaroual, Identification and quantification by 1H nuclear magnetic resonance spectroscopy of seven plasticizers in PVC medical devices, Anal Bioanal Chem 409 (2017) 1271–1280. https://doi.org/10.1007/s00216-016-0053-4.

[155] T. Radaniel, S. Genay, N. Simon, F. Feutry, F. Quagliozzi, C. Barthélémy, M. Lecoeur, V. Sautou, B. Décaudin, P. Odou, L. Bernard, D. Bourdeaux, P. Chennell, D. Richard, B. Pereira, V. Sautou, N. Azaroual, Christine Barthélémy, B. Décaudin, T. Dine, F. Feutry, S. Genay, N. Kambia, M. Lecoeur, P. Odou, N. Simon, C. Vaccher, R. Cueff, E. Feschet, C. Breysse, Quantification of five plasticizers used in PVC tubing through high performance

liquid chromatographic-UV detection, J Chromatogr B Analyt Technol Biomed Life Sci 965 (2014) 158–163. https://doi.org/10.1016/j.jchromb.2014.06.027.

[156] J. Mazurek, A. Laganà, V. Dion, S. Etyemez, C. Carta, M.R. Schilling, Investigation of cellulose nitrate and cellulose acetate plastics in museum collections using ion chromatography and size exclusion chromatography, J Cult Herit 35 (2019) 263–270. https://doi.org/10.1016/j.culher.2018.05.011.

[157] B. Kemper, D.A. Lichtblau, Extraction of plasticizers: An entire and reproducible quantification method for historical cellulose acetate material, Polym Test 80 (2019) 106096. https://doi.org/10.1016/j.polymertesting.2019.106096.

[158] S. Da Ros, A.E. Aliev, I. del Gaudio, R. King, A. Pokorska, M. Kearney, K. Curran, Characterising plasticised cellulose acetate-based historic artefacts by NMR spectroscopy: A new approach for quantifying the degree of substitution and diethyl phthalate contents, Polym Degrad Stab 183 (2021) 109420. https://doi.org/10.1016/j.polymdegradstab.2020.109420.

[159] K. Sutherland, C. Schwarzinger, B.A. Price, The application of pyrolysis gas chromatography mass spectrometry for the identification of degraded early plastics in a sculpture by Naum Gabo, J Anal Appl Pyrolysis 94 (2012) 202–208. https://doi.org/10.1016/j.jaap.2011.12.016.

[160] L. Castle, S.M. Jickells, J. Nichol, S.M. Johns, J.W. Gramshaw, Determination of high- and low-molecular-mass plasticisers in stretch-type packaging films, J Chromatogr A 675 (1994) 261–266. https://doi.org/10.1016/0021-9673(94)85283-9.

[161] C.H. Dong, Y.F. Liu, W.F. Yang, X.L. Sun, G.Q. Wang, Simultaneous determination of phthalate plasticizers in PVC packaging materials using homogeneous-ultrasonic extraction-GC-MS assisted with continuous wavelet transform, Analytical Methods 5 (2013) 4513–4517. https://doi.org/10.1039/C3AY40574E.

[162] P. Gimeno, S. Thomas, C. Bousquet, A.F. Maggio, C. Civade, C. Brenier, P.A. Bonnet, Identification and quantification of 14 phthalates and 5 non-phthalate plasticizers in PVC medical devices by GC–MS, Journal of Chromatography B 949–950 (2014) 99–108. https://doi.org/10.1016/J.JCHROMB.2013.12.037.

[163] M. Driffield, E. Bradley, L. Castle, A. Lloyd, M. Parmar, D. Speck, D. Roberts, S. Stead, Use of atmospheric pressure solids analysis probe time-of-flight mass spectrometry to screen for plasticisers in gaskets used in contact with foods, Rapid Communications in Mass Spectrometry 29 (2015) 1603–1610. https://doi.org/10.1002/RCM.7255.

[164] S. Schulz, S. Wagner, S. Gerbig, H. Wächter, D. Sielaff, D. Bohn, B. Spengler, DESI MS based screening method for phthalates in consumer goods, Analyst 140 (2015) 3484–3491. https://doi.org/10.1039/C5AN00338E.

[165] F. Lotz, P. Baar, B. Spengler, S. Schulz, Development of a handheld liquid extraction pen for on-site mass spectrometric analysis of daily goods, Analyst 146 (2021) 3004–3015. https://doi.org/10.1039/D0AN02281K.

[166] T. Rothenbacher, W. Schwack, Rapid and nondestructive analysis of phthalic acid esters in toys made of poly(vinyl chloride) by direct analysis in real time

single-quadrupole mass spectrometry, Rapid Communications in Mass Spectrometry 23 (2009) 2829–2835. https://doi.org/10.1002/RCM.4194.

[167] R. Zhang, Y. Yue, R. Hua, W. Yan, Factors affecting the separation of phthalate esters, and their analysis, by HPTLC, Journal of Planar Chromatography - Modern TLC 20 (2007) 321–326. https://doi.org/10.1556/JPC.20.2007.5.2.

[168] E. Dytkiewitz, W. Schwack, Quantification of plasticizers in poly(vinyl chloride) commodities by high-performance thin-layer chromatography, Journal of Planar Chromatography - Modern TLC 25 (2012) 238–243. https://doi.org/10.1556/JPC.25.2012.3.9.

[169] W. Burns, The chromatographic behaviour of the commoner ester type plasticisers, Journal of Applied Chemistry 5 (2007) 599–609. https://doi.org/10.1002/jctb.5010051103.

[170] W.A. Foreman, D.R. Paulson, Partial Analysis of Vinyl-Asbestos Floor Tile A tic experiment for beginning organic chemistry, J Chem Educ 49 (1972) 572–573. https://pubs.acs.org/sharingguidelines (accessed April 14, 2022).

[171] J.W. Copius Peereboom, The analysis of plasticizers by micro-adsorption chromatography, J Chromatogr A 4 (1960) 323–328. https://doi.org/10.1016/S0021-9673(01)98409-2.

[172] L. Fishbein, P.W. Albro, Chromatographic and biological aspects of the phthalate esters, J Chromatogr A 70 (1972) 365–412. https://doi.org/10.1016/S0021-9673(00)92702-X.

[173] J. Bloom, Application des chromatographies sur couche mince et gaz-liquide à l'analyse qualitative et quantitative des esters des acides aliphatiques dicarboxyliques, J Chromatogr A 115 (1975) 570–580. https://doi.org/10.1016/S0021-9673(01)98961-7.

[174] M. Swiatecka, H. Zowall, IDENTIFICATION OF PLASTICIZERS IN PLASTICS BY THIN-LAYER CHROMATOGRAPHY : SWIATECKA, M. (Translated by NASA Technical Translation), Polimery 14 (1969) 165–166. https://archive.org/details/nasa_techdoc_19720006940 (accessed April 13, 2022).

[175] J. Nematollahi, W.L. Guess, J. Autian, Plasticizers in medical application I Analysis and toxicity evaluation of dialkyl benzenedicarboxylates, J Pharm Sci 56 (1967) 1446–1453. https://doi.org/10.1002/jps.2600561115.

[176] R. Takeshita, H. Yoshida, Separation of Phthalate Esters by Thin-Layer Chromatography Using Polyamide, Eisei Kagaku 23 (1977) 383–387. https://doi.org/10.1248/jhs1956.23.383.

[177] H. van Bekkum, H.M.A. Buurmans, B.M. Wepster, A.M. van Wijk, Ester hydrolysis in concentrated sulfuric acid, Recueil Des Travaux Chimiques Des Pays-Bas 88 (1969) 301–306. https://doi.org/10.1002/RECL.19690880307.

[178] D.Y. Maeng, V.F. McNeill, Kinetics of alkaline hydrolysis of synthetic organic esters, Int J Chem Kinet 54 (2022) 218–222. https://doi.org/10.1002/KIN.21552.

[179] D.A. Nelson, TLC detection of phthalate esters with anisaldehyde and Dragendorff reagents, Anal Biochem 29 (1969) 171–173. https://doi.org/10.1016/0003-2697(69)90022-0.

[180] S. Levinson, Detection of Diethylphthalate, Ind Eng Chem 17 (1925) 929. https://doi.org/10.1021/IE50189A019.

[181] J.A. Handy, L.F. Hoyt, Diethylphthalate IV, The Journal of the American Pharmaceutical Association (1912) 15 (1926) 454–461. https://doi.org/10.1002/JPS.3080150608.

[182] C. Guinn Barr, Investigations on the fluorometric determination of malic and succinic acids in apple tissue, Plant Physiol 23 (1948) 443–454.

[183] C.E. Frohman, J.M. Orten, THE FLUOROMETRIC DETERMINATION OF POLYCAR-BOXYLIC ACIDS FOLLOWING CHROMATOGRAPHY, Journal of Biological Chemistry 205 (1953) 717–723.

[184] T. Takahashi, K. Sakaguchi, On Colour Reactions of Dibasic Acids of Fatty Series, Especially of Fumaric Acid, Bulletin of the Agricultural Chemical Society of Japan 2 (1926) 97–101. https://doi.org/10.1080/03758397.1926.10856784.

[185] Personal communication with APC Pure supplier, (2022).

[186] T.C.J. Ovenston, A scheme for the chromatographic examination of propellant explosives, Analyst 74 (1949) 344–351. https://doi.org/10.1039/AN9497400344.

[187] Stains for Developing TLC Plates, n.d. https://www.chemistry.mcmaster.ca/adronov/resources/Stains_for_Developing_TLC_Plates.pdf (accessed July 7, 2022).

[188] S.K. Bharti, R. Roy, Quantitative 1H NMR spectroscopy, TrAC Trends in Analytical Chemistry 35 (2012) 5–26. https://doi.org/10.1016/J.TRAC.2012.02.007.

[189] ICH Topic Q 2 (R1) Validation of Analytical Procedures: Text and Methodology Step 5, (1995). http://www.emea.eu.int (accessed June 29, 2022).

[190] T. Schoenberger, Guideline for qNMR analysis, 2020. https://enfsi.eu/wp-content/uploads/2017/06/qNMR-Guideline_version001.pdf (accessed June 29, 2022).

[191] Y. Lee, Y. Matviychuk, B. Bogun, C.S. Johnson, D.J. Holland, Quantification of mixtures of analogues of illicit substances by benchtop NMR spectroscopy, Journal of Magnetic Resonance 335 (2022). https://doi.org/10.1016/j.jmr.2021.107138.

[192] L. Sassu, S. Puligheddu, C. Puligheddu, S. Palomba, E. Muru, C. Mattia, C. Allevi, Application of benchtop low-field NMR spectrometers in the refining industry: A multivariate calibration approach for rapid characterization of crude oils, Magnetic Resonance in Chemistry 58 (2020). https://doi.org/10.1002/mrc.5093.

[193] S.L. Draper, E.R. McCarney, Benchtop nuclear magnetic resonance spectroscopy in forensic chemistry, Magnetic Resonance in Chemistry (2021). https://doi.org/10.1002/mrc.5197.

[194] H.Y. Yu, S. Myoung, S. Ahn, Recent applications of benchtop nuclear magnetic resonance spectroscopy, Magnetochemistry 7 (2021). https://doi.org/10.3390/magnetochemistry7090121.

[195] P.H.J. Keizers, F. Bakker, J. Ferreira, P.F.K. Wackers, D. van Kollenburg, E. van der Aa, A. van Beers, Benchtop NMR spectroscopy in the analysis of substandard and falsified medicines as well as illegal drugs, J Pharm Biomed Anal 178 (2020). https://doi.org/10.1016/j.jpba.2019.112939.

[196] T.A. van Beek, Low-field benchtop NMR spectroscopy: status and prospects in natural product analysis, Phytochemical Analysis (2020) 1–14. https://doi.org/10.1002/pca.2921.

[197] M. Grootveld, B. Percival, M. Gibson, Y. Osman, M. Edgar, M. Molinari, M.L. Mather, F. Casanova, P.B. Wilson, Progress in low-field benchtop NMR spectroscopy in chemical and biochemical analysis, Anal Chim Acta (2019). https://doi.org/10.1016/j.aca.2019.02.026.

[198] B.C. Percival, M. Grootveld, M. Gibson, Y. Osman, M. Molinari, F. Jafari, T. Sahota, M. Martin, F. Casanova, M.L. Mather, M. Edgar, J. Masania, P.B. Wilson, Low-field, benchtop NMR spectroscopy as a potential tool for point-of-care diagnostics of metabolic conditions: Validation, protocols and computational models, 2019. https://doi.org/10.3390/ht8010002.

[199] J.F. Araneda, T. Mendonça Barbosa, P. Hui, M.C. Leclerc, J. Ma, A.F.G. Maier, S.D. Riegel, Incorporating Benchtop NMR Spectrometers in the Undergraduate Lab: Understanding Resolution and Circumventing Second-

Order Effects, J Chem Educ 98 (2021). https://doi.org/10.1021/acs.jchemed.0c01182.

[200] S.K. Bharti, R. Roy, Quantitative 1H NMR spectroscopy, TrAC - Trends in Analytical Chemistry 35 (2012) 5–26. https://doi.org/10.1016/j.trac.2012.02.007.

[201] Y. Lee, Y. Matviychuk, D.J. Holland, Quantitative analysis using external standards with a benchtop NMR spectrometer, Journal of Magnetic Resonance (2020). https://doi.org/10.1016/j.jmr.2020.106826.

[202] B. Gouilleux, B. Charrier, S. Akoka, P. Giraudeau, Gradient-based solvent suppression methods on a benchtop spectrometer, Magnetic Resonance in Chemistry (2017). https://doi.org/10.1002/mrc.4493.

[203] G. Assemat, B. Gouilleux, D. Bouillaud, J. Farjon, V. Gilard, P. Giraudeau, M. Malet-Martino, Diffusion-ordered spectroscopy on a benchtop spectrometer for drug analysis, J Pharm Biomed Anal 160 (2018) 268–275. https://doi.org/10.1016/j.jpba.2018.08.011.

[204] K. Hatada, T. Kitayama, K. Ute, Application of High-Resolution NMR Spectroscopy to Polymer Chemistry, Annu Rep NMR Spectrosc 26 (1993) 99–210. https://doi.org/10.1016/S0066-4103(08)60059-9.

[205] J. King, D.I. Bower, W.F. Maddams, H. Pyszora, The measurement of the tacticity of poly(vinyl chloride) by 13C nuclear magnetic resonance spectroscopy, Die Makromolekulare Chemie 184 (1983) 879–891. https://doi.org/10.1002/MACP.1983.021840421.

[206] P. D'Antuono, E. Botek, B. Champagne, J. Wieme, M.F. Reyniers, G.B. Marin, P.J. Adriaensens, J.M. Gelan, A joined theoretical-experimental investigation on the1H and13C NMR signatures of defects in poly(vinyl chloride), Journal of Physical Chemistry B 112 (2008) 14804–14818. https://doi.org/10.1021/JP805676Q.

[207] B. Blümich, Low-field and benchtop NMR, Journal of Magnetic Resonance (2019). https://doi.org/10.1016/j.jmr.2019.07.030.

[208] J. Rönnols, E. Danieli, H. Freichels, F. Aldaeus, Lignin analysis with benchtop NMR spectroscopy, Holzforschung 74 (2020) 226–231. https://doi.org/10.1515/hf-2018-0282.

[209] M. Schilling, M. Bouchard, H. Khanjian, T. Learner, A. Phenix, R. Rivenc, Application of chemical and thermal analysis methods for studying cellulose ester plastics., Acc Chem Res 43 (2010) 888–896. https://doi.org/10.1021/ar1000132.

[210] H. Kono, H. Hashimoto, Y. Shimizu, NMR characterization of cellulose acetate: Chemical shift assignments, substituent effects, and chemical shift additivity, Carbohydr Polym 118 (2015) 91–100. https://doi.org/10.1016/j.carbpol.2014.11.004.

[211] H. Kono, C. Oka, R. Kishimoto, S. Fujita, NMR characterization of cellulose acetate: Mole fraction of monomers in cellulose acetate determined from carbonyl carbon resonances, Carbohydr Polym 170 (2017) 23–32. https://doi.org/10.1016/j.carbpol.2017.04.061.

[212] S. Genay, F. Feutry, M. Masse, C. Barthélémy, V. Sautou, P. Odou, B. Décaudin, N. Azaroual, Identification and quantification by 1H nuclear magnetic resonance spectroscopy of seven plasticizers in PVC medical devices, Anal Bioanal Chem 409 (2017) 1271–1280. https://doi.org/10.1007/s00216-016-0053-4.

[213] A. Duchowny, A. Adams, Compact NMR spectroscopy for low-cost identification and quantification of PVC plasticizers, Molecules 26 (2021). https://doi.org/10.3390/molecules26051221.

[214] G. Dal Poggetto, L. Castañar, R.W. Adams, G.A. Morris, M. Nilsson, Relaxation-encoded NMR experiments for mixture analysis: REST and beer, Chemical Communications 53 (2017) 7461–7464. https://doi.org/10.1039/C7CC03150E.

[215] D.A. Jayawickrama, C.K. Larive, E.F. McCord, D.C. Roe, Polymer additives mixture analysis using pulsed-field gradient NMR spectroscopy, Magnetic Resonance in Chemistry 36 (1998) 755–760. https://doi.org/10.1002/(SICI)1097-458X(1998100)36:10<755::AID-OMR362>3.0.CO;2-O.

[216] G. Dal Poggetto, L. Castanar, R.W. Adams, G.A. Morris, M. Nilsson, Dissect and Divide: Putting NMR Spectra of Mixtures under the Knife, J Am Chem Soc 141 (2019). https://doi.org/10.1021/jacs.8b13290.

[217] P.G. Takis, P.G. Takis, B. Jiménez, B. Jiménez, C.J. Sands, C.J. Sands, E. Chekmeneva, E. Chekmeneva, M.R. Lewis, M.R. Lewis, SMolESY: An efficient and quantitative alternative to on-instrument macromolecular 1H-NMR signal

suppression, Chem Sci 11 (2020) 6000–6011. https://doi.org/10.1039/d0sc01421d.

[218] G. Mitchell, F. France, A. Nordon, P.L. Tang, L.T. Gibson, Assessment of historical polymers using attenuated total reflectance-Fourier transform infrared spectroscopy with principal component analysis, Herit Sci 1 (2013) 1–10. https://doi.org/10.1186/2050-7445-1-28.

[219] P. Peets, K. Kaupmees, S. Vahur, I. Leito, Reflectance FT-IR spectroscopy as a viable option for textile fiber identification, Herit Sci 7 (2019). https://doi.org/10.1186/s40494-019-0337-z.

[220] C. Cucci, G. Bartolozzi, V. Marchiafava, M. Picollo, E. Richardson, Study of semi-synthetic plastic objects of historic interest using non-invasive total reflectance FT-IR, Microchemical Journal 124 (2016) 889–897. https://doi.org/10.1016/j.microc.2015.06.010.

[221] E.M. Angelin, S.F. de Sá, I. Soares, M.E. Callapez, J.L. Ferreira, M.J. Melo, M. Bacci, M. Picollo, Application of Infrared Reflectance Spectroscopy on Plastics in Cultural Heritage Collections: A Comparative Assessment of Two Portable Mid-Fourier Transform Infrared Reflection Devices, Appl Spectrosc 75 (2021) 818–833. https://doi.org/10.1177/0003702821998777.

[222] J. Bell, P. Nel, B. Stuart, Non-invasive identification of polymers in cultural heritage collections: evaluation, optimisation and application of portable FTIR (ATR and external reflectance) spectroscopy to three-dimensional polymer-based objects, Herit Sci 7 (2019) 1–18. https://doi.org/10.1186/S40494-019-0336-0/TABLES/7.

[223] D. Saviello, L. Toniolo, S. Goidanich, F. Casadio, Non-invasive identification of plastic materials in museum collections with portable FTIR reflectance spectroscopy: Reference database and practical applications, Microchemical Journal 124 (2016) 868–877. https://doi.org/10.1016/j.microc.2015.07.016.

[224] B. Lavédrine, A. Fournier, G. Martin, Preservation of plastic artefacts in museum collections, CTHS, Paris (2012).

[225] C. van Aubel, L. Beerkens, A. Boelens, K. te Brake-Baldock, A. Brokerhof, S. de Groot, P. ’t Hoen, H. van Keulen, T. van Oosten, O. van Rooijen, T. Scholte, Plastic Identification Tool, (2019). https://plastic-en.tool.cultureelerfgoed.nl/ (accessed July 9, 2023).

[226] F. Rosi, C. Miliani, P. Gardner, A. Chieli, A. Romani, M. Ciabatta, R. Trevisan, B. Ferriani, E. Richardson, L. Cartechini, Unveiling the composition of historical plastics through non-invasive reflection FT-IR spectroscopy in the extended near- and mid-Infrared spectral range, Anal Chim Acta 1169 (2021) 338602. https://doi.org/10.1016/J.ACA.2021.338602.

[227] M. Picollo, G. Bartolozzi, C. Cucci, M. Galeotti, V. Marchiafava, B. Pizzo, Comparative Study of Fourier Transform Infrared Spectroscopy in Transmission, Attenuated Total Reflection, and Total Reflection Modes for the Analysis of Plastics in the Cultural Heritage Field, Appl Spectrosc 68 (2014) 389–397. https://doi.org/10.1366/13-07199.

[228] F. Rosi, C. Miliani, P. Gardner, A. Chieli, A. Romani, M. Ciabatta, R. Trevisan, B. Ferriani, E. Richardson, L. Cartechini, Unveiling the composition of historical plastics through non-invasive reflection FT-IR spectroscopy in the extended

near- and mid-Infrared spectral range, Anal Chim Acta 1169 (2021) 338602. https://doi.org/10.1016/J.ACA.2021.338602.

[229] H. Al Salloum, J. Saunier, A. Dazzi, J. Vigneron, A. Etcheberry, C. Marlière, C. Aymes-Chodur, J.M. Herry, M. Bernard, E. Jubeli, N. Yagoubi, Characterization of the surface physico-chemistry of plasticized PVC used in blood bag and infusion tubing, Materials Science and Engineering: C 75 (2017) 317–334. https://doi.org/10.1016/J.MSEC.2017.02.057.

[230] A. Vichi, G. Eliazyan, S.G. Kazarian, Study of the Degradation and Conservation of Historical Leather Book Covers with Macro Attenuated Total Reflection-Fourier Transform Infrared Spectroscopic Imaging, ACS Omega 3 (2018) 7150–7157. https://doi.org/10.1021/acsomega.8b00773.

[231] K.S. Irvin, J.H. Potgieter, C. Liauw, R. Sparkes, S. Potgieter-Vermaak, The quantification of di-octyl terephthalate and calcium carbonate in polyvinyl chloride using Fourier transform-infrared and Raman spectroscopy, J Appl Polym Sci 139 (2022). https://doi.org/10.1002/app.52372.

[232] A. V Ewing, S.G. Kazarian, Recent advances in the applications of vibrational spectroscopic imaging and mapping to pharmaceutical formulations, Spectrochim Acta A Mol Biomol Spectrosc 197 (2018) 10–29. https://linkinghub.elsevier.com/retrieve/pii/S1386142517310296.

[233] M. BELTRÁN, A. MARCILLA, FOURIER TRANSFORM INFRARED SPECTROSCOPY APPLIED TO THE STUDY OF PVC DECOMPOSITION, Eur Polym J 33 (1997) 1135–1142. https://doi.org/10.1016/S0014-3057(97)00001-3.

[234] D.L. Tabb, J.L. Koenig, Fourier Transform Infrared Study of Plasticized and Unplasticized Poly(vinyl chloride), Macromolecules 8 (1975) 929–934. https://doi.org/10.1021/ma60048a043.

[235] N. González, M.J. Fernández-Berridi, Application of Fourier transform infrared spectroscopy in the study of interactions between PVC and plasticizers: PVC/plasticizer compatibility versus chemical structure of plasticizer, J Appl Polym Sci 101 (2006) 1731–1737. https://doi.org/10.1002/APP.23381.

[236] N. González, M.J. Fernández-Berridi, Fourier transform infrared spectroscopy in the study of the interaction between PVC and plasticizers: PVC/plasticizer compatibility, J Appl Polym Sci 107 (2008) 1294–1300. https://doi.org/10.1002/APP.26651.

[237] K. Burns, J.H. Potgieter, S. Potgieter-Vermaak, I.D.V. Ingram, C.M. Liauw, A comparative assessment of the use of suitable analytical techniques to evaluate plasticizer compatibility, J Appl Polym Sci (2023). https://doi.org/10.1002/APP.54104.

[238] H. Lai, Z. Wang, P. Wu, B.I. Chaudhary, S.S. Sengupta, J.M. Cogen, B. Li, Structure and diffusion behavior of trioctyl trimellitate (TOTM) in PVC film studied by ATR-IR spectroscopy, Ind Eng Chem Res 51 (2012). https://doi.org/10.1021/ie300007m.

[239] N. Tokhadze, P. Chennell, L. Bernard, C. Lambert, B. Pereira, B. Mailhot-Jensen, V. Sautou, Impact of alternative materials to plasticized PVC infusion tubings on drug sorption and plasticizer release, Sci Rep 9 (2019). https://doi.org/10.1038/s41598-019-55113-x.

[240] T. Rijavec, D. Ribar, J. Markelj, M. Strlič, I. Kralj Cigić, Machine learning-assisted non-destructive plasticizer identification and quantification in historical PVC objects based on IR spectroscopy, Sci Rep 12 (2022). https://doi.org/10.1038/s41598-022-08862-1.

[241] O. Madden, G. Gordon, K.C. Cobb, A.M. Spencer, Depth profiling laminated glass with a fiber optic probe customized for adjustable working distance, Journal of Raman Spectroscopy 45 (2014) 1318–1321. https://doi.org/10.1002/jrs.4550.

[242] A. Neves, E.M. Angelin, É. Roldão, M.J. Melo, New insights into the degradation mechanism of cellulose nitrate in cinematographic films by Raman microscopy, Journal of Raman Spectroscopy 50 (2019) 202–212. https://doi.org/10.1002/jrs.5464.

[243] C. Paris, C. Coupry, Fourier transform Raman spectroscopic study of the first cellulose-based artificial materials in heritage, Journal of Raman Spectroscopy 36 (2005) 77–82. https://doi.org/10.1002/jrs.1288.

[244] O. Madden, K.C. Cobb, A.M. Spencer, Raman spectroscopic characterization of laminated glass and transparent sheet plastics to amplify a history of early aviation “glass,” Journal of Raman Spectroscopy 45 (2014) 1215–1224. https://doi.org/10.1002/jrs.4618.

[245] O. Madden, K.C. Cobb, A.M. Spencer, Raman spectroscopic characterization of laminated glass and transparent sheet plastics to amplify a history of early aviation “glass,” Journal of Raman Spectroscopy 45 (2014) 1215–1224. https://doi.org/10.1002/jrs.4618.

[246] A. Klisińska-Kopacz, B. Łydżba-Kopczyńska, M. Czarnecka, T. Koźlecki, J. del Hoyo Mélendez, A. Mendys, A. Kłosowska-Klechowska, M. Obarzanowski, P. Frączek, Raman spectroscopy as a powerful technique for the identification of polymers used in cast sculptures from museum collections, Journal of Raman Spectroscopy 50 (2019) 213–221. https://doi.org/10.1002/jrs.5407.

[247] J. Moskowitz, K. Carlos, L. Lindahl-Ackerman, K.L. Reese, T. Begley, B.J. Yakes, Portable Raman Spectroscopy for Screening of Phthalate Plasticizers in Food Contact Production Line Tubing and Bottle Cap Gaskets, ACS Food Science and Technology (2022). https://doi.org/10.1021/ACSFOODSCITECH.2C00059/SUPPL_FILE/FS2C00059_SI_001.PDF.

[248] L. Cséfalvayová, M. Strlič, H. Karjalainen, L. Cséfalvayová, M. Strlič, H. Karjalainen, Quantitative NIR chemical imaging in heritage science, Anal Chem 83 (2011) 5101–5106. https://doi.org/10.1021/ac200986p.

[249] A. Adams, R. Kwamen, B. Woldt, M. Graß, Nondestructive Quantification of Local Plasticizer Concentration in PVC by 1H NMR Relaxometry, Macromol Rapid Commun 36 (2015) 2171–2175. https://doi.org/10.1002/marc.201500409.

[250] A. V. Ewing, S.G. Kazarian, Recent advances in the applications of vibrational spectroscopic imaging and mapping to pharmaceutical formulations, Spectrochim Acta A Mol Biomol Spectrosc 197 (2018) 10–29.

[251] D. Caballero, M. Bevilacqua, J.M. Amigo, Application of hyperspectral imaging and chemometrics for classifying plastics with brominated flame retardants, Journal of Spectral Imaging 8 (2019). https://doi.org/10.1255/jsi.2019.a1.

[252] N.B. Joshi, D.E. Hirt, Evaluating bulk-to-surface partitioning of erucamide in LLDPE films using FT-IR microspectroscopy, Appl Spectrosc 53 (1999) 11–16. https://doi.org/10.1366/0003702991945380.

[253] G. Geertz, R. Brüll, J. Wieser, R. Maria, M. Wenzel, K. Engelsing, J. Wüst, M. Bastian, M. Rudschuck, Stabiliser diffusion in long-term pressure tested polypropylene pipes analysed by IR microscopy, Polym Degrad Stab 94 (2009) 1092–1102. https://doi.org/10.1016/j.polymdegradstab.2009.03.020.

[254] R. Maria, K. Rode, R. Brüll, F. Dorbath, B. Baudrit, M. Bastian, E. Brendlé, Monitoring the influence of different weathering conditions on polyethylene pipes by IR-microscopy, Polym Degrad Stab 96 (2011) 1901–1910. https://doi.org/10.1016/j.polymdegradstab.2011.07.004.

[255] E. Joseph, C. Ricci, S.G. Kazarian, R. Mazzeo, S. Prati, M. Ioele, Macro-ATR-FT-IR spectroscopic imaging analysis of paint cross-sections, Vib Spectrosc 53 (2010) 274–278. https://doi.org/10.1016/j.vibspec.2010.04.006.

[256] A. Dazzi, C.B. Prater, AFM-IR: Technology and Applications in Nanoscale Infrared Spectroscopy and Chemical Imaging, Chem Rev 117 (2017) 5146–5173. https://doi.org/10.1021/acs.chemrev.6b00448.

[257] G. Lorenzetti, J. Striova, A. Zoppi, E.M. Castellucci, Confocal Raman microscopy for in depth analysis in the field of cultural heritage, in: J Mol

Struct, Elsevier, 2011: pp. 97–103. https://doi.org/10.1016/j.molstruc.2010.12.057.

[258] M. Mauricio-Iglesias, V. Guillard, N. Gontard, S. Peyron, Raman depth-profiling characterization of a migrant diffusion in a polymer, J Memb Sci 375 (2011) 165–171. https://doi.org/10.1016/j.memsci.2011.03.039.

[259] S. Sommer, M. Koch, A. Adams, Terahertz Time-Domain Spectroscopy of Plasticized Poly(vinyl chloride), Anal Chem 90 (2018) 2409–2413. https://doi.org/10.1021/acs.analchem.7b04548.

[260] G. Pastorelli, T. Trafela, P.F. Taday, A. Portieri, D. Lowe, K. Fukunaga, M. Strlič, Characterisation of historic plastics using terahertz time-domain spectroscopy and pulsed imaging, Anal Bioanal Chem 403 (2012) 1405–1414. https://doi.org/10.1007/s00216-012-5931-9.

[261] M. Sardashti, B.A. Baldwin, D.J. O'Donnell, NMR imaging of polyethylene pipes, J Polym Sci B Polym Phys 33 (1995) 571–576. https://doi.org/10.1002/polb.1995.090330405.

[262] L.A. Weisenberger, J.L. Koenig, NMR Imaging of Diffusion Processes in Polymers: Measurement of the Spatial Dependence of Solvent Mobility in Partially Swollen PMMA Rods, Macromolecules 23 (1990) 2445–2453. https://doi.org/10.1021/ma00211a007.

[263] S. Widmaier, W.I. Jung, K. Pfeffer, M. Pfeffer, O. Lutz, MRI and determination of T1 and T2 of solid polymers using a 1.5 T whole-body imager, Magn Reson Imaging 11 (1993) 733–737. https://doi.org/10.1016/0730-725X(93)90016-7.

[264] K. Punčochová, A. V. Ewing, M. Gajdošová, N. Sarvašová, S.G. Kazarian, J. Beránek, F. Štěpánek, Identifying the mechanisms of drug release from amorphous solid dispersions using MRI and ATR-FTIR spectroscopic imaging, Int J Pharm 483 (2015) 256–267. https://doi.org/10.1016/j.ijpharm.2015.02.035.

[265] S. Baumgartner, G. Lahajnar, A. Sepe, J. Kristl, Quantitative evaluation of polymer concentration profile during swelling of hydrophilic matrix tablets using 1H NMR and MRI methods, European Journal of Pharmaceutics and Biopharmaceutics 59 (2005) 299–306. https://doi.org/10.1016/j.ejpb.2004.08.010.

[266] B. Keneghan, A Survey of Synthetic Plastic and Rubber Objects in the Collections of the Victoria and Albert Museum, Museum Management and Curatorship 7775 (2007) 321–331. https://doi.org/10.1080/09647770101001903.

[267] N. Balcar, A. Lattuati-Derieux, A. Vila, Analysis of degradation products founds in surveys, in: Preservation of Plastic Artefacts in Museum Collections, 2012: pp. 302–308. http://popart-highlights.mnhn.fr/collection-survey/analysis-of-degradation-products-founds-in-surveys/index.html.

[268] K. Hoeyng, S. Etyemez, K. McCormick, M. Schilling, A. Phenix, Curling, ripples, dimples: Observations from a condition survey of animation cels, Studies in Conservation 61 (2016) 294–296. https://doi.org/10.1080/00393630.2016.1188615.

[269] M. Picollo, G. Bartolozzi, C. Cucci, M. Galeotti, V. Marchiafava, B. Pizzo, Analysis of degradation products founds in surveys, Appl Spectrosc 68 (2014) 389–397. https://doi.org/10.1366/13-07199.

[270] M. Hoerger, Participant dropout as a function of survey length in internet-mediated university studies: Implications for study design and voluntary participation in psychological research, Cyberpsychol Behav Soc Netw 13 (2010). https://doi.org/10.1089/cyber.2009.0445.

[271] Who we are - Plart Foundation, (n.d.). https://fondazioneplart.it/en/plart-foundation/ (accessed February 14, 2022).

[272] About us | Museum of Design in Plastics, (n.d.). https://www.modip.ac.uk/about (accessed February 14, 2022).

[273] M. Nelles, Icon 2019 Membership Survey Final Report, London, 2019.

[274] M. Nelles, Icon 2015 Membership Survey Full Report, London, 2016.

[275] A. Calmes, Practical Aspects of Plastics Found in Archives, Restaurator 13 (1992) 23–36. https://doi.org/10.1515/REST.1992.13.1.23/MACHINEREADABLECITATION/RIS.

[276] C. Chu, P. Nel, Plastics in Australian Archives: An Industry Survey Regarding Prevalence, Condition, and Preservation Strategies, Studies in Conservation (2021). https://doi.org/10.1080/00393630.2021.1996093.

[277] S. Burslem, H. Ellory-van Dekker, M. Downing, R. Parkinson, J. Stirling, T. Szrajber, H. Worthy, British Museum Object Names Thesaurus, (1999).

https://terminology.collectionstrust.org.uk/British-Museum-objects/ (accessed March 10, 2024).

[278] British Standards Institute, PD 5454:2012 Publication Guide for the storage and exhibition of archival, (2012) 68.

[279] Library of Congress, Care, Handling, and Storage of Motion Picture Film, (n.d.). https://www.loc.gov/preservation/care/film.html#Storage (accessed March 10, 2024).

[280] S. Williams, Care of Objects Made from Rubber and Plastic - Canadian Conservation Institute (CCI) Notes 15/1, CCI Notes (2015).

[281] K. Curran, M. Underhill, J. Grau-Bové, T. Fearn, L.T. Gibson, M. Strlič, Classifying Degraded Modern Polymeric Museum Artefacts by Their Smell, Angewandte Chemie International Edition 57 (2018) 7336–7340. https://doi.org/10.1002/anie.201712278.

[282] G. Bartolozzi, C. Cucci, V. Marchiafava, M. Picollo, S. Lorenzo, PolIReS IFAC-CNR - Polimers Infrared Reflectance Spectra database, (n.d.). https://spectradb.ifac.cnr.it/polires/ (accessed May 31, 2023).

[283] S. Primpke, M. Wirth, C. Lorenz, G. Gerdts, Reference database design for the automated analysis of microplastic samples based on Fourier transform infrared (FTIR) spectroscopy, Anal Bioanal Chem 410 (2018) 5131–5141. https://doi.org/10.1007/S00216-018-1156-X/FIGURES/6.

[284] H. De Frond, R. Rubinovitz, C.M. Rochman, μATR-FTIR Spectral Libraries of Plastic Particles (FLOPP and FLOPP-e) for the Analysis of Microplastics, Anal

Chem 93 (2021) 15878–15885. https://doi.org/10.1021/acs.analchem.1c02549.

[285] I. del Gaudio, E. Hunter-Sellars, I.P. Parkin, D. Williams, S. da Ros, K. Curran, Water sorption and diffusion in cellulose acetate: The effect of plasticisers, Carbohydr Polym 267 (2021) 118185. https://doi.org/10.1016/J.CARBPOL.2021.118185.

[286] A.M. Abdelghany, M.S. Meikhail, N. Asker, Synthesis and structural-biological correlation of PVC\PVAc polymer blends, Journal of Materials Research and Technology 8 (2019) 3908–3916. https://doi.org/10.1016/j.jmrt.2019.06.053.

[287] C. van Aubel, Identification of plastics by looking, touching and smelling - V&A Blog, V&A Conservation Journal (2017) 16–17. https://www.vam.ac.uk/blog/caring-for-our-collections/identification-of-plastics-by-looking-touching-and-smelling.

[288] C. van Aubel, O. van Rooijen, Plastic Identification Tool, (2019). https://plastic-en.tool.cultureelerfgoed.nl/ (accessed March 19, 2023).

[289] D.O. Hummel, Atlas of Plastics Additives, Springer Berlin Heidelberg, Berlin, Heidelberg, 2002. https://doi.org/10.1007/978-3-642-56211-2.

[290] J. Du, E. Diaz, M. Carl, W. Bae, C.B. Chung, G.M. Bydder, Ultrashort echo time imaging with bicomponent analysis, Magn Reson Med 67 (2012) 645–649. https://doi.org/10.1002/mrm.23047.

[291] O. Jolliet, L. Huang, P. Hou, P. Fantke, High Throughput Risk and Impact Screening of Chemicals in Consumer Products, Risk Analysis 41 (2021) 627–644. https://doi.org/10.1111/RISA.13604.

[292] M. Al-Natsheh, M. Alawi, M. Fayyad, I. Tarawneh, Simultaneous GC–MS determination of eight phthalates in total and migrated portions of plasticized polymeric toys and childcare articles, Journal of Chromatography B 985 (2015) 103–109. https://doi.org/10.1016/J.JCHROMB.2015.01.010.

[293] L. Bernard, R. Cueff, D. Bourdeaux, C. Breysse, V. Sautou, Analysis of plasticizers in poly(vinyl chloride) medical devices for infusion and artificial nutrition: comparison and optimization of the extraction procedures, a pre-migration test step, Anal Bioanal Chem 407 (2015) 1651–1659. https://doi.org/10.1007/s00216-014-8426-z.

[294] L. Bernard, D. Bourdeaux, B. Pereira, N. Azaroual, C. Barthélémy, C. Breysse, P. Chennell, R. Cueff, T. Dine, T. Eljezi, F. Feutry, S. Genay, N. Kambia, M. Lecoeur, M. Masse, P. Odou, T. Radaniel, N. Simon, C. Vaccher, C. Verlhac, M. Yessaad, B. Décaudin, V. Sautou, Analysis of plasticizers in PVC medical devices: Performance comparison of eight analytical methods, Talanta 162 (2017) 604–611. https://doi.org/10.1016/j.talanta.2016.10.033.

[295] Ministry of Environment and Food, Survey and health assessment of phthalates in toys and other products for children, Danish Environmental Protection Agency, 2015. https://www2.mst.dk/udgiv/publications/2015/06/978-87-93352-44-5.pdf (accessed March 10, 2024).

[296] T. Kawakami, K. Isama, A. Matsuoka, Analysis of phthalic acid diesters, monoester, and other plasticizers in polyvinyl chloride household products in Japan, Journal of Environmental Science and Health, Part A 46 (2011) 855–864. https://doi.org/10.1080/10934529.2011.579870.

[297] G. McCombie, S. Biedermann, G. Suter, M. Biedermann, Survey on plasticizers currently found in PVC toys on the Swiss market: Banned phthalates are only a minor concern, Http://Dx.Doi.Org/10.1080/10934529.2016.1274176 52 (2017) 491–496. https://doi.org/10.1080/10934529.2016.1274176.

[298] M. Dreyfus, Phthalates and Phthalate Substitutes in Children's Toys, (2010). https://www.cpsc.gov/s3fs-public/pdfs/blk_media_phthallab.pdf (accessed March 10, 2024).

[299] N. Mac Fhionnlaoich, S. Ibsen, L.A. Serrano, A. Taylor, R. Qi, S. Guldin, A Toolkit to Quantify Target Compounds in Thin-Layer-Chromatography Experiments, J Chem Educ 95 (2018) 2191–2196. https://doi.org/10.1021/acs.jchemed.8b00144.

[300] Bromothymol Blue solution Safety Data Sheet - Honeywell Fluka, (2017). https://lab.honeywell.com/sm/api/rc/documents/download/32822-100ML_SDS_GB_E?appId=7868&catNo=32822-100ML&matnr=10236471&lang=E&country=GB&type=SDS (accessed July 10, 2022).

[301] Bromothymol blue 0.05% in ethanol (20%) | VWR, (n.d.). https://uk.vwr.com/store/product/4642442/bromothymol-blue-0-05-in-ethanol-20 (accessed July 10, 2022).

[302] Summary of Key Physical data for Baker Analyzed HPLC Solvents, (n.d.). https://macro.lsu.edu/howto/solvents/Summary%20of%20Key%20Physical%20data%20for%20Baker%20Analyzed%20HPLC%20Solvents.htm (accessed July 15, 2022).

[303] Chapter 7 Thin-layer chromatography of polymers, in: Journal of Chromatography Library, Elsevier, 1983: pp. 361–413. https://doi.org/10.1016/S0301-4770(08)61042-8.

[304] N. Repina, O. Konovalova, D. Kalinin, D. Edamenko, Thin-layer chromatographic separation of a number of bile acids with mobile phases based on surfactants, JPC – Journal of Planar Chromatography – Modern TLC 33 (2020) 271–279. https://doi.org/10.1007/s00764-020-00034-z.

[305] P. Harmon, R. Otter, A review of common non-ortho-phthalate plasticizers for use in food contact materials, Food and Chemical Toxicology 164 (2022) 112984. https://doi.org/10.1016/j.fct.2022.112984.

7 Division of labour/ Author contribution statement

Dr Simoni Da Ros performed some of the work described in section 3.2.4. Dr Stephen Wastling operated the MRI instrument and analysed the data described in section 3.2.5.

8 Appendix

8.1 Additional sample information

	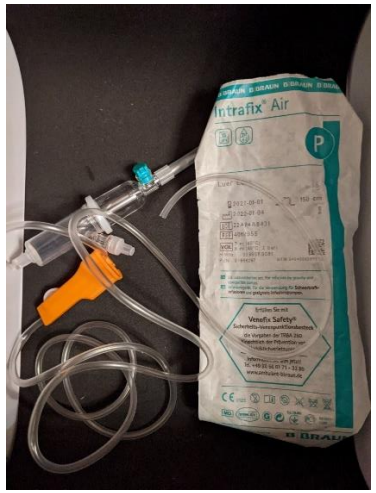		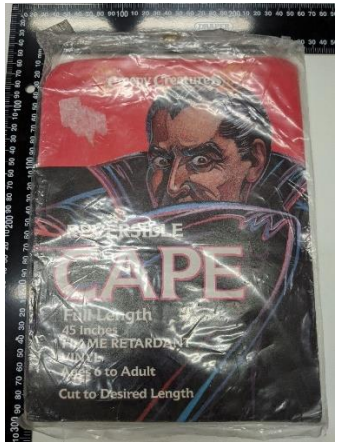	
BAL	**BBI**	**BBI**	**BLC & RDC**	**BLC & RDC**

				
COC	DOD	DOD	DOG	DOG

	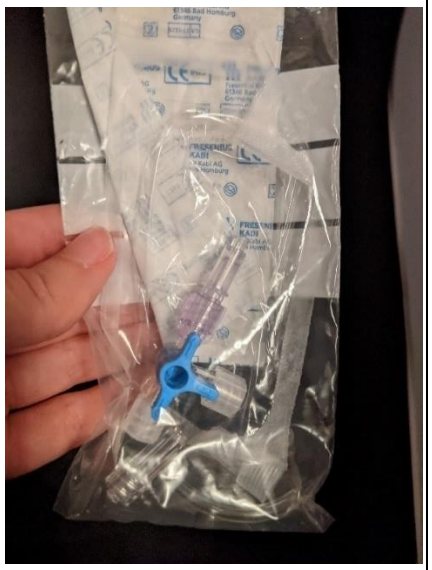		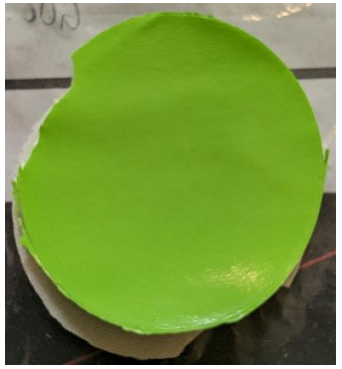	
ERA	FKB	FMO	GOC	GRG

			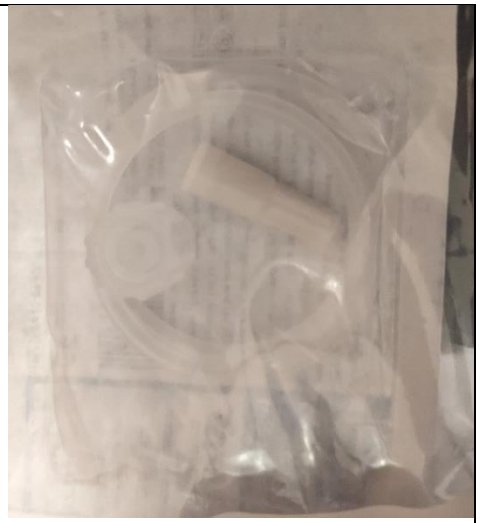
HEI	MCS	NIP	NIP

				
NOD	NOD	PEN	PEN	PHC

				
PIL	PIL	PNK	SNO	SNO

				
SUC	TBW	TCS	VYG	VYG

		 Boots vinyl toy designed for baby hands: soft, hygienic and washable ages 6-15 mths
WHD	YED	YED

8.2 Comparison of ATR-FTIR spectra to open-source polymer ATR-FTIR spectroscopy libraries.

Table 43 Comparison of ATR-FTIR spectra to open-source polymer ATR-FTIR spectroscopy libraries. Matches were quantified using Pearson's correlation coefficient (r). Correct matches are shown in bold.

Sample	spectra ID	Top match and correlation coefficient per ATR-FTIR spectroscopy library						Primpke 'other' match n.b. limited to solid polymers
		FLOPP-e	r %	FLOPP	r %	Primpke	r %	
BAL	balloon	PC	73.69	Rubber	95.24	PE	92.36	-
BBI	bbraun intrafix	**PVC**	59.46	PET	88.56	Other	88.14	epoxide_resin
DOD	donald inner	PP	67.41	**PVC**	98.18	Other	76.63	polyester_epoxide
	donald outer	**PVC**	74.98	**PVC**	94.1	PET	82.65	-
DOG	white dog inner	**PVC**	65.54	**PVC**	86.9	Other	80.88	poly(diallyl_isophthalate)
	white doll shoe inner cut	PP	65.77	**PVC**	94.62	Other	79.37	polyester_epoxide
	white doll shoe outer cut	**PVC**	72.65	**PVC**	94.52	Other	81.47	polyester_epoxide

ERA	eraser inner cut	PU	70.05	**PVC**	94.58	Other	72.15	vinyl_chloride_vinyl_acetate_hydroxy propyl_acrylate
FMO	white fimo	PU	69.97	Polyester	94.38	Other	86.28	vinyl_chloride_vinyl_acetate_hydroxy propyl_acrylate
GOC	green oil cloth cloth down	**PVC**	69.95	PU	94.44	PET	98.6	-
	green oil cloth pvc down	PU	74.75	PET	87.86	**PVC**	84.36	-
GRG	green giant inner cut	**PVC**	68.01	**PVC**	94.71	Other	82.99	vinyl_chloride_vinyl_acetate_hydroxy propyl_acrylate
	green giant mid	**PVC**	67.43	**PVC**	88.34	Other	82.88	vinyl_chloride_vinyl_acetate_hydroxy propyl_acrylate
	green giant outer cut	**PVC**	68.34	**PVC**	91.07	Other	82	vinyl_chloride_vinyl_acetate_hydroxy propyl_acrylate
HEI	heidelberger	**PVC**	58.43	**PVC**	92.8	Other	87.97	epoxide_resin

MCS	medium sheet outer	**PVC**	65.27	**PVC**	92.99	Other	83.61	vinyl_chloride_vinyl_acetate_hydroxy propyl_acrylate
NIP	nipro butterfly set	**PVC**	60.51	**PVC**	93.11	Other	83.79	vinyl_chloride_vinyl_acetate_hydroxy propyl_acrylate
NOD	noddy inner	**PVC**	65.82	PU	99.26	Other	87.4	poly(diallyl_isophthalate)
	noddy outer	**PVC**	69.67	**PVC**	93.17	Other	84.95	poly(diallyl_isophthalate)
PEN	penguin white mid	**PVC**	69.86	**PVC**	90.55	Other	82.25	polyester_epoxide
	penguin white outer	**PVC**	69.52	**PVC**	93.98	Other	82.22	polyester_epoxide
PHC	phone case	PU	65.42	PVC	93.98	PU	95.26	-
PIL	pilsbury inner cut	**PVC**	69.69	**PVC**	93.57	Other	82.36	poly(diallyl_isophthalate)
	pilsbury outercut	**PVC**	77.22	**PVC**	92.66	PET	82.89	-
PNK	pink pig	**PVC**	74.2	PET	88.43	PET	79.48	-
	pink pig thin ear	**PVC**	73.1	**PVC**	77.03	Other	82.11	poly(diallyl_isophthalate)
SNO	snoopy inner cut	**PVC**	64.73	**PVC**	79.81	Other	85.67	poly(diallyl_isophthalate)
	snoopy outer cut	**PVC**	66.83	**PVC**	77.05	Other	85.2	poly(diallyl_isophthalate)

SUC	sucker outer	**PVC**	57.1	**PVC**	94.77	Other	89.04	epoxide_resin
TCS	thick clear sheet inner	PMMA	71.98	**PVC**	88.65	**PVC**	75.31	-
	thick clear sheet mid	PMMA	72.61	**PVC**	92.6	**PVC**	78.46	-
	thick clear sheet outer	PMMA	71.88	**PVC**	98.24	**PVC**	75.57	-
TWB	trump white	**PVC**	66.76	**PVC**	95.44	Other	81.47	polyester_epoxide
VYG	vygon	**PVC**	60.44	PEA	86.37	Other	85.78	vinyl_chloride_vinyl_acetate_hydroxy propyl_acrylate
YED	yellow dog inner	**PVC**	66.6	**PVC**	94.46	Other	85.24	poly(diallyl_isophthalate)
	yellow dog inner sliver	**PVC**	66.7	**PVC**	93.71	Other	82.75	poly(diallyl_isophthalate)
	yellow dog outer paint	**PVC**	67.45	**PVC**	88.62	**PVC**	86.87	-

8.3 Cost evaluation of proposed TLC method (as of November 2023)

Table 44: Equipment and chemicals used in this work (at least 5 samples per plate)

Equipment	**Est. upfront item cost**	**Equivalent consumables cost per plate run (5-8 samples)**	**Notes**
TLC plates (x 1)	£100	£1	Polymer backed plates readily available - 100 plates (5 x 10 cm).
Optional: UV lamp	£100-300		254 nm lamp
1 µL Micropipette (x 1)	£50-100	-	Reusable if cleaned in acetone (avoiding dissolution of marks). It can also be hand-pulled from heated glass pipettes.
Hexane (500 mL)	£9-20	£0.20	Dependent on amount bought – £/mL varies
Ethyl acetate (100 mL)	£3-30	£0.07	Not restricted
Acetone (100 mL)	£2-20	£0.02	Not restricted
Benzyl Benzoate (100 mL)	£6.85	£0.01	Not restricted
0.04% Bromocresol green stain (100 mL)	£2.95	-	Reusable if stored in dark.
Filter paper	£5	-	Reusable. £5 per 100.
Chamber for elution and stains	£7	-	Reusable. Any wide neck (>5 cm) and flat-based sealable jar
Estimated cost	***£185-£600 upfront***	***£1.80 per run***	**1 plate could contain up to 8 samples**

Q1: What is your job role? (Tick all that apply)

- ☐ Curator
- ☐ Conservator / Collections Care Manager
- ☐ Scientist

Q2: Are you involved in the curation/care of plastic objects at your organisation?

◯ Yes ◯ No

Your career

Note: if you have answered/chosen item [2] in question 2, skip the following question

Q3: How long have you worked in the heritage sector?

◯ 0-1 years ◯ 1-5 years ◯ 5-10 years ◯ 10+ years

Your expertise

Note: if you have answered/chosen item [2] in question 2, skip the following question

Q4: What is your area of expertise? (Tick all that apply)

- ☐ Plastics
- ☐ Metals
- ☐ Textiles
- ☐ Organics (incl wood)
- ☐ Paper
- ☐ Paintings
- ☐ Stone
- ☐ Glass & ceramics
- ☐ Photographic material
- ☐ Preventive Conservation
- ☐ Other

If you have chosen "other", please specify:

Your expertise

Note: if you have answered/chosen at least one of the following items: [1] in question 4, skip the following question
Note: if you have answered/chosen item [2] in question 2, skip the following question

Q5: Do you have any specialized knowledge of plastics?

◯ Yes ◯ No

Your experience

Note: if you have answered/chosen item [2] in question 5 AND NOT answered/chosen at least one of the following items: [1] in question 4, skip the following question
Note: if you have answered/chosen item [2] in question 2, skip the following question

Q6: Through which of the following have you gained your knowledge of plastics? (tick all that apply)

- ☐ Through work experience e.g knowledge gained informally over your career
- ☐ Short term courses e.g Continuing Professional Development
- ☐ Scientific degree e.g materials science, chemistry
- ☐ Conservation degree (with study of plastics)
- ☐ Other degree level study; please give degree

If you have chosen "other", please specify:

Your experience

Note: if you have answered/chosen item [2] in question 5 AND NOT answered/chosen at least one of the following items: [1] in question 4, skip the following question
Note: if you have answered/chosen item [2] in question 2, skip the following question

Q7: How long have you worked with plastics?

☐ years

Note: if you have answered/chosen item [2] in question 2, skip the following question

Q8: Does your organisation have other staff with specialized knowledge of plastic materials?

◯ Yes ◯ No

Your collection

Note: if you have answered/chosen item [2] in question 2, skip the following question

Q9: Which of these statements do you agree with?

- ◯ Plastic objects make up a major proportion of our collection
- ◯ Plastic objects make up a moderate proportion of our collection
- ◯ Plastic objects make up a minor proportion of our collection

Note: if you have answered/chosen item [2] in question 2, skip the following question

Q10: What type of objects contain plastic at your organisation? (tick all that apply)

- ☐ sculpture
- ☐ archival media e.g film, audio tapes.
- ☐ military objects (armour, equipment, clothing)
- ☐ games/toys/sporting equipment
- ☐ furniture
- ☐ food products/packaging
- ☐ personal ornament (incl jewellery, spectacles)
- ☐ miscellaneous/ other; please give details
- ☐ paintings
- ☐ agricultural equipment
- ☐ science/medicine
- ☐ musical instruments
- ☐ household (incl fixtures, fittings, components)
- ☐ textile/clothing
- ☐ religious/ritual equipment

If you have chosen "other", please specify:

Note: if you have answered/chosen item [2] in question 2, skip the following question

Q11: Are you concerned about plastics in your collection?

◯ I am very concerned ◯ I am somewhat concerned ◯ I am not concerned

Note: if you have answered/chosen item [3] in question 11, skip the following question
Note: if you have answered/chosen item [2] in question 2, skip the following question

Q12: What are the main areas of concern?

Acquisition

Note: if you have answered/chosen item [2] in question 2, skip the following question

Q13: Assuming a plastic object is to be acquired, are you likely to be involved in its acquisition?

◯ Always ◯ Sometimes ◯ Never

Acquisition

Note: if you have answered/chosen item [3] in question 13, skip the following question
Note: if you have answered/chosen item [2] in question 2, skip the following question

Q14: What is your role during acquisition?

Acquisition

Note: if you have answered/chosen item [2] in question 2, skip the following question

Q15: Who makes the final decision regarding acquisition? (tick all that apply)

☐ Curatorial staff ☐ Conservation staff ☐ Other

If you have chosen "other", please specify:

Acquisition

Note: if you have answered/chosen item [2] in question 2, skip the following question

Q16: Does your organisation follow a formal acquisition procedure/process?

◯ Yes ◯ No

Acquisition

Note: if you have answered/chosen item [2] in question 2, skip the following question

Q17: Is a condition assessment undertaken as part of acquisition?

◯ Always ◯ Sometimes ◯ Never

Acquisition

Note: if you have answered/chosen item [3] in question 17, skip the following question
Note: if you have answered/chosen item [2] in question 2, skip the following question

Q18: When is the condition assessment typically performed?

◯ Before acquisition ◯ After acquisition

Acquisition

Note: if you have answered/chosen item [3] in question 17, skip the following question
Note: if you have answered/chosen item [2] in question 2, skip the following question

Q19: Who undertakes the assessment? (tick all that apply)

☐ Curatorial staff ☐ Conservation staff ☐ External experts ☐ Other

If you have chosen "other", please specify:

Acquisition

Note: if you have answered/chosen item [2] in question 2, skip the following question

Q20: Do you seek to identify any of the components of a plastic object (e.g polymer, additive) as part of the acquisition process?

◯ Always ◯ Sometimes ◯ Never

Identification of plastic type

Note: if you have answered/chosen item [2] in question 2, skip the following question

Q21: At your organisation, other than at acquisition, what else may trigger efforts to identify a plastic material? (tick all that apply)

☐ Nothing ☐ Exhibition ☐ Loan
☐ Desire for collection knowledge ☐ To inform conservation strategy ☐ Result of condition assessment
☐ Other, please give details

If you have chosen "other", please specify:

Identification of plastic type

Note: if you have answered/chosen item [3] in question 20 AND answered/chosen at least one of the following items: [1] in question 21, skip the following question
Note: if you have answered/chosen item [2] in question 2, skip the following question

Q22: Are you involved in identifying a plastic material?

◯ Yes ◯ No

Identification of plastic type

Note: if you have answered/chosen item [3] in question 20 AND answered/chosen at least one of the following items: [1] in question 21, skip the following question
Note: if you have answered/chosen item [2] in question 22, skip the following question
Note: if you have answered/chosen item [2] in question 2, skip the following question

Q23: What method(s) do YOU use for identification? (tick all that apply)

- ☐ ID flow charts
- ☐ Knowledge of object history
- ☐ Infrared Spectroscopy (FT-IR in mid infrared region)
- ☐ Other spectroscopy (Near Infrared, Raman, NMR or multi/hyperspectral imaging)
- ☐ Chromatography (GC/MS, SPME-GC/MS, Py-GC/MS)
- ☐ Polarisation filters

Identification of plastic type

Note: if you have answered/chosen item [3] in question 20 AND answered/chosen at least one of the following items: [1] in question 21, skip the following question
Note: if you have answered/chosen item [2] in question 2, skip the following question

Q24: Are others involved in identification? (tick all that apply)

◯ Yes ◯ No

Identification of plastic type

Note: if you have answered/chosen item [3] in question 20 AND answered/chosen at least one of the following items: [1] in question 21, skip the following question
Note: if you have answered/chosen item [2] in question 24, skip the following question
Note: if you have answered/chosen item [2] in question 2, skip the following question

Q25: Who else is involved in plastic identification? (please tick all that apply)

- ☐ Curatorial colleagues
- ☐ Conservator/scientist colleagues
- ☐ External partner e.g outsourced chemical analysis
- ☐ Other

If you have chosen "other", please specify:

Identification of plastic type

Note: if you have answered/chosen item [3] in question 20 AND answered/chosen at least one of the following items: [1] in question 21, skip the following question
Note: if you have answered/chosen item [2] in question 24, skip the following question
Note: if you have answered/chosen item [2] in question 2, skip the following question

Q26: What methods do they use? (tick all that apply)

- ☐ Infrared Spectroscopy (FT-IR in mid-infrared region)
- ☐ Other spectroscopy (e.g. Near-infrared, Raman, Nuclear Magnetic Resonance (NMR), or multi/hyperspectral imaging)
- ☐ Chromatography (GC/MS, SPME-GC/MS, Py-GC/MS)
- ☐ Polarisation filters
- ☐ ID flow charts
- ☐ Knowledge of object history
- ☐ Don't know
- ☐ Other

If you have chosen "other", please specify:

Identification of plastic type

Note: if you have answered/chosen item [2] in question 2, skip the following question

Q27: Which of these statements do you agree with?

Polymer type has been positively identified for ...

- ◯ no plastic object in the collection
- ◯ some plastic objects in the collection
- ◯ most plastic objects in the collection
- ◯ all plastic objects in the collection

Identification of plastic type

Note: if you have answered/chosen item [2] in question 2, skip the following question
Note: if you have answered/chosen at least one of the following items: [1] in question 1, skip the following question

Q28: Are there any barriers to polymer identification at your organisation?

◯ Yes ◯ No

Identification of plastic type

Note: if you have answered/chosen item [2] in question 28, skip the following question
Note: if you have answered/chosen item [2] in question 2, skip the following question
Note: if you have answered/chosen at least one of the following items: [1] in question 1, skip the following question

Q29: If yes, what barriers are there to polymer identification at your organisation? (please tick all that apply)

☐ Funding ☐ Equipment ☐ Time ☐ Expertise ☐ Other

If you have chosen "other", please specify:

Note: if you have answered/chosen item [2] in question 2, skip the following question
Note: if you have answered/chosen at least one of the following items: [1] in question 1, skip the following question

Q30: Do you have any standard procedures or guidelines at your organisation for conserving plastic objects incl. temperature, relative humidity and lighting levels for display and/or storage?

◯ No ◯ Yes, please give details

If you have chosen "other", please specify:

Note: if you have answered/chosen item [2] in question 2, skip the following question
Note: if you have answered/chosen at least one of the following items: [1] in question 1, skip the following question

Q31: How do you monitor the condition of your plastic objects? (please tick all that apply)

☐ We don't
☐ Regular condition assessment (e.g scheduled annual assessment)
☐ Ad hoc condition assessment (e.g triggered due to upcoming event or conservation need)

Note: if you have answered/chosen at least one of the following items: [1] in question 31, skip the following question
Note: if you have answered/chosen item [2] in question 2, skip the following question
Note: if you have answered/chosen at least one of the following items: [1] in question 1, skip the following question

Q32: What triggers a condition assessment to be undertaken? (please tick all that apply)

☐ Response to output from sensors/indicators
☐ Prompted by exhibition
☐ Routine assessment e.g yearly/monthly etc
☐ Response to visual change of object
☐ Prompted by loan
☐ Other, please state

If you have chosen "other", please specify:

Note: if you have answered/chosen item [2] in question 2, skip the following question
Note: if you have answered/chosen at least one of the following items: [1] in question 1, skip the following question

Q33: Which of these have you observed? (please tick all that apply)

☐ None
☐ Cracking
☐ Brittleness
☐ Shape deformation (shrinkage, warping)

- ☐ Bloom (crystallite formation on surface)
- ☐ Sweating
- ☐ Discolouration
- ☐ Smell
- ☐ VOC emission (e.g as suggested by AD strip / other indicator)
- ☐ Abrasion
- ☐ Other

If you have chosen "other", please specify:

Note: if you have answered/chosen item [2] in question 2, skip the following question
Note: if you have answered/chosen at least one of the following items: [1] in question 1, skip the following question

Q34: How are your plastic objects stored? (please tick all that apply)

- ☐ Open (non-enclosed)
- ☐ Closed
- ☐ Air-tight
- ☐ Fridge
- ☐ Freezer
- ☐ Other

If you have chosen "other", please specify:

Note: if you have answered/chosen item [2] in question 2, skip the following question
Note: if you have answered/chosen at least one of the following items: [1] in question 1, skip the following question

Q35: What storage materials do you use? (e.g cardboard box, metal canister)

- ☐ Cardboard
- ☐ Metal
- ☐ Plastic
- ☐ Other (please give details)

If you have chosen "other", please specify:

Note: if you have answered/chosen item [2] in question 2, skip the following question
Note: if you have answered/chosen at least one of the following items: [1] in question 1, skip the following question

Q36: Do you isolate any plastic objects? If so, what and why?

Note: if you have answered/chosen item [2] in question 2, skip the following question
Note: if you have answered/chosen at least one of the following items: [1] in question 1, skip the following question

Q37: Do you monitor VOC (volatile organic compound) emissions from plastics (e.g acids)?

◯ Yes ◯ No

Note: if you have answered/chosen item [2] in question 37, skip the following question
Note: if you have answered/chosen item [2] in question 2, skip the following question
Note: if you have answered/chosen at least one of the following items: [1] in question 1, skip the following question

Q38: If yes, what method do you use?

e.g SPME, AD strips or other indicator

Please give details

Note: if you have answered/chosen item [2] in question 2, skip the following question
Note: if you have answered/chosen at least one of the following items: [1] in question 1, skip the following question

Q39: What sources do you consult to inform care of plastic objects? (tick all that apply)

- ☐ None
- ☐ Scientific literature
- ☐ Colleagues at your organisation
- ☐ Guidelines/Standards
- ☐ Conservation literature
- ☐ Conferences/conference proceedings
- ☐ External experts
- ☐ Other, please give details

If you have chosen "other", please specify:

Note: if you have answered/chosen item [2] in question 2, skip the following question

Q40: Which of these statements do you agree with? (tick all that apply)In the majority of cases I describe/catalogue a plastic object…

- ☐ with the term 'plastic'
- ☐ with it's polymer type(s) e.g Cellulose acetate, PVC, PTFE
- ☐ with its common name e.g acetate, acrylic
- ☐ with its brand name e.g Celluloid, Teflon
- ☐ Other

If you have chosen "other", please specify:

Research

Note: if you have answered/chosen item [2] in question 2, skip the following question

Q41: Is your organisation actively researching plastic conservation methods?

◯ Yes ◯ No

Research

Note: if you have answered/chosen item [2] in question 41, skip the following question
Note: if you have answered/chosen item [2] in question 2, skip the following question

Q42: Is the research in collaboration with anyone, or purely in-house research? (please tick all that apply)

☐ In-house reasearch ☐ External partner e.g academia/industry

Note: if you have answered/chosen item [2] in question 2, skip the following question

Q43: If you would like to tell us more about ongoing projects, please add any details in the box below (optional)

Q44: If you’d like to share your organisation name and/or country please add to the box below (optional)

Thank you for taking part! On clicking finish, you'll be redirected to our mail list sign up. If you'd like to be informed of our survey results please add your email address there.

Privacy &GDPR

The collected survey data and mailing lists are seperate; we will not be able to link your responses to your email address.

Please note, we collect &store your email address using MailChimp - whose servers are based in the US, therefore by using this service we are transferring data outside of the EU/EEA. We have opted out of MailChimp being able to use our subscriber details in their data science projects. MailChimp's privacy may be viewed here https://mailchimp.com/legal/privacy

8.4 *apriori* mined association rules for two plasticisers, sorted by 'confidence'.

ID	rules (x => y)	support	confidence	coverage	lift	count	number of samples in dataset
29	{MeEster} => {DINCH}	2%	100%	2%	3.24	2	120
35	{MeEster} => {ESBO}	2%	100%	2%	1.28	2	120
6	{ESBO} => {DEHA}	100%	100%	100%	1.00	1	1
7	{DEHA} => {ESBO}	100%	100%	100%	1.00	1	1
63	{DINCH} => {ESBO}	30%	97%	31%	1.24	36	120
73	{TXIB} => {ESBO}	28%	97%	28%	1.24	33	120
69	{ATBC} => {ESBO}	26%	86%	30%	1.10	31	120
75	{DOTP} => {ESBO}	43%	81%	53%	1.03	51	120
45	{TBC} => {ESBO}	4%	71%	6%	0.91	5	120
67	{DIDP} => {DINP}	5%	67%	7%	4.70	12	261
27	{DPHP} => {ESBO}	2%	67%	3%	0.85	2	120
55	{DEHP} => {ESBO}	5%	55%	9%	0.70	6	120
76	{ESBO} => {DOTP}	43%	54%	78%	1.03	51	120
59	{TXIB} => {ATBC}	14%	51%	28%	1.42	22	155
311	{DIBP} => {DNOP}	1%	50%	2%	15.75	1	126
491	{DNOP} => {DINP}	1%	50%	3%	9.79	2	137
49	{DNOP} => {DEHP}	1%	50%	3%	4.24	2	144
31	{MeEster} => {ATBC}	1%	50%	2%	1.67	1	120
33	{MeEster} => {DOTP}	1%	50%	2%	0.95	1	120
23	{DINP} => {ESBO}	1%	50%	2%	0.64	1	120
682	{DINP} => {DEHP}	8%	49%	16%	1.30	24	307
581	{DBP} => {DINP}	2%	47%	5%	2.90	7	298
602	{DBP} => {DEHP}	2%	47%	5%	1.20	7	298
57	{TXIB} => {DINCH}	13%	47%	28%	1.44	20	155
68	{DINCH} => {ATBC}	14%	45%	30%	1.38	24	177
411	{TBC} => {TXIB}	3%	43%	6%	1.51	3	120
43	{TBC} => {DOTP}	3%	43%	6%	0.82	3	120
631	{DIBP} => {DEHP}	3%	42%	6%	1.75	5	189
691	{ATBC} => {DINCH}	14%	41%	33%	1.38	24	177
58	{DINCH} => {TXIB}	13%	40%	32%	1.44	20	155
60	{ATBC} => {TXIB}	14%	39%	36%	1.42	22	155
64	{ESBO} => {DINCH}	30%	38%	78%	1.24	36	120
431	{DBP} => {DIBP}	2%	38%	4%	5.91	3	189

74	{ESBO} => {TXIB}	28%	35%	78%	1.24	33	120
694	{DIDP} => {DEHP}	2%	33%	7%	0.90	6	261
20	{DEHA} => {DOTP}	2%	33%	5%	0.79	1	59
19	{DEHA} => {DEHP}	1%	33%	3%	0.56	1	110
70	{ESBO} => {ATBC}	26%	33%	78%	1.10	31	120
61	{TXIB} => {DOTP}	9%	33%	28%	0.66	14	155
683	{DINP} => {DIDP}	5%	32%	14%	4.70	12	261
501	{DINP} => {DNOP}	1%	29%	5%	9.79	2	137
391	{TBC} => {ATBC}	2%	29%	6%	0.95	2	120
741	{ATBC} => {DOTP}	9%	28%	33%	0.56	16	177
321	{DNOP} => {DIBP}	1%	25%	3%	15.75	1	126
441	{DIBP} => {DBP}	2%	25%	6%	5.91	3	189
352	{DPHP} => {DIDP}	1%	25%	2%	3.28	1	197
371	{DPHP} => {DEHP}	1%	25%	2%	0.97	1	197
54	{DEHP} => {ATBC}	2%	25%	8%	0.93	3	142
39	{DPHP} => {DOTP}	1%	25%	2%	0.63	1	197
693	{DEHP} => {DINP}	8%	21%	38%	1.30	24	307
401	{DIBP} => {DOTP}	1%	20%	3%	0.39	1	172
641	{DINP} => {DOTP}	2%	19%	13%	0.47	7	291
751	{DOTP} => {ATBC}	9%	18%	49%	0.56	16	177
62	{DOTP} => {TXIB}	9%	18%	50%	0.66	14	155
551	{DBP} => {DOTP}	1%	18%	4%	0.44	2	247
82	{DEHP} => {DOTP}	5%	17%	27%	0.43	12	263
612	{DIBP} => {DINP}	1%	17%	6%	1.75	2	189
592	{DINP} => {DBP}	2%	15%	16%	2.90	7	298
37	{TBC} => {DINCH}	1%	14%	6%	0.46	1	120
51	{DBP} => {DIDP}	0%	13%	3%	1.81	1	261
80	{DINCH} => {DOTP}	3%	12%	22%	0.31	7	261
50	{DEHP} => {DNOP}	1%	12%	12%	4.24	2	144
83	{DOTP} => {DEHP}	5%	12%	40%	0.43	12	263
642	{DEHP} => {DIBP}	3%	11%	24%	1.75	5	189
621	{DINP} => {DIBP}	1%	11%	10%	1.75	2	189
351	{TOTM} => {DOTP}	1%	10%	8%	0.20	1	128
42	{TXIB} => {TBC}	3%	9%	28%	1.51	3	120
552	{ATBC} => {DEHP}	2%	8%	27%	0.93	3	142
81	{DOTP} => {DINCH}	3%	7%	39%	0.31	7	261
362	{DIDP} => {DPHP}	1%	7%	8%	3.28	1	197
56	{ESBO} => {DEHP}	5%	6%	78%	0.70	6	120
701	{DEHP} => {DIDP}	2%	6%	37%	0.90	6	261
611	{DEHP} => {DBP}	2%	6%	39%	1.20	7	298
65	{DOTP} => {DINP}	2%	6%	41%	0.47	7	291
52	{DIDP} => {DBP}	0%	6%	7%	1.81	1	261
402	{ATBC} => {TBC}	2%	6%	30%	0.95	2	120
30	{DINCH} => {MeEster}	2%	5%	31%	3.24	2	120

46	{ESBO} => {TBC}	4%	5%	78%	0.91	5	120
44	{DOTP} => {TBC}	3%	5%	53%	0.82	3	120
692	{DINCH} => {DEHP}	1%	4%	20%	0.19	2	226
21	{DOTP} => {DEHA}	2%	4%	42%	0.79	1	59
681	{DEHP} => {DINCH}	1%	4%	23%	0.19	2	226
601	{TXIB} => {DEHP}	1%	3%	22%	0.10	1	154
32	{ATBC} => {MeEster}	1%	3%	30%	1.67	1	120
38	{DINCH} => {TBC}	1%	3%	31%	0.46	1	120
591	{DEHP} => {TXIB}	1%	2%	29%	0.10	1	154
36	{ESBO} => {MeEster}	2%	2%	78%	1.28	2	120
28	{ESBO} => {DPHP}	2%	2%	78%	0.85	2	120
381	{DEHP} => {DPHP}	1%	2%	26%	0.97	1	197
561	{DOTP} => {DBP}	1%	2%	42%	0.44	2	247
34	{DOTP} => {MeEster}	1%	2%	53%	0.95	1	120
361	{DOTP} => {TOTM}	1%	2%	49%	0.20	1	128
201	{DEHP} => {DEHA}	1%	2%	60%	0.56	1	110
40	{DOTP} => {DPHP}	1%	1%	40%	0.63	1	197
41	{DOTP} => {DIBP}	1%	1%	51%	0.39	1	172
24	{ESBO} => {DINP}	1%	1%	78%	0.64	1	120

R code used to mine association rules between two additives

```
library(arules)
library(arulesViz)
library(tidyr)
library(tidyverse)

#import data
readfile <- read.csv("data.csv")
adname <- colnames(readfile)
adname[1]="ESBO"
colnames(readfile) <- c(adname)
df <- apply(combn(adname,2),2,paste,collapse='-')
df<-str_split_fixed(df, "-", 2)

# initiate a list for storage
subrules_names <- list()

#loop through combinations
x <- 1

while (x <= nrow(df)) {
  a <- df[x, 1]
  b <- df[x, 2]
  filename <- paste(a,b,".txt")

  # Create logical vectors indicating NA values in columns a and b
  na_a <- is.na(readfile[, a])
```

```
  na_b <- is.na(readfile[, b])


# Subset dataframe to drop rows where either A or B contains NA, the remaining samples were tested for both A and B
  readfile_drop <- readfile[!(na_a | na_b), ]
  tr <- transactions(readfile_drop)
  rules <- apriori(tr,parameter=list(support = 0.1, conf = 0.5, minlen=2,maxlen=2))
  subrules_a <- subset(rules, (lhs %pin% c(a)) & (rhs %pin% c(b)))
  subrules_b <- subset(rules, (lhs %pin% c(b)) & (rhs %pin% c(a)))
  subrules <- union(subrules_a, subrules_b)
  write(subrules, filename)


  # Dynamically name subrules
  subrule_name <- paste("subrules_", x, sep = "")
  assign(subrule_name, subrules)


  # Append subrule name to the list
  subrules_names[[x]] <- subrule_name


  x <- x + 1
}


all_subrules <- Reduce(union, lapply(subrules_names, get))
img <- plot(all_subrules, method = "grouped matrix", measure="confidence", rhs_max=20)
all_subrules <- sort(all_subrules, by = "confidence")


write(all_subrules,'confidence.txt')
```

8.5 *apriori* mined association rules for >2 plasticisers.

Rule	LHS	RHS	support	confidence	coverage	lift	count
8	{DEHP,DIDP}	{DINP}	0.014327	0.833333	0.017192	5.935374	5
9	{DOTP,DINP}	{DEHP}	0.017192	0.857143	0.020057	2.578818	6
10	{DOTP,DEHP}	{DINP}	0.017192	0.5	0.034384	3.561224	6
11	{TXIB,DINCH}	{ATBC}	0.028653	0.5	0.057307	3.008621	10
12	{TXIB,DINCH}	{ESBO}	0.045845	0.8	0.057307	2.970213	16
13	{TXIB,ATBC}	{ESBO}	0.045845	0.727273	0.063037	2.700193	16
14	{ESBO,ATBC}	{TXIB}	0.045845	0.516129	0.088825	4.189047	16
15	{DOTP,TXIB}	{ESBO}	0.037249	0.928571	0.040115	3.447568	13
16	{DOTP,DINCH}	{ATBC}	0.011461	0.571429	0.020057	3.438424	4
17	{ATBC,DINCH}	{ESBO}	0.045845	0.666667	0.068768	2.475177	16
18	{ESBO,ATBC}	{DINCH}	0.045845	0.516129	0.088825	3.105673	16
19	{DOTP,DINCH}	{ESBO}	0.014327	0.714286	0.020057	2.651976	5
20	{DOTP,ATBC}	{ESBO}	0.025788	0.5625	0.045845	2.088431	9
21	{ESBO,DEHP}	{DOTP}	0.014327	0.833333	0.017192	2.464689	5
22	{TXIB,ATBC,DINCH}	{ESBO}	0.025788	0.9	0.028653	3.341489	9
23	{ESBO,TXIB,DINCH}	{ATBC}	0.025788	0.5625	0.045845	3.384698	9
24	{ESBO,TXIB,ATBC}	{DINCH}	0.025788	0.5625	0.045845	3.384698	9
25	{ESBO,ATBC,DINCH}	{TXIB}	0.025788	0.5625	0.045845	4.565407	9

Rules were mined from McCombie et al’s dataset with a threshold confidence of 0.5, and support of 0.01.

8.6 ATR-FTIR spectra of samples

Sample BBI

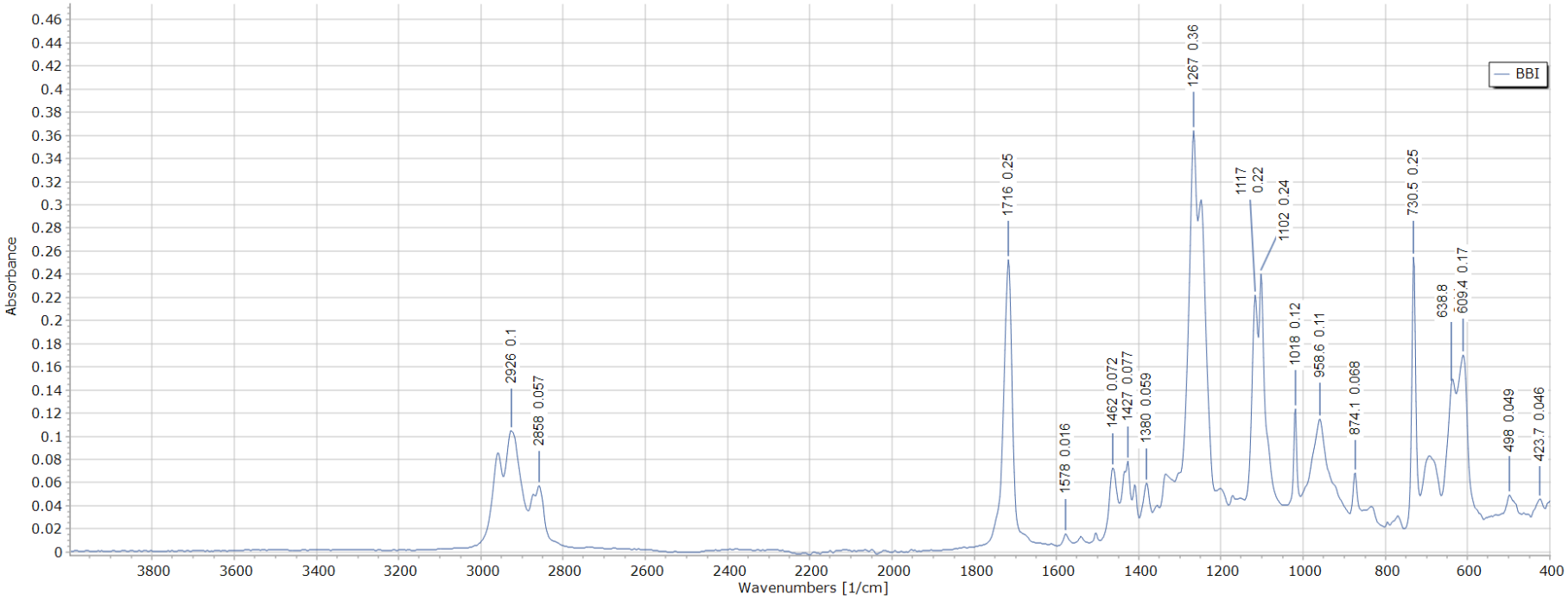

Sample BLK

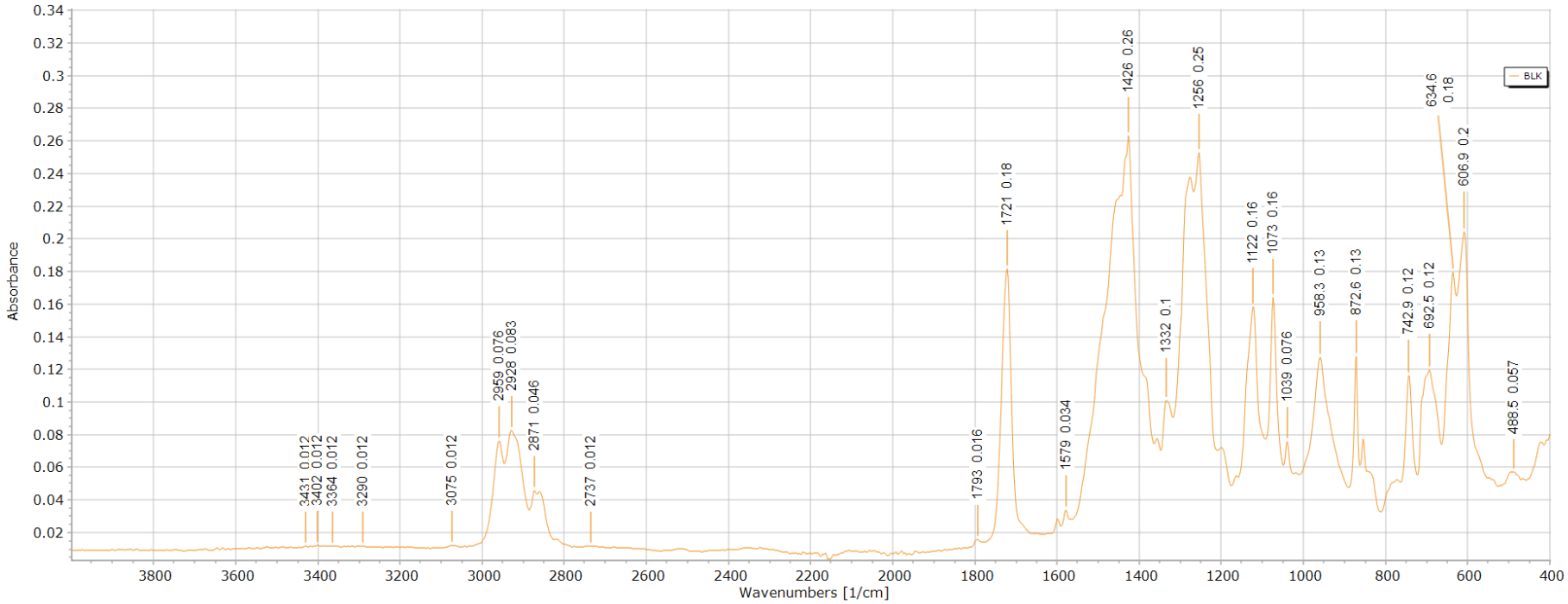
Absorbance
Wavenumbers [1/cm]
BLK
3431 0.012
3402 0.012
3364 0.012
3290 0.012
3075 0.012
2959 0.076
2928 0.083
2871 0.046
2737 0.012
1793 0.016
1721 0.18
1579 0.034
1426 0.26
1332 0.1
1256 0.25
1122 0.16
1073 0.16
1039 0.076
958.3 0.13
872.6 0.13
742.9 0.12
692.5 0.12
634.6 0.18
606.9 0.2
488.5 0.057

Sample COC

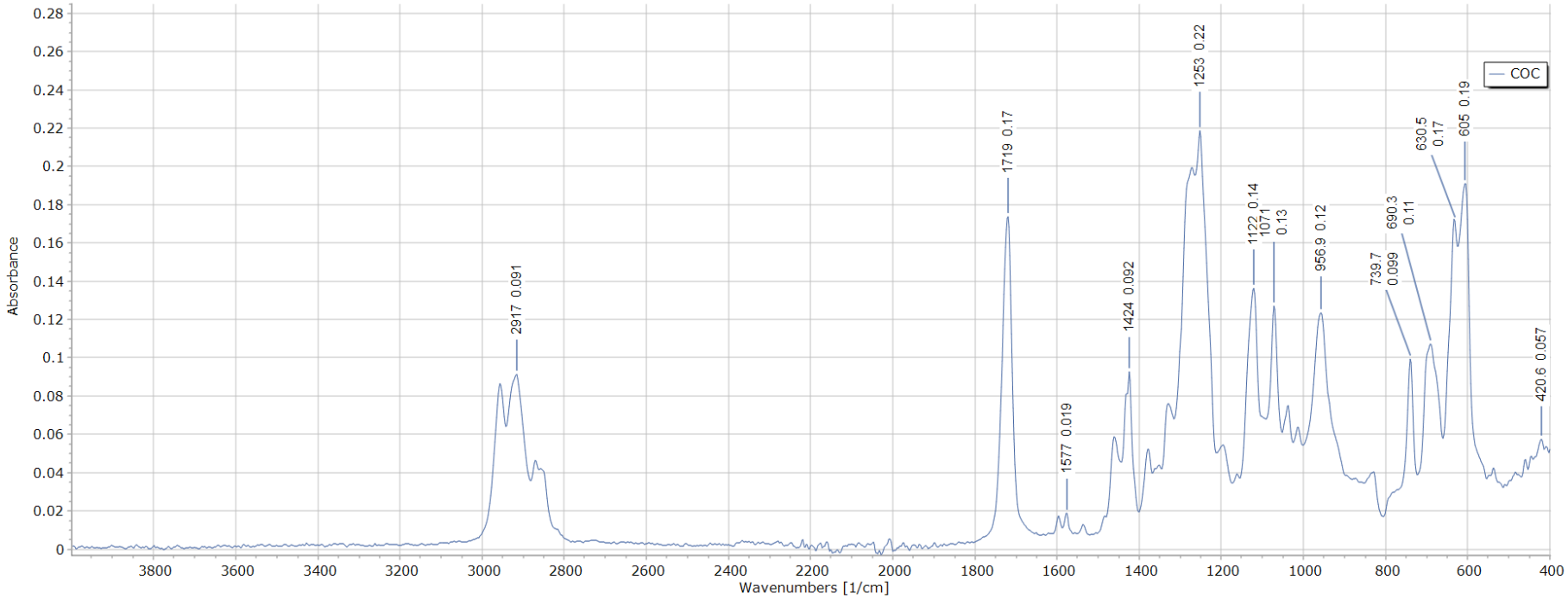
COC
Absorbance
Wavenumbers [1/cm]
2917 0.091
1719 0.17
1577 0.019
1424 0.092
1253 0.22
1122 0.14
1071 0.13
956.9 0.12
739.7 0.099
690.3 0.11
630.5 0.17
605 0.19
420.6 0.057

Sample DOD

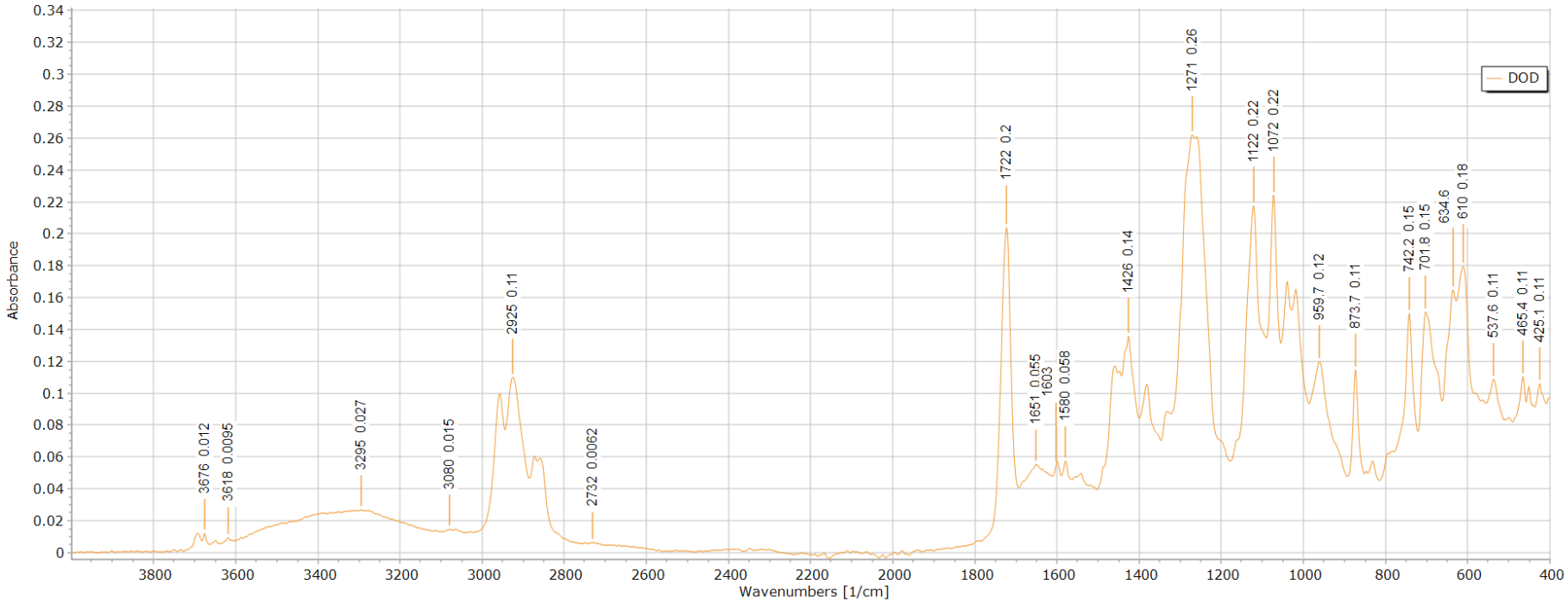
DOD
Absorbance
Wavenumbers [1/cm]
3676 0.012
3618 0.0095
3295 0.027
3080 0.015
2925 0.11
2732 0.0062
1722 0.2
1651 0.055
1603
1580 0.058
1426 0.14
1271 0.26
1122 0.22
1072 0.22
959.7 0.12
873.7 0.11
742.2 0.15
701.8 0.15
634.6
610 0.18
537.6 0.11
465.4 0.11
425.1 0.11

Sample DOG

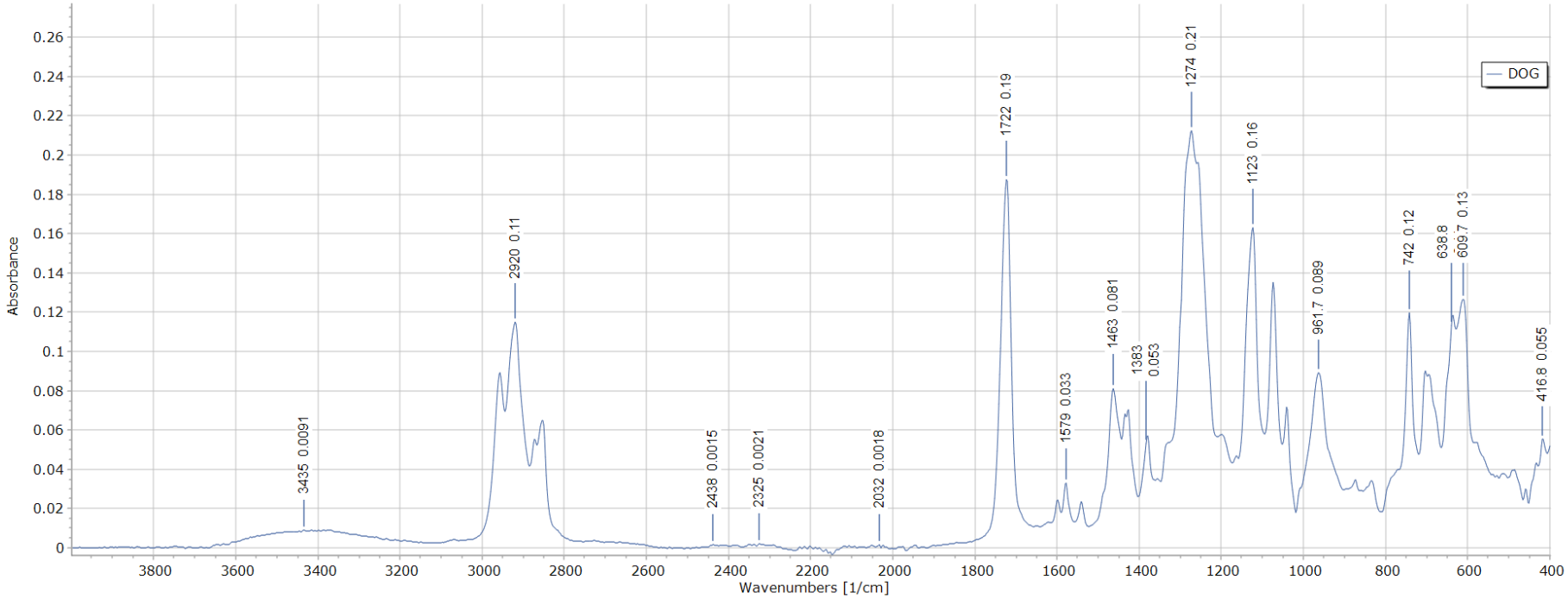
DOG
Absorbance
Wavenumbers [1/cm]
3435 0.0091
2920 0.11
2438 0.0015
2325 0.0021
2032 0.0018
1722 0.19
1579 0.033
1463 0.081
1383
0.053
1274 0.21
1123 0.16
961.7 0.089
742 0.12
638.8
609.7 0.13
416.8 0.055

Sample ERA

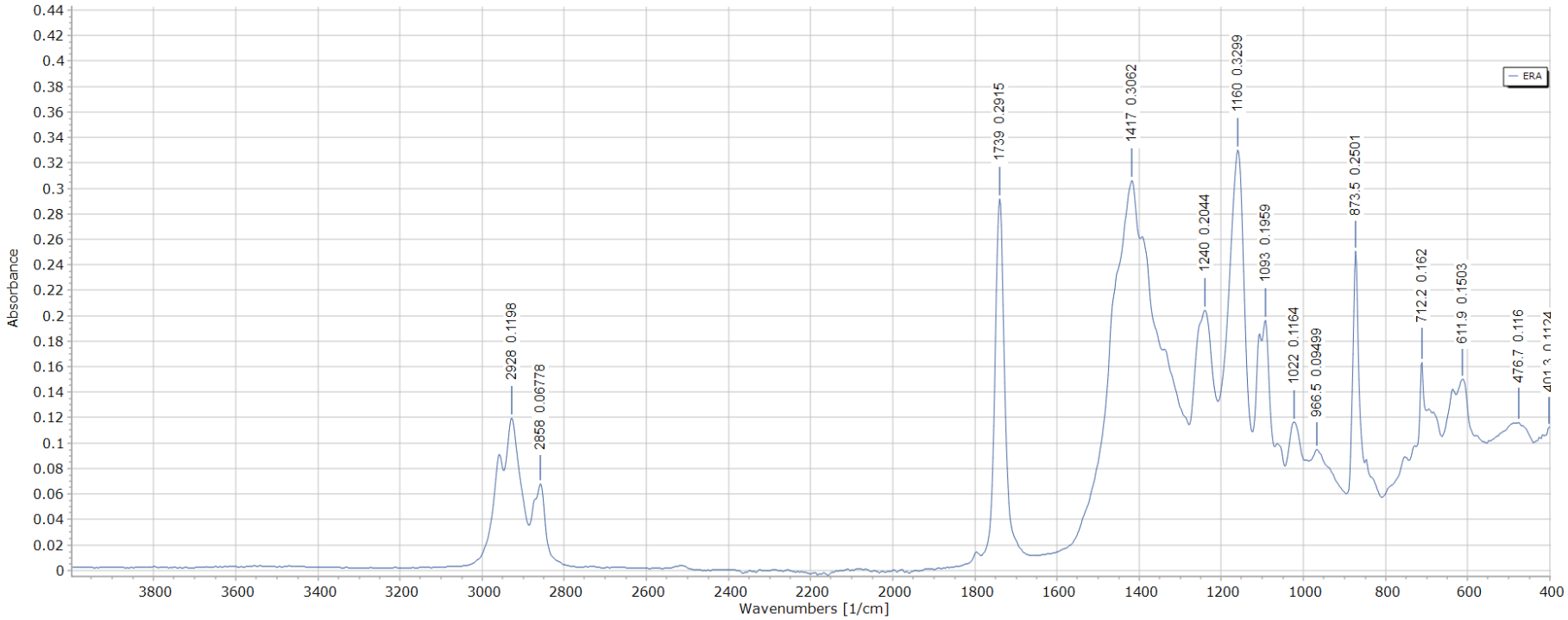
ERA
Absorbance
Wavenumbers [1/cm]
2928 0.1198
2858 0.06778
1739 0.2915
1417 0.3062
1240 0.2044
1160 0.3299
1093 0.1959
1022 0.1164
966.5 0.09499
873.5 0.2501
712.2 0.162
611.9 0.1503
476.7 0.116

Sample FKB

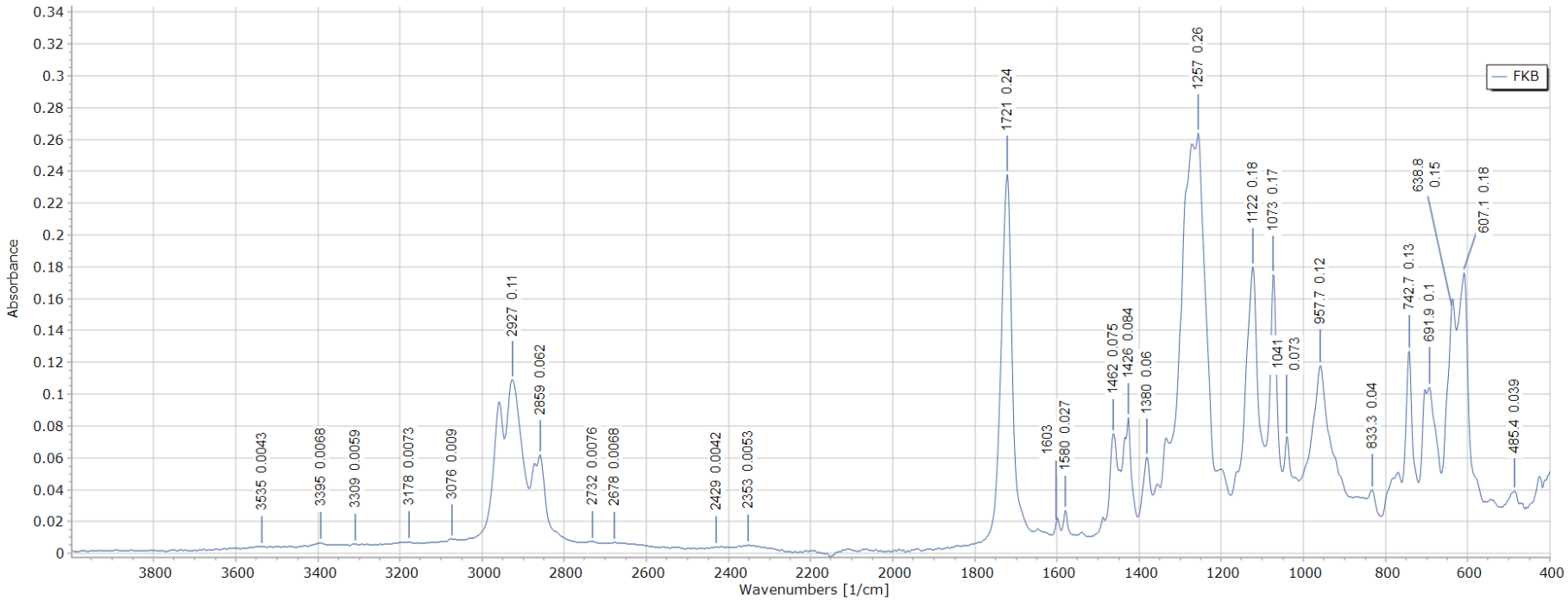
FKB
Absorbance
Wavenumbers [1/cm]
3535 0.0043
3395 0.0068
3309 0.0059
3178 0.0073
3076 0.009
2927 0.11
2859 0.062
2732 0.0076
2678 0.0068
2429 0.0042
2353 0.0053
1721 0.24
1603
1580 0.027
1462 0.075
1426 0.084
1380 0.06
1257 0.26
1122 0.18
1073 0.17
1041
0.073
957.7 0.12
833.3 0.04
742.7 0.13
691.9 0.1
638.8
0.15
607.1 0.18
485.4 0.039

Sample FMO

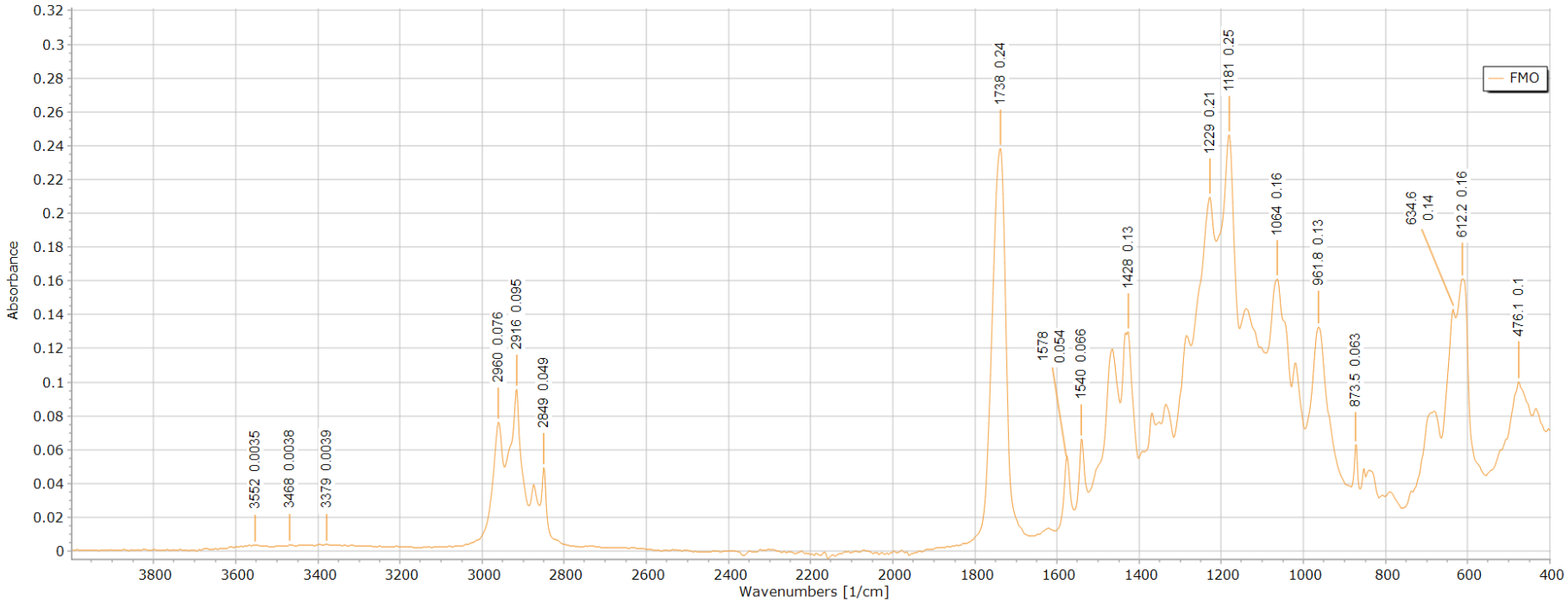
FMO
Absorbance
Wavenumbers [1/cm]
3552 0.0035
3468 0.0038
3379 0.0039
2960 0.076
2916 0.095
2849 0.049
1738 0.24
1578 0.054
1540 0.066
1428 0.13
1229 0.21
1181 0.25
1064 0.16
961.8 0.13
873.5 0.063
634.6 0.14
612.2 0.16
476.1 0.1

Sample GOC

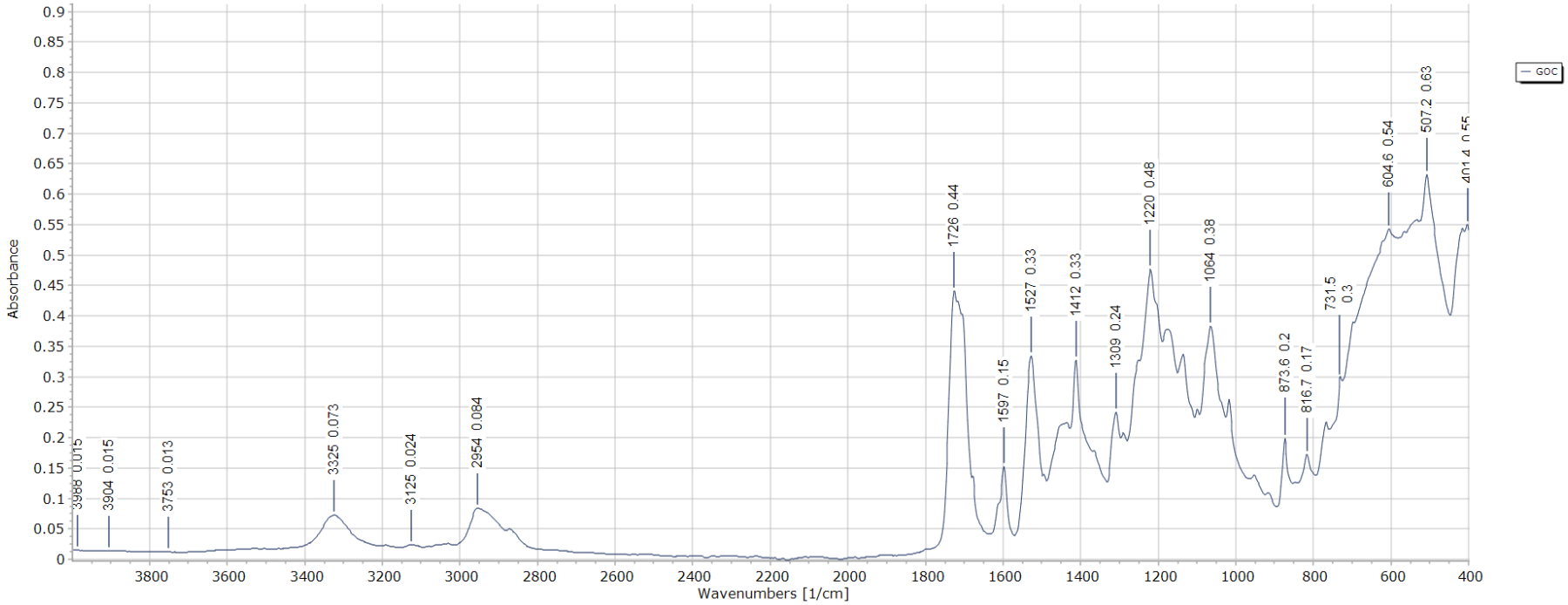
Absorbance
Wavenumbers [1/cm]
GOC
3988 0.015
3904 0.015
3753 0.013
3325 0.073
3125 0.024
2954 0.084
1726 0.44
1597 0.15
1527 0.33
1412 0.33
1309 0.24
1220 0.48
1064 0.38
873.6 0.2
816.7 0.17
731.5 0.3
604.6 0.54
507.2 0.63

Sample GRG

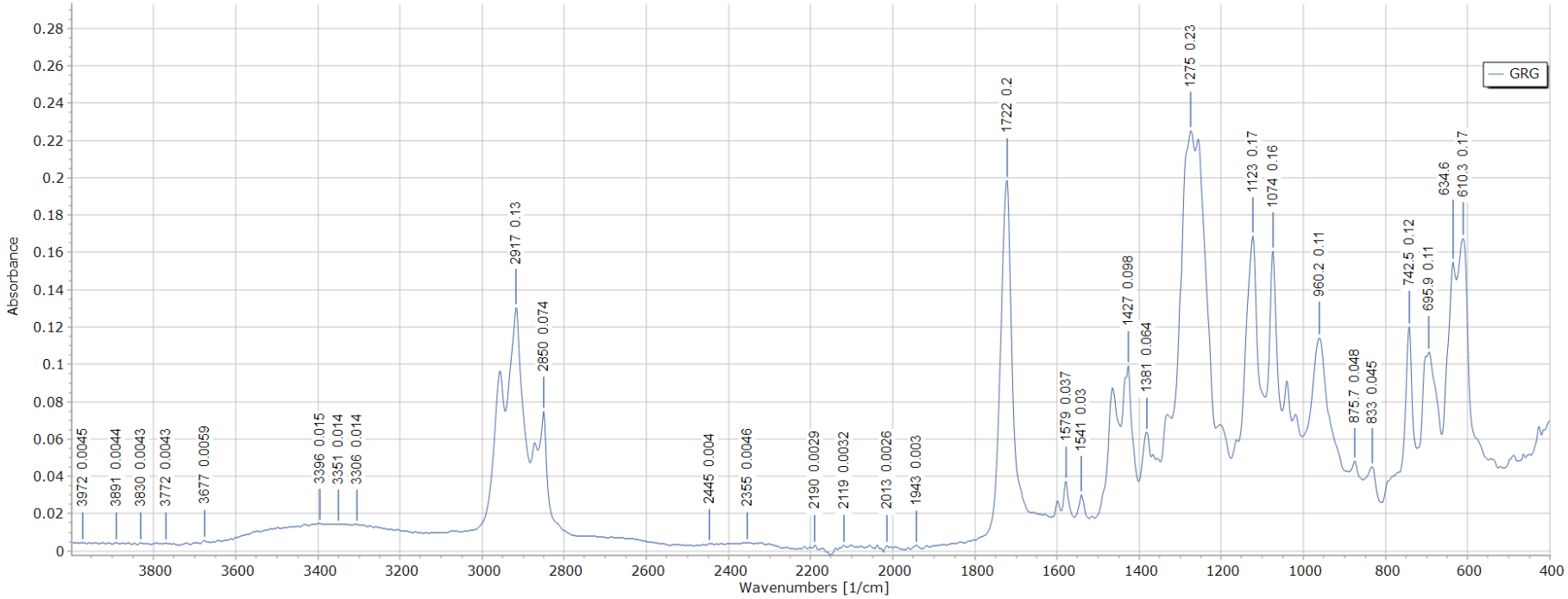
GRG
Absorbance
Wavenumbers [1/cm]
3972 0.0045
3891 0.0044
3830 0.0043
3772 0.0043
3677 0.0059
3396 0.015
3351 0.014
3306 0.014
2917 0.13
2850 0.074
2445 0.004
2355 0.0046
2190 0.0029
2119 0.0032
2013 0.0026
1943 0.003
1722 0.2
1579 0.037
1541 0.03
1427 0.098
1381 0.064
1275 0.23
1123 0.17
1074 0.16
960.2 0.11
875.7 0.048
833 0.045
742.5 0.12
695.9 0.11
634.6
610.3 0.17

Sample HEI

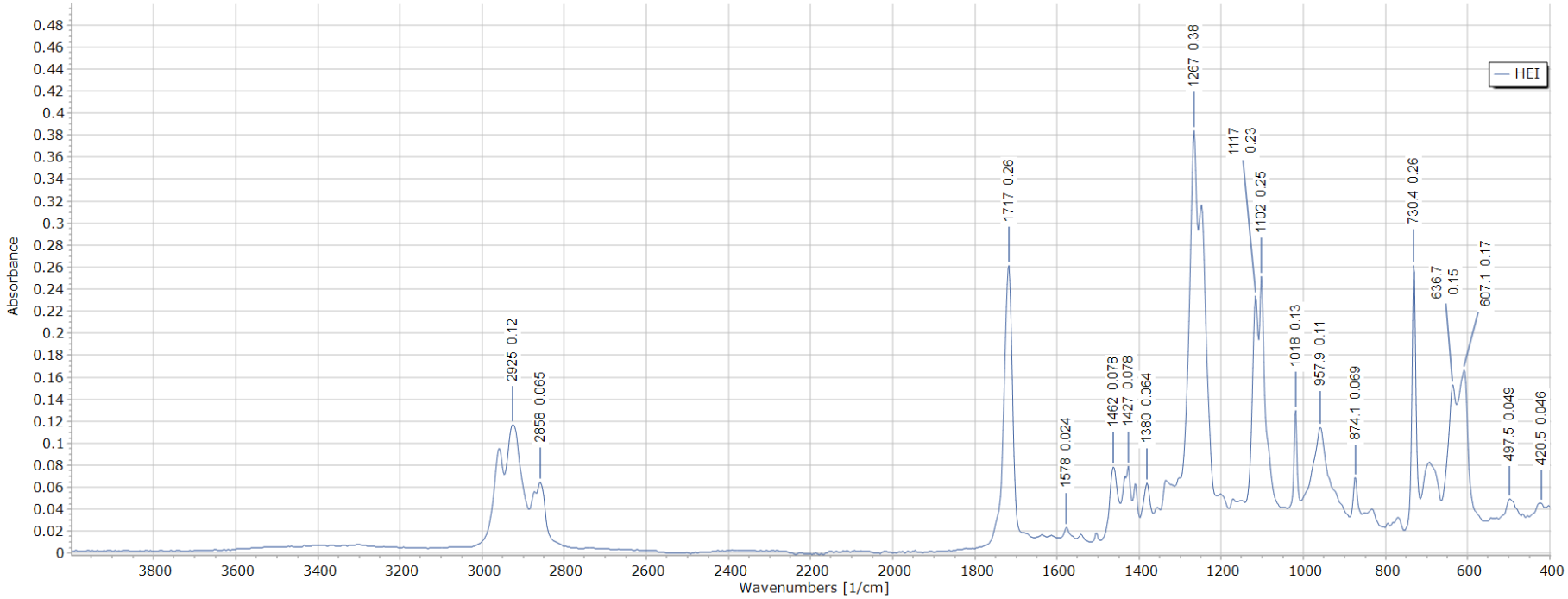
HEI
Absorbance
Wavenumbers [1/cm]
2925 0.12
2858 0.065
1717 0.26
1578 0.024
1462 0.078
1427 0.078
1380 0.064
1267 0.38
1117 0.23
1102 0.25
1018 0.13
957.9 0.11
874.1 0.069
730.4 0.26
636.7 0.15
607.1 0.17
497.5 0.049
420.5 0.046

Sample MCS

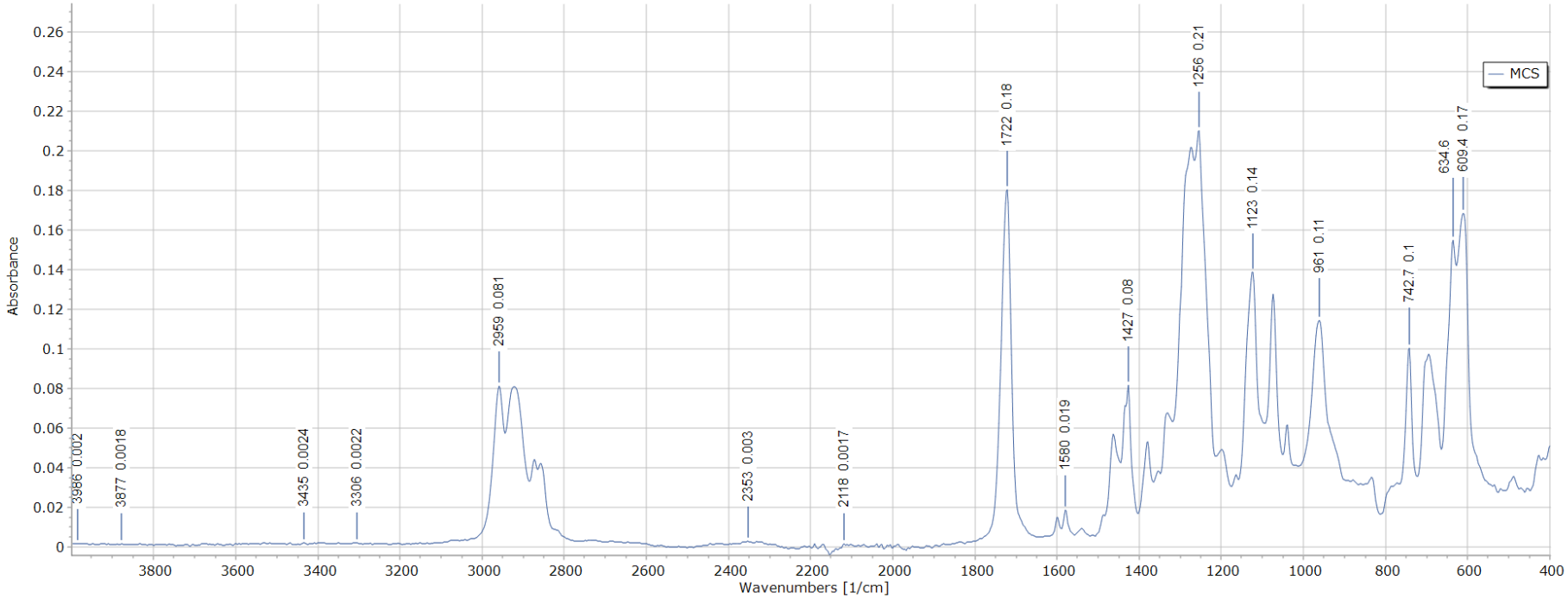
MCS
Absorbance
Wavenumbers [1/cm]
3986 0.002
3877 0.0018
3435 0.0024
3306 0.0022
2959 0.081
2353 0.003
2118 0.0017
1722 0.18
1580 0.019
1427 0.08
1256 0.21
1123 0.14
961 0.11
742.7 0.1
634.6
609.4 0.17

Sample NIP

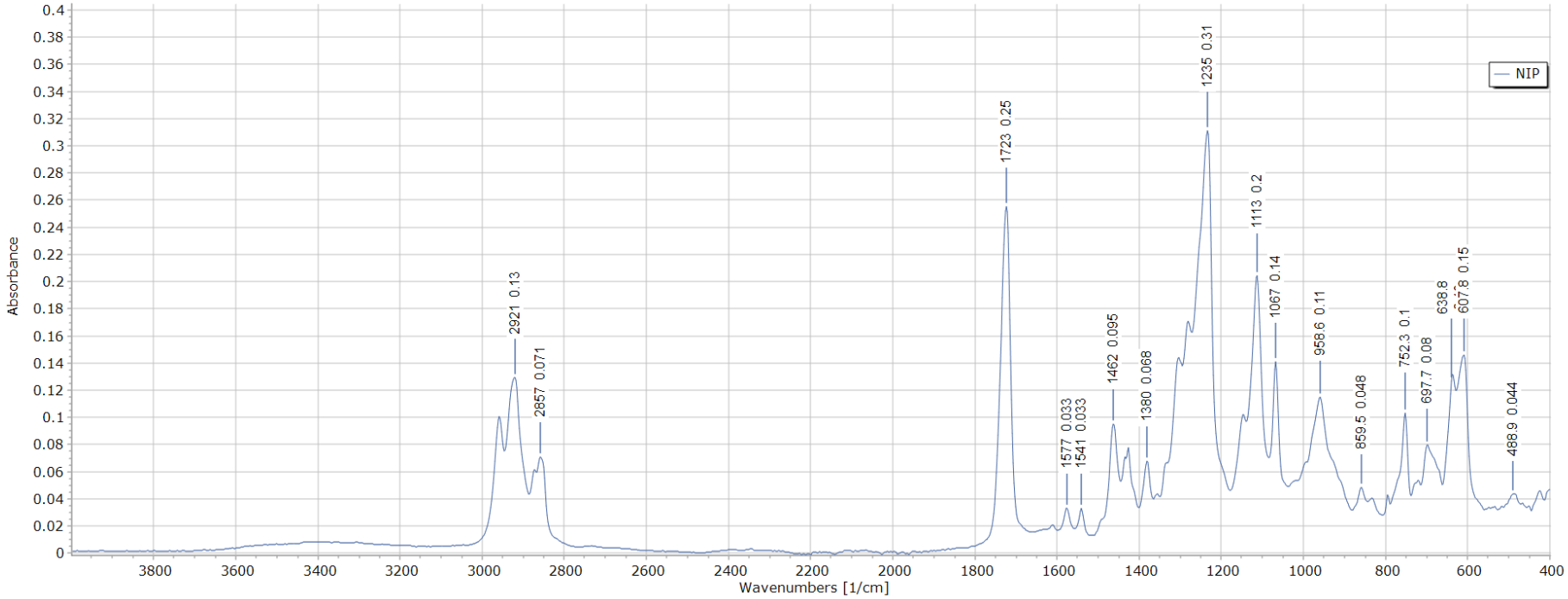
NIP
Absorbance
Wavenumbers [1/cm]
2921 0.13
2857 0.071
1723 0.25
1577 0.033
1541 0.033
1462 0.095
1380 0.068
1235 0.31
1113 0.2
1067 0.14
958.6 0.11
859.5 0.048
752.3 0.1
697.7 0.08
638.8
607.8 0.15
488.9 0.044

Sample NOD

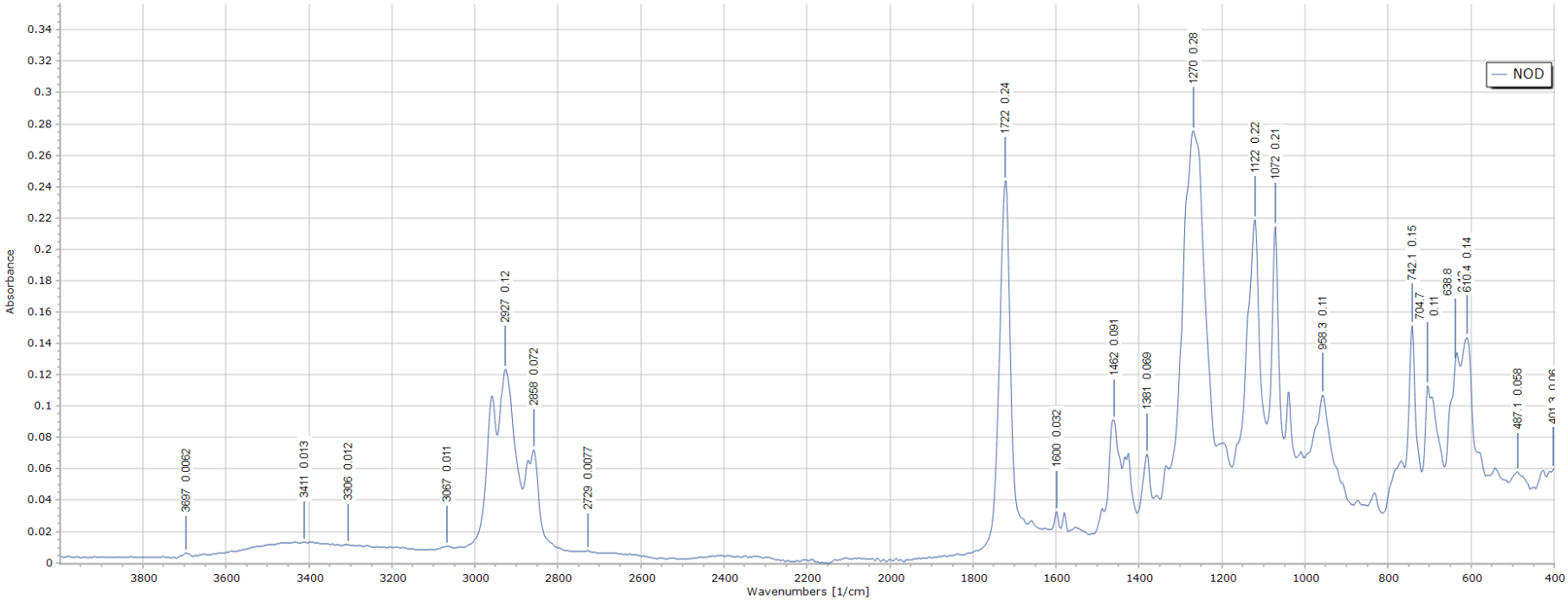
NOD
Absorbance
Wavenumbers [1/cm]
3697 0.0062
3411 0.013
3306 0.012
3067 0.011
2927 0.12
2858 0.072
2729 0.0077
1722 0.24
1600 0.032
1462 0.091
1381 0.069
1270 0.28
1122 0.22
1072 0.21
958.3 0.11
742.1 0.15
704.7 0.11
638.8
610.4 0.14
487.1 0.058

Sample PEN

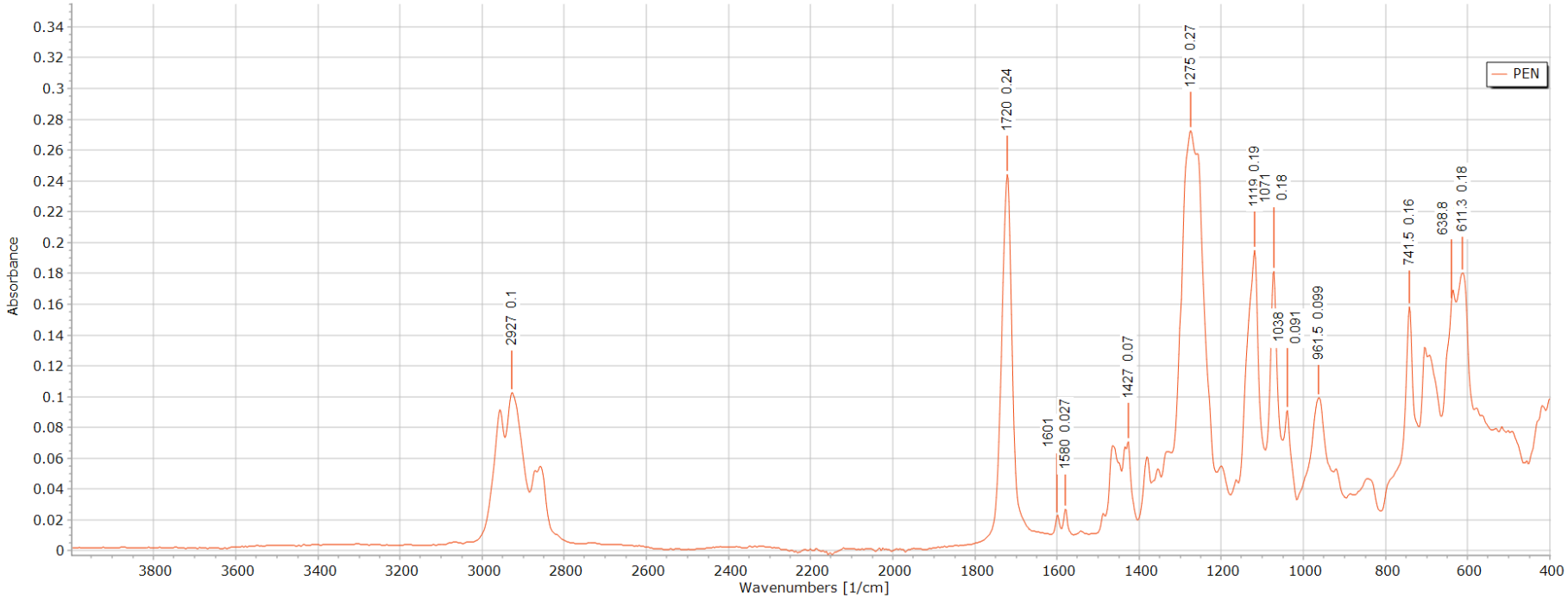
PEN
Absorbance
Wavenumbers [1/cm]
2927 0.1
1720 0.24
1601
1580 0.027
1427 0.07
1275 0.27
1119 0.19
1071
0.18
1038
0.091
961.5 0.099
741.5 0.16
638.8
611.3 0.18

Sample PHC

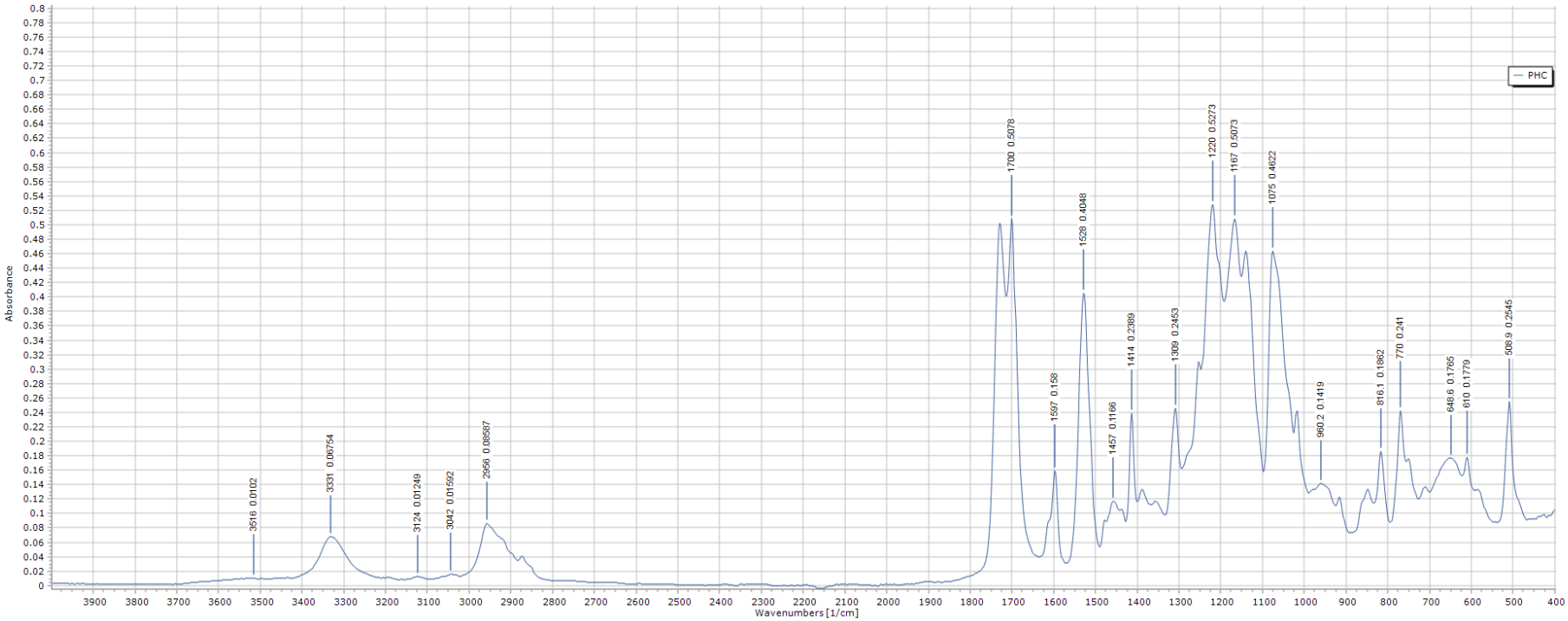
PHC
Absorbance
Wavenumbers [1/cm]
3516 0.0102
3331 0.06754
3124 0.01249
3042 0.01592
2956 0.06587
1700 0.5078
1597 0.158
1528 0.4048
1457 0.1166
1414 0.2389
1309 0.2453
1220 0.5273
1167 0.5073
1075 0.4622
960.2 0.1419
816.1 0.1862
770 0.241
648.6 0.1765
610 0.1779
508.9 0.2545

Sample PIL

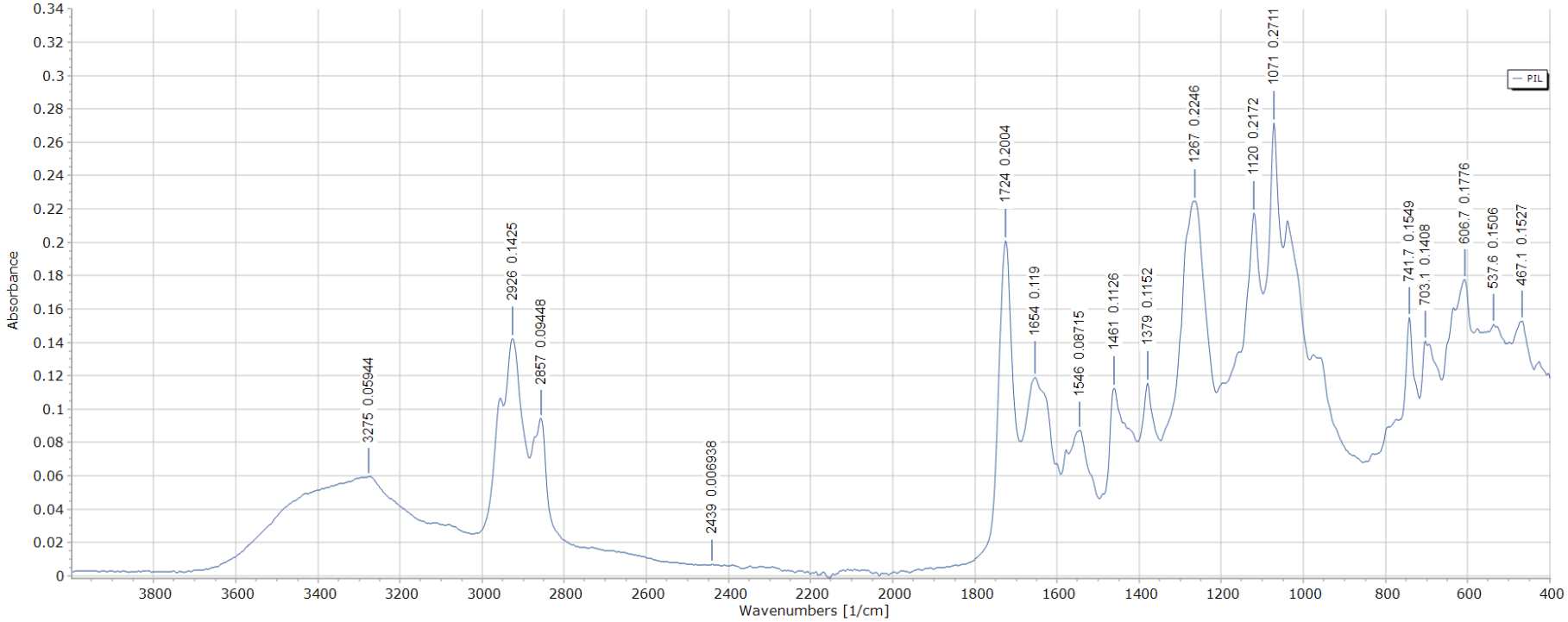
Absorbance
Wavenumbers [1/cm]
PIL
3275 0.05944
2926 0.1425
2857 0.09448
2439 0.006938
1724 0.2004
1654 0.119
1546 0.08715
1461 0.1126
1379 0.1152
1267 0.2246
1120 0.2172
1071 0.2711
741.7 0.1549
703.1 0.1408
606.7 0.1776
537.6 0.1506
467.1 0.1527

Sample PNK

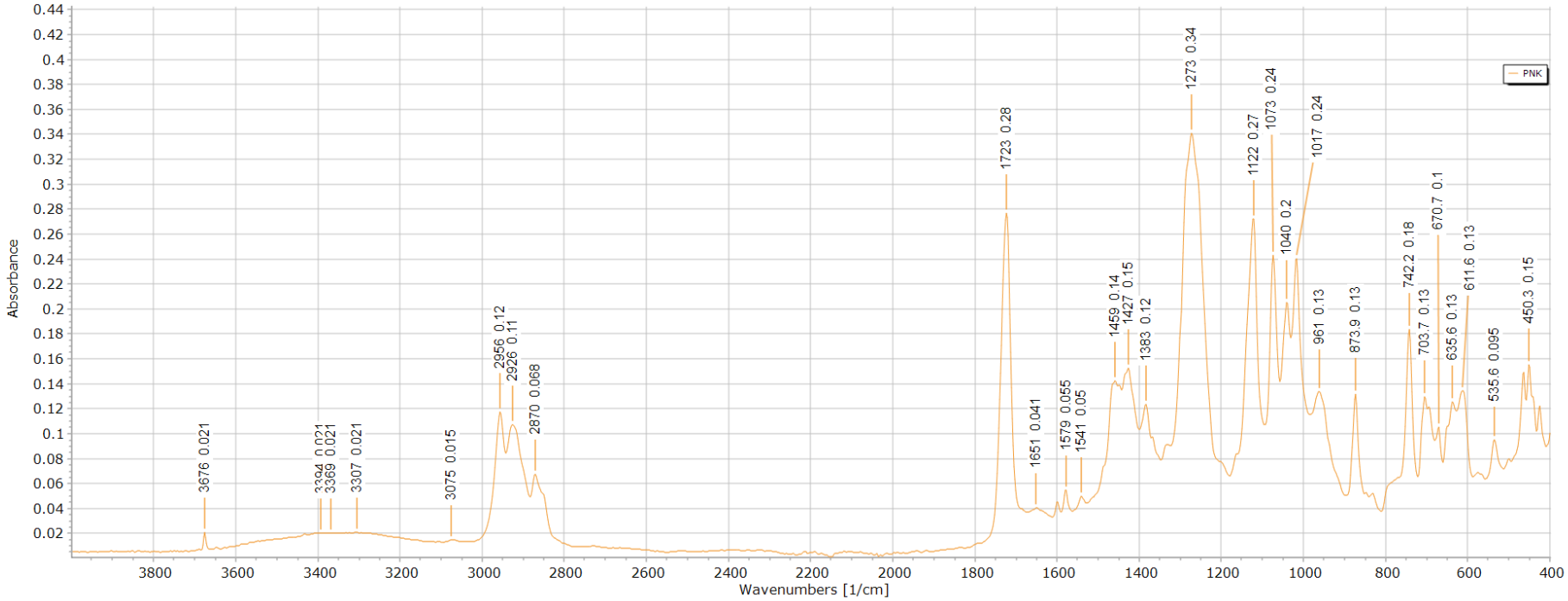
Absorbance
Wavenumbers [1/cm]
PNK
3676 0.021
3394 0.021
3369 0.021
3307 0.021
3075 0.015
2956 0.12
2926 0.11
2870 0.068
1723 0.28
1651 0.041
1579 0.055
1541 0.05
1459 0.14
1427 0.15
1383 0.12
1273 0.34
1122 0.27
1073 0.24
1040 0.2
1017 0.24
961 0.13
873.9 0.13
742.2 0.18
703.7 0.13
670.7 0.1
635.6 0.13
611.6 0.13
535.6 0.095
450.3 0.15

Sample RDC

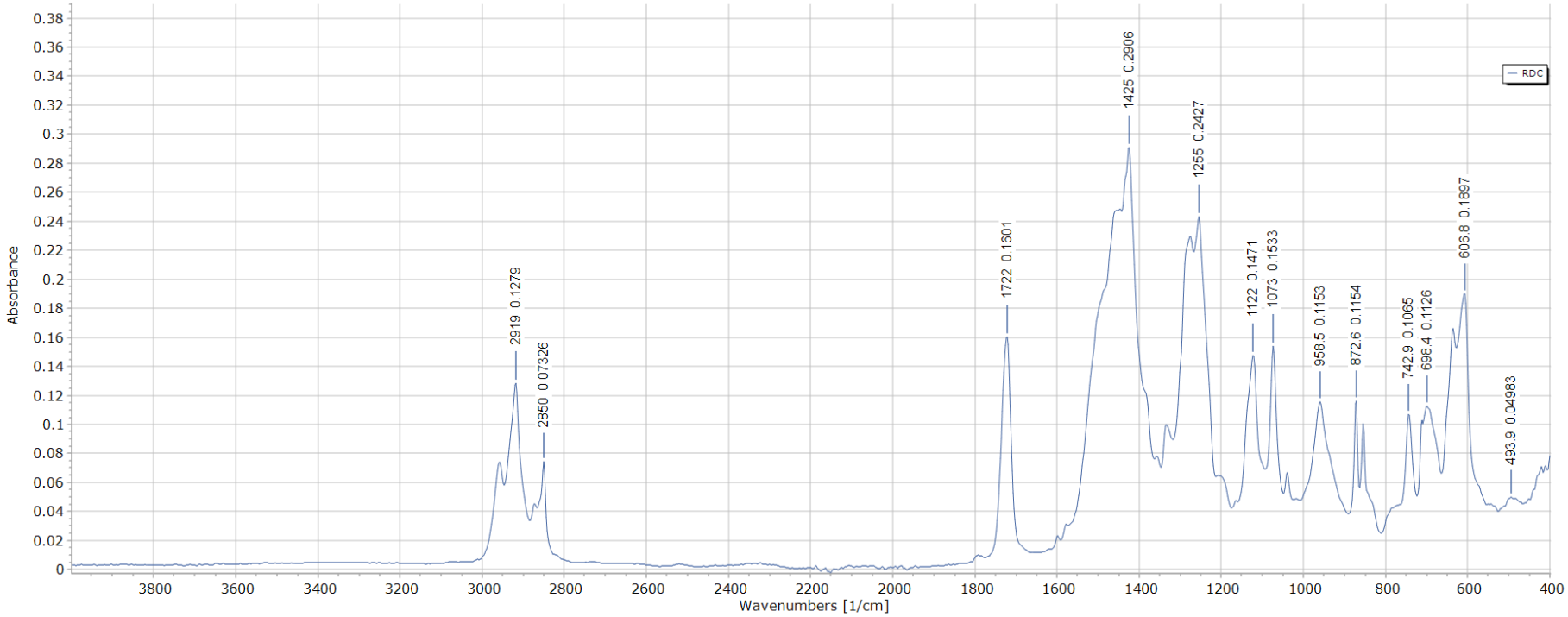
RDC
Absorbance
Wavenumbers [1/cm]
2919 0.1279
2850 0.07326
1722 0.1601
1425 0.2906
1255 0.2427
1122 0.1471
1073 0.1533
958.5 0.1153
872.6 0.1154
742.9 0.1065
698.4 0.1126
606.8 0.1897
493.9 0.04983

Sample SNO

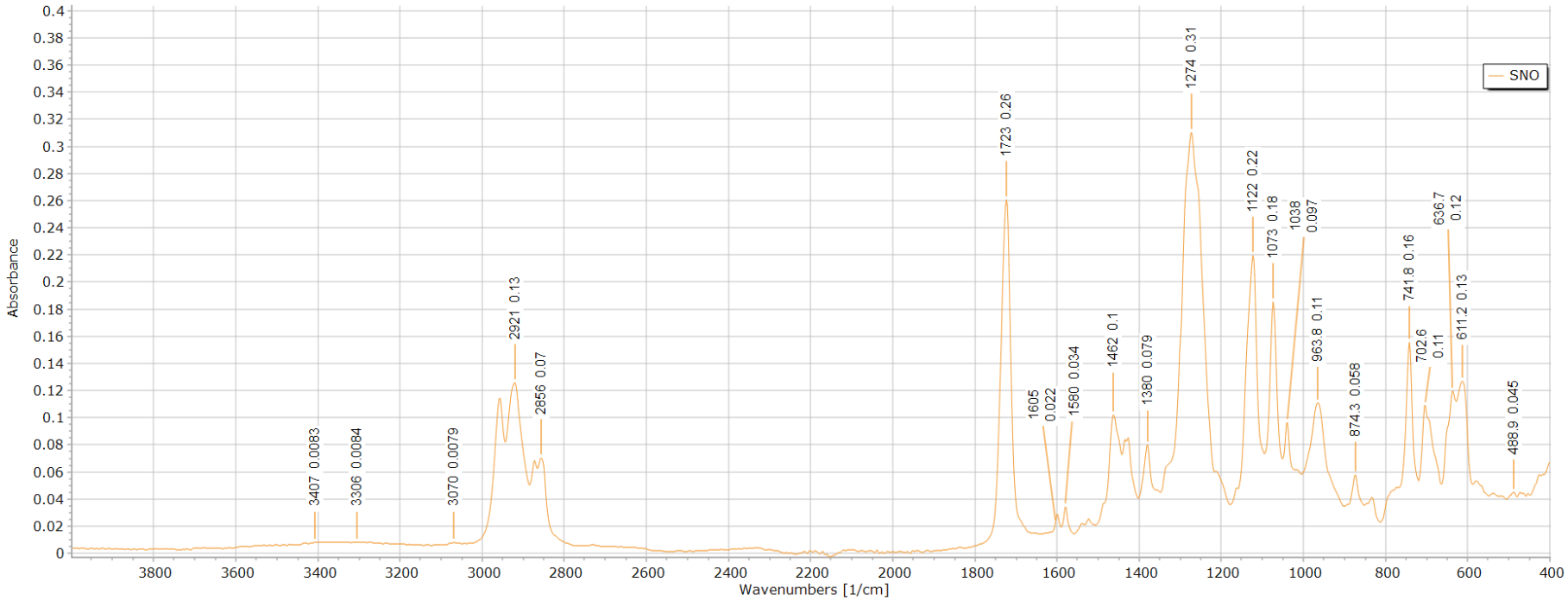
SNO
Absorbance
Wavenumbers [1/cm]
3407 0.0083
3306 0.0084
3070 0.0079
2921 0.13
2856 0.07
1723 0.26
1605 0.022
1580 0.034
1462 0.1
1380 0.079
1274 0.31
1122 0.22
1073 0.18
1038 0.097
963.8 0.11
874.3 0.058
741.8 0.16
702.6 0.11
636.7 0.12
611.2 0.13
488.9 0.045

Sample SUC

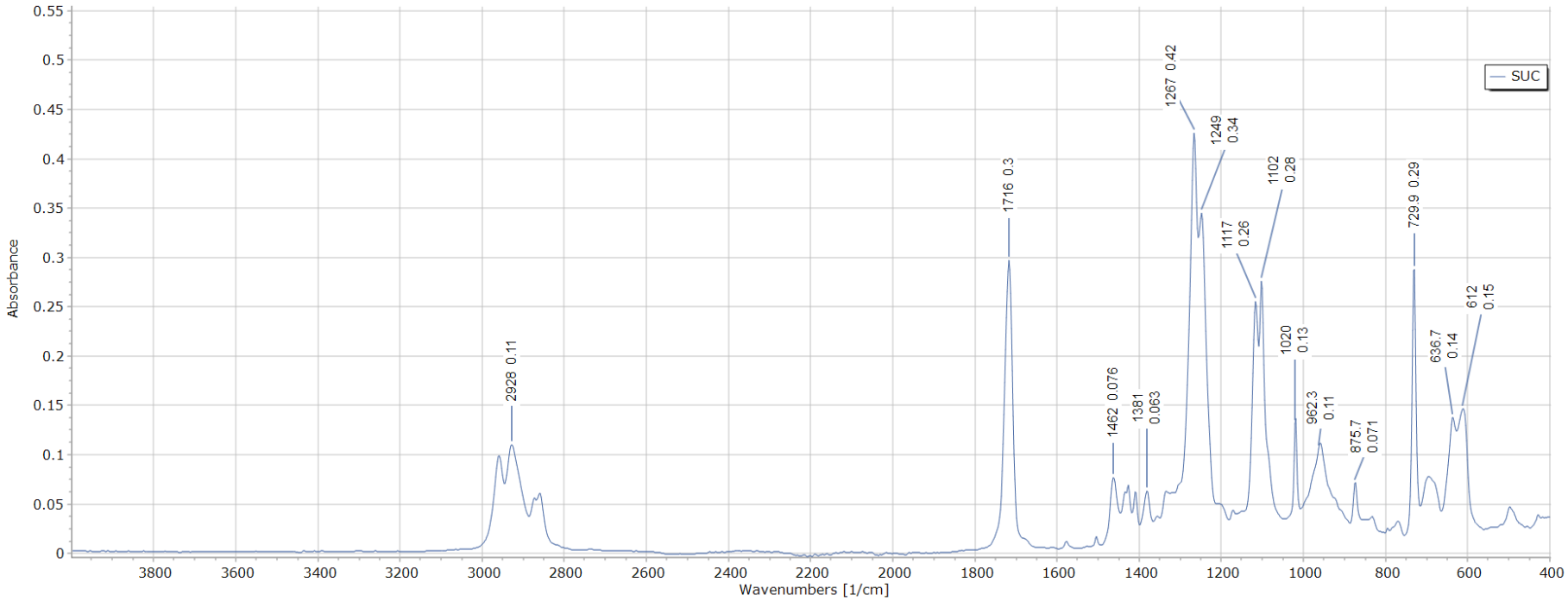
SUC
Absorbance
Wavenumbers [1/cm]
2928 0.11
1716 0.3
1462 0.076
1381 0.063
1267 0.42
1249 0.34
1117 0.26
1102 0.28
1020 0.13
962.3 0.11
875.7 0.071
729.9 0.29
636.7 0.14
612 0.15

Sample TCS

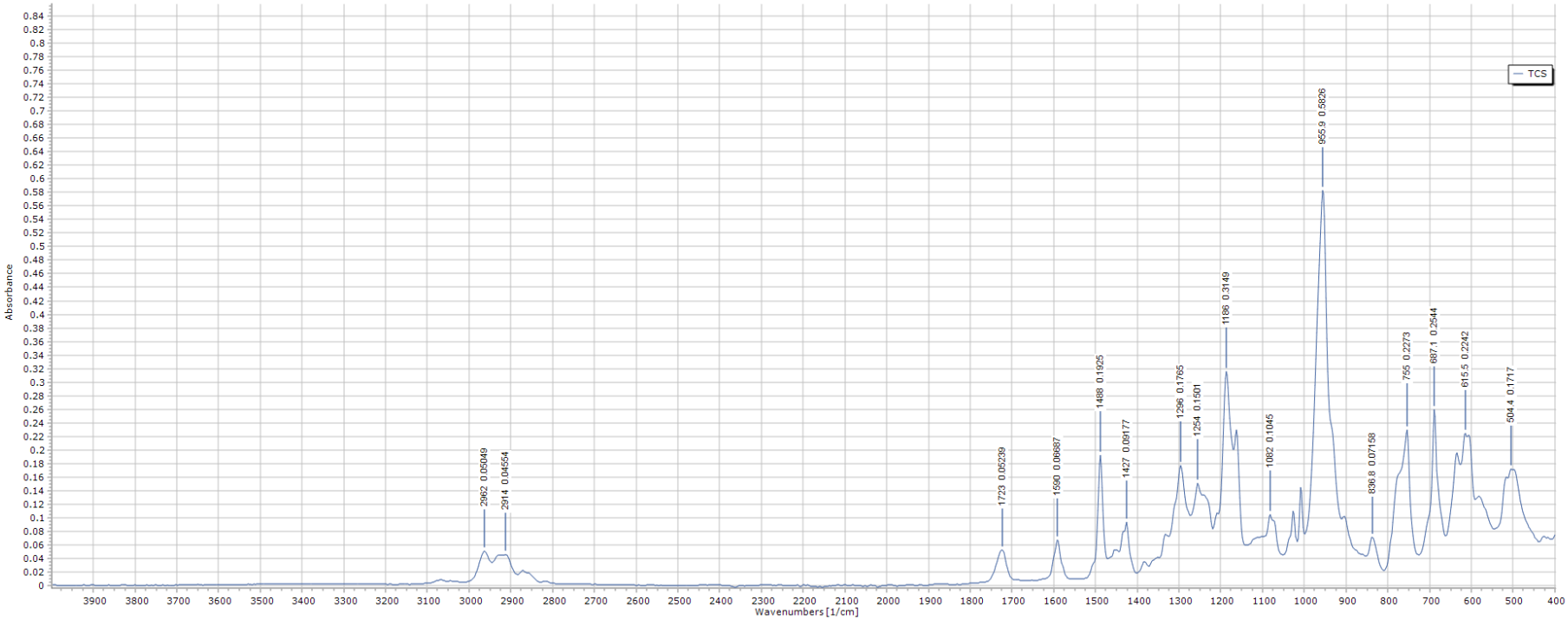
TCS
Absorbance
Wavenumbers [1/cm]
2962 0.05049
2914 0.04554
1723 0.05239
1590 0.06687
1488 0.1925
1427 0.09177
1296 0.1765
1254 0.1501
1186 0.3149
1082 0.1045
955.9 0.6826
836.8 0.07168
755 0.2273
697.1 0.2544
615.5 0.2242
504.4 0.1717

Sample TBW

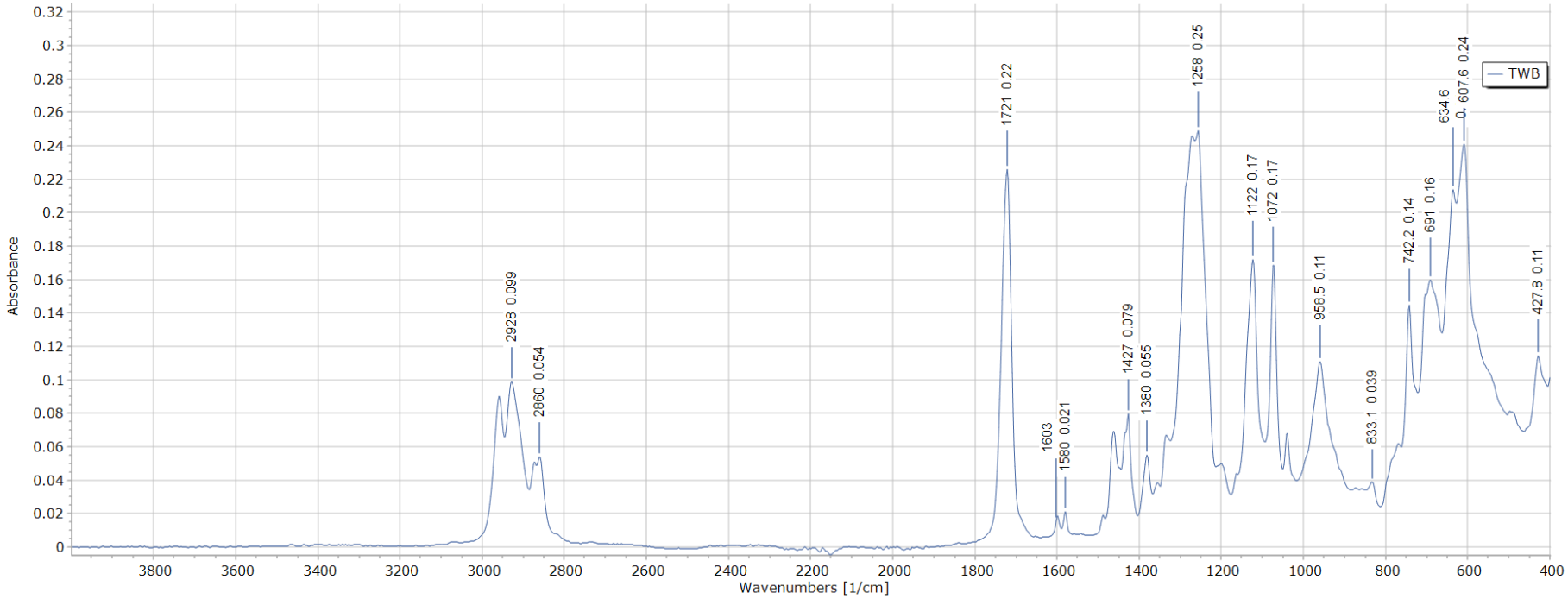
TWB
Absorbance
Wavenumbers [1/cm]
2928 0.099
2860 0.054
1721 0.22
1603
1580 0.021
1427 0.079
1380 0.055
1258 0.25
1122 0.17
1072 0.17
958.5 0.11
833.1 0.039
742.2 0.14
691 0.16
634.6
607.6 0.24
427.8 0.11

Sample VYG

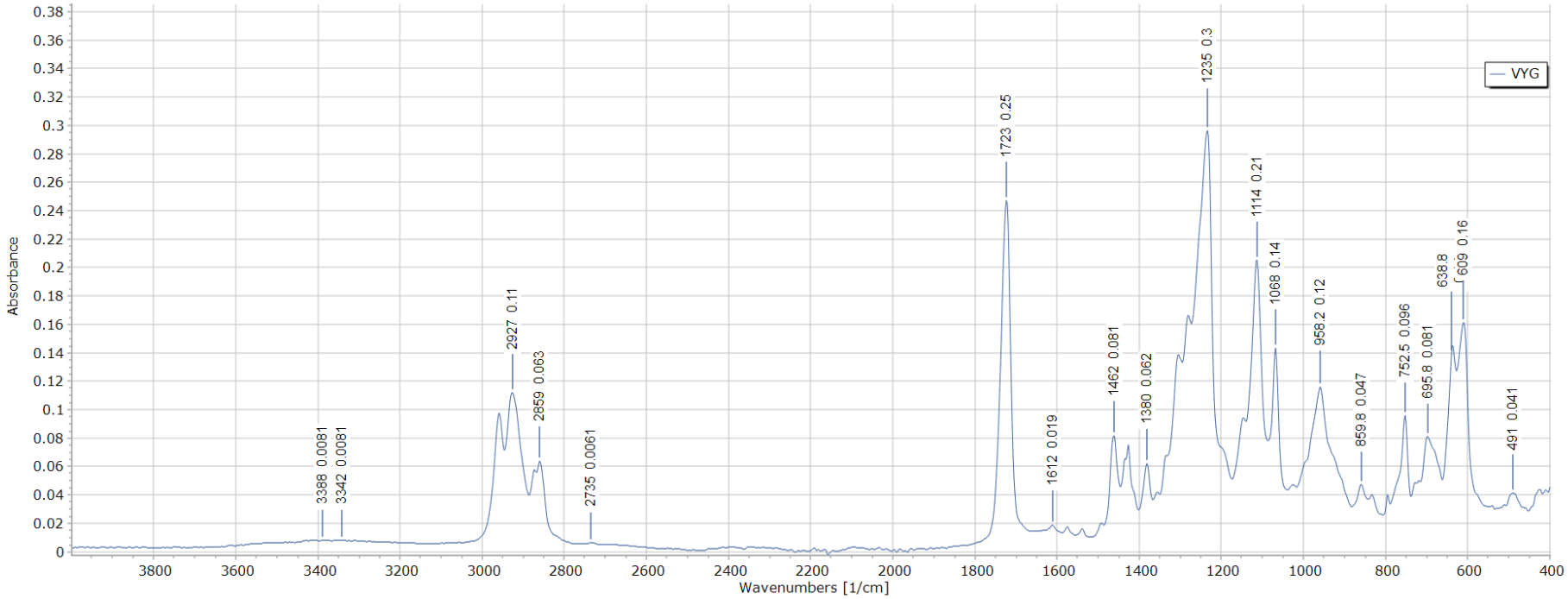
VYG
Absorbance
Wavenumbers [1/cm]
3388 0.0081
3342 0.0081
2927 0.11
2859 0.063
2735 0.0061
1723 0.25
1612 0.019
1462 0.081
1380 0.062
1235 0.3
1114 0.21
1068 0.14
958.2 0.12
859.8 0.047
752.5 0.096
695.8 0.081
638.8
609 0.16
491 0.041

Sample WHD

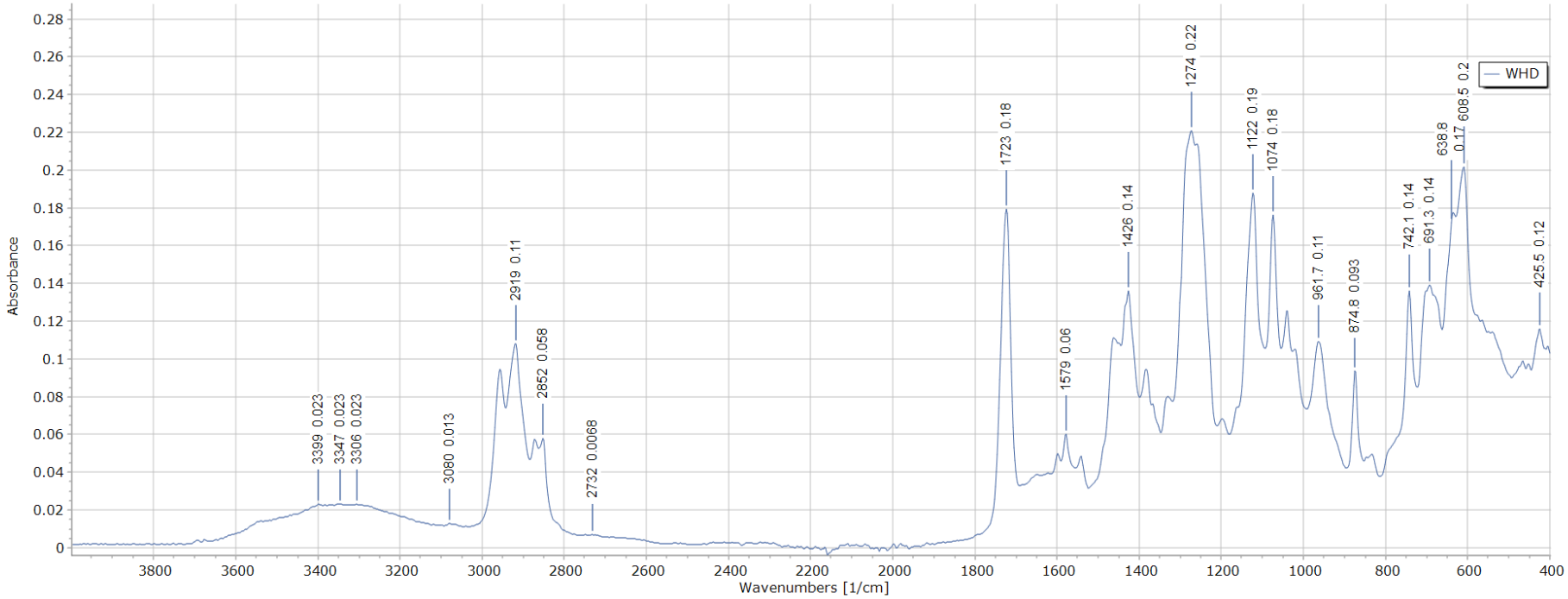
WHD
Absorbance
Wavenumbers [1/cm]
3399 0.023
3347 0.023
3306 0.023
3080 0.013
2919 0.11
2852 0.058
2732 0.0068
1723 0.18
1579 0.06
1426 0.14
1274 0.22
1122 0.19
1074 0.18
961.7 0.11
874.8 0.093
742.1 0.14
691.3 0.14
638.8 0.17
608.5 0.2
425.5 0.12

8.7 KKT - ER-FTIR spectra of samples (1800-400 cm^{-1})

Sample BBI

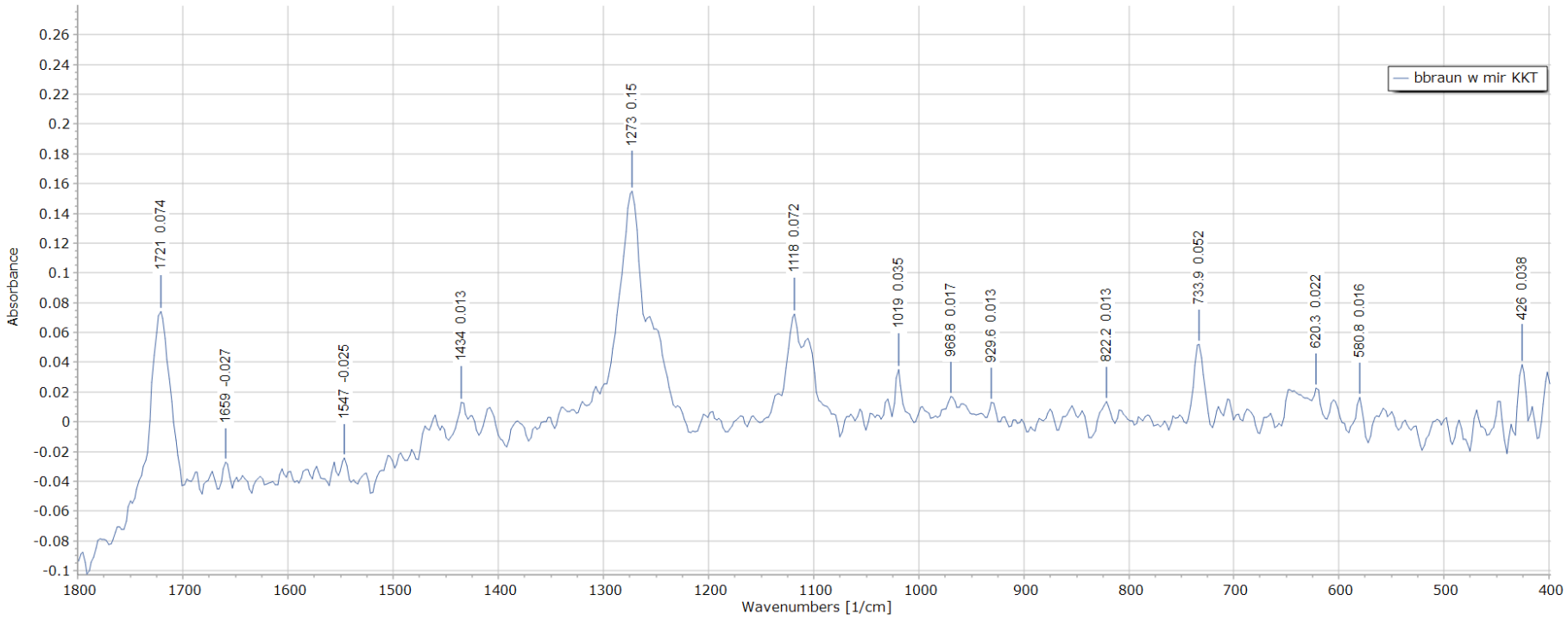

Sample BLK

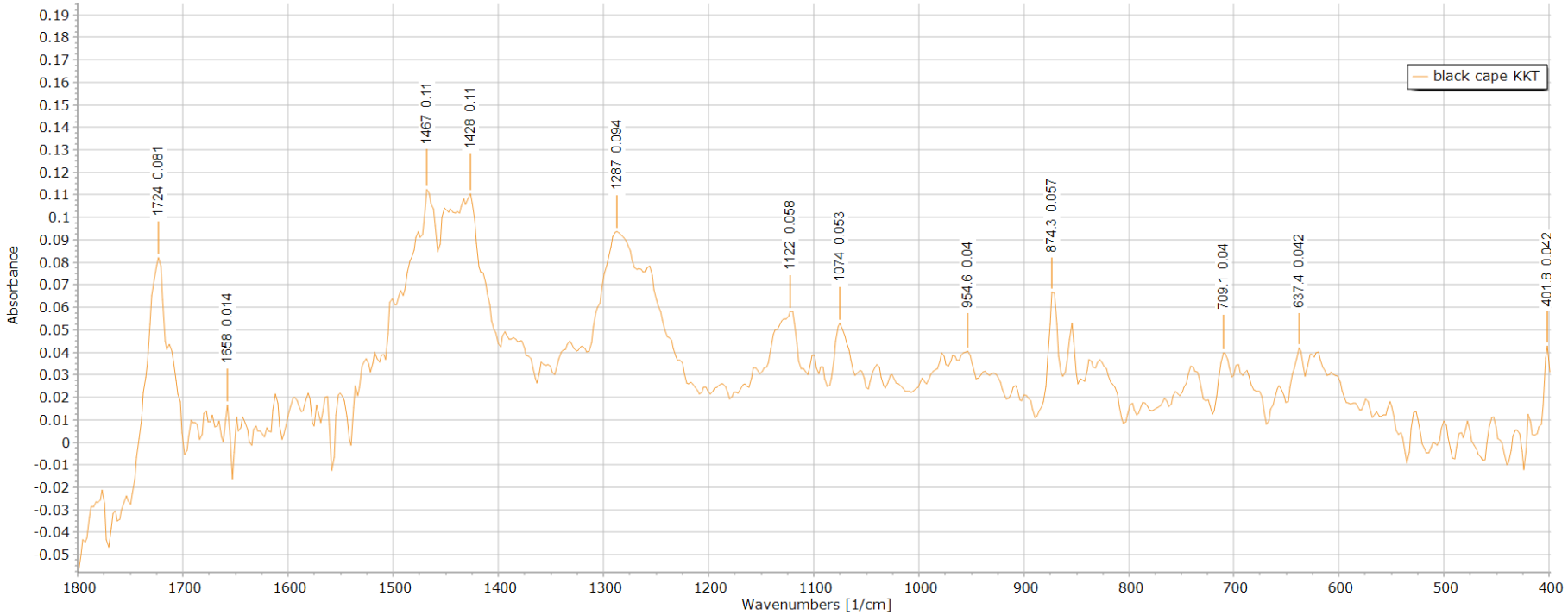
black cape KKT
Absorbance
Wavenumbers [1/cm]
1724 0.081
1658 0.014
1467 0.11
1428 0.11
1287 0.094
1122 0.058
1074 0.053
954.6 0.04
874.3 0.057
709.1 0.04
637.4 0.042
401.8 0.042

Sample COC

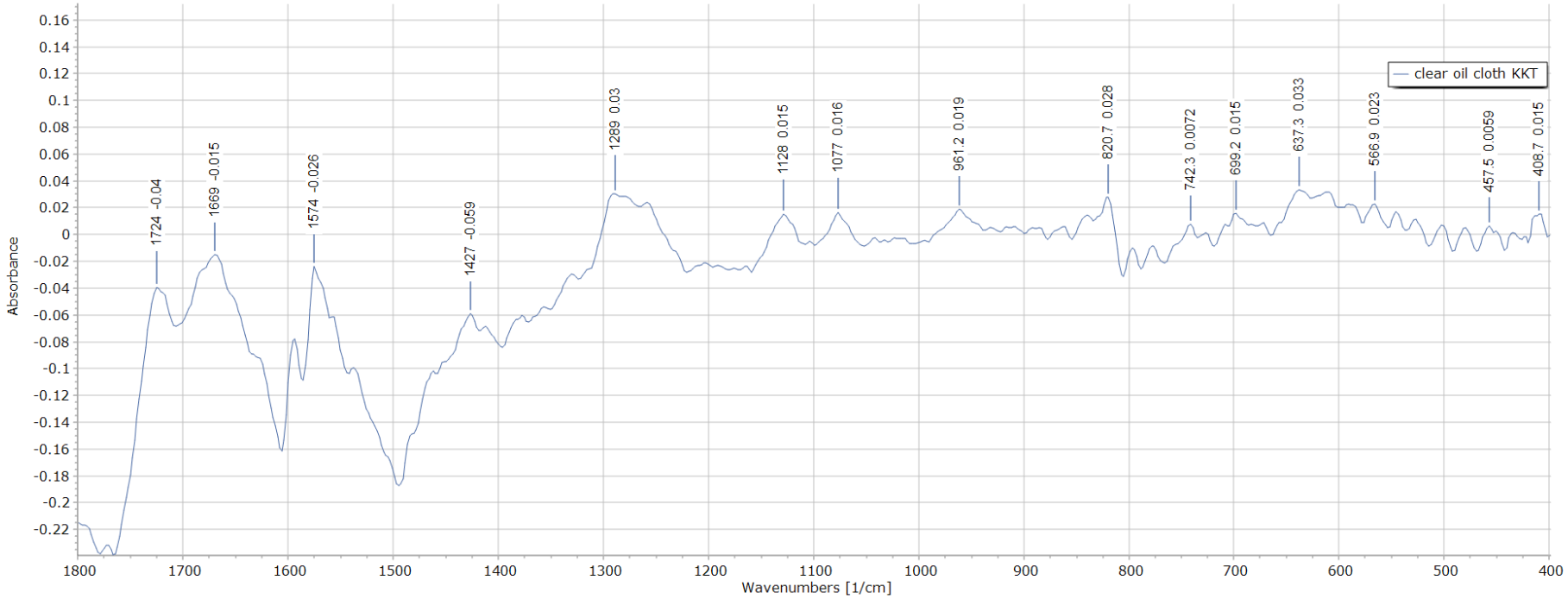
clear oil cloth KKT
Absorbance
Wavenumbers [1/cm]
1724 -0.04
1669 -0.015
1574 -0.026
1427 -0.059
1289 0.03
1128 0.015
1077 0.016
961.2 0.019
820.7 0.028
742.3 0.0072
699.2 0.015
637.3 0.033
566.9 0.023
457.5 0.0059
408.7 0.015

Sample DOD

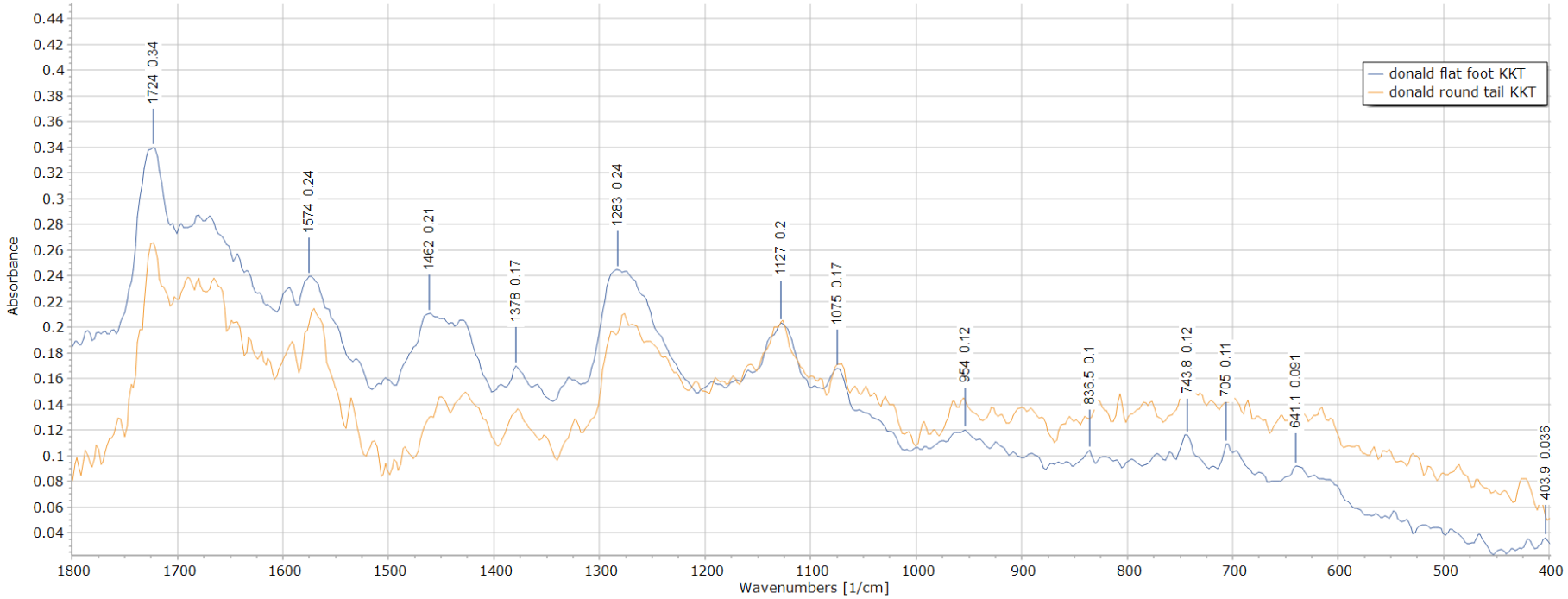
donald flat foot KKT
donald round tail KKT
Absorbance
Wavenumbers [1/cm]
1724 0.34
1574 0.24
1462 0.21
1378 0.17
1283 0.24
1127 0.2
1075 0.17
954 0.12
836.5 0.1
743.8 0.12
705 0.11
641.1 0.091
403.9 0.036

Sample DOG

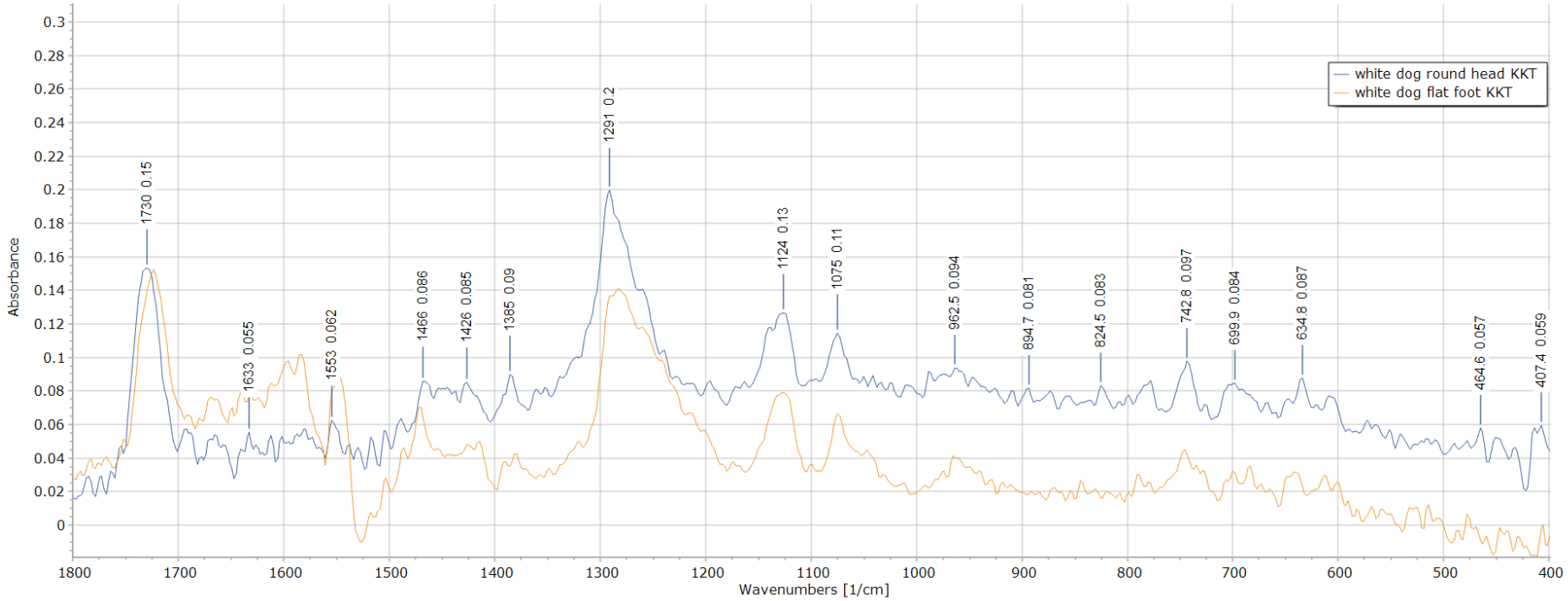
white dog round head KKT
white dog flat foot KKT
Absorbance
Wavenumbers [1/cm]
1730 0.15
1633 0.055
1553 0.062
1466 0.086
1426 0.085
1385 0.09
1291 0.2
1124 0.13
1075 0.11
962.5 0.094
894.7 0.081
824.5 0.083
742.8 0.097
699.9 0.084
634.8 0.087
464.6 0.057
407.4 0.059

Sample ERA

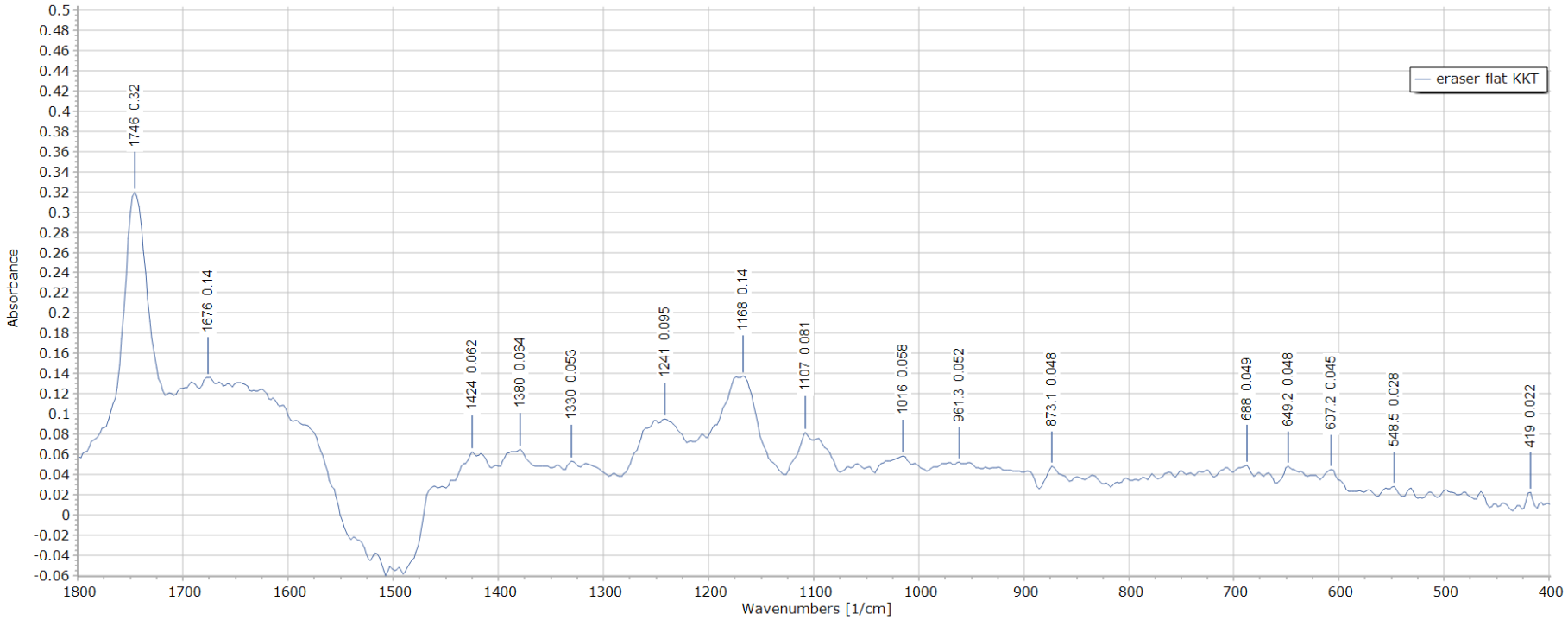
eraser flat KKT
Absorbance
Wavenumbers [1/cm]
1746 0.32
1676 0.14
1424 0.062
1380 0.064
1330 0.053
1241 0.095
1168 0.14
1107 0.081
1016 0.058
961.3 0.052
873.1 0.048
688 0.049
649.2 0.048
607.2 0.045
548.5 0.028
419 0.022

Sample FMO

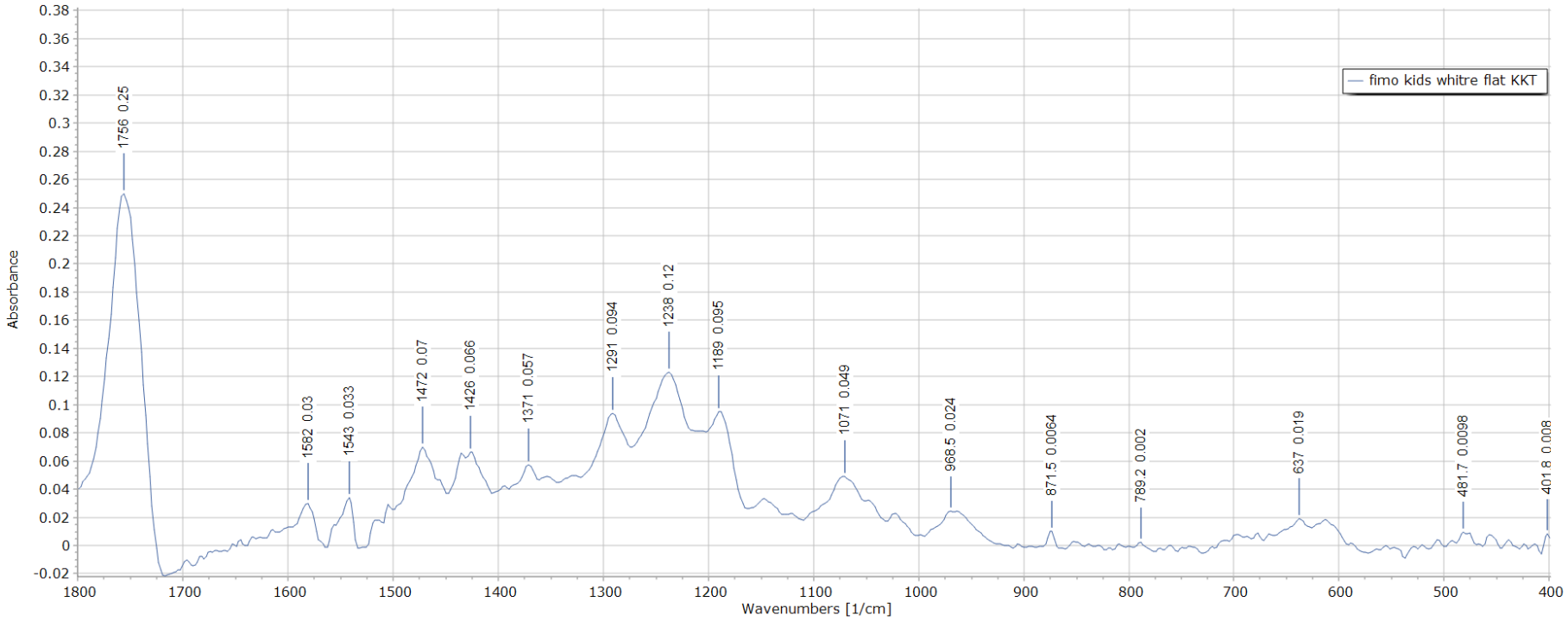
fimo kids whitre flat KKT
Absorbance
Wavenumbers [1/cm]
1756 0.25
1582 0.03
1543 0.033
1472 0.07
1426 0.066
1371 0.057
1291 0.094
1238 0.12
1189 0.095
1071 0.049
968.5 0.024
871.5 0.0064
789.2 0.002
637 0.019
481.7 0.0098
401.8 0.008

Sample GOC

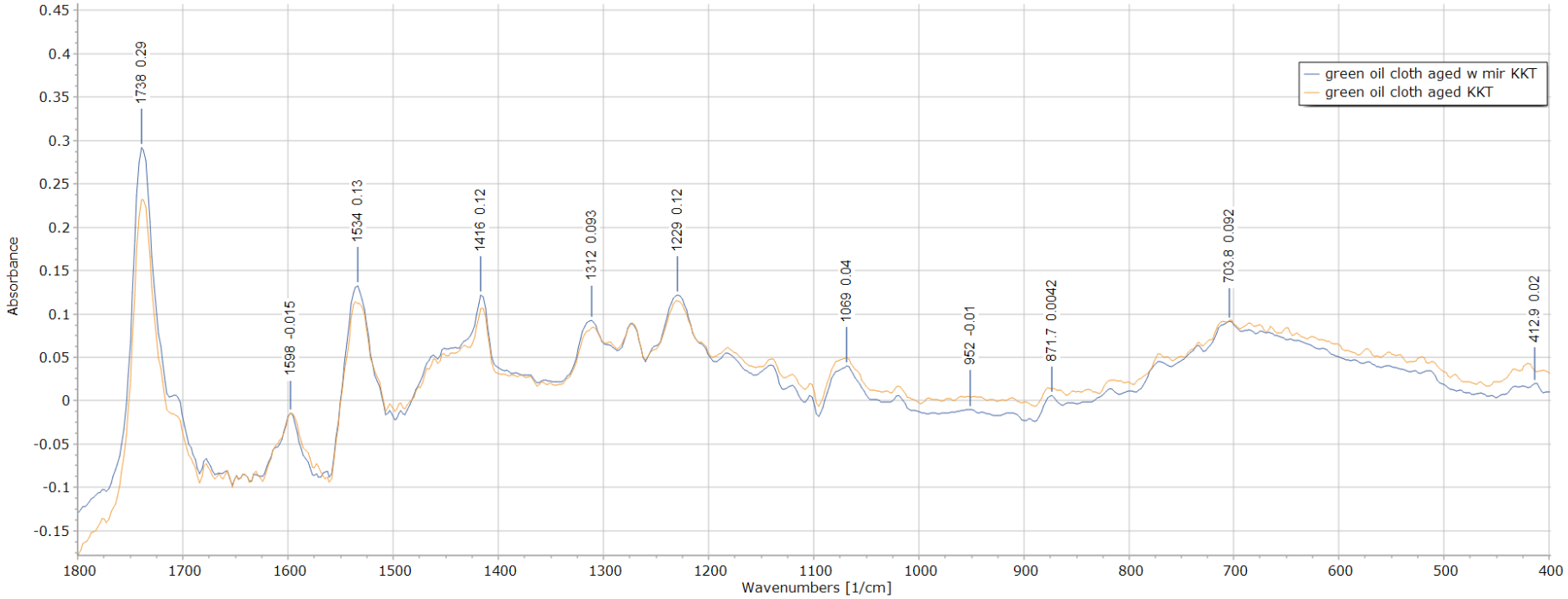
green oil cloth aged w mir KKT
green oil cloth aged KKT
1738 0.29
1598 -0.015
1534 0.13
1416 0.12
1312 0.093
1229 0.12
1069 0.04
952 -0.01
871.7 0.0042
703.8 0.092
412.9 0.02
Absorbance
Wavenumbers [1/cm]

Sample GRG

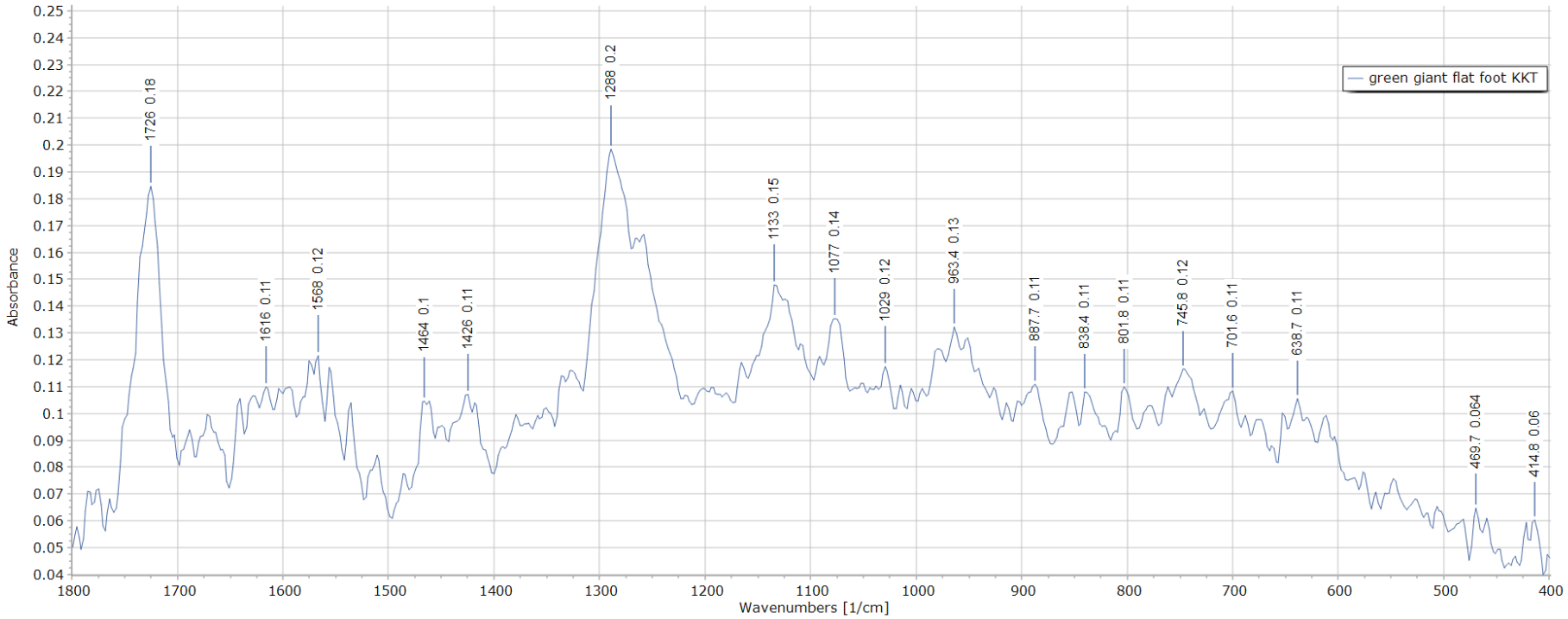
green giant flat foot KKT
Absorbance
Wavenumbers [1/cm]
1726 0.18
1616 0.11
1568 0.12
1464 0.1
1426 0.11
1288 0.2
1133 0.15
1077 0.14
1029 0.12
963.4 0.13
887.7 0.11
838.4 0.11
801.8 0.11
745.8 0.12
701.6 0.11
638.7 0.11
469.7 0.064
414.8 0.06

Sample MCS

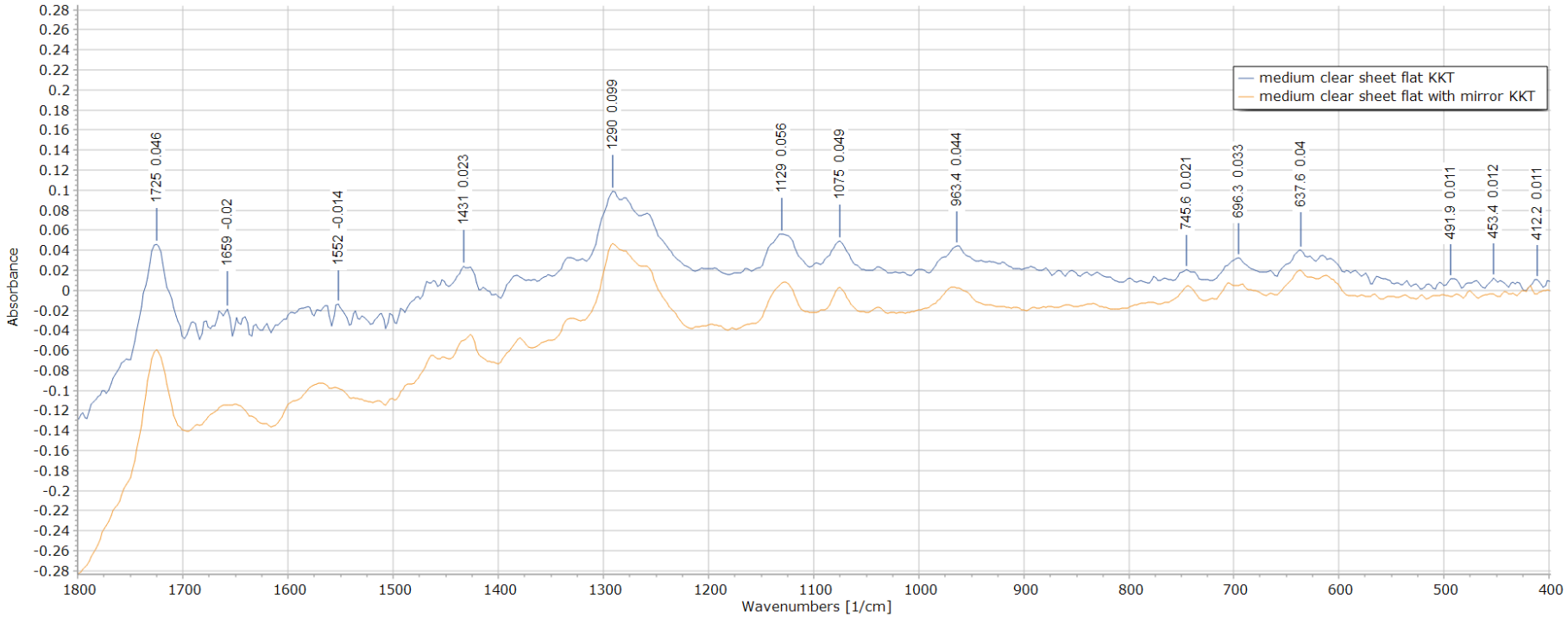
medium clear sheet flat KKT
medium clear sheet flat with mirror KKT
1725 0.046
1659 -0.02
1552 -0.014
1431 0.023
1290 0.099
1129 0.056
1075 0.049
963.4 0.044
745.6 0.021
696.3 0.033
637.6 0.04
491.9 0.011
453.4 0.012
412.2 0.011
Absorbance
Wavenumbers [1/cm]

Sample NOD

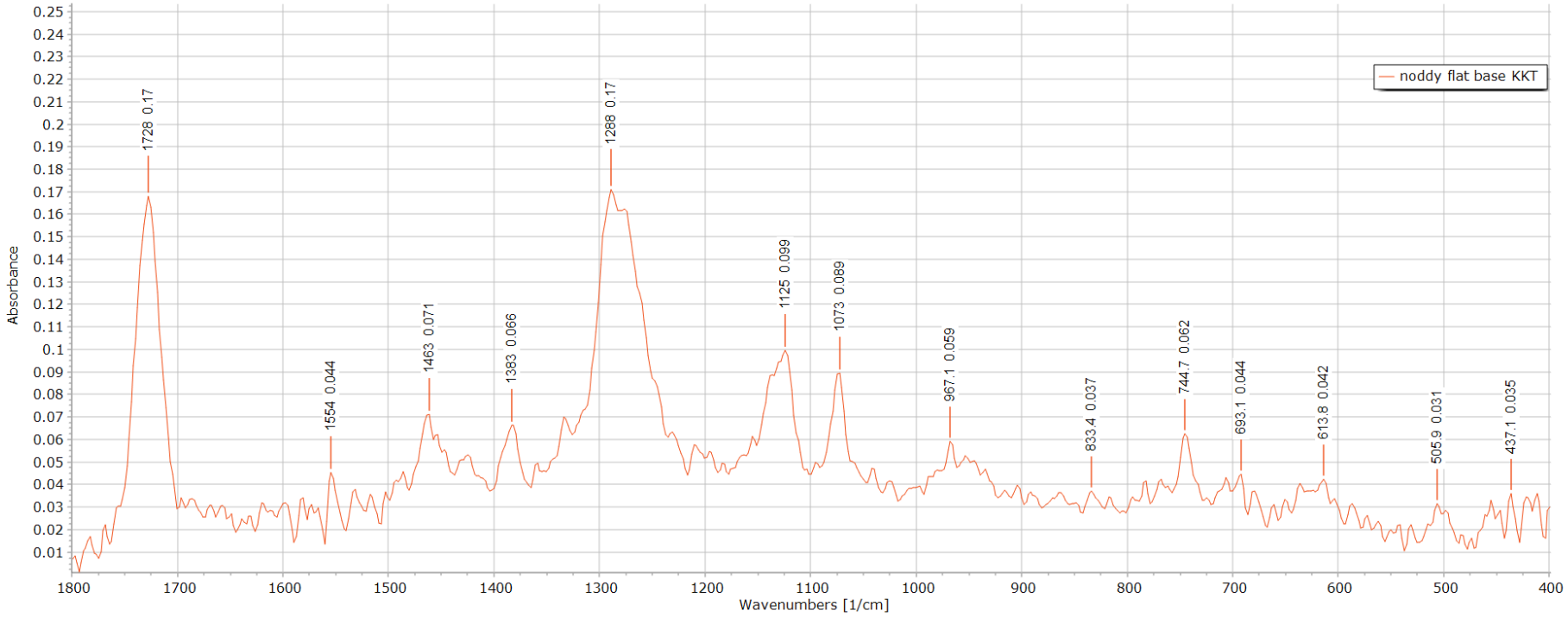
noddy flat base KKT
Absorbance
Wavenumbers [1/cm]
1728 0.17
1554 0.044
1463 0.071
1383 0.066
1288 0.17
1125 0.099
1073 0.089
967.1 0.059
833.4 0.037
744.7 0.062
693.1 0.044
613.8 0.042
505.9 0.031
437.1 0.035

Sample PEN

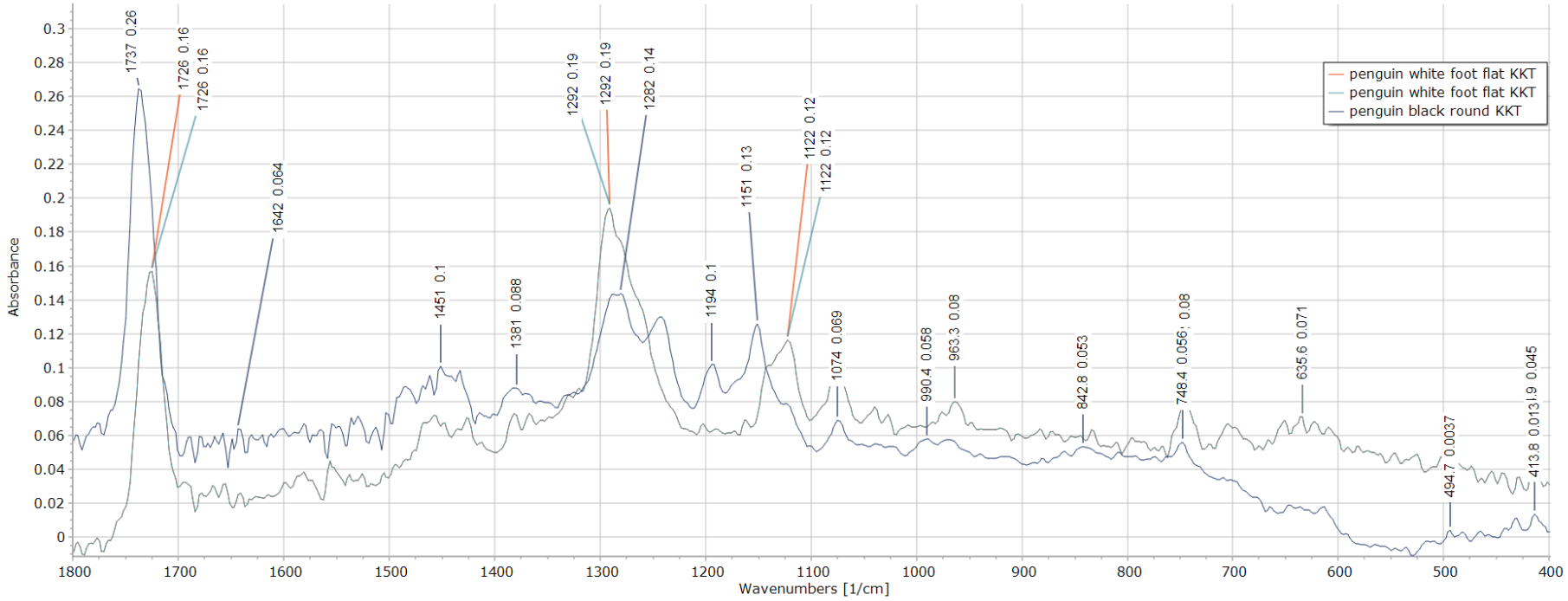
penguin white foot flat KKT
penguin white foot flat KKT
penguin black round KKT
Absorbance
Wavenumbers [1/cm]
1737 0.26
1726 0.16
1726 0.16
1642 0.064
1451 0.1
1381 0.088
1292 0.19
1292 0.19
1282 0.14
1194 0.1
1151 0.13
1122 0.12
1122 0.12
1074 0.069
990.4 0.058
963.3 0.08
842.8 0.053
748.4 0.056
635.6 0.071
494.7 0.0037
413.8 0.045

Sample PHC

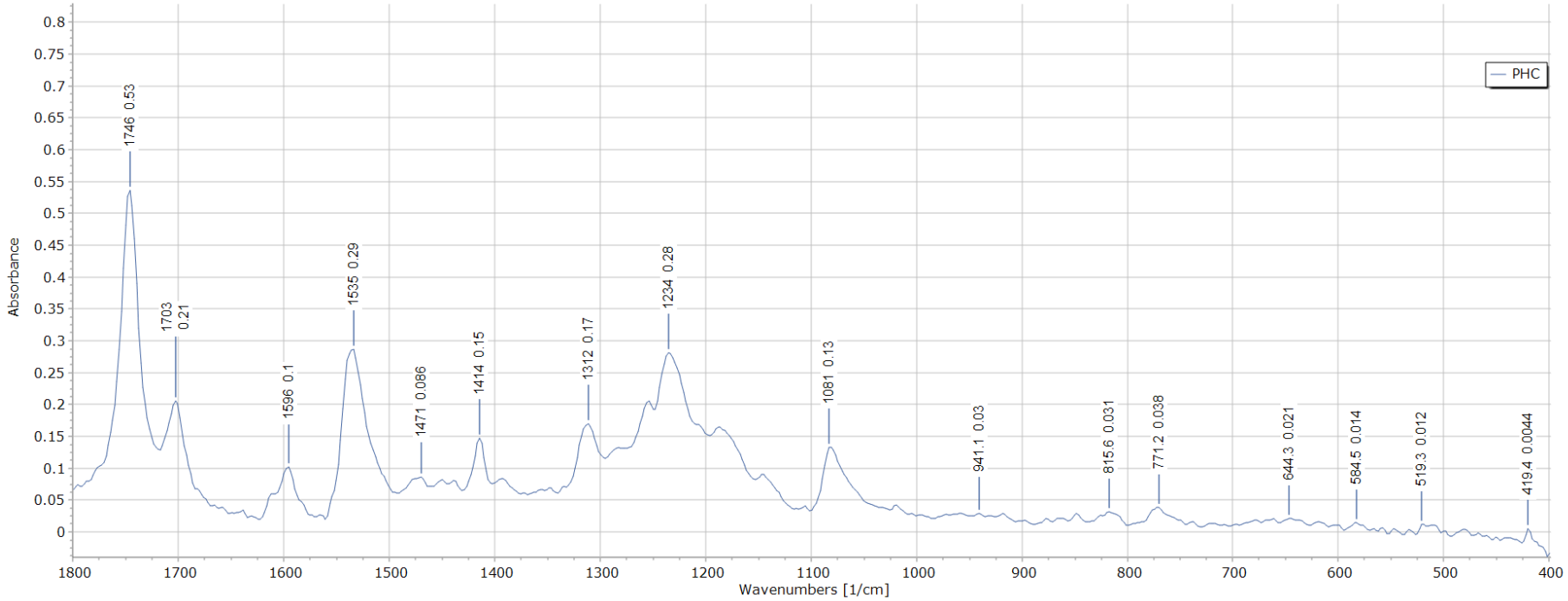
PHC
Absorbance
Wavenumbers [1/cm]
1746 0.53
1703 0.21
1596 0.1
1535 0.29
1471 0.086
1414 0.15
1312 0.17
1234 0.28
1081 0.13
941.1 0.03
815.6 0.031
771.2 0.038
644.3 0.021
584.5 0.014
519.3 0.012
419.4 0.0044

Sample PIL

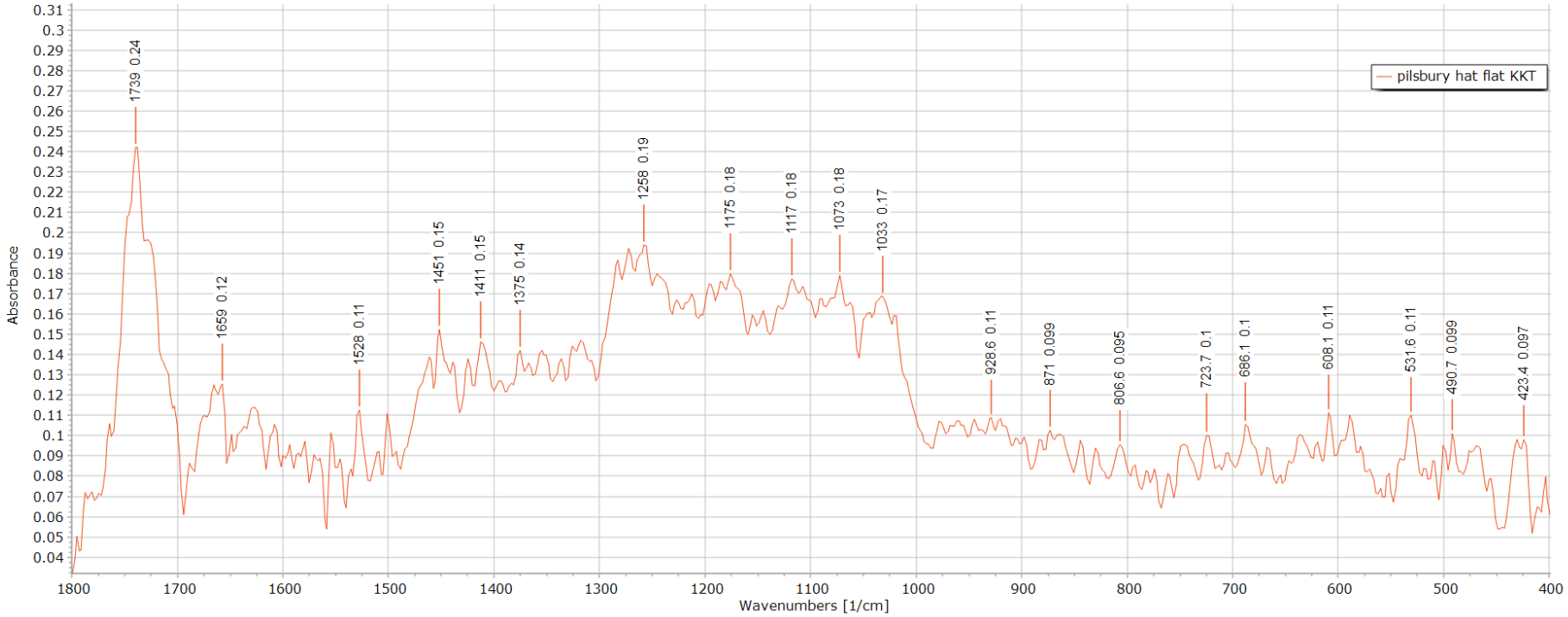
pilsbury hat flat KKT
Absorbance
Wavenumbers [1/cm]
1739 0.24
1659 0.12
1528 0.11
1451 0.15
1411 0.15
1375 0.14
1258 0.19
1175 0.18
1117 0.18
1073 0.18
1033 0.17
928.6 0.11
871 0.099
806.6 0.095
723.7 0.1
686.1 0.1
608.1 0.11
531.6 0.11
490.7 0.099
423.4 0.097

Sample PNK

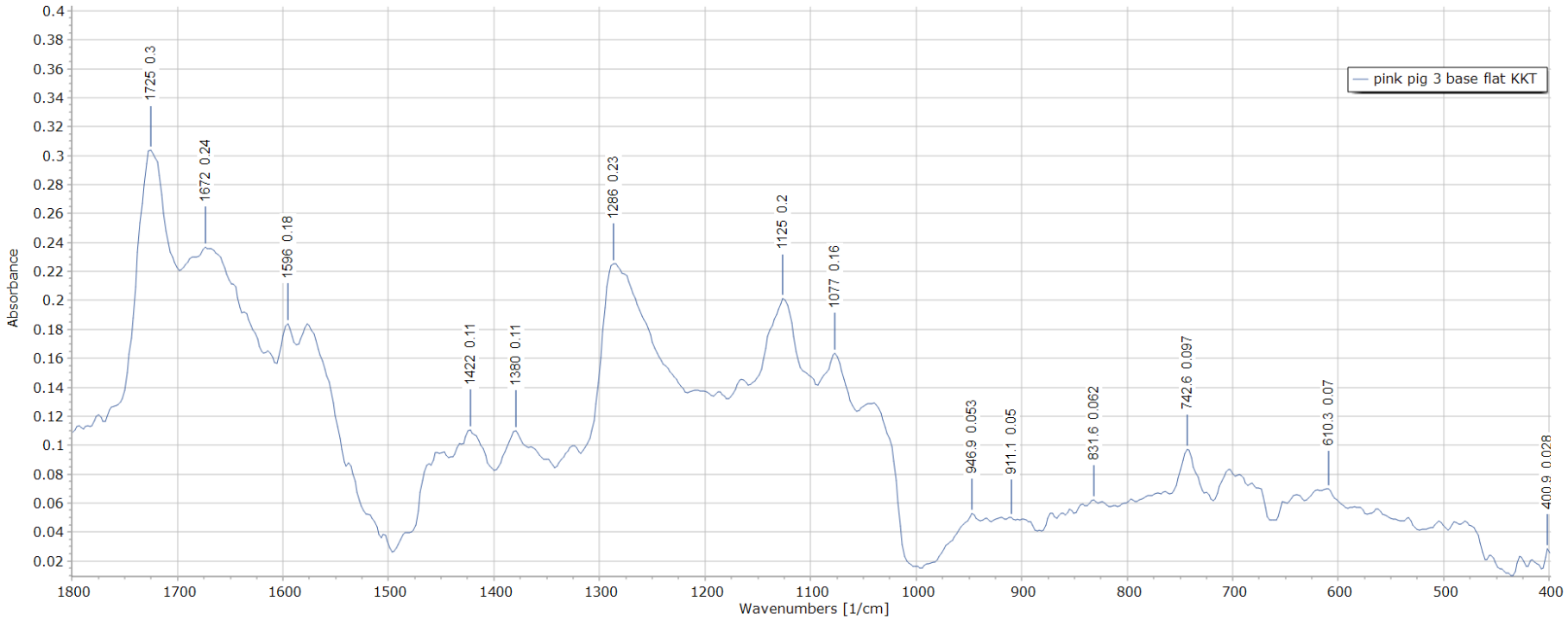
pink pig 3 base flat KKT
Absorbance
Wavenumbers [1/cm]
1725 0.3
1672 0.24
1596 0.18
1422 0.11
1380 0.11
1286 0.23
1125 0.2
1077 0.16
946.9 0.053
911.1 0.05
831.6 0.062
742.6 0.097
610.3 0.07
400.9 0.028

Sample RDC

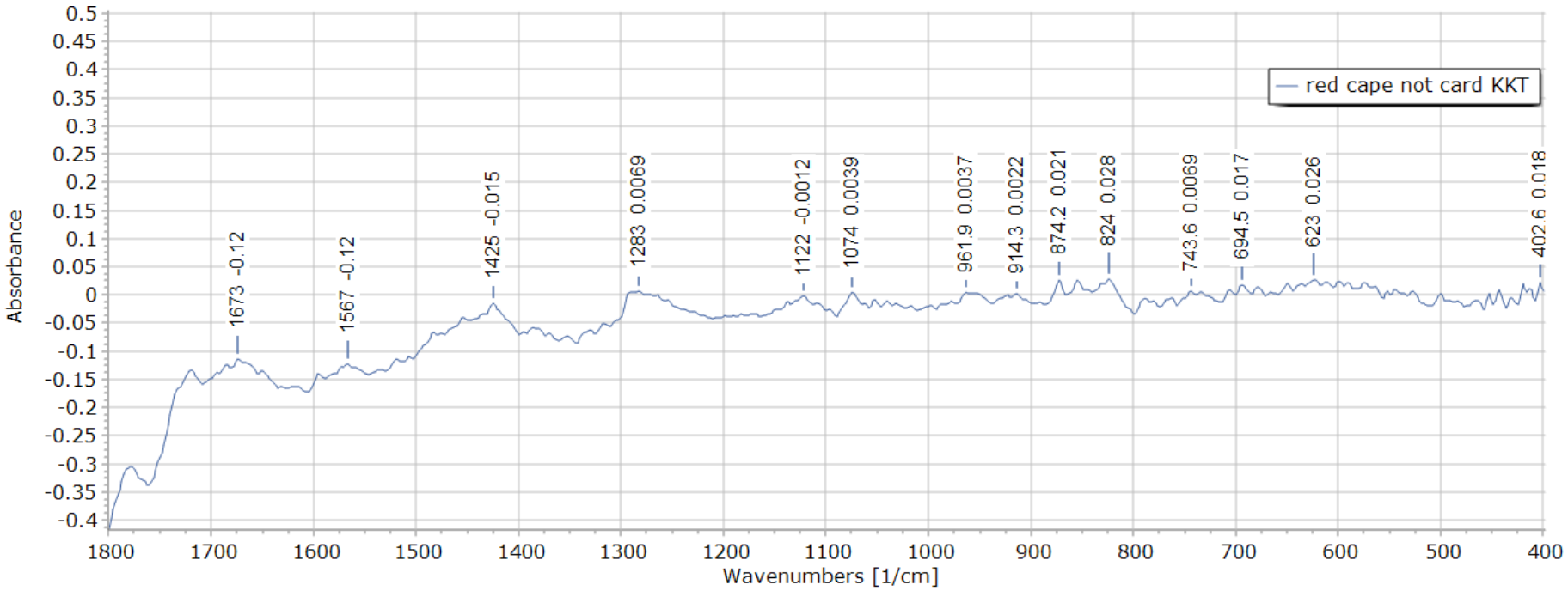
red cape not card KKT
Absorbance
Wavenumbers [1/cm]
1673 -0.12
1567 -0.12
1425 -0.015
1283 0.0069
1122 -0.0012
1074 0.0039
961.9 0.0037
914.3 0.0022
874.2 0.021
824 0.028
743.6 0.0069
694.5 0.017
623 0.026
402.6 0.018

Sample SNO

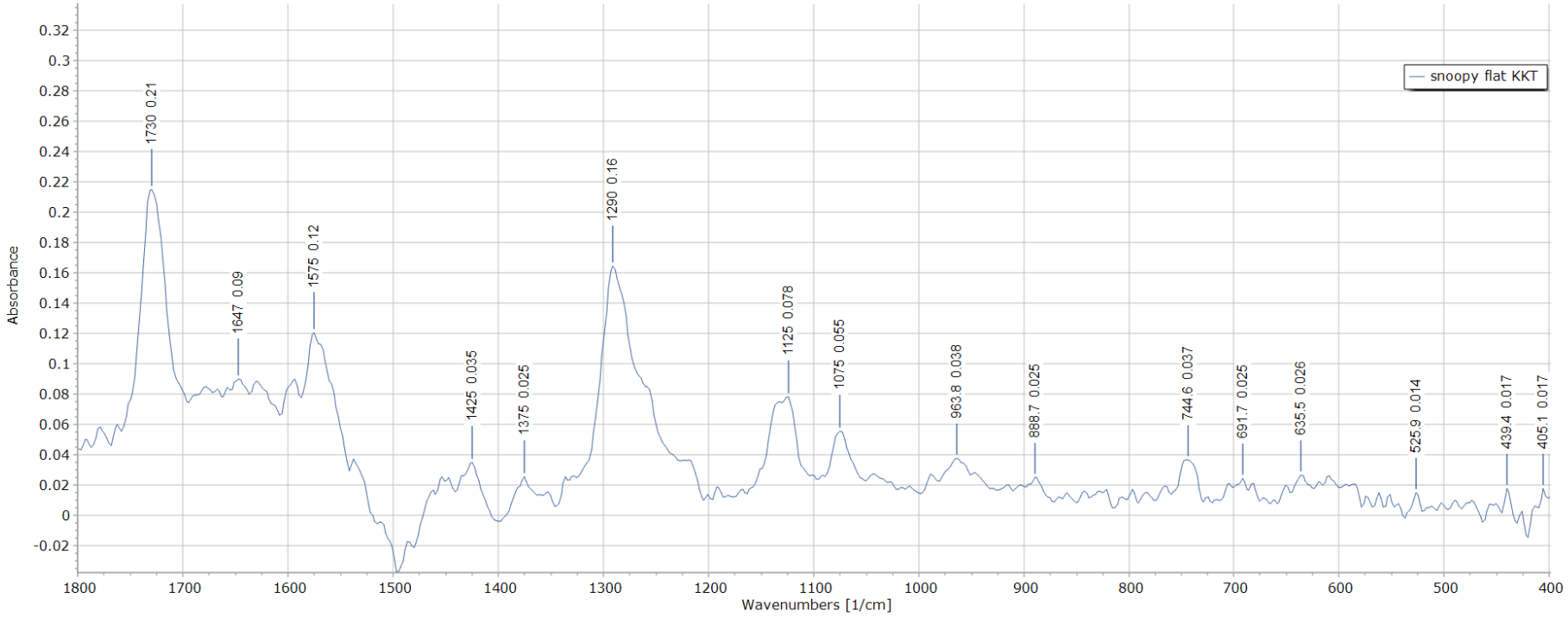
snoopy flat KKT
Absorbance
Wavenumbers [1/cm]
1730 0.21
1647 0.09
1575 0.12
1425 0.035
1375 0.025
1290 0.16
1125 0.078
1075 0.055
963.8 0.038
888.7 0.025
744.6 0.037
691.7 0.025
635.5 0.026
525.9 0.014
439.4 0.017
405.1 0.017

Sample SUC

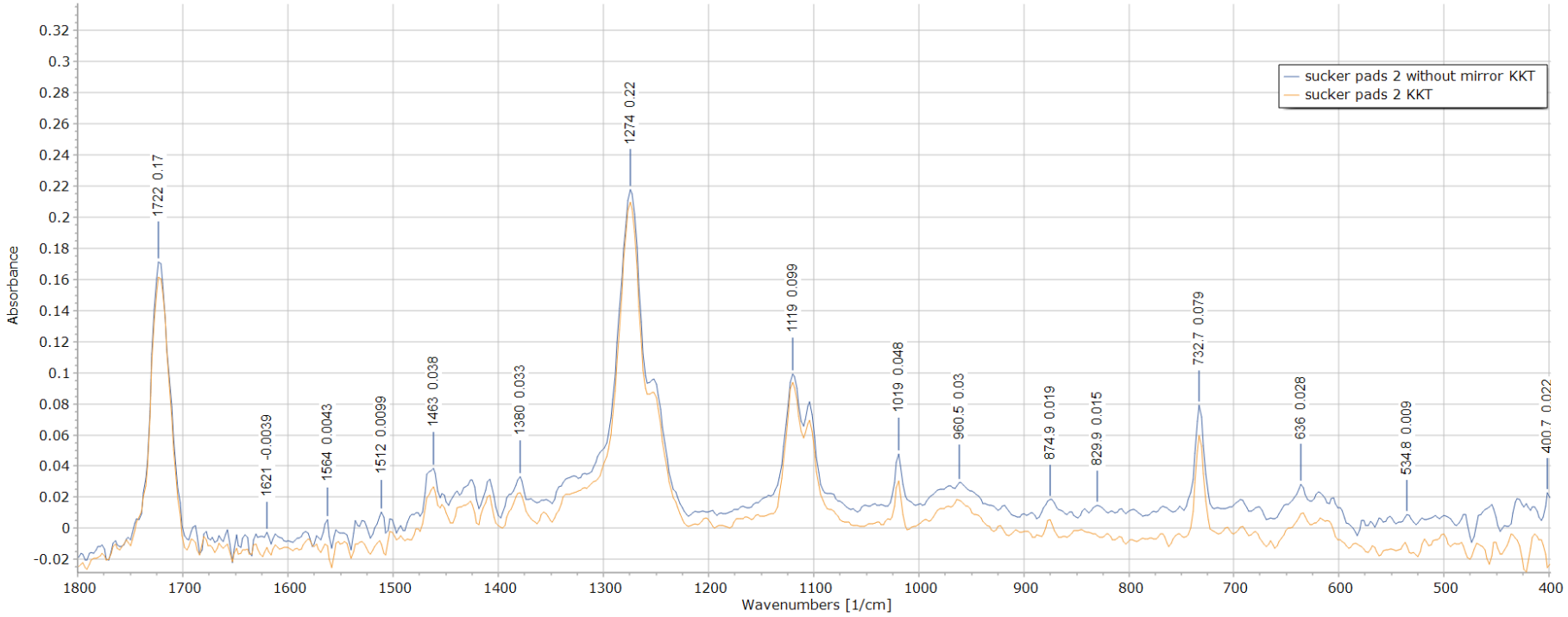
sucker pads 2 without mirror KKT
sucker pads 2 KKT
Absorbance
Wavenumbers [1/cm]
1722 0.17
1621 -0.0039
1564 0.0043
1512 0.0099
1463 0.038
1380 0.033
1274 0.22
1119 0.099
1019 0.048
960.5 0.03
874.9 0.019
829.9 0.015
732.7 0.079
636 0.028
534.8 0.009
400.7 0.022

Sample TCS

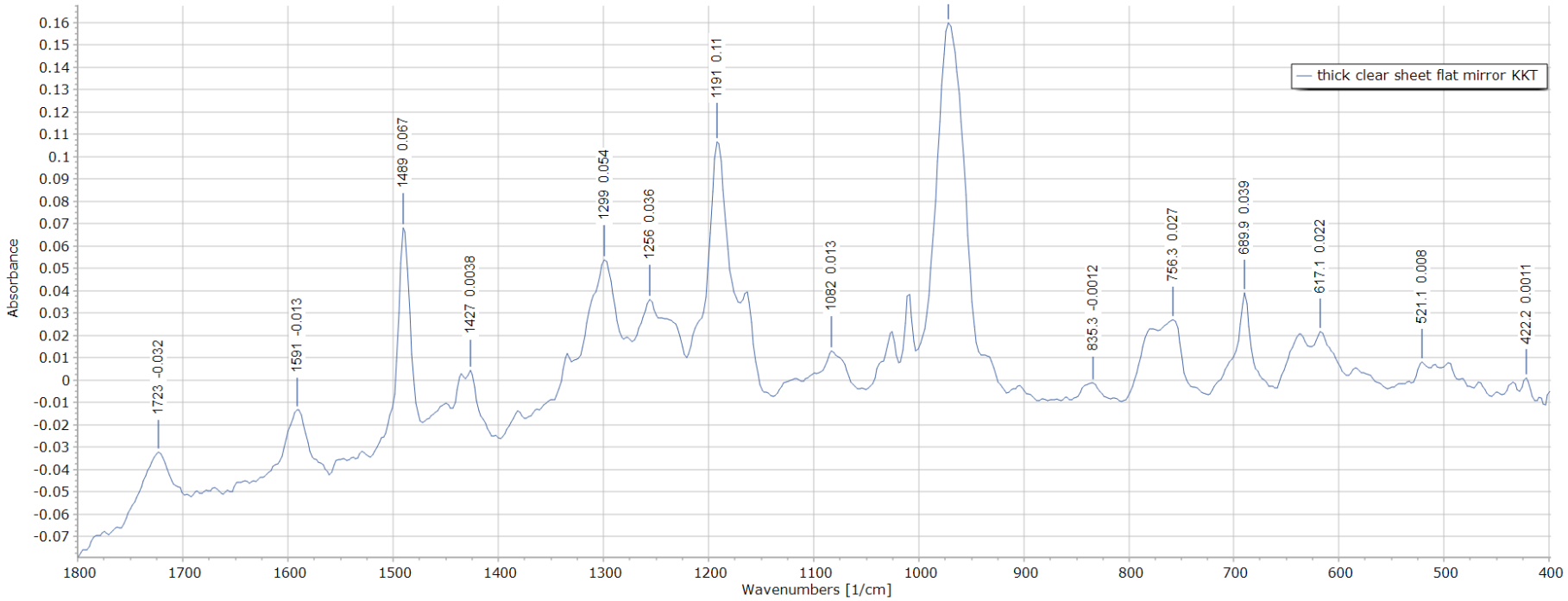
thick clear sheet flat mirror KKT
Absorbance
Wavenumbers [1/cm]
1723 -0.032
1591 -0.013
1489 0.067
1427 0.0038
1299 0.054
1256 0.036
1191 0.11
1082 0.013
835.3 -0.0012
756.3 0.027
689.9 0.039
617.1 0.022
521.1 0.008
422.2 0.0011

Sample WHD

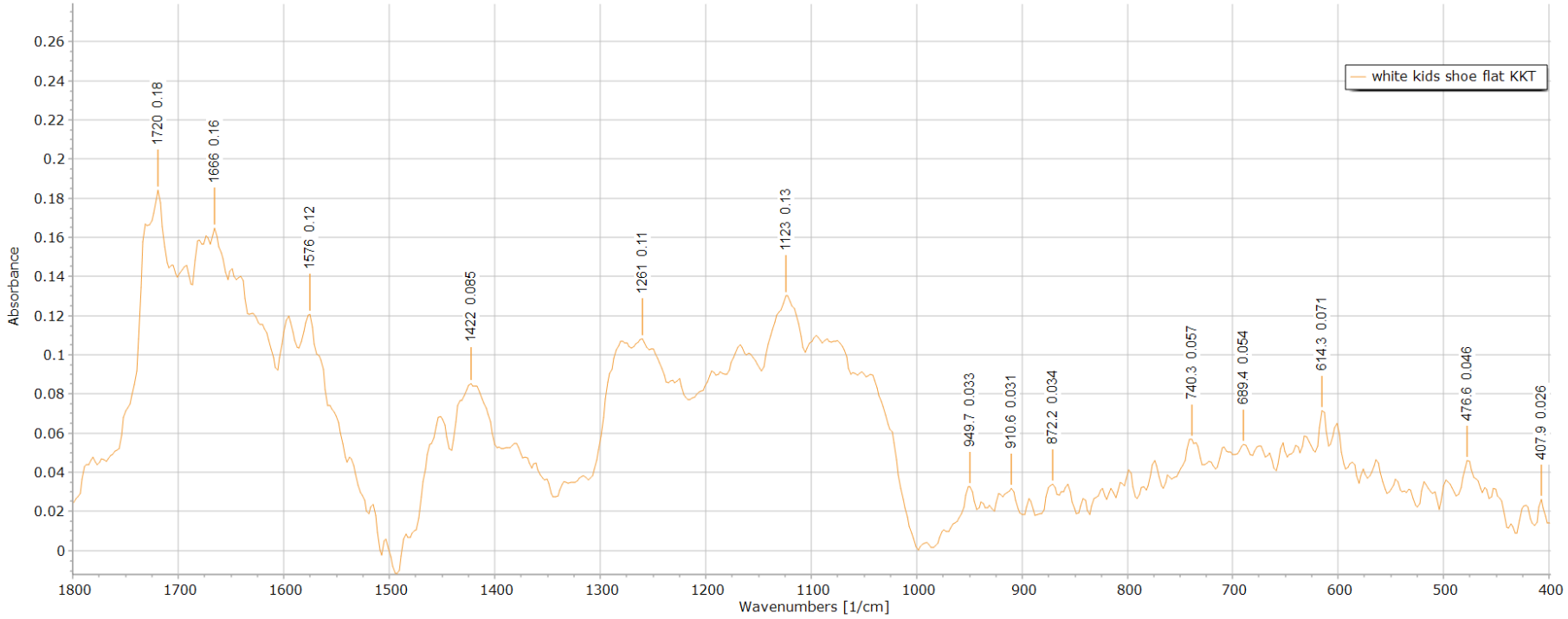
white kids shoe flat KKT
Absorbance
Wavenumbers [1/cm]
1720 0.18
1666 0.16
1576 0.12
1422 0.085
1261 0.11
1123 0.13
949.7 0.033
910.6 0.031
872.2 0.034
740.3 0.057
689.4 0.054
614.3 0.071
476.6 0.046
407.9 0.026

Sample YED

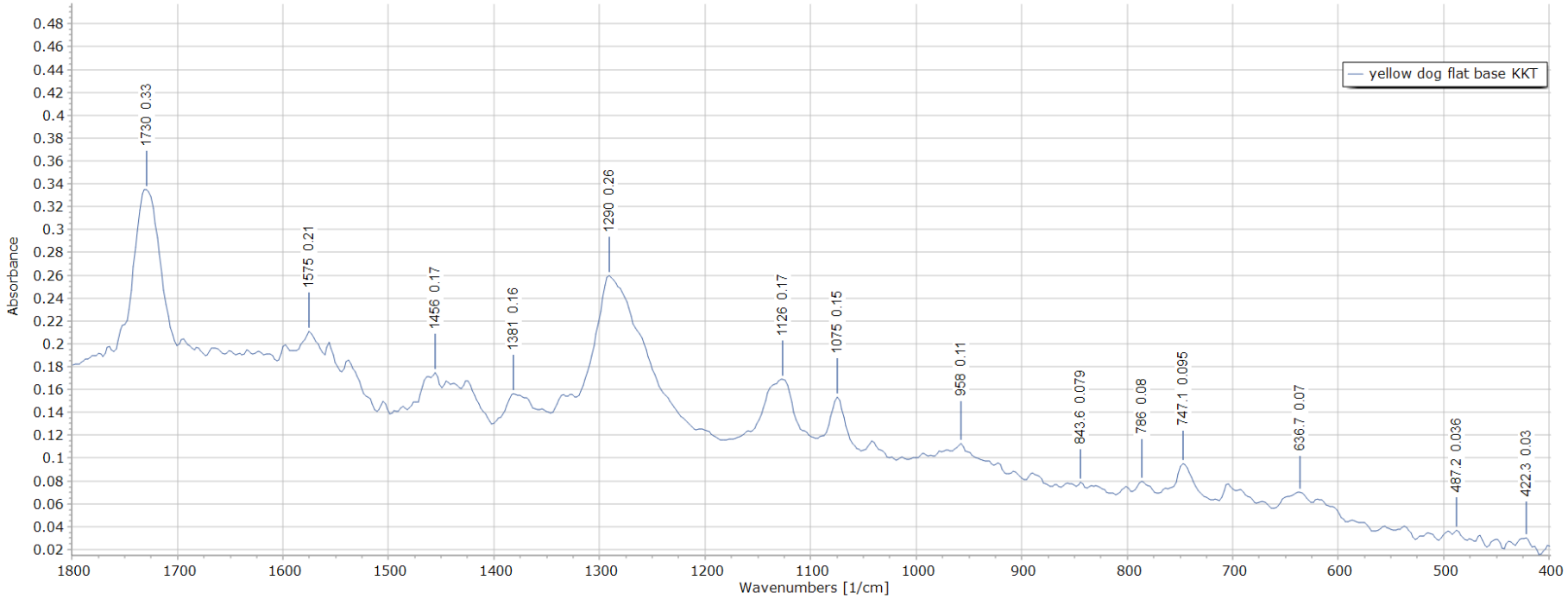
yellow dog flat base KKT
Absorbance
Wavenumbers [1/cm]
1730 0.33
1575 0.21
1456 0.17
1381 0.16
1290 0.26
1126 0.17
1075 0.15
958 0.11
843.6 0.079
786 0.08
747.1 0.095
636.7 0.07
487.2 0.036
422.3 0.03